Nitric oxide and central autonomic control of blood pressure: A neuroanatomical study of nitric oxide and cGMP expression in the brain and spinal cord

Kellysan Powers-Martin

This thesis was submitted in fulfilment of the requirements for the degree of Doctor of Philosophy (Biomedical Science), Murdoch University.

July 2008

Declaration

I declare that this thesis is my own account of my research and contains work that has not been previously submitted for a degree at any other tertiary educational institution.

Kellysan Powers-Martin

Abstract

Essential hypertension is defined as a chronic elevation of blood pressure of unknown cause. Though a definitive trigger for this change in blood pressure has not been established, there is a strong association with an upregulation of sympathetic output from the central nervous system. There are a number of central autonomic nuclei involved in the maintenance of blood pressure, including the brainstem regions of the nucleus tractus solitarii (NTS), caudal ventrolateral medulla (CVLM), rostral ventrolateral medulla (RVLM), the sympathetic preganglionic neurons (SPNs) within the intermediolateral cell column (IML) of the spinal cord, as well as forebrain regions such as the paraventricular nucleus (PVN) of the hypothalamus. Within these centers, a vast number of neurotransmitters have been identified that contribute to the control of blood pressure, including glutamate, angiotensin II, serotonin, neurotensin, neuropeptide Y, opioids and catecholamines. Recognition of the role of nitric oxide (NO) and its multiple influences over the neural control of blood pressure is gaining increasing significance.

Nitric oxide is a unique modulatory molecule that acts as a non-conventional neurotransmitter. As NO is a gas with a short half-life of 4 – 6 seconds, its' synthesising enzyme, nitric oxide synthase (NOS) is often used as a marker of location of production. Once activated, the best-known "receptor" for NO is soluble guanylate cyclase (sGC), which drives the production of cyclic guanosine monophosphate (cGMP). Identifying the presence of cGMP can therefore be used to determine sites receptive to NO. Previous studies examining the role of NO in the central autonomic control of blood pressure have focused predominantly upon application of either excitatory or inhibitory drugs into the key central autonomic regions and assessing pressor or depressor effects. This thesis aims instead to study

the neuroanatomical relationship and functional significance of NO and cGMP expression in the brain and spinal cord of a hypertensive and normotensive rat model.

In the first experimental chapter (Chapter 3), a comparative neuroanatomical analysis of neuronal NOS expression and its relationship with cGMP in the SPN of mature Spontaneously Hypertensive Rats (SHR) and their controls, Wistar Kyoto (WKY) was undertaken. Fluorescence immunohistochemistry confirmed the expression of nNOS in the majority of SPN located within the IML region of both strains. However, a strain specific anatomical arrangement of SPN cell clusters was evident and while there was no significant difference between the total number of SPN in each strain, there were significantly fewer nNOS positive SPN in the SHR animals. All nNOS positive SPN were found to express cGMP, and a novel subpopulation of nNOS negative, cGMP-positive SPN was identified. These cells were located in the medial edge of the IML SPN cell group. These results suggest that cGMP is a key signalling molecule in SPN, and that a reduced number of nNOS positive SPN in the SHR may be associated with the increase in sympathetic tone seen in essential hypertension.

The second experimental chapter (Chapter 4) aimed to determine if reduced numbers of nNOS containing SPN translated into reduced detectable cGMP. The functional significance of cGMP signalling in the two strains was then examined. Based on previous work by our group, it was predicted that reduced nNOS in the SHR would translate into reduced cGMP and that intrathecal administration of exogenous cGMP in the spinal cord would drive a differential pressor response in the two animal strains. Immunohistochemical techniques confirmed that within each SPN, the relative level of cGMP expression was significantly reduced in the SHR when compared to the WKY. Intrathecal application of 8-bromo-cGMP, a drug

analogous to cGMP, increased blood pressure in both strains and had a differential and dose dependent effect, causing only a small increase in blood pressure in anaesthetised WKY animals, while driving a significant pressor response in the SHR. This finding raised the novel hypothesis that in the SHR, reduced nNOS expression is not a driver of hypertension, but is instead a protective mechanism limiting the potent pressor effects of cGMP within SPN.

The third experimental chapter (Chapter 5) examines the expression of neuronal and inducible isoforms of NOS (nNOS, iNOS) within the RVLM of SHR and WKY rats. Reverse transcription-polymerase chain reaction (RT-PCR) was used to analyse the level of mRNA expression and immunohistochemistry was then used to further analyse protein levels of nNOS. Total RNA was extracted and reverse transcribed from the RVLM of mature male WKY and SHR. Quantitative real-time PCR indicated that relative to WKY, mRNA levels for nNOS was significantly higher in RVLM of the SHR. This was confirmed immunohistochemically. When compared to iNOS, nNOS was expressed at significantly higher levels overall, however there was no difference in iNOS mRNA expression between the two strains. This demonstration of differential expression levels of nNOS and iNOS in the RVLM raises the possibilities that (i) NO production is up-regulated in the RVLM in SHR in response to increased sympathetic activity in order to re-establish homeostatic balance or alternatively that (ii) an alteration in the balance between nNOS and iNOS activity may underlie the genesis of augmented sympathetic vasomotor tone during hypertension.

The fourth experimental chapter (Chapter 6) extends the observations in Chapter 5 through examination of the expression of cGMP and sGC within the RVLM. There is strong functional evidence to suggest that NO signalling in the

RVLM relies on cGMP as an intracellular signalling molecule and that this pathway is impaired in hypertension. Immunohistochemistry was used to assess cGMP expression as a marker of active NO signalling in the C1 region of the RVLM, again comparing SHR and WKY animals. Fluorescence immunohistochemistry on sections of the RVLM, double labelled for cGMP and either nNOS or phenylethylamine methyl-transferase (PNMT) failed to reveal cGMP positive neurons in the RVLM from aged animals of either strain, despite consistent detection of cGMP immunoreactivity neurons in the nucleus ambiguus from the same or adjacent sections. This was demonstrated both in the presence and absence of the phosphodiesterase inhibitor isobutylmethylxanthine (IBMX) and in young vs. aged animals. *In-vitro* incubation of RVLM slices in the NO donor DETA-NO or NMDA did not reveal any additional cGMP neuronal staining within the RVLM. In all studies, cGMP was prominent within the vasculature. Soluble guanylate cyclase immunoreactivity was found throughout the RVLM, although it did not co-localise with the PNMT or nNOS neuronal populations. Overall, results suggest that within the RVLM, cGMP is not detectable in the resting state and cannot be elicited by phosphodiesterase inhibition, NMDA receptor stimulation or NO donor application. A short time course of cGMP signalling or degradation not inhibited by the phosphodiesterase inhibitor utilised (IBMX) in the RVLM cannot be excluded.

The final experimental chapter (Chapter 7) examines cGMP expression in magnocellular and preautonomic parvocellular neurons of the PVN. Retrograde tracing techniques and immunohistochemistry were used to visualise cGMP immunoreactivity within functionally, neurochemically and topographically defined PVN neuronal populations in Wistar rats. Basal cGMP immunoreactivity was readily observed in the PVN, both in neuronal and vascular profiles. Cyclic GMP

immunoreactivity was significantly higher in magnocellular compared to preautonomic neuronal populations. In preautonomic neurons, the level of cGMP expression was independent on their subnuclei location, innervated target or neurochemical phenotype. The data presented in this chapter indicates a highly heterogeneous distribution of basal cGMP levels within the PVN, and supports work by others indicating that constitutive NO inhibitory actions on preautonomic PVN neurons are likely mediated indirectly through activation of interneurons.

Summary

Together, these studies comprise a detailed analysis of the neuroanatomical expression of NO and its signalling molecule cGMP in key central autonomic regions involved in the regulation of blood pressure. Under resting or basal conditions, the studies demonstrate notable differences in the expression of NO synthesising enzymes between normotensive and hypertensive animals, and correlating changes in the downstream signalling molecule cGMP. In the spinal cord, novel functional differences in cGMP activity were also demonstrated. In the RVLM, although differences in nNOS were demonstrated, cGMP expression could not be readily detected in either the WKY or SHR, while in contrast within the PVN, cGMP was detected in both magnocellular and parvocellular neuronal populations.

Conclusion

This thesis gives insight into the physiological role of NO and cGMP as mediators of central blood pressure control. The results presented indicate that the NO-cGMP dependent signalling pathway may not be the dominant driver responsible for maintaining high blood pressure in the SHR model of essential hypertension, and that there is no globally consistent pattern of expression, and indeed the role of NO as a mediator of pressor and depressor function may vary between the autonomic

regions examined. Further, it is possible that this pathway is only recruited during activation of reflex homeostatic pathways or during times of marked physiological stress, and that the differences we see in basal expression between the normotensive and SHR animals are instead a result of compensatory mechanisms.

Acknowledgements

What to say without sounding cliché? There are of course the obvious thank-yous – Jackie for driving me nuts, Doug for always sounding terrified of me on the phone, and Leonard for….ummm, what do you look like again? Ok, just joking. Jackie you are an amazingly intelligent person who I truly admire. Doug, though you don't say much, what you do say is gold. Leonard, you always strive to make me think

However, a thesis is an embodiment of work for which many more people need to be given credit for.

To my fellow colleagues – thank you all for your various inputs. I can't believe there are so many of you, Paula, Anna, Yelena, Courtney, Raihana, Su Ann, Little Jo, Gael, Niloufer and John – thanks for all the good times. Rhonda – thankyou thank you, thank you for your patience and talent to teach; Steve, thanks for all the IT assistance. Varun and Vasyl, you were a pleasure to work with. To the current inhabitants of our office, Ben, Kathryn, Penny and Tammy, thank-you so much for this year – I would have never made it without you. Words cannot say how much you guys mean to me. I will miss the good times, our lovely "pets", and the constant support. A big thank-you has to go to Trish, as well – for all the times she's propped me up this year. Lastly, Susannah – who has made sure I finish these last 18 months, no matter how much I wanted to give up. SusieQ, you're one of my closest friends, my best friend through my PhD.

Another set of thanks has to go to the wonderful people I have met interstate and internationally, Anne Goodchild, Paul Pilowsky, Deborah Spingell, Javier Stern and Vinicia Biancardi. Anne, you are an amazing scientist, with such patience I'll never forget and Paul, thank you for your invaluable insight. Deb, thankyou for all your hard work. The three of you should all take credit in helping me become the scientist I am today. To Javier and Vinicia, thank you for helping me feel so welcome in the USA, and for your input and advice on everything.

To my awesome friends, thank-you for keeping me sane and grounded, without your patience, coffees, dinners and so forth, I would surely have lost the plot. A big thank-you to my closest friends, in no particular order Grace, Cindy, Lee Lee,

David, Jacqui, Catherine, Andrea, Emily, Emma and Lorraine I owe you all afternoon tea and bickies.

Lastly, to my wonderful family. My mum, for giving me my fighting spirit, and my dad for giving me that balancing calm. I love you both so much, and just want you to say thank-you for everything. My little family of animals, thank-you for those cuddles, particular Lily and Saffy. Lastly, a huge thank-you goes to Rob, words cannot express how much you mean to me. You have seen me at my best and my worst, and you were always there, still loving me and picking up the pieces. I will never be able to thank-you enough. Oh and I need help formatting this….so don't go anywhere yet. And can I have my thumb drive back please? Thanks hunny.

"Science has made us gods

even before we are worthy of being men"

Jean Rostand – French biologist (1894 – 1977)

Publications arising from this thesis

Edwards MA, Loxley RA, **Powers-Martin K**, Lipski J, McKitrick DJ, Arnolda LF, Phillips JK.

Unique levels of expression of N-methyl-D-aspartate receptor subunits and neuronal nitric oxide synthase in the rostral ventrolateral medulla of the spontaneously hypertensive rat.

Brain Research: Molecular Brain Research 2004; 129(1-2): 33-43.

Powers-Martin K, McKitrick DJ, Arnolda LF, Phillips JK.

Distinct subpopulations of cyclic guanosine monophosphate (cGMP) and neuronal nitric oxide synthase (nNOS) containing sympathetic preganglionic neurons in spontaneously hypertensive and Wistar-Kyoto rats.

The Journal of Comparative Neurology 2006; 497(4): 566-74.

Powers-Martin K, Barron AM, Auckland C, McCooke J, McKitrick DJ, Arnolda LF, Phillips JK

Immunohistochemical assessment of cyclic guanosine monophosphate (cGMP) and soluble guanylate cyclase (sGC) within the rostral ventrolateral medulla

Journal of Biomedical Science 2008; 15(6): 801-12.

Powers-Martin K, Phillips JK, Biancardi VC, Stern JE.

Heterogeneous Distribution of Basal Cyclic Guanosine Monophosphate (cGMP) within Distinct Neuronal Populations in the Hypothalamic Paraventricular Nucleus

American Journal of Physiology: Regulatory, Integrative and Comparative Physiology 2008; 295(4): R1341-50.

Other publications arising from period of candidature

Springell DA, **Powers-Martin K**, Phillips JK, Pilowsky PM, Goodchild AK.

Phosphorylated extracellular signal-regulated kinase 1/2 immunoreactivity identifies a novel subpopulation of sympathetic preganglionic neurons.

Neuroscience. 2005; 133(2): 583-90.

Table of Contents

List of Figures

List of Tables

Abbreviations

2K1C	2 kidney 1 clip
8-Br-cGMP	8-Bromo-cGMP
A1	adrenergic groups
aCSF	artificial cerebrospinal fluid
ADH	antidiuretic hormone
AMPA	a-amino-3-hydroxy-5-methyl-4-isoxazole propionic acid
Ang II	angiotensin II
ANP	atrial
ANS	autonomic nervous system
anti α-SMA	anti a smooth muscle actin
AVP	arginine vasopressin
BH_4	(6R)-6,5,7,8-tetrahydrobiopterin
BNP	brain natriuretic peptide
BP	blood pressure
CAA	central autonomic area
cGMP	cyclic guanosine monophosphate
CGRP	calcitonin gene-related peptide
ChAT	choline acetyl transferase
cNOS	constitutive NOS
CNP	C-type natriuretic peptide
CNS	central nervous system
CO_2	carbon dioxide
CRH	corticotropic releasing hormone
CSN	commissural subnucleus
Ct	cycle threshold
CVLM	caudal ventrolateral medulla
CY2	cyanine
CY3	indocarbocyanine
CY5	indodicarbocyanine
DAB	diaminobenzidase
DAF-2	4,5-diaminofluorescein-2-diacetate
DBH	dopamine b oxidase
DC	dorsal cap
dNTPs	deoxynucleoside-triphosphate
eNOS	endothelial NO synthase
ERK	extracellular signal-related kinase
FG®	Fluorogold®
FITC	fluorescein isothiocyanate
GABA	g-aminobutyric acid
GCs	guanylyl cyclases
HIF-1α	hypoxic inducible factor 1 alpha
HR	heart rate
IBMX	inhibitor isobutylmethylxanthine

IM	intramuscular
IML	intermediolateral lateral cell column
io	inferior olive
IP	intraperitoneal
IR	immunoreactivity
L-arg	L-arginine
LM	lateral magnocellular
MAP	mean arterial pressure
MM	medial magnocellular
mRNA	messenger RNA
NA	nucleus ambiguus
NaN_3	sodium azide
NAPDH	nicotinamide-adenine-dinucleotide phosphate
NMDA	N-methyl-D-aspartate
nNOS	Neuronal NOS
NO	nitric oxide
NOS	NO synthase
NR1	N-methyl-D-aspartate receptor 1
NR2	N-methyl-D-aspartate receptor 2
NRS	normal rabbit serum
NSE	neuronal specific enolase
NTS	nucleus tractus solitarii
ODQ	1H-[1,2,4] oxadiazole [4,3-a] quinoxaline-1-one
OT	oxytocin
OVLT	organum vascularis lamina terminalis
PaPo	posterior parvocellular
PB	phosphate buffer
PDE	phosphodiesterases
p-ERK1/2	phosphorylated extracellular signal regulated kinase 1/2
PKG	protein kinase G
PNMT	phenylethanolamine-n-methyltransferase
PPE	preproenkephalin
PSD95	post synaptic density protein
PVN	paraventricular nucleus of the hypothalamus
RSNA	renal sympathetic nerve activity
RT-PCR	polymerase chain reaction
RVLM	rostral ventrolateral medulla
sd	standard deviation
SEM	standard error of the mean
SFO	subfornical organ
sGC	soluble guanylate cyclase
SHR	Spontaneously Hypertensive Rat
SND	sympathetic nervous discharge
SON	supraoptic nucleus
SPN	sodium nitroprusside
SPN	sympathetic preganglionic neurons

TH	tyrosine hydroxylase
TPBS	Tris phosphate buffered saline
VM	ventromedial parvocellular
WKY	Wistar Kyoto

1. Literature review

1.1. Regulation of blood pressure

1.1.1. Hypertension

Homeostasis, the regulation of the internal environment, is dependent on efficient and appropriate blood flow to all regions of the body. This flow is determined by pressure gradients within the cardiovascular system which we routinely gauge through assessment of mean arterial pressure (MAP) (Bernard, 1865; Dampney et al., 2002). Various stressors in a daily routine can cause blood pressure (BP) to fluctuate dramatically, but ultimately, over a 24-hour period it is a tightly controlled variable (Guyenet, 2006). However, in response to ongoing stressors that challenge the maintenance of BP, individuals may lose the ability to maintain MAP within the normal physiological range (Monahan, 2007). Hypertension is diagnosed when there is chronic elevation of the 24-hour average BP, and can be classified as one of either two broad categories of hypertension essential (or primary) hypertension, and secondary hypertension (Guyenet, 2006).

Essential hypertension is defined as a rise in BP of unknown cause that increases risk for cerebral, cardiac, and renal events (Messerli et al., 2007). It is generally agreed that essential hypertension arises from a combination of genetic and environmental influences (Folkow, 1982). Human population studies have shown that the development of hypertension has some genetic basis (Staessen et al., 2003) with at least 17 human genes having been identified with either hypertension or

hypotension (Lifton et al., 2001). However, interventional studies show that environmental changes, such as diet, exercise and salt intake can affect BP, regardless of genetic disposition, indicating that environmental factors are powerful contributors to essential hypertension (Fagard, 2001; Graudal et al., 1998; Sacks et al., 2001).

Secondary hypertension is diagnosed in patients whose increase in BP has an identifiable cause (Messerli et al., 2007). The most common cause is chronic renal disease, which can be brought on by diabetes, glomerulonephritis, or polycystic kidney disease (Fesler et al., 2005; Phillips, 2005; Textor, 2004). Other known factors include phaeochromocytoma, Cushing's syndrome and primary aldosteronism (Barzon et al., 2002; Sawka et al., 2003).

Present statistics indicate that 20 – 30% of the worldwide population is afflicted with hypertension (Mackay and Mensah, 2004; Staessen et al., 2003), and given that its' prevalence rises with age, between 60 – 70% of those over 60 are afflicted (Staessen et al., 2003). While hypertension itself has no physical symptoms, the secondary effects of hypertension can be devastating. For example, one of the most consistent and powerful predictors of stroke is elevated BP (Zhang et al., 2006). Estimates published by the World Health Organisation indicate that up to 15 million people each year suffer from stroke, of whom ~5 million die and another ~5 million are left permanently disabled (Mackay and Mensah, 2004). Furthermore, population mortality trends show that those who have suffered a stroke have symptoms similar to those who suffer from hypertension (Luepker et al., 2006; Wolf-Maier et al., 2003) with elevated systolic BP >115mmHg and above explaining 60% of the population-attributable risk of stroke (Lawes et al., 2006). Hypertension also aggregates with other disorders, such as abdominal obesity, dyslipidaemia, glucose intolerance,

hyperinsulinaemia and hyperuricaemia, indicating that these are likely to have hypertension as a contributing factor (Staessen et al., 2003).

A number of early studies have shown that the onset and early stages of human hypertension is characterised by augmented sympathetic activity at both rest and during physical and psychological stressors (Egan et al., 1987; Julius, 1986; Nestel, 1969). Plasma adrenaline (Goldstein, 1983) and noradrenaline (Esler et al., 1986) levels are higher in younger persons with hypertension (under the age of 40), and muscle sympathetic nervous activity is elevated in individuals in the early stages of hypertension (Anderson et al., 1989b). Together, these data suggest that augmented sympathetic output may contribute to the development of hypertension (Anderson et al., 1989b).

1.1.2. The baroreceptor reflex

Blood pressure is a function of vascular resistance and cardiac output, two variables that are tightly controlled by the autonomic nervous system (ANS). It is in a constant state of flux, and is regulated over short and long-term time frames, through changes in vasomotor tone and sodium fluid balance (Staessen et al., 2003). Vasomotor tone refers to the degree of vascular contractility and reflects sympathetic drive, with increased peripheral resistance being another key factor driving hypertensive states (Staessen et al., 2003). These mechanisms are affected to various degrees by genetic and environmental factors, and are controlled by local factors, circulating hormones, and the central nervous system (Staessen et al., 2003). The kidneys play a key role in regulating sodium and fluid balance, which is central in long-term BP control through the control of blood volume. Abnormalities in kidney function can therefore contribute significantly to the pathophysiology of renal

hypertension via this and other mechanisms including effects on sympathetic drive (Guyton, 1990; Phillips, 2005).

Within the central nervous system, a number of centres act as a unit to maintain BP, within the actions of the baroreceptor reflex. The stimulus for the baroreflex originates at the level of the baroreceptors (Fig 1.1). These receptors are highly specialised stretch sensitive nerve endings, and are located in various regions of the cardiovascular system, such as the carotid artery, aorta, and the cardiopulmonary region (Aicher et al., 2000; Averill and Diz, 2000; Dampney, 1994). An increase in BP within the arterial wall, for example by the arterial pulse wave, causes the wall to distort activating the receptors (Aicher et al., 2000; Dampney, 1994; Spyer, 1994).

Once activated the baroreceptors send afferent impulses to the central nervous system, via the vagus and carotid sinus nerves (Averill, 2000). The primary response to stimulation of these stretch receptors (by an increase in BP) is a resultant fall in BP, mediated by inhibition of the tonic activity of sympathetic vascular innervation and therefore reduction of total peripheral resistance, and excitation of the cardiovagal motor neurons, driving bradycardia and reducing cardiac output (Aicher et al., 2000). The work presented in this thesis has focused on the sympathetic control of vasomotor tone, as a key regulator of BP.

Figure 1.1: Location of baroreceptors

Baroreceptors (seen in yellow in the aortic arch and left and right carotid sinuses) are located within the aortic arch and the carotid sinus. These specialised receptors detect the pressure of blood flowing past them, and send inputs to the central nervous system to alter vascular tone and cardiac output. Image taken from http://www.cvphysiology.com/Blood%20Pressure/bp012%20baroreceptor%20anat.gif.

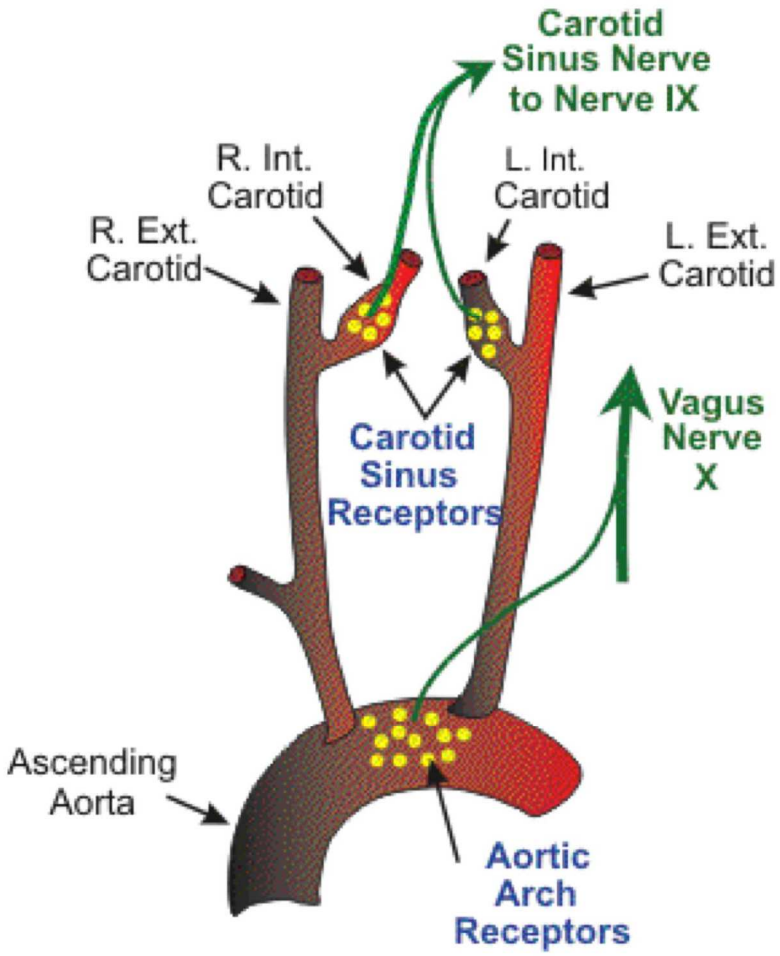

Figure 1. Location and innervation of arterial baroreceptors.

The primary central sympathetic components of the baroreceptor reflex are located within the medulla oblongata and thoracic spinal cord, though there are many supramedullary premotor centres that can modulate the final output of the baroreceptor reflex (Aicher et al., 2000). For example, the hypothalamus has been shown to elicit sympathoexcitation via both the medulla and spinal cord, which increases BP and HR (Coote et al., 1998). For the purposes of this review, I shall focus on three key regions in the medulla, then the sympathetic preganglionic neurons (SPNs) of the spinal cord and the paraventricular nucleus of the hypothalamus (PVN), discussing their roles in the homeostatic control of blood pressure, perturbations associated with hypertension and specific neuromodulators involved in regulating their activity. The review will follow the path of the baroreceptor reflex, beginning with the point where the baroreceptors terminate in the nucleus tractus solitarii (NTS), progressing to the caudal ventrolateral medulla (CVLM), the rostral ventrolateral medulla (RVLM), and then the SPNs (Fig 1.2) being final integration point of the baroreceptor reflex. I will then discuss the specific issues relation to the PVN.

1.1.3. Transmitters in hypertension

Many neurotransmitters and neuropeptides have been shown to signal within the baroreceptor reflex. These include classical neurotransmitters, such as γ-aminobutyric acid (GABA), and L-glutamate (Averill, 2000), as well as angiotensin II (Boscan et al., 2001; Campagnole-Santos et al., 1988; Paton and Kasparov, 1999; Schreihofer and Guyenet, 2002), serotonin (N'Diaye et al., 2001), neurotensin (Seagard et al., 2000), neuropeptide Y (Kubo and Kihara, 1990), opioids (Li et al., 1996) and catecholamines (Sved et al., 1992). In recent years, studies have shown

that nitric oxide (NO) is an important factor in the maintenance of cardiovascular autonomic control (Chowdhary and Townend, 1999), and is critical to the maintenance of normal BP (Huang et al., 1995). In experimental animals, it has been shown that NO regulates vasomotor tone and arterial pressure, at least in part, by modulating sympathetic neural outflow (Sartori et al., 2005). Furthermore, it has been shown now in a number of experimental models of hypertension that NO signalling appears to be impaired (Sartori et al., 2005).

In this thesis, the central tenant of many of the studies presented is that altered NO signalling in central autonomic nuclei is linked to hypertension, as either an initiating or secondary response mechanism.

In this chapter, I will present the mechanisms underlying NO signalling and then introduce the afore mentioned central autonomic regions involved in the baroreceptor reflex, and discuss how these areas are affected by NO both in the normal physiological condition and during altered states of BP.

Figure 1.2: Centres involved in the baroreceptor reflex

Pathway of the baroreceptor reflex. Input from the baroreceptors (not shown) are first relayed to the NTS, progressing to the CVLM, then the RVLM of the medulla, before terminating at the SPNs before relaying signals to the peripheral nervous system, via the sympathetic post ganglionic neurons.

Key elements and effectors of the baroreceptor pathway

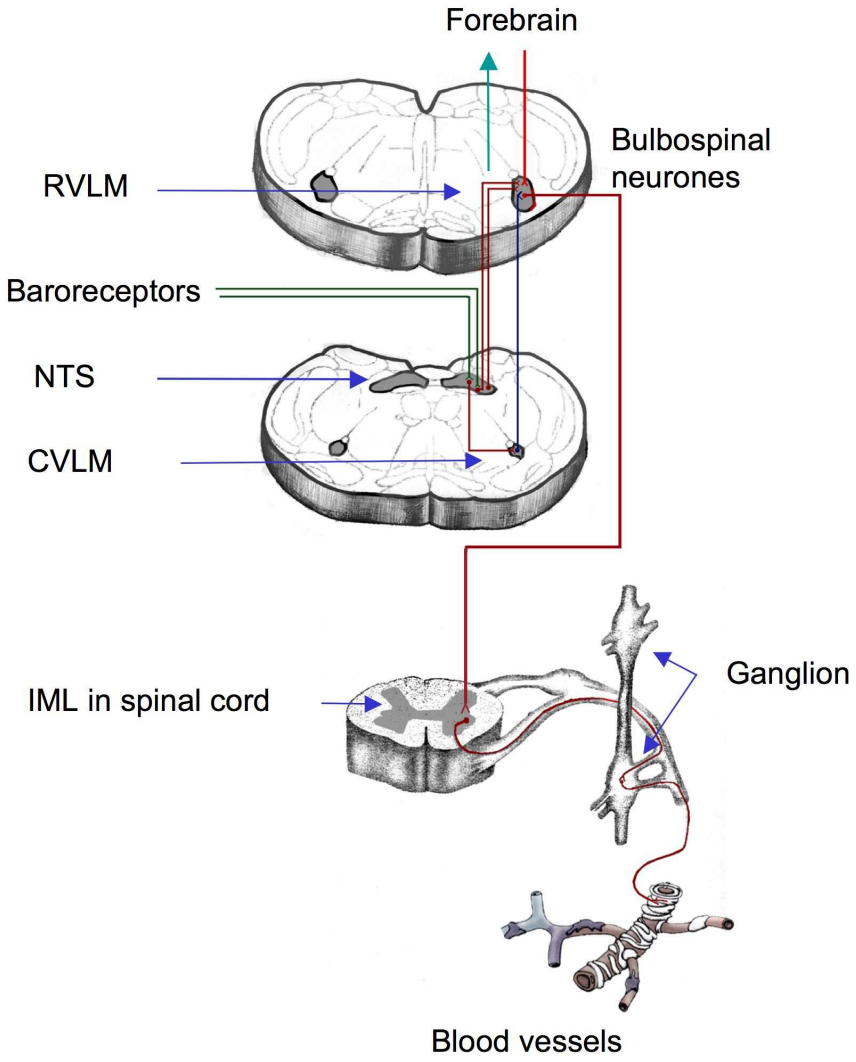

With thanks to Mr Mark Edwards for this image

1.2. Nitric oxide

1.2.1. Definition

Nitric oxide is a ubiquitous modulatory molecule that acts as a non-conventional neurotransmitter in the central nervous system (CNS) (Schuman and Madison, 1994). It is a colourless, odourless gas (Bruckdorfer, 2005), with a short half life of about 4 - 6 seconds (Cannon, 1998; Furchgott, 1983; Thomas et al., 2001) and is a diatomic free radical (Bruckdorfer, 2005; McDonald and Murad, 1995) which can be a potent toxin to the body (Cary et al., 2006). Nitric oxide has a low molecular weight, is reasonably hydrophobic and is membrane permeable, so it can not be stored for long periods of time, but theoretically is able to reach anywhere within cells and tissues (Baranano and Snyder, 2001). Nitric oxide is formed only after activation of its synthesising enzyme NO synthase (NOS) and is therefore highly regulated (Baranano and Snyder, 2001).

1.2.2. Location and production of NO

Being a gas, NO is difficult to visualise, so NOS is often used as a marker to indicate the capacity of a cell to produce NO. There are three NOS enzymes which use L-arginine as a substrate (Nathan and Xie, 1994). All isoforms require co-factors for synthesis, including reduced nicotinamide-adenine-dinucleotide phosphate (NADPH), flavin adenine dinucleotide, flavin mononucleotide and (6R)-6,5,7,8-tetrahydrobiopterin (BH_4) (Hevel and Marletta, 1992; Mayer et al., 1991; Pollock et al., 1991; Stuehr et al., 1991). Once these elements are combined with oxygen, the subsequent reaction is the production of citrulline, NADP and the free radical NO (Alderton et al., 2001). Many cells are capable of synthesising NO (Li and

Forstermann, 2000) and this include central nervous system (CNS) regions involved in cardiovascular control (Bhat et al., 1995; Chang et al., 2003; Kantzides and Badoer, 2005).

1.2.3. General function

Since it's discovery, studies have shown that NO is involved in many physiological processes throughout the body. In peripheral organs, such as the digestive, respiratory and urogenital organs, NO acts in a neurotransmitter-like manner, in that it is released from nitrergic nerves to mediate smooth muscle relaxation (Rand and Li, 1995; Toda et al., 2005; Toda and Okamura, 2003). Within the CNS, NO is associated with many functions, including learning and memory formation, feeding, sleeping, reproductive behaviour as well as sensory and motor function (Garthwaite, 2008). Nitric oxide most often acts as a local paracrine factor influencing physiological functions of cells in the immediate locale of its production (Horn et al., 1994). Dysregulation of NO is known to contribute to a myriad of diseases including heart disease, hypertension, stroke, gastrointestinal distress, erectile dysfunction and neurodegeneration (Bredt, 1999; Dawson and Dawson, 1998; Takahashi, 2003).

An important function of NO is in the regulation of sympathetic outflow within the CNS (Krukoff, 1999). This includes general inhibition of sympathetic activity (Kantzides and Badoer, 2005; Sakuma et al., 1992) and reduction of BP (Togashi et al., 1992) and conversely it has been shown to stimulate pressor responses (Hirooka et al., 1996; Malik et al., 2007). This is covered in more detail in later sections discussing NO and the specific autonomic regions.

1.2.4. Nitric oxide synthase isoforms

Overview

There are three isoforms of NOS that catalyse the formation of NO (McDonald and Murad, 1995). The three isoforms are generated from separate genes on different loci (Griffith and Stuehr, 1995), but each of the genes have a similar genomic structure, suggesting a common ancestral NOS gene (Alderton et al., 2001). All 3 isoforms are self sufficient enzymes with two major functional domains fused into a single polypeptide. Each isoform has a different physiological function, despite the fact that they all produce NO (Bruckdorfer, 2005).

The biosynthesis of NO by NOS involves the conversion of L-arginine ($_L$-arg) to $_L$-citrulline (Masters et al., 1996). Nitric oxide synthase functions as a dimer made of two identical monomers that are functionally and structurally divided into 2 domains, the C-terminal reductase domain, and an N-terminal oxygenase domain (Hemmens and Mayer, 1998). The C-terminal reductase domain contains binding sites for NADPH, which carries electrons from one reaction to another, flavin adenine dinucleotide, involved in changing redox states, and flavin mononucleotide, involved in oxidoreductases (Alderton et al., 2001). The N-terminal contains binding sites for haem, which detects oxygen and BH_4, which is essential for the synthesis of NO by NOS (Andrew and Mayer, 1999). Between the two regions lies the calmodulin binding domain, which plays a key role in both the structure and function of the enzyme. The reductase and oxygenase domains of NOS are distinct catalytic unis, which together provide the complete machinery required for NO production (Andrew and Mayer, 1999).

Biosynthesis of NO involves a two-step oxidation of $_{L}$-arg to $_{L}$-citrulline, with concomitant production of NO. L-arginine is hydroxylated to form N^{G}- hydroxy-L-arginine, which is then further oxidated with NADPH to form $_{L}$-citrulline and NO (Andrew and Mayer, 1999). The manner in which this reaction is initiated differs between the isoforms and is discussed below.

Endothelial nitric oxide synthase

As the name suggests, endothelial NO synthase (eNOS) was first discovered within the endothelial layer of blood vessels (Furchgott and Zawadzki, 1980). The gene for eNOS is located on chromosome 7, and the protein encodes for a 1203 amino acid sequence (Alderton et al., 2001). In their seminal experiment, Furgott and Zawadzki found that strips of rabbit aorta with intact endothelium relaxed in response to acetylcholine, but constricted in response to this same agonist when the endothelium had been rubbed off (Cannon, 1998; Furchgott and Zawadzki, 1980). The substance responsible for this relaxation, initially called endothelium-derived relaxing factor, was subsequently found to be NO. Endothelial NOS is found within the caveolae of the endothelial cell plasma membrane (Garcia-Cardena et al., 1996; Shaul et al., 1996), which is where receptors for agents that regulate endothelial activity accumulate. Though it was originally purified and cloned from vascular endothelium, its expression has been reported in cardiomyocytes, blood platelets, and hippocampal neurons (Arnal et al., 1999).

Endothelial NOS attaches to the membrane with hydrophobic anchors, (Bruckdorfer, 2005), and only minute amounts of eNOS are required for a reaction to occur. Regulated by influx of calcium into the cell, the production of eNOS is stimulated by blood flow through the arteries (Bruckdorfer, 2005). Shear stress, which is exerted by the blood stream on the endothelial cell surface, regulates

endothelial autacoid production and gene transcription (Davies, 1995; Takahashi et al., 1997), and it has been demonstrated in numerous vascular preparations that shear stress leads to vasodilation through the release of endothelial NO and/or prostaglandins (de Wit et al., 1997; Koller and Kaley, 1990; Koller et al., 1993; Pohl et al., 1991). The main role of eNOS within the vasculature is to therefore regulate changes in blood flow and pressure in response to local stimuli (Bruckdorfer, 2005).

Neuronal nitric oxide synthase

Located on chromosome 12; the neuronal NOS (nNOS) gene encodes for an 144 amino acid protein (Alderton et al., 2001) and is the largest of the 3 isoforms. Neuronal NOS is located primarily within neurons of both the central and peripheral nervous system (Alderton et al., 2001; Patel et al., 2001), though its expression has been demonstrated in other cell types, including smooth muscle and cardiac cells (Casadei, 2006; Webb et al., 2006). Neuronal NOS is located within the cytoplasm, and unlike eNOS has no anchors (Bruckdorfer, 2005). Instead, nNOS has a post synaptic density protein (PSD95), Drosophila disc large tumour suppressor, and zonula occludens-1 protein (zo-1) (PDZ domain), that targets nNOS to synaptic sites in the brain (Alderton et al., 2001).

Functionally, NO released from nerves is involved in a wide range of neurotransmitter functions throughout the body including regulation of gastro-intestinal function, penile erection, neuronal control of blood flow and central neuronal signalling. Within the CNS, there is strong support for it having a role in plasticity, as it plays a key role as a modulator of responses to glutamate.

Both nNOS and eNOS are expressed constitutively in mammals and collectively are called constitutive NOS (cNOS) (Li and Poulos, 2005).

Inducible nitric oxide synthase

The gene for iNOS is located on chromosome 17, and encodes for a 133 kDA 1203 amino acid protein (Alderton et al., 2001). Unlike endothelial and nNOS, iNOS is activated by external stimuli, such as bacterial lipopolysaccharide (Bruckdorfer, 2005), produces a large amount of NO, and has long lasting activity of 24 hours or more (Bruckdorfer, 2005). Though there is evidence that iNOS can produce NO in all tissues, it is mainly localised to macrophages, hepatocytes and smooth muscle (McDonald and Murad, 1995). Functionally, iNOS contributes a non-specific immune component as part of the inflammatory response.

Constitutive NOS activity is controlled by calmodulin binding in a calcium concentration dependent manner (Li and Poulos, 2005). In sharp contrast, iNOS has calmodulin bound permanently as an additional subunit, and hence is not regulated by calmodulin binding, but instead is under transcriptional control (Li and Poulos, 2005).

In addition to regulation by Ca2+/calmodulin, nNOS possesses several phosphorylation sites. Phosphorylation sites for cGMP-dependent protein kinases, protein kinase C or Ca2+/calmodulin-dependent protein kinase (CaMK)II have been found on purified nNOS enzymes, but their effects on the activity of nNOS have been found to be modest and sometimes contradictory (Nakane et al., 1991; Bredt et al., 1992; Dinerman et al., 1994b). Ca2+/calmodulin-dependent protein kinase, a co-resident with NMDA receptors and nNOS at synapses (Kennedy, 2000), has been found to inhibit NO formation by ~50%, probably by affecting Ca2+/calmodulin binding (Hayashi et al., 1999; Komeima et al., 2000). In the cultured neurones, phosphorylated nNOS was concentrated in dendritic spines but the phosphorylation process was slow, taking 15 min to be detectable (Rameau et al., 2004), suggesting

that CaMKII is likely to be not a dynamic regulator of nNOS activity but more a longer-term gain controller.

1.2.5. Nitric oxide signalling mechanisms

As a membrane permeable neuronal messenger, NO produces its biological actions through distinct signal transduction pathways (Ahern et al., 2002; Stamler et al., 1997). Its most well known role is the activation of the second messenger cyclic guanosine monophosphate (cGMP) (Chowdhary and Townend, 1999).

The soluble guanylate cyclase - cyclic GMP cascade

As NO diffuses across membranes (Dawson and Dawson, 1998), it binds with a family of enzymes referred to as the guanylyl cyclases (GCs), which synthesise cGMP from intracellular guanosine triphosphate (Krumenacker et al., 2004). There are two main classes of GCs, one that is located in the membranous compartment or organelles, and one in the cytosolic compartment (Murad, 1994; Schmidt, 1992; Vles et al., 2000; Wedel and Garbers, 1997). The membrane bound GCs, otherwise known as particulate GC are large transmembrane molecules that have a receptor domain at the outside of the cell and an intracellular catalytic site (Vles et al., 2000). Particulate GC is activated through interaction with peptide hormones such as atrial, brain and C-type natriuretic peptides, with the receptor domain (Vles et al., 2000). In contrast, soluble guanylate cyclase (sGC) is only activated by NO. It can respond to nanomolar concentrations of NO and catalyse the conversion of GTP to 3'5' cGMP and pyrophosphate (Bredt, 1999; Cary et al., 2006; Dawson and Dawson, 1998). The sGC receptors are composed of two subunits, an alpha (α) and beta (β) heterodimer, of which there are 2 known isoforms $\alpha1\beta1$ and $\alpha2\beta1$ (Garthwaite, 2008).

The production of cGMP by sGC is the mechanism by which NO exerts most of its physiological effects as a cell signalling molecule (Krumenacker et al., 2004). Cyclic GMP binds to target proteins such as cGMP dependant protein kinases such as protein kinase G (PKG) (Jaffrey and Snyder, 1995), cGMP regulated ion channels (Zagotta and Siegelbaum, 1996) and several families of phosphodiesterases (Ahern et al., 2002; Pineda et al., 1996), resulting in specific down stream outputs (Bredt, 1999; Cary et al., 2006; Dawson and Dawson, 1998). Within brain cells, NO activates the associated guanylyl cyclase activity with no observable delay (with a 20-ms sampling time) and, on removal of NO, the activity decays with a half-time of 200 ms (Bellamy and Garthwaite, 2001).

The actions of cGMP have been predominantly studied by binding cGMP agonists to its regulatory sites on either cyclic nucleotide-gated (CNG) ion channels (Kaupp and Seifert, 2002) or hyperpolarization-activated, cyclic nucleotide-modulated (HCN) channels (Craven and Zagotta, 2006). Cyclic GMP also binds directly to a number of the phosphodiesterase enzymes (PDE), particularly PDE2, 5 and in retinal photoreceptor cells, PDE6. This results in heightened catalytic activity and cGMP breakdown. Probably the most widespread mechanism employed by cGMP is activation of PKG, which exists in three forms, PKG1α and PKG1β (splice variants), and PKGII, which is anchored to the plasma membrane by nitrosylation (Garthwaite, 2008). The three forms are found in different locations of the brains with PKG1α is concentrated in cerebellum and dorsal root ganglia, and PKG1β the hippocampus and olfactory bulb. Conversely, PKGII has a more widespread distribution in the brain with a particular abundance in the thalamus (Feil et al., 2005; Hofmann et al., 2006; Vaandrager et al., 2005). Several substrates for PKG have been identified (Schlossmann and Hofmann, 2005) and many of its actions are exerted at

the level of phosphatases, leading indirectly to increased or decreased levels of phosphorylation of effector proteins (Garthwaite, 2008).

Nitrosylation of protein thiols

In addition to the well-described cGMP pathway, there are many biological functions that can be attributed to the actions of NO (Broillet, 1999). This includes the modification of proteins through direct chemical reactions such as the nitrosylation of protein thiols (Davis et al., 2001).

The transfer of NO group to cysteine sulfhydryls on proteins is known as S-nitrosylation (Broillet, 1999), where by NO forms stable covalent interactions with free thiol groups of proteins (Foster et al., 2003). Direct action of NO on proteins has been shown to involve cysteine or tyrosine residues (Broillet, 1999; Stamler, 1994) and metals such as the haem-Fe^{++} interaction (Butler et al., 1995). The nitrosylation of thiols involves joining NO with oxygen, which causes changes in enzymatic activity (Bruckdorfer, 2005).

S-Nitrosylation requires higher concentrations of NO than does activation of sGC and tends to proceed with slower kinetics than cGMP-mediated actions (Ahern et al., 2002). Physiological studies show that the range of ion channels and receptors that are affected by S-Nitrosylation is as many as the ones affected by cGMP (Ahern et al., 2002). These include Ca^{2+}, Na^{+}, cyclic-nucleotide-gated channels, glutamate receptors and N-methyl-D-aspartate (NMDA) receptors. S-Nitrosylation is known to affect exocytosis, synaptic transmission and synaptic plasticity (Bruckdorfer, 2005).

Activation of NMDA receptors

The major excitatory neurotransmitter within the central nervous system is L-Glutamate (Collingridge and Lester, 1989). L-Glutamate functions via activation of

excitatory amino acid ionotropic and metabotropic receptors (Collingridge and Lester, 1989; Nakanishi, 1992). There are 3 main types of amino acid ionotropic receptors; (i) NMDA receptors, (ii) α-amino-3-hydroxy-5-methyl-4-isoxazole propionic acid (AMPA) receptors, and (iii) kainate receptors (Collingridge and Lester, 1989). In addition to the capacity for NO to nitrosylate the NMDA receptor, NOS activation has been linked to excitatory input via NMDA receptors.

The NMDA receptor is a ligand-gated ion channel, permeable to sodium, calcium, and potassium (Nakanishi, 1992). To date, one N-methyl-D-aspartate receptor 1 (NR1) subunit, and four N-methyl-D-aspartate receptor 2 (NR2) subunits (NR2A–D) have been identified and cloned (Kimura et al., 2000). Functional NMDA receptor complexes are formed by different combinations of the subunits (Contestabile, 2000; Kimura et al., 2000). The NR1 unit is the obligatory subunit and contains all the fundamental properties necessary for a functional receptor-channel complex, including a binding site (Hollmann and Heinemann, 1994; Kaczmarek et al., 1997; Nakanishi, 1992), however homomeric combinations of NR1 lead to a receptor with low affinity for binding (Contestabile, 2000). Instead, functional receptors are combinations of the NR1 with at least one of the NR2 subunits. Different combinations of the NR1 with the NR2 subunits can alter the functional properties of the NMDA receptor (Monyer et al., 1994), modify the characteristics of currents elicited, calcium conductance and regulation by other modulators (Contestabile, 2000).

NMDA receptors occur selectively at the post synaptic density of excitatory synapses (Moriyoshi et al., 1991) and although there are several distinct calcium stores at the synapse, only influx through the NMDA receptor efficiently activates nNOS (Kiedrowski et al., 1992). Neuronal NOS does not directly bind to the NMDA

receptor, instead interact via the post synaptic protein PSD-95/SAP90 (PSD-95) (Brenman et al., 1996), which is a membrane-associated guanylate kinase (Cho et al., 1992; Kistner et al., 1993). PSD-95 has 3 PDZ domains, small modular protein-protein interaction interfaces that mediate assembly of protein complexes at cell junctions. Neuronal NOS is unique in that it has it's own PDZ domain, which is critical in allowing nNOS to target specific cellular membranes (Brenman and Bredt, 1997). The tail end of the NMDA receptor binds to one of the PDZ domain of the PSD-95, while nNOS PDZ domain binds to another of the PSD-95 PDZ domains (Christopherson et al., 1999), forming a ternary signalling complex, critical to efficient coupling of calcium influx through the NMDA receptor (Christopherson et al., 1999).

Linkage of NMDA neurotransmission and NO production occurs when a presynaptic neuron is depolarised and glutamate crosses the synapse, binding to the NMDA receptor (Nelson et al., 2003). This causes displacement of a magnesium ion from the receptor, allowing an influx of extra cellular calcium into the cell through the NMDA receptor (Lodish et al., 1997), which instigates NOS to produce NO. Studies have shown that the activation of the NMDA receptor by glutamate stimulates constitutive forms of NOS (Crane et al., 1997; Crane et al., 1998; Dawson and Snyder, 1994), i.e. nNOS (in the brain) and eNOS (in the vasculature). NMDA stimulation with glutamate and the associated increase in NO in turn has been shown to increase cGMP (Garthwaite et al., 1988; Garthwaite and Garthwaite, 1987; Garthwaite et al., 1989). Nitric oxide can subsequently influence the release of glutamate from surrounding presynaptic terminals (Matsuo et al., 2001) and it can interact in an autocrine fashion with thiol groups on the NMDA receptor, causing a

conformational change (S-nitrosylation) that serves to inactivate receptor function (Gbadegesin et al., 1999; Gow et al., 2000).

Within the CNS, NMDA receptor modulation by NO in key central autonomic nuclei can influence sympathetic outflow and BP responses. For example, microinjection of NMDA into the NTS causes a dose dependent increase in NO levels within the NTS, and a decrease in BP that is the same as that seen when NO agonists are applied to the NTS (Matsuo et al., 2001). Furthermore, both the response to microinjection of NMDA and NO is attenuated when NOS inhibitors are applied (Matsuo et al., 2001).

1.3. Nitric Oxide and autonomic areas

There is a considerable amount of evidence supporting a role for NO as a key central autonomic regulator of cardiovascular function, with substantial data showing modulation of sympathetic activity and corresponding changes in BP in several species (del Carmen Garcia et al., 1997), including the rat (Minami et al., 1995; Mollace et al., 1992; Sakuma et al., 1992), cat (Hegde et al., 1994; Shapoval et al., 1991) and dog (Nakahara et al., 1995; Nakahara et al., 2000). This review will now focus on the role of NO in the key central autonomic regions that are the focus of this thesis.

1.4. Nucleus tractus solitarii

Stimulation of the NTS, the first relay station in the baroreflex arc, elicits a decrease in renal sympathetic nerve activity (RSNA), BP and heart rate (HR) (del Carmen Garcia et al., 1997). Analysis of nNOS messenger RNA (mRNA) expression during the development and maintenance of hypertension in the NTS of the

hypertensive Spontaneously Hypertensive Rat (SHR) model and their normotensive genetic control, the Wistar Kyoto (WKY) showed that SHRs had significantly higher nNOS mRNA expression, compared to the WKY, although nNOS mRNA expression decreased as in both strains with aging (Ferrari and Fior-Chadi, 2005). Interestingly, both nNOS protein and mRNA levels increased in the SHR prior to the onset of hypertension. Whether this is causal is unclear, however previous studies showing that NOS activity increases with age indicates that nNOS may be a compensatory response to elevated levels of BP, as the central nervous system may be trying to offset the increased sympathetic output (Qadri et al., 2003).

1.4.1. Location

The NTS is located within the brain stem, dorsal to the RVLM and in the rat, it consists of a column of cells on each side of the fourth ventricle (Sapru, 1994). At the rostral edge of the area postrema, the bilateral columns of the NTS cells merge in the midline to form the commissural subnucleus (CSN) (Sapru, 1994). The CSN of the NTS is approximately 0.5mm rostral to 1mm caudal to the calamus scriptorius (Sapru, 1994). The most critical region pertaining to cardiovascular control are concentrated in the most caudal regions of the NTS (Loewy, 1990), for example, aortic baroreceptors send their central processes to make synaptic contacts with second order cells that are contained within the dorsal caudal NTS (Dean and Seagard, 1995). These neurons then may make contact with either third order neurons in the NTS, or may send axons out of the NTS to other brain areas, such as the hypothalamus, RVLM or CVLM (Andresen et al., 2004).

1.4.2. Function

The NTS is pivotal in assimilating and integrating a multitude of viscerosensory processes, including cardiovascular, respiratory, gustatory, hepatic and renal control mechanisms (Lawrence and Jarrott, 1996). It is the first central relay for baroreceptor control (Lawrence and Jarrott, 1996), as afferent baroreceptor fibres from the carotid sinus and aortic arch terminate primarily in the intermediate portion of the NTS (Andresen and Kunze, 1994; Ciriello, 1983) and form excitatory synaptic contacts with second-order neurons (Aicher et al., 1999; Velley et al., 1991). The carotid chemoreceptors (chemoreflex) and the cardiopulmonary afferent C-fibres (Bezold-Jarisch reflex), both of which have involved in the regulation arterial pressure, also have their first synapse in the NTS (Machado et al., 1997). Activation of the baroreflex or Bezold-Jarisch reflex increases parasympathetic drive to the heart and decreases sympathetic drive to the heart and vessels to normalise BP (Machado et al., 1997), whereas activation of the chemoreflex increases both sympathetic and parasympathetic drive which results in an increase in arterial pressure and intensifies the bradycardic response (Haibara et al., 1995; Marshall, 1994). The activation of these cardiovascular afferents release excitatory amino acids within the NTS, which prompts excitation of different postsynaptic neurons that the NTS projects to, including the CVLM and RVLM (Machado et al., 1997).

1.4.3. Nitric oxide in the NTS

Moderately stained small and medium sized nNOS immunoreactive cells are found in low density throughout the NTS at both caudal and rostral levels (Simonian and Herbison, 1996). When NO donors are injected into the NTS, sympathetic responses such as hypotension and bradycardia are elicited, indicating that NO is

involved in the regulation of sympathetic output (Ferrari and Fior-Chadi, 2005). The microdialysis of nitrosothiol, an important component of NO mediated biological events, increases the release of glutamate, which is the most utilised neurotransmitter at barosensitive terminals within the NTS (Lawrence and Jarrott, 1993; 1996). Together, these data indicate that NO is an important modulator of autonomic output within the NTS.

1.5. Caudal ventrolateral medulla

The NTS influences the output of the RVLM by stimulating the bulbospinal vasomotor neurons that mediate tonic and reflex adjustments of sympathetic outflow (Haselton and Guyenet, 1989; Morrison et al., 1988). Although there are studies showing direct connections between the RVLM and NTS (Ross et al., 1985), electrophysiological (Agarwal and Calaresu, 1991; Jeske et al., 1993) and pharmacological (Blessing, 1988; Willette et al., 1984c) experiments show that baroreceptor information is modulated by the CVLM (Aicher et al., 1995; Jeske et al., 1995; McKitrick et al., 1992). Furthermore, anatomical studies indicate that GABAergic neurons in the CVLM receive numerous inputs from NTS areas that receive primary baroreceptor afferent fibers (Dampney, 1994; Hirooka, 2006; McKitrick et al., 1992). Coupled with the evidence showing that this is a vasodepressor area, the CVLM constitutes the necessary inhibitory link in the baroreceptor reflex mediating the control of sympathetic vasomotor outflow.

1.5.1. Location

Located caudal to the RVLM, the CVLM has been defined to the region ventral and overlapping the nucleus ambiguus (NA), mainly dorsal to, but extending ventrally into the medial aspect of the lateral reticular nucleus (Bonham and Jeske,

1989; Gordon and McCann, 1988; Willette et al., 1983). Rostrally, it terminates at the RVLM, though there is evidence for some overlap (Sved et al., 2000). In other species this may differ. For example, in the rabbit, there is the inter ventrolateral medulla, which lies between the RVLM and CVLM (Dampney et al., 2003b). Furthermore, not only is the area spread over a large region, but there is evidence that shows that there are at least 2 distinct populations of cells, the rostral CVLM and caudal CVLM, otherwise known as the caudal pressor area (Sved et al., 2000), the two areas appearing to have distinct functional differences (Pilowsky and Goodchild, 2002).

1.5.2. Function

In 1973, Guertzenstein reported that the application of neuroactive drugs thought to excite neurons on the ventral surface of the most caudal regions of the cat brainstem elicited dramatic decreases in arterial pressure (Guertzenstein, 1973; Sved et al., 2000). When the CVLM is stimulated chemically, such as through microinjection of L-glutamate, there is a significant reduction in sympathetic nerve activity (Blessing and Reis, 1982; 1983; Cravo et al., 1991) and vasodilation of vessels in the renal mesenteric and hind limb vascular beds vasodilate (Willette et al., 1987) resulting in a decrease in BP. This result is consistent in a number of species, such as the cat, rabbit and rat (Blessing and Reis, 1982; Gatti et al., 1986; Willette et al., 1983). Conversely, lesions to the CVLM neurons result in an increase in BP (Willette et al., 1984b), associated with significant increases in sympathetic nerve activity (Blessing and Reis, 1982). Indeed, this acute hypertension can be of such impact that is leads to ventricular failure and pulmonary oedema (Blessing et al., 1982; Cravo et al., 1991; Willette et al., 1987). Stimulation of CVLM neurons appears to also decrease HR, independent of the actions of nearby pre-cardiac neurons

in the nucleus ambiguus (McKitrick and Calaresu, 1997). As part of the baroreflex pathway therefore, the CVLM receives prominent projections from the region of the NTS and then projects to RVLM bulbospinal neurons that project to the SPNs (Aicher et al., 1995; Jeske et al., 1995), and functions to provide the necessary inhibitory inputs needed to regulate the baroreceptor reflex.

There are however some discrepancies associated with lesion studies of the CVLM. While the majority of studies show that lesioning the CVLM results in an increase in BP (Sved et al., 2000), some studies show that despite the increase in BP after lesioning, the baroreceptor reflex remains intact (Granata et al., 1985; Imaizumi et al., 1985). Studies by Cravo and colleagues (Cravo et al., 1991) found that the site of chemical lesioning affected the outcome, in that injections into the rostral portion of the CVLM destroyed the baroreceptor response, but injections into the caudal region, though increasing BP, did not affect the baroreceptor response. Furthermore, local injections of glutamate into the caudal pressor area do not appear to decrease MAP, and in fact increase BP (Seyedabadi et al., 2006), providing support that the rostral and caudal regions of the CVLM appear to have distinct functions (Sved et al., 2000).

1.5.3. Nitric oxide in CVLM

Neurons positively labeled for nNOS can be found scattered throughout the CVLM (Simonian and Herbison, 1996), of which, 8% of these neurons project to the CVLM (Kantzides and Badoer, 2005). The majority of nNOS positive, RVLM projecting neurons are located at the caudal end of the CVLM (Kantzides and Badoer, 2005). Microinjections studies have shown that NO influences the blood pressure responses elicited from the CVLM, as microinjections of L-arginine ($_{L}$-Arg) a NO promoter produces a hypertensive effect, where as N(G)-nitro-L-arginine methyl ester

L-NAME, an nNOS inhibitor produces a significant hypotensive effect (Lage et al., 1999).

1.6. Rostral ventrolateral medulla

The CVLM sends GABAergic (inhibitory) monosynaptic projections to the RVLM. The importance of the RVLM as a critical region in the maintenance of BP was discovered over a century ago (Owsjannikow, 1871, cited in Madden, 2003 #193), though this discovery was largely ignored till over a century later, when Guertzenstein and Feldberg examined the effects of drug application to the ventral surface of the brain stem on BP (Feldberg and Guertzenstein, 1972; 1976; Guertzenstein, 1973; Guertzenstein and Silver, 1974). This region was further refined to the area ventral of the retrofacial nucleus, at the level of the rostral portion of the inferior olive, where it was found that microinjection of glutamate (Goodchild and Dampney, 1985) or other neuroexcitatory amino acids (Dampney et al., 1987) caused a significant increase in BP, and that bilateral destruction led to a profound fall in BP (Dampney et al., 1987).

The RVLM is the final site within the brainstem that integrates the various influences on BP from higher centres such as the paraventricular hypothalamus, lateral hypothalamus, midbrain periaqueductal gray (Dampney, 1994), and it has been shown that inhibition of this region causes BP to drop by as much as the total removal of supraspinal influences (Madden and Sved, 2003). Given that this region is so influential on BP, it is of high significance.

1.6.1. Location

The RVLM is located in the ventral portion of the brainstem, beginning immediately caudal to the facial nucleus, lateral to the inferior olives, and ventral to

the nucleus ambiguus (Phillips et al., 2001), This relatively small area is anatomically heterogeneous, containing many cell groups such as nucleus reticularis rostroventrolateralis, gigantocellular nucleus paragigantocellularis lateralis and the external and semi compact formations of the nucleus ambiguus (Andrezik et al., 1981; Guyenet, 1990; Newman, 1985; Ruggiero et al., 1989). One of the most common ways to differentiate this heterogenous population of cells is by the identification of the neurochemical phenotype of neurons with the region.

1.6.2. Receptors and transmitters

The RVLM neuronal cell population can be divided into two main categories, the C1 neurons and non-C1 neurons. The C1 neurons are adrenergic neurons, identified on the basis of their expression of phenylethanolamine-n-methyltransferase (PNMT) (Hokfelt et al., 1984b; Jeske and McKenna, 1992; Ross et al., 1981; Ross et al., 1984a), which is the enzyme that is responsible for converting noradrenaline to adrenaline (Brownstein and Palkovits, 1984). The remainder of the baroreceptor neurons are broadly categorised as the non-C1 population.

Throughout the brainstem, the catecholamine groups, first described by Dahlstroem and Fuxe (Dahlstroem and Fuxe, 1964) are grouped into the A1 – A12 groups (noradrenergic), and the C1 – C3 (adrenergic) and can be collectively visualised with tyrosine hydroxylase (TH), the enzyme that converts tyrosine into dopa (Hokfelt et al., 1984a). Within the ventrolateral medulla, PNMT positive neurons extend from the caudal pole of the facial nucleus to the level of the calamus scriptorius (Ruggiero et al., 1985). The traditionally defined C1 cell group can be subdivided into two distinct divisions (1) a cell column originating in the CVLM and extending rostrally and ventrally towards the ventral surface of the RVLM and (2) a

cell cluster developing rostral and medial to the column and expanding close to the surface of the RVLM (Ruggiero et al., 1985).

The noradrenergic neurons are confined mainly to two groups: the A1 cell groups, in the ventromedial medulla oblongata, and the A2 group, located in the dorsal vagal complex (Hokfelt et al., 1984b). Both cell groups start caudally in the upper cervical spinal cord (Hokfelt et al., 1984b). The main group of A1 cell bodies are located in the ventrolateral medulla oblongata, at caudal levels ventrolateral to the most rostral part of the ventral horn cells. At the rostral end, they are primarily located dorsolateral to the lateral reticular nucleus, with only a few cells in this nucleus. The A2 group extends rostrally to the area postrema, where they intermingle somewhat, with the most caudal cells of the magnocellular C2 group (Hokfelt et al., 1984b). A third group of neurons, the A5 cell group has also been implicated in cardiovascular control (Hokfelt et al., 1984a). The A5 noradrenaline group form a continuous column, starting at the level of the ventrolateral pons medial to the trigeminal and facial nerves and extending in a caudal direction approximately to the level where the C1 neurons begin, and slightly overlap them (Hokfelt et al., 1984c).

C1 cells

The C1 group is composed of rostral and caudal subdivisions. The rostral C1 region contains barosensitive neurons with axons that project to the spinal cord (Kanjhan et al., 1995; Lipski et al., 1995; Schreihofer and Guyenet, 1997), providing tonic, excitatory drive to SPNs (Sun, 1995; Guyenet et al., 1996), while caudal C1 neurons project to the hypothalamus and forebrain regions (Stornetta et al., 1999; Tucker et al., 1987; Verberne et al., 1999).

In addition to their adrenergic phenotype, many C1 cells express other peptides as well such as enkephalin and neuropeptide Y, whose roles in regards to

cardiovascular control has yet to be defined (Pilowsky and Goodchild, 2002). While C1 neurons show the ability to produce catecholamines, specifically adrenaline, their use of adrenaline needs to be questioned, as high performance liquid chromatography was unable to reveal the presence of adrenaline in the IML of the spinal cord, where PNMT containing bulbospinal neurons terminate (Sved, 1989). Furthermore, some species, such as the rabbit, guinea pig and sheep do not express PNMT, indicating that perhaps adrenaline is not contributing to sympathetic output in the RVLM (McLachlan et al., 1989; Tillet, 1988). Also, it has been shown that some of the most rostral C1 neurons do not express aromatic L-amino acid decarboxylase, which converts dopa to dopamine, also critical in adrenaline synthesis (Phillips et al., 2001), which implies that a percentage of C1 neurons may not synthesise catecholamines (Phillips et al., 2001).

C1 and non C1 receptors and transmitters

There have been many studies into the receptors and transmitters present within the RVLM including adrenergic receptors and transmitters, neuropeptides such as angiotensin II, amino acids such as GABA, and opioid signalling mechanisms (Dampney et al., 2003a; Guyenet et al., 2002).

Immunohistochemically, it has been shown that bulbospinal neurons express alpha-2 receptors, and this has been substantiated functionally as a significant population of barosensitive neurons as they are inhibited by clonidine (Allen and Guyenet, 1993), a powerful agonist for the alpha-2 adrenoreceptor. Reja et al. have shown that the level of alpha-2 adrenoreceptor cDNA is significantly less in SHRs compared to WKY controls (Reja et al., 2002b), and it has also been shown that alpha-2 adrenoreceptor knock-out mice express elevated levels of catecholamines, HR and BP (Gavras and Gavras, 2001).

Within the RVLM, both angiotensin II (Ang II) and Ang II receptors have been demonstrated in a number of species (Allen et al., 1988a; Allen et al., 1987; Allen et al., 1988b; Lind et al., 1985; Mendelsohn et al., 1988), and microinjection of Ang II into the RVLM causes an increase in sympathetic nerve activity and arterial pressure, which can be blocked by Ang II antagonists (Muratani et al., 1991). Overall, the renin-angiotensin system has been shown to play an important role in the development of hypertension, as blockade of this system results in resetting of the baroreflex function, and improves the sensitivity for control of heart rate and sympathetic nerve activity (Averill and Diz, 2000).

During resting conditions, bulbospinal neurons in the RVLM are strongly inhibited by GABA (Schreihofer and Guyenet, 2002). Iontophoretic experiments reveal that application of the $GABA_A$ receptor antagonist bicuculline increases the firing rate of bulbospinal neurons (Sun and Guyenet, 1985), and microinjection of bicuculline causes an increase in sympathetic nerve activity and BP (Kubo and Kihara, 1987; Willette et al., 1984a). This indicates that GABA is involved in tonically inhibiting the activity of RVLM neurons, which ultimately lowers sympathetic nerve activity and BP (Schreihofer and Guyenet, 2002).

A small subset of RVLM neurons also express preproenkephalin (PPE) mRNA, (Guyenet et al., 2002), and in situ hybridisation studies, coupled with retrograde labelling indicates that most of these neurons project to the SPNs (Guyenet et al., 2002). Hypotension induced by hydralazine (a vasodilator) causes the PPE neurons to express *c-fos* suggesting opioids are utilised during hypotension (Guyenet et al., 2002).

*1.6.3. **Projections***

The RVLM is critical as a cardiovascular control centre where inputs from higher centres are modified. The RVLM has also been identified as an area that heavily innervates the spinal cord region containing SPNs and which, when stimulated either electrically or chemically, caused a marked increase in blood pressure (Ross et al., 1983; 1984a; Ross et al., 1984b).

Projections to the RVLM

There are a number of centres that project to the RVLM that are involved in BP control. These include the central nucleus of the amygdala, important in the control of BP during or in response to stressful or fearful stimuli (Saha, 2005), the NTS and CVLM (Colombari et al., 2001), covered in previous sections, the paratrigeminal nucleus, which has been implicated in BP control as it causes a pressure response when stimulated by bradykinin (de Sousa Buck et al., 2001) and of specific relevance to this project, from the PVN (Badoer, 2001).

The PVN, which is later discussed in detail further on (section 1.8), is a major integrative site for autonomic function (Badoer, 2001). It has 2 distinct cell populations, of which the parvocellular neurons project to the RVLM. It has been shown that electrical or chemical stimulation of the PVN leads to a pressor response and the activation of *c-fos* in the RVLM, suggesting that the stimulation of PVN neurons leads to the activation of RVLM neurons (Krukoff et al., 1994). Furthermore, the pressor response from electrical stimulation of the PVN can be inhibited by microinjection into the RVLM of choline inhibitors, indicating that it is working through the RVLM via a cholinergic pathway (Kubo et al., 2000). Also, during experimental haemorrhage it has been shown that a specific population of

RVLM projecting PVN neurons are activated, however these cells are not activated by the administration of hypotension inducing drugs, indicating that RVLM projecting PVN neurons are important in detecting specific functional responses, in this case, changes in blood volume (Badoer, 1998).

Projections from the RVLM

C1 cells

The majority of C1 neurons project to the spinal cord, where they provide a dense plexus of terminals in the thoracic IML (Kantzides and Badoer, 2005; Madden and Sved, 2003; Ross et al., 1984a) and synapse on SPNs (Milner et al., 1988). Along the length of the RVLM, more rostral C1 cells project to the spinal cord than caudal C1 cells (Kanjhan et al., 1995; Lipski et al., 1995; Phillips et al., 2001; Schreihofer and Guyenet, 1997) which have an increased proportion of neurons that project to the hypothalamus and forebrain areas (Stornetta et al., 1999; Tucker et al., 1987; Verberne et al., 1999). Terminal projections from C1 neurons have been identified in the dorsal motor vagal complex, A1 area, raphe pallidus and obscurus of the caudal RVLM, and also within the locus coeruleus and nucleus subcoeruleus of the rostral RVLM (Card et al., 2006). In the midbrain, projections from the RVLM can be found in the periaquaductal gray, while forebrain projections from C1 neurons project predominantly to the hypothalamus (Card et al., 2006).

Non-C1 cells

Only a subset of neurons that project to the SPNs contain PNMT- i.e. only 50 – 70% of spinally projecting RVLM neurons are actually C1 cells, - the rest are non C1 cells (Madden and Sved, 2003). Non-C1 neurons from the mid RVLM region project to the medullary respiratory neurons, and innervate phrenic motor neurons

(Dobbins and Feldman, 1994; Ellenberger and Feldman, 1990; Ellenberger et al., 1992), as well as to various regions in the brainstem, midbrain and diencephalon (Card et al., 2006). Like C1 cells, there are also a percentage of non-C1 cells that have reciprocal projection to the spinal cord (Burman et al., 2004; Stornetta et al., 2001) and hypothalamus (Verberne et al., 1999), showing that these cells are capable of influencing autonomic output. Many of the non-C1 cells are highly active at rest and are barosensitive (Guyenet et al., 2001). They have lightly myelinated axons and could be a source of supraspinal glutamatergic drive from the RVLM to vasomotor SPNs. It has not been identified as yet whether non-C1 cells release glutamate (Madden et al., 1999).

1.6.4. Function

As described, the RVLM is an essential brain region involved in the tonic generation of sympathetic nerve activity (Sun et al., 1988), and the integration of a number of autonomic and somatic functions, including the control of BP and respiration. Activation of specific RVLM neurons has been shown to increase arterial pressure, by increasing peripheral resistance, the secretion of catecholamines and cardiac output (Campos Junior and Guertzenstein, 1989; Feldberg and Guertzenstein, 1972). Bulbospinal neurons in the RVLM respond to a variety of visceral, somatic and supramedullary inputs (Guyenet et al., 1996). Stimulation of this region via electrical or chemical stimulation elicits marked increases in BP and sympathetic nerve activity (Ross et al., 1983; 1984a; Ross et al., 1984b) whilst destruction of the RVLM region as a whole results in a reduction in sympathetic nerve discharge (Kantzides and Badoer, 2005).

Indeed, inhibition of the RVLM causes BP to decrease by as much as is seen with total removal of supraspinal influences, for example with cervical spinal cord

transection (Madden and Sved, 2003). The region is also essential for many neurally mediated cardiovascular reflexes, including those stimulated by aortic and carotid baroreceptors, carotid chemoreceptors, muscle afferents, and cardiopulmonary receptors (Granata et al., 1985; Guyenet, 1990; Kiely and Gordon, 1993; Koshiya et al., 1993; Stornetta et al., 1989; Verberne and Guyenet, 1992).

In addition to cardiovascular control, subpopulations of neurons in the RVLM are involved in nociception and are activated by peripheral noxious stimuli, with stimulation of the medial RVLM able to alter nociceptive transmission (Babic and Ciriello, 2004). Neurons in the medial RVLM are also involved in the regulation of breathing (Dobbins and Feldman, 1994; Ellenberger and Feldman, 1990; Ellenberger et al., 1992).

Functional subpopulations C1 cells vs. non-C1 cells

C1 cells are tonically active and powerfully inhibited by elevations of BP (Ross et al., 1984a). As the majority of rostral C1 cells project to the SPNs in the spinal cord, it would suggest that they are critical for the maintenance of tonic sympathetic outflow (Madden and Sved, 2003). However, destruction of C1 neurons reduces the pressor response elicited by glutamate stimulation by only 40% (Madden and Sved, 2003) and while it reduces reflex sympathoexcitation in response to decreased BP it does not abolish it (Madden and Sved, 2003). This suggests that the C1 neurons are involved in the sympathoexcitation evoked from the RVLM, although not essential for the process. It is possible that because unilateral lesions have only destroyed a percentage of C1 cells, remaining C1 neurons are sufficient to attenuate the responses described. However, experiments involving bilateral lesioning of the C1 neurons, as well as experiments where spinally projecting C1 neurons are destroyed have yielded similar results; C1 neurons are not essential for RVLM-

mediated maintenance of resting sympathetic vasomotor tone (Madden and Sved, 2003), but do contribute to baroreceptor-evoked sympathoexcitation and other sympathoexcitatory reflexes (Madden and Sved, 2003).

However, C1 cells are not the only cells involved in the regulation of BP. Electrophysiological studies using indirect criteria, such as juxtacellular labelling to distinguish between putative C1 neurons and non-C1 neurons, show that both C1 and non C1 cells respond to changes in arterial pressure (Haselton and Guyenet, 1989; Schreihofer and Guyenet, 1997). Furthermore, studies using hypotension-evoked Fos expression as a means of identifying barosensitive neurons conclusively demonstrated that spinally projecting C1 neurons and non-C1 neurons in the RVLM were both responsive to decreases in BP (Chan and Sawchenko, 1994; Sved et al., 1994).

1.6.5. Changes in the RVLM during hypertension

The RVLM has been studied in a number of different hypertensive models, showing major changes between the normotensive and hypertensive state. An enhanced pressor response to microinjections of glutamate into the RVLM has been demonstrated in rats with Goldblatt 2 Kidney 1 Clip (2K1C) hypertension (induced by partial obstruction of one renal artery) (Bergamaschi et al., 1995). Further, 2K1C rats respond to blockade of RVLM glutamatergic synapses with a decrease in blood pressure, while normotensive rats do not, indicating a change of sensitivity of the glutamate receptors in the RVLM of this model (Colombari et al., 2001). In the SHR, electrical stimulation of the RVLM produces greater pressor responses than in control WKY (Lin et al., 1995) and it has also been demonstrated that SHR rats have approximately 2.5 times more TH mRNA expression in the C1 and A1 regions of the RVLM, compared to their normotensive controls (Reja et al., 2002a). These data

indicate both functional and neurochemical alterations in the RVLM in the hypertensive state.

1.6.6. Nitric Oxide in the RVLM

Location

The expression of NO in the RVLM has been examined through its synthesising enzyme NOS in a number of immunohistochemical and cytochemical studies. Neuronal NOS positive neurons can been found scattered throughout the gigantocellular reticular and lateral paragigantocellular nucleus (Nazu and Thippeswamy, 2002), with their dendrites producing a lattice-like appearance in the region (Simonian and Herbison, 1996). More clustered groups of nNOS neurons can be seen in the medial, lateral and ventrolateral portions of the RVLM (Nazu and Thippeswamy, 2002). Interesting, NOS expressing neurons appear to be distinct from other neurochemically defined cell populations within the RVLM, and do not appear to co-localise with any of the known classical transmitter systems (Nazu and Thippeswamy, 2002). Studies have shown that although NOS and TH/PNMT immunoreactive neurons are widely distributed in the RVLM, the two do not coexist in any neurons. Furthermore, only a small number of cells retrogradely labeled from the spinal cord showed co-localisation with NOS producing cells (Nazu and Thippeswamy, 2002). This suggests that the RVLM contains a well-defined group of neurons that express NO that are distinct from the adrenergic C1 group and have only limited monosynaptic projections to the spinal cord (Iadecola et al., 1993; Ohta et al., 1993).

Function

There is significant evidence showing that NO can influence the output of the RVLM (Chan et al., 2003a; Chan et al., 2001a), although, the actual response is controversial. It has been shown that microinjections of sodium nitroprusside, a NO donor and $_{L}$ -Arg, into the RVLM of cats reduced arterial pressure and sympathetic nerve activity, while microinjection of N^{G-} methyl-$_{L}$-Arg, a non selective NOS inhibitor, increased them (Shapoval et al., 1991). Hirooka et al. (Hirooka et al., 1996) however, reported conflicting results showing that in rabbits a decrease in BP and sympathetic nerve activity in response to NO donors. This may be species related, but in the rat, both pressor (Martins-Pinge et al., 1997) and depressor (Kagiyama et al., 1997) responses have been reported in response to NO donors. Regardless, NO does effect the RVLM, and its control over BP and one of the aims of this thesis is to further define the significance of NO production in the region.

With regards to NO signalling in the RVLM, there is strong functional evidence to show cGMP dependent and independent mechanism of action (Chan et al., 2003b), however, expression of cGMP or changes in cGMP levels in this region, has not been documented and is one of the goals of this thesis.

1.7. Sympathetic preganglionic neurons

Sympathetic preganglionic neurons are the last point in the central nervous system where autonomic output can be modulated (Minson et al., 1997). Sympathetic preganglionic neurons are located within the spinal cord, predominantly between cervical segments C8 and lumbar segment L2, and project to sympathetic postganglionic neurons, whose axons in turn innervate autonomic targets including

vascular smooth muscle, penile tissue and the heart (Anderson, 1998; Giuliano and Rampin, 2004; Janig and McLachlan, 1987).

1.7.1. Topographic organisation

The SPNs are topographically organised into four distinct nuclei, the nucleus intermediolateral lateral cell column (IML), the nucleus intermediolateralis thoraco-lumbalis pars funicularis, the nucleus intercalatus spinalis and the nucleus intercalatus pars paraependymalis (Petras and Cummings, 1972). Approximately 85% of SPNs can be found within the IML, which occupies the lateral dorsal horn of the spinal grey matter (Lee et al., 1996). The SPNs are arranged in a ladder like pattern, with "*the uprights formed by neurons of the IML and central CA area, and their rostrocaudal oriented dendrites. The rungs of the ladder are primarily formed by the mediolaterally-oriented dendrites of the SPNs*" (Ezerman and Forehand, 1996) which are clustered approximately 200 microns apart.

1.7.2. Receptors, transmitters, and function

As the major excitatory input to post ganglionic neurons supplying a variety of target organs, SPNs play host to a large number of receptors, and have a large source of neurotransmitters, with multiple functional outcomes. This next section will cover 3 of the main categories of neurotransmitter synaptic input to the SPNs, the monoamines, amino acids and other neurotransmitters including peptides, and discuss their sources and functional significance.

Monoamines

Anatomical studies indicate that the IML receives a dense noradrenergic innervation (Dahlstrom and Fuxe, 1965), with many noradrenergic terminals localised

in clusters around SPN cell bodies (McCall, 1988). Furthermore, autoradiograph studies indicate there are high concentrations of alpha2-adrenergic receptors within SPNs (McCall, 1988). The main source of adrenergic input appears to come from the A5 cell group, which is rostral of the RVLM (Blessing et al., 1981; Dahlstrom and Fuxe, 1965) both of which have direct connections to SPNs in the IML. Microiontophoretic studies indicate that these inputs inhibit the activity of SPNs, as stimulation of the A5 area inhibits the firing rates of SPNs (Coote et al., 1981; De Groat and Ryall, 1967),

Interestingly, microiontophoretic administration of adrenaline has been shown to inhibit the activity of SPN (McCall, 1988), as does the application of alpha 1-AR agonists (Aghajanian and Rogowski, 1983). This is in conflict to the purportedly excitatory role of the C1- bulbospinal adrenergic cell group, and indicates that in regards to monoamines, SPN are a complex population of neurons and that other co-transmitter inputs may assume greater functional significance.

Amino acids

Amino acid neurotransmitters are crucial in the control of most central neurons, including SPNs (Llewellyn-Smith, 2002). Sympathetic preganglionic neurons are densely innervated by axon terminals containing glutamate immunoreactivity (Llewellyn-Smith et al., 1998; Llewellyn-Smith et al., 1992). This innervation arises from supraspinal sources, such as the RVLM (Morrison, 2003), as well as from intraspinal sources, as glutamate immunoreactive input to SPN remains after complete spinal cord transection (Llewellyn-Smith et al., 1997a; Llewellyn-Smith et al., 2007). Sympathetic preganglionic neurons respond to glutamate with fast excitatory post-synaptic potentials mediated by NMDA and/or non-NMDA receptors (Deuchars et al., 1995; Inokuchi et al., 1992b; Sah and McLachlan, 1995),

while glutamate antagonists profoundly affect SPNs autonomic responses (Llewellyn-Smith et al., 2007). For example, intrathecal administration of kynurenate, a broad-spectrum antagonist for glutamate receptors, reduces BP and HR (Verberne et al., 1990), and direct application of kynurenate, using iontophoretic or pneumatic pressure injection, decreases the activity of SPNs (Morrison, 2003).

Studies have also shown that there is a dense network of GABA-like immunoreactive processes that surrounds the soma and dendrites of SPNs (Llewellyn-Smith, 2002; McCall, 1988). These GABAergic inputs come from supraspinal sites, such as the ventral medulla, (Llewellyn-Smith, 2002), as well as from intraspinal sources (Llewellyn-Smith, 2002), and cause fast inhibitory post synaptic potentials (Backman and Henry, 1983; Inokuchi et al., 1992a; Yoshimura and Nishi, 1982).

Alternative transmitters

There are a wide variety of other neurotransmitters concentrated in SPNs, including acetylcholine, which is found in all SPN including those which innervate the chromaffin cells and ganglionic cells of the adrenal medulla (Murphy et al., 2003) and enkephalin, which is found specifically in those SPN that innervate adrenergic chromaffin cells (Pelto-Huikko et al., 1985) and function to regulate the release of catecholamines into the circulation (Llewellyn-Smith, 2002; Llewellyn-Smith et al., 2007). Furthermore, there is a subset of SPN innervating the adrenal medulla that express phosphorylated extracellular signal–regulated kinase (Springell et al., 2005). The secretion of adrenaline and noradrenaline from adrenal medullary chromaffin cells is an important contributor to the homeostatic responses to a variety of challenges including cold exposure, haemorrhage, myocardial ischemia, shock and hypoglycaemia (Brown and Fisher, 1984; Maddens and Sowers, 1987; Vollmer, 1996; Vollmer et al., 1997; Yamaguchi, 1992; Young et al., 1984).

A subpopulation of SPNs express neuropeptide Y (Gibbins, 1992). They can be further divided into neurons that synapse directly onto vasodilator neurons, which express substance P, or that synapse directly on vasoconstrictor neurons, which express calcitonin gene-related peptide (CGRP) (Gibbins, 1992). Intrathecal administration of substance P, or its analogues increases the firing rate of SPNs, and subsequently increases BP (McCall, 1988), while intrathecal administration of substance P antagonists drops BP to spinally transected animal levels.

There is a vast amount of evidence showing that there are monosynaptic connections between the PVN and SPNs (Ranson et al., 1998). As discussed in the next section, the PVN expresses oxytocin (OT) and arginine vasopressin (AVP), and SPNs contain receptors for both these transmitters (McCall, 1988). Superfusion of AVP over spinal slices causes SPN to depolarise, while intrathecal administration of AVP increases BP (McCall, 1988). Functionally, it has been shown that neurons from the PVN projecting to the SPNs are activated when there is a decrease in blood volume (Badoer, 2001), indicating that PVN neurons are likely able to influence the autonomic output of the SPNs.

1.7.3. Changes in SPNs during hypertension

Whilst there have been many studies demonstrating the neuroanatomical functional differences in the NTS, CVLM and RVLM between hypertensive models and their genetic normotensive counterparts, there has been very little information regarding changes at the level of the SPN in association with hypertension. Minson et al has shown that SHRs have increased c-Fos expression compared to its normotensive control, the Wistar Kyoto (Minson et al., 1996). Furthermore, Tang et al have demonstrated a decreased proportion of NOS containing SPN from the intermediolateralis pars funicularis that project to the superior cervical ganglion (Tang

et al., 1995a). One of the goals of this thesis is to extend this knowledge, by examining the nNOS expression in SPN of the IML within the thoracic spinal cord.

1.7.4. Nitric Oxide in the SPNs

Within the IML, NOS containing SPNs have been identified as an anatomically distinct population of cells, and in the Sprague-Dawley rat, up to 70% of the SPNs in the IML (between T2 and T13) contain nNOS (Anderson, 1992). Functional responses to NO driven by SPN are controversial, with both pressor or depressor responses documented (del Carmen Garcia et al., 1997; Koga et al., 1999; Lee et al., 1996).

Intrathecal administration of endogenous NOS attenuates pressor responses induced by NMDA (Arnolda, 2002) suggesting a role for NO as a modulator of descending excitatory cardiovascular signals. Evidence for spinal NO as a functional regulator of BP is evidenced by its role in mediating hypotensive reactions to haemorrhage. In a study by Lu et al. (Lu et al., 1999) intrathecal administration of NOS inhibitors significantly attenuated the precipitous decrease in BP seen with severe haemorrhage.

1.8. Paraventricular hypothalamus

In addition to the reflex BP control pathways modulated by the brainstem and spinal cord regions, superimposed upon this is input from higher regions that serve to maintain homeostasis in response to both acute and chronic stressors. One of these regions involved in control vascular sympathetic responses is the PVN (Stern et al., 2003).

*1.8.1. **Location***

The PVN is located within the hypothalamus and is a complex, heterogenous region containing both large magnocellular neurons and small parvocellular neurons (Shafton et al., 1998), which are associated with neuroendocrine and autonomic outflow respectively. The neurons of the PVN can be divided in a variety of ways, including on the basis of cytoarchitecture, cellular characteristics, (i.e. magnocellular and parvocellular) (Swanson and Kuypers, 1980), or chemically coded neurotransmitter subpopulation (Swanson and Sawchenko, 1983), or by projection target (Swanson and Sawchenko, 1983). The regions of the PVN involved in BP control are located either side along the entire length of the third ventricle of the hypothalamus over a distance of ~4.25mm in the rat (de Wardener, 2001). In addition to the PVN, other hypothalamic regions involved in BP control in this region are the medial preoptic nucleus, which arches upward and posteriorly over the ventricle (Lind, 1988), and the supraoptic nucleus (Sawchenko and Swanson, 1982).

Subpopulations

Magnocellular neurons

The magnocellular subdivisions of the PVN contain large cells that synthesise AVP (otherwise known as antidiuretic hormone, ADH) or OT (Benarroch, 2005). These cells give rise to the hypothalamus-neurohypophyseal system and project to the posterior pituitary where they release AVP or OT into the blood stream (Engelmann et al., 2004; Renaud and Bourque, 1991). The majority of magnocellular neurons lie in the magnocellular balls within the lateral and medial magnocellular region of the PVN (Paxinos and Watson, 1998), with the oxytocinergic cells lying in a ring around the vasopressinergic neuron mass.

Parvocellular neurons

The smaller neurons of the PVN make up the parvocellular neuronal population. The medial parvocellular subdivision of the PVN synthesises corticotropic releasing hormone (CRH) and somatostatin and cells from this region project to the neurohemal zone of the median eminence, where they regulate secretion from the anterior pituitary (Sawchenko et al., 1996). Neurons of the anterior, ventral and posterior parvocellular subdivisions of the rat PVN project to autonomic nuclei of the brain stem and spinal cord. These autonomic PVN neurons may be immunoreactive to contain AVP, OT, CRH, TH, angiotensin, somatostatin, enkephalin or neurotensin in different combinations (Hallbeck et al., 2001; Jansen et al., 1995).

1.8.2. Receptors and transmitters

Synaptic control of the PVN is extremely complex. Excitatory inputs, which are mediated by glutamate (Herman et al., 2004) act on the PVN via both AMPA and NMDA receptors (Benarroch, 2005; Herman et al., 2004).

The PVN also receives inhibitory inputs that are mediated by GABA (Herman et al., 2004) primarily by $GABA_A$ receptors, although presynaptic $GABA_B$ receptors may also regulate both glutamatergic and GABAergic neurotransmission in the PVN (Benarroch, 2005). GABAergic inhibition of the PVN comes from several different sources; GABA provides the tonic inhibitory effect of baroreceptors and atrial receptors over magnocellular AVP secretion (Benarroch, 2005; Yang and Coote, 2003). Furthermore, GABAergic inputs from the nucleus of the stria terminals and dorsomedial nucleus of the hypothalamus relay inhibitory limbic influences on CRH PVN neurons in response to external stressors (Herman et al., 2004).

The catecholaminergic A1/C1 groups are critical for activation of the PVN in response to stressors such as hypoxia, hypovolemia, or cytokines (Sawchenko et al., 2000). Noradrenaline, acting via postsynaptic α1 receptors, activates magnocellular AVP neurons (Boudaba et al., 2003), parvocellular CRH neurons (Chen et al., 2004b) and sympathoexcitatory neurons in the PVN. Activation of presynaptic α2 receptors reduces release of GABA from inhibitory synapses on sympathoexcitatory PVN neurons (Li et al., 2005). Activation of NMDA receptors leads to an increase in intracellular Ca^{2+} and NO production in the PVN (Herman et al., 2003). Other excitatory neurotransmitter inputs to PVN to the RVLM may be mediated by glutamate, AVP (acting via V1 receptors), or AngII (via AT1 receptors) (Dampney et al., 2003a).

1.8.3. Projections

Two major areas that project to the PVN are the subfornical organ (SFO), and organum vascularis lamina terminalis (OVLT) (Bains and Ferguson, 1995). These circumventricular organs contain neurons with secreting granules and vacuoles and fenestrated capillaries, an arrangement which allows the neurons to monitor levels of substances unable to penetrate the blood brain barrier (de Wardener, 2001), thereby providing a route of communication from the periphery to the central autonomic control regions such as the PVN.

The PVN has reciprocal connections to various centres of the brain including the supraoptic nucleus, NTS, RVLM and spinal cord (Luiten et al., 1985; Swanson and Kuypers, 1980; Swanson and Sawchenko, 1983; Zhang et al., 1997), which have been demonstrated using various techniques including classical electrophysiology experiments and neuroanatomical studies with tracer (Magoun, 1940). For example,

using anterograde tracing, it was shown that projections to the autonomic centres in the spinal cord came from the dorsal portion of the hypothalamus (Kuypers and Maisky, 1975). This was further refined in 1976, with retrograde tracing methods, revealing that the majority of the hypothalamic innervation of SPNs comes from within the PVN (Saper et al., 1976). Experiments using electrical stimulation of the various cholinergic and adrenergic groups (A1) of the medulla, combined with electrophysiological identified PVN neurons, confirmed reciprocal connections between the PVN neurons and RVLM neurons (Saphier, 1993).

Projections from the PVN can be broken down into two main domains. The first is the posterior pituitary gland, which is involved in endocrine homeostasis within the body (Swanson and Kuypers, 1980), the second is to key CNS regions are involved in autonomic control, such as the cardiovascular centres in the medulla (RVLM and NTS) as well as SPN within the IML (Hardy, 2001; Li et al., 2003a; Pyner and Coote, 1999; Ranson et al., 1998; Swanson and Kuypers, 1980). The PVN-IML pathway is especially important in regulation of the haemodynamic responses to stress and osmolarity changes in the blood (Coote, 1995).

1.8.4. Function

Integrative function

The PVN is involved in integrating inputs from interoceptors, humoral centres and limbic centres (Sawchenko et al., 2000). Interoceptive inputs have both direct and indirect pathways into the PVN. These inputs arise from the visceral receptors, nociceptors and thermoreceptors and reach all subdivisions of the PVN (Sawchenko et al., 2000). Humoral signals such as steroid levels, glucose levels, and blood osmolality reach the PVN by different mechanisms, having effects on the

circumventricular organs, which then relay this information to the PVN (Benarroch, 2005). Limbic inputs from the orbitomedial prefrontal cortex and amygdala, related to emotional responses to external stressors, are relayed primarily via the bed nucleus of the hypothalamus (Sawchenko et al., 2000).

The PVN also receives abundant intrahypothalamic projections. These include inputs from the dorsomedial nucleus in response to stress, the suprachiasmatic nucleus, which is critical for circadian control of autonomic and endocrine function, and from the arcuate nucleus and perifornical area, which are involved in control of food intake and energy metabolism (Ferguson and Samson, 2003).

Finally, the PVN plays an important role in the integration of autonomic and endocrine homeostatic responses (Swanson and Sawchenko, 1980). Through reciprocal interconnections with autonomic centres in the brain, the PVN integrates and moderates cardiovascular centres (Horn et al., 1994), sexual behaviour (Mani et al., 1994), control of autonomic outflow (Martin and Haywood, 1992) and vasomotor tone and BP (Porter and Brody, 1985; Zhang and Ciriello, 1985a; b).

Autonomic regulation

The PVN has been implicated in several aspects of cardiovascular control, such as sympathoexcitatory responses to stress (Badoer, 2001; Blair et al., 1996; Coote et al., 1998) and renal vasoconstriction (Cham and Badoer, 2008). There have been several neurochemically distinct groups of PVN neurons identified that project, both ipsilaterally and contralaterally, via the hypothalamic decussation (Toth et al., 1999) to autonomic nuclei of the brain stem and spinal cord. The autonomic PVN neurons constitute a heterogeneous population consisting of cells with unique morphological and physiological properties (Stern, 2001). Separate populations of pre-autonomic PVN neurons selectively control functionally distinct subpopulations

of preganglionic sympathetic or parasympathetic neurons (Coote et al., 1998; Portillo et al., 1998). For example, the PVN sends direct projections to cardiac (Coote, 1995; Ranson et al., 1998) and renal (Coote et al., 1998) sympathoexcitatory neurons. Stimulation of the PVN leads to an increase in BP, HR, and renal sympathetic nerve activity (Coote et al., 1998) and while spinally projecting PVN neurons are inhibited by baroreceptor and atrial afferents, they are activated by systemic hypotension (Coote et al., 1998). The PVN elicits sympathoexcitation both via direct projections to SPNs in the IML and via collateral projections to neurons of the RVLM that in turn send excitatory inputs to the IML (Coote et al., 1998; Shafton et al., 1998). Overall, it is apparent that the PVN is critical in both influencing and integrating various inputs that control autonomic outflow.

1.8.5. Changes in PVN during hypertension

The functional cerebral changes that have been detected in the brains of hypertensive animals occur predominantly in the hypothalamus and the medulla (de Wardener, 2001). Furthermore, it has been shown that when the PVN of SHR, Dahl salt sensitive and rats with renal hypertension is lesioned, there are decreases in blood pressure (Ciriello et al., 1984; Goto et al., 1981; Herzig et al., 1991; Takeda et al., 1991), and it has been proposed that hypertension is due to an increase in medullary pressor activity due to suppression from superior medullary inhibitory activity (Chalmers, 1998; Chalmers and Pilowsky, 1991).

A number of differences within the PVN have been identified between hypertensive and normotensive animal models. At the age of 4 weeks, the mRNA levels of AVP within the PVN are 3 fold higher within the SHR, compared to the WKY, while their mRNA expression of OT is 35% lower (van Tol et al., 1988). Also, it has been shown that blockade of glutamate receptors within the PVN

decreases the spontaneous firing activity of spinally PVN neurons within SHR rats, but has no effect in WKY (Li et al., 2008). When examined with radioimmunoassay, Dahl salt sensitive rats show a higher expression of NOS activity, compared to controls (Serino et al., 2001). Together, these data indicate augmented activity within the PVN during hypertension.

1.8.6. Nitric oxide in the PVN

Nitric oxide has a major role in regulating the activity of PVN neurons and has been shown to inhibit both magnocellular AVP producing (Kadekaro, 2004) and sympathoexcitatory PVN neurons (Li et al., 2003a; Qadri et al., 2003).

Location

Neuronal NOS is densely found throughout the PVN (Bredt et al., 1990; Miyagawa et al., 1994; Vincent and Kimura, 1992). It is produced by magnocellular neurons expressing OT but not by vasopressinergic neurons (Miyagawa et al., 1994; Vacher et al., 2003). Nitric oxide produced in the PVN can induce cGMP synthesis in astrocytes, as well as in GABAergic, catecholaminergic, glutamatergic and serotenergic fibres (Vacher et al., 2003). However, only 30% of preautonomic neurons in the PVN express NO under basal conditions – the majority of expression is otherwise found in magnocellular neurons. This indicates that NO may be a bridging molecule between the two subpopulations (Stern et al., 2003), and functionally could be important, as it may be the mechanism through with magnocellular and pre-autonomic cells are communicating (Stern et al., 2003).

Interestingly, despite a number of studies looking at NO in the PVN, very little work has looked a down stream NO signalling and whether similar subpopulations of PVN neurons can be identified. While Vacher et al have looked at cGMP expression

in PVN neurons in the mouse, their findings show that nNOS expression is limited to OT expressing magnocellular neurons (Vacher et al., 2003) where as studies in rats have shown nNOS in expression in both AVP and OT magnocellular neurons (Arevalo et al., 1992; Bredt et al., 1991; Hatakeyama et al., 1996), indicating that down stream signalling may also differ between species. Of particular relevance to this thesis is the expression of cGMP and on of the aims of this thesis is to examine cGMP defined by PVN target innervations in the rat.

Function

Microinjection studies are often utilised to gain information about the effects of various neurotransmitters in the PVN, and the irrespective effects on sympathetic nervous discharge (SND) (Kenney et al., 2003).

Paraventricular hypothalamus neurons appear to be under a strong, NO-mediated tonic inhibitory influence (Stern, 2004). In particular, NO appears to have a strong influence over cells within the PVN that project to the RVLM. When the relatively selective nNOS inhibitor 7-NI is applied to these neurons, the firing activity of RVLM-projecting PVN neurons is increased (Stern et al., 2003). Conversely, the ongoing activity of RVLM projecting neurons is strongly inhibited by NO (Stern, 2004). Perfusion of the PVN with NO containing CSF or microinjection of NO donor, sodium nitroprusside into the PVN elicits a significant reduction in arterial BP (Horn et al., 1994). This supports a role for NO as an important inhibitory molecule controlling the electrical activity of pre-autonomic PVN neurons, and indicates that these neurons are tonically inhibited by an endogenous NO source (Stern et al., 2003). Mechanistically, it has been shown that NO suppresses the firing activity of spinally projecting PVN neurons through the potentiation of GABAergic synaptic inputs (Li et al., 2003a).

As hyperactivity of PVN neurons plays an important part in the maintenance of increased sympathetic vasomotor tone in certain types of hypertension, decreased GABAergic inhibition of presympathetic neurons in PVN may be responsible for the elevated level of sympathetic outflow in hypertension. Nitric oxide may therefore work as a “brake’ preventing excessive excitation of PVN neurons and sustained increases in sympathetic outflow.

1.9. This Thesis

The demonstrated importance of neuronal NO in many of the key sites that participate in central autonomic regulation leads to the prediction that disease states associated with altered autonomic outflow may also exhibit altered central NO mechanisms.

This project was undertaken to further understand NO signalling mechanisms within brain regions known to contribute to the maintenance of autonomic outflow. Specifically, we aimed to characterise the differences in basal NO expression between the SHR and its control strain, the WKY, in regions known to influence sympathetic activity, focussing on the SPNs RVLM, and PVN. Given that previous work shows that the addition or subtraction of NO to these regions affects MAP, we hypothesised that basal expression of NO and cGMP would differ between the two animal strains. To test this theory, we used different combinations of mRNA analysis, histochemistry, immunohistochemistry and retrograde labelling, to assess difference in gene and protein levels between the two strains. In the spinal cord, we went further and examined functional differences through assessment of blood pressure responses to intrathecal administration of cGMP donors.

2. General materials and methods

Materials and methods general to the thesis are described in the following chapter. Specific details pertinent to the individual experimental chapters are provided with the relevant chapter. All animal experimentation was undertaken with full ethics approval from Animal Ethics Committees of the following institutions; Murdoch University, (Murdoch), Western Australia; The University of Western Australia, (Crawley), Western Australia; and University of Cincinnati, (Cincinnati) OH, USA.

2.1. Animals

Animals were obtained from the Animal Resources Centre (WA) or Harlan (Wisconsin, USA). Animals were housed on a 12 hour light-dark cycle with access to standard rat chow and water ad libitum. Environmental enrichment was provided through chewing blocks and peanuts, and animals were group housed where possible. Male rats were used in all experiments (aged 7 weeks through to 12 months, total *n=118*). The strains Wistar, Wistar Kyoto (WKY) and Spontaneously Hypertensive Rat (SHR) were used as detailed in each chapter. The Wistar rat is an outbred strain of albino rat developed at the Wistar Institute (Philadelphia, PA). Spontaneously hypertensive rats were derived from a Wistar colony at Kyoto University, selected on the basis of increased blood pressure (Louis and Howes, 1990; Okamoto and Aoki, 1963). The Wistar Kyoto strain were derived from the same Wistar strain as the SHR, but were selected instead as normotensive genetic controls (Johnson et al., 1992).

2.2. Assessment of blood pressure

2.2.1. Systolic pressure readings via tail cuff recording

Systolic blood pressure was measured in conscious rats with the tail-cuff method (NIBP controller, AD Instruments, Castle Hill, Australia). One to two weeks prior to blood pressure testing, rats were trained for handling, restraint and inflation of the tail cuff. For recordings, rats were placed inside a restrainer with a heat lamp used to ensure an ambient temperature of ~28°C. An inflatable cuff (AD Instruments, Bella Vista, NSW, Australia) and microphone (AD Instruments,) were placed around the rat's tail. The animal was allowed to settle for a period of 2 - 3 minutes. The cuff was inflated to above systolic pressure (>250 mmHg), preventing blood flow into the tail and then slowly deflated. Systolic pressure was recorded as that point when pulsatile measurements of blood flow were first detected (Fig 2.1). The process was recorded with Chart (AD Instruments). A minimum of 4 recordings were made for each rat and the average taken as systolic blood pressure. Average systolic blood pressures for the three strains of rats used in this study were: Wistar: 106.5 ± 8.3, $n = 30$, WKY: 126 ± 9.2, $n = 37$ and SHR: 180 ± 26.4, $n = 31$.

Figure 2.1: Blood pressure trace of a SHR and WKY

Illustration of blood pressure trace recording results. Figure depicts the blood pressure reading from an SHR (A) and WKY (B) respectively. The SHR blood pressure reading is 188.1 (cross), while the WKY is significantly lower, at 126.2 (cross). An average of a minimum of 4 recordings was used to determine each animal's systolic blood pressure.

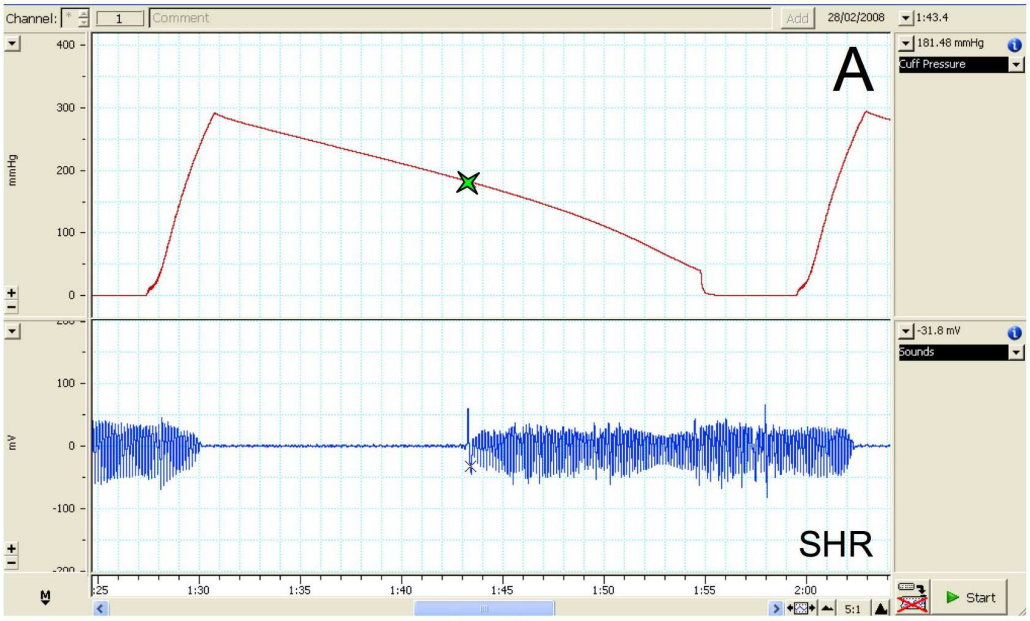
Channel:
1
Comment
Add
28/02/2008
1:43.4
181.48 mmHg
Cuff Pressure
A
mmHg
400
300
200
100
0
-31.8 mV
Sounds
mV
100
0
-100
SHR
1:25
1:30
1:35
1:40
1:45
1:50
1:55
2:00
5:1
Start

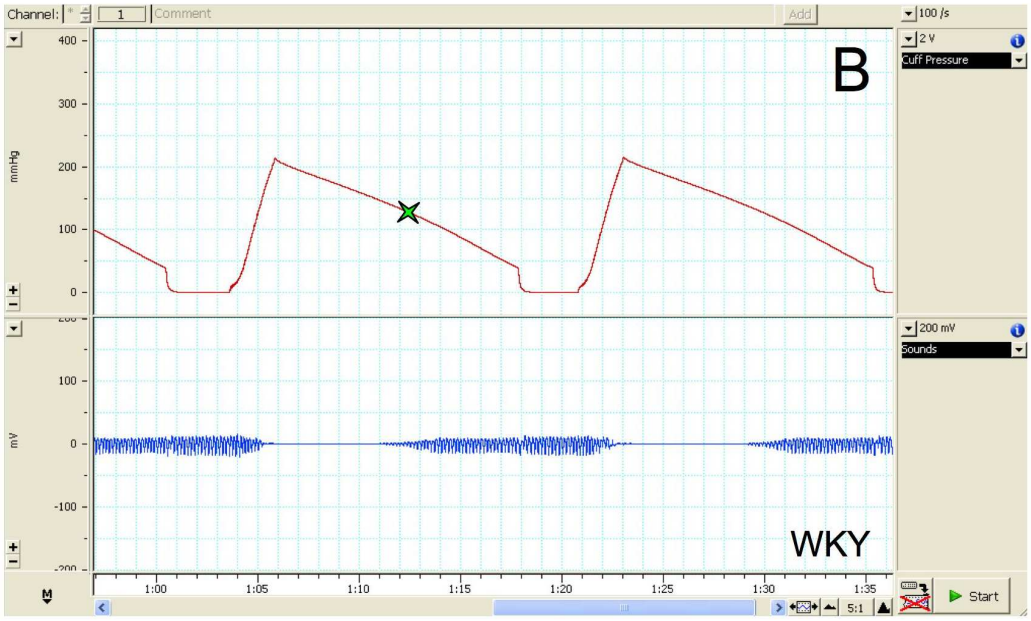
Channel:
1
Comment
Add
100 /s
2 V
Cuff Pressure
B
mmHg
400
300
200
100
0
200 mV
Sounds
mV
100
0
-100
WKY
1:00
1:05
1:10
1:15
1:20
1:25
1:30
1:35
5:1
Start

2.3. Surgical procedures

All surgical and perfusion procedures were performed under general anaesthesia. One hour prior to anaesthesia, food was withheld from animals to reduce gastrointestinal contents. Depth of anaesthesia was assessed using responses to both noxious stimuli (tail pinching/toe pinching) and the blink reflex.

2.3.1. Retrograde labelling of IML sympathetic preganglionic neurons

Fluorogold® (FG®) is a retrograde tracer used commonly in neuronal studies (Ju et al., 1989), and has been shown to be effective in labelling all sympathetic preganglionic neurons (SPNs) of the spinal cord when injected into the intraperitoneal (IP) space (Anderson, 1992; Anderson and Edwards, 1994; Anderson et al., 1989a; Hamilton et al., 1995). It was used in these studies to confirm the identity of SPNs in the intermediolateral cell column (IML) of the spinal cord. Fluorogold® powder (Fluorochrome, Denver Colorado) was diluted in sterile saline (0.9 % NaCl) to create a 2% (w/v) solution. The 2 % FG® solution was aliquoted (100 µl) into sterile microtubes and stored at -80°C. On the day of use, the 2% FG® solution was thawed at room temperature and diluted in 1ml of sterile saline to provide a 0.2% solution for injection. Animals were physically restrained and bilateral IP) injections of FG® were made (0.5ml each side). Animals were euthanased 14 days post injection as detailed in section 2.4.

2.4. Perfusion and fixation

Fixation was achieved by cardiac perfusion through the left ventricle and aorta to enable rapid and complete fixation of body tissues. Prior to perfusion, rats were

anaesthetised with O_2/CO_2 (oxygen 20% carbon dioxide 80%) and sodium pentobarbitone (Thiobarb, Jurox, Rutherford, Australia; 100mg/kg) administered IP.

2.4.1. Immunohistochemical experiments

Once anaesthetised, the abdomen and thoracic cavity of the animal was opened. A 22-gauge blunted needle, attached to a peristaltic pump (Harvard Apparatus, Massachusetts, USA) was inserted via the left ventricle into the aorta and clamped in place. The right auricle was cut to allow the outflow of blood and perfusate. Thirty ml of ice cold heparinised saline (0.9% NaCl containing heparin 2 I.U/ml [Jurox, Rutherford, Australia]) was perfused through the animal (6ml per minute), followed by 180ml of ice-cold 4% formalin diluted in 0.9% saline at the same rate. The spinal cord (for IML experiments) and brain [for rostral ventrolateral medulla (RVLM) and paraventricular hypothalamus (PVN) experiments] were then removed and post fixed in 4 % formalin for 4 h at 4°C. Brainstem and spinal cord blocks was washed in 0.1M phosphate buffer (PB; pH 7.4, 3 x 10 min), then stored in 0.1M phosphate buffered saline containing 10 mM Tris base (TPBS; pH 7.4), plus 0.3% Triton X 100 (Tx), and either 0.1% Sodium Azide (NaN_3; Sigma, Castle Hill, Newcastle, Australia) for fluorescence microscopy studies, or 0.05% Thimerosal (Sigma) for light microscopy studies. Hypothalamic blocks (see section 2.5.1) were cryoprotected by being placed in 30% sucrose solution for 3 days and then frozen down and stored at -80°C.

2.5. Immunohistochemistry

2.5.1. ***Sectioning***

Spinal Cord

The fixed cord was washed for 30 minutes (min) in 0.1M PB. The pia was removed and the cord mounted ventral surface down on a cutting block with super glue (Selleys, NSW, Australia). Additional support was provided with 2% w/v Agar (Sigma). Horizontal sections (50μm) were cut using a vibrating microtome (Vibratome, St Louis, MO, USA) and placed in 0.1M PB. Sections were mounted temporarily on glass slides and viewed under UV fluorescence light using an Olympus BX 51 microscope (Olympus, Mt Waverly, VIC, Australia). The presence of Fluorogold® labelled cells within the IML region, as well as within the central autonomic area (CAA) confirmed the identification of slices containing retrogradely labelled SPN. Sections then underwent fluorescent or peroxidase immunohistochemistry as required.

RVLM

Hindbrains were dissected from the spinal cord at the level of the obex, and the forebrain at the junction between cerebrum and cerebellum. Any remaining pia mater was removed and the hindbrain was washed once for 30 min in 0.1M PB. Coronal sections (50 μm) sections were cut using a Vibratome and placed in 0.1 M PB. A stereomicroscope (Wild M7 S, Wild Heerbrugg, Switzerland) was used to determine anatomical landmarks. Sections containing the RVLM region were defined as those contained within the region extending caudally 600-800 μm from the caudal pole of the facial nucleus. This corresponds to 12.5mm to 11.7mm caudal to Bregma

(Paxinos and Watson, 1998). The region was bounded laterally by the spinal trigeminal tract, medially by the inferior olive and pyramids, and dorsally by the compact formation of the nucleus ambiguus.

Hypothalamus (PVN)

Experiments performed on the hypothalamus were carried out at the Genome Research Facility, University of Cincinnati

The hypothalamus was dissected from the brainstem, at the junction between the cerebrum and cerebellum, and trimmed at the optic chiasm. Hypothalamic tissue was placed into the cryostat (Leica CM 3050S, Wetzlar, Germany) and allowed to warm to -20°C. Hypothalamic sections (25 µm) were cut coronally in a rostro-caudal fashion. Sections were placed in 0.1M PBS. Anatomical landmarks were confirmed using a stereomicroscope (Leica), the rostral portion being identified by flattening and broadening of the supra optic nucleus, and the loss of the mamillothalamicus nucleus, the caudal end located by the moving of the fornix below the zona inserta, corresponding to 1.3 mm to 2.1 mm caudal to Bregma (Paxinos and Watson, 1998).

2.5.2. Immunofluorescence immunohistochemistry

RVLM and spinal cord

Following sectioning, sections were incubated in 50 % ethanol for 30 min and then washed in TPBS (2 x 15 min). Sections were incubated for one hour at room temperature in blocking solution containing donkey serum (10% Chemicon, Temecula, CA, USA), diluted in TPBS with 0.3% Tx and 0.1% NaN_3. Sections were then incubated free floating in primary antibody diluted in blocking solution, either singly or in combinations as detailed in the respective chapters. Details regarding all

antibodies used are provided in Table 2.1. Details of experiments confirming specificity are provided in the relevant experimental chapter. Sections were incubated for 24 hours at room temperature, then 72-96 hours at 4°C. Following incubation with the primary antibodies, sections were washed in TPBS (3 x 30 min) and then incubated for either 4 hours at room temperature, or overnight at 4ºC in species-specific secondary antibodies (Table 2.1) diluted in TPBS containing 0.3% Tx, 0.1% NaN_3, and donkey serum (1%). Sections were then washed TPBS (3 x 30 min), mounted on glass slides (Starfrost, ProSciTech, Thuringowa, QLD, Australia) and coverslipped in Prolong Antifade (Molecular Probes, Mt Waverley, VIC, Australia).

Table 2.1: Antibody Details

Antigen and Host Species	Source	Catalogue #	Lot #
Primary Detection Antibodies			
Anti cGMP: Rabbit	Chemicon (Temecula CA)	AB303	24091218
Anti neuronal NOS: Mouse	Sigma (St Louis, MO)	N2280	022K4838
Anti Oxytocin: Mouse	Chemicon	AB153	220541143
Anti Vasopressin: Guinea Pig	Peninsula Laboratories (San Carlos, CA)	T-5048	031088-2
Anti ChAT: Goat	Chemicon	AB144P	22041143
Anti FG: Rabbit	Chemicon	AB153	22061290
Secondary Detection Antibodies			
Cy2: Donkey anti goat	Jackson (West Grove, PA)	705-096-147	70600
Cy3: Donkey anti-rabbit	Jackson	711-166-152	59892
Cy5: Donkey anti-mouse	Jackson	715-096-151	58916
FITC: Donkey anti-guinea pig	Jackson	705-096-147	58196
FITC: Donkey anti mouse	Jackson	715-096-150	76041
AlexaFluor 568: Donkey anti mouse	Molecular Probes (Mt Waverly, Aus)	A-21203	93D1-1

Table 2.1. Source, catalogue and lot number of antibodies use throughout this thesis. Cyclic guanosine monophosphate (cGMP); nitric oxide synthase (NOS), choline acetyltransferase (ChAT), fluoroscein isothiocyanate (FITC), Fluorogold (FG), Cyanine 2 (Cy2), Indocarbocyanine 3 (Cy3) and Indodicarbocyanine (Cy5).

Hypothalamus

Hypothalamic sections were washed in 0.01M PBS (2 x 5 min), and transferred in to a blocking solution containing 0.01M PBS with 0.01% Triton X and 10% goat serum (Chemicon) and 0.04% NaN_3 for one hour at room temperature. Sections were washed 3 times for 5 min in 0.01M PBS, prior to incubation with the primary antibody/antibodies diluted in the same blocking solution overnight at room temperature. Sections were washed again 3 times for 5 min in 0.1M PBS, before being incubated with the secondary antibody diluted in blocking solution as above, for 4 hours at room temperature in a darkened environment. Sections were again washed (0.1M PBS, 1 x 5min), and then mounted on glass slides (Starfrost) using Vectashield (Vector Laboratories, Burlingame, CA, USA).

For both the fluorescence immunohistochemistry and immunoperoxidase immunohistochemistry (below), negative controls were run in parallel by omitting the primary antibody and incubating sections in blocking solution only.

2.5.3. Immunoperoxidase immunohistochemistry

Following sectioning, tissue was washed in 0.1M PB overnight. Sections were incubated in 30% methanol and washed twice in TPBS for 15 min. Sections were then incubated in a blocking solution of TPBS containing 10% goat serum, 0.3% Tx, 0.05% thimerosal (Sigma) and 20% avidin blocking solution (Vector Laboratories) for 1 hour and then washed TPBS (2 x 5 min). Primary antibodies were diluted in blocking solution (TPBS with 0.3% Tx, 0.05% thimerosal, 10% goat serum) and 20% biotin blocking solution (Vector Laboratories) and the tissue was incubated free floating for 72 hours at room temperature. Sections were washed in TBPS (3 x 20 min), and incubated overnight at 4°C with a biotinylated anti goat

secondary antibody (Vector Laboratories) diluted to 1:500 in TPBS with 0.3% Tx, 0.05% thimerosal and 1 % goat serum. After washing in TPBS (3 x 30 min), sections were incubated in a solution containing avidin-biotin peroxidase complex (1:500; Vectastain) diluted in TPBS with 0.3 % Tx and 0.05 % Thimerosal overnight at 4°C. Sections were washed in TPBS (3 x 5 min) and incubated with diaminobenzidase (DAB) solution, containing 0.02% hydrogen peroxide, 0.02% buffer (Vector Laboratories) and 0.04% DAB diluted in distilled H_20 (dH_2O) for 2 mins. The reaction was terminated by diluting in dH_2O. Sections were washed twice in dH_20, mounted on glass slides (Starfrost), and allowed to air-dry. They were then dehydrated in ethanol (70 %, 80 %, 90 % and 100 %; 1 x 2 min each) and then xylene (2 x 5 min) and cover slipped in Ultra Mount (Lomb Scientific, Taren Point, NSW, Australia).

2.6. Imaging

2.6.1. Confocal microscopy

A BioRad MRC-1024 confocal laser scanning microscope (Carl Zeiss Pty. Ltd. North Ryde, NSW, Australia) was used to examine fluorescent labelling using filter settings specific for identification of the secondary antibody fluorophores (fluorescein isothiocyanate [FITC], cyanine [CY2], indocarbocyanine [CY3] and indodicarbocyanine [CY5]). Each fluorochrome was viewed separately in single channel mode to improve scanning accuracy and no "bleed through" was observed. To excite FITC labelled and CY2 secondary antibodies, excitation was set at 488nm, while 568nm excitation was used for CY3, and 650 for CY5. Collection filters for FITC/CY2 were set to 510, while CY3 was set at 580 and CY5 670. Images were captured as either single images or by taking 4 – 6 optical "slices" through the

sections as a "z" series imaging 10 – 30 microns of tissue, and then reconstructed as a single two-dimensional image using Confocal Assistant Software (BioRad, Hercules, California, USA). Figures were assembled and labelled using Photo Shop software (version 7, Adobe Systems, Mountain View, CA). Overall colour balance and contrast were adjusted, but no other modifications were made.

2.6.2. Light microscopy

NADPH and DAB immunohistochemistry

Sections processed using DAB immunohistochemistry and NADPH diaphorase histochemistry (Chapters 3 and 4) were examined using an Olympus BX51 light microscope (Olympus) under bright field microscopy. Images were taken using DP-Controller Software (Olympus, version 3.1). Figures were assembled and labelled using Photo Shop software (Adobe Systems), and labelled using Microsoft PowerPoint (version 11.2, Microsoft PowerPoint for Mac, Microsoft Corporation, WA, USA)

2.7. Analysis

The specific statistical tests and software utilised are described within each chapter.

3. Distinct subpopulations of cyclic guanosine monophosphate (cGMP) and neuronal nitric oxide synthase (nNOS) containing sympathetic preganglionic neurons in Spontaneously Hypertensive and Wistar-Kyoto rats

3.1. Introduction

Despite having different initiating mechanisms, many forms of chronic hypertension demonstrate increased activity of the sympathetic nervous system (Campese and Krol, 2002; Esler and Kaye, 1998; Rahn et al., 1999) and the therapeutic value of down-regulating sympathetic activity in these conditions is now evident (Esler and Kaye, 1998). In experimental models of hypertension induced by long-term inhibition of nitric oxide (NO) sympathetic activity is increased (Souza et al., 2001). While much research has been directed towards the deficiency of endothelial NO in hypertension, it is becoming increasingly evident that central neuronal NO influences cardiovascular homeostasis, and that impaired NO production may contribute to autonomic dysfunction observed in both essential and secondary hypertension (Chowdhary and Townend, 2001; Patel et al., 2001). Nitric oxide may influence excitatory neuronal responses by chemical modification (s-nitrosylation) of the NMDA receptor, thereby reducing co-incident excitatory responses to glutamate (Ahern et al., 2002). Alternatively, NO can stimulate soluble guanylate cyclase (sGC), and activate intracellular target proteins via the production of cyclic

guanosine-3',5'-monophosphate (cGMP). Target proteins include protein kinase G, cGMP gated ion channels and/or cGMP-stimulated or inhibited phosphodiesterases (Lucas et al., 2000).

Sympathetic preganglionic neurons (SPNs) receive extensive monosynaptic inputs from the paraventricular nucleus (PVN), rostral ventrolateral medulla (RVLM), medullary raphe and A5 area, all of which are critical to the maintenance of vascular tone (Sved et al., 2001). In the rat, SPN are situated in the thoraco-lumbar spinal cord, with approximately 85% located in the intermediolateral cell column (IML) and the rest distributed in the central autonomic area (CAA) and intercalated nuclei and the dorsolateral funiculus (Strack et al., 1988). It has been shown previously that under basal conditions, the SPN of the spontaneously hypertensive rat (SHR) has increased *c-fos* expression compared to its normotensive control, the Wistar Kyoto (Minson et al., 1996), suggesting that these neurons are likely to contribute to the elevated blood pressure in this model of hypertension.

There is considerable evidence that neuronal NO is a critical neurotransmitter regulating the activity of the SPN. In the Sprague-Dawley rat, up to 70% of the SPN contain neuronal NO synthase (nNOS) (Anderson, 1992) and while a pressor role for NO in the spinal cord has been demonstrated (Hakim et al., 1995; Lee et al., 1996), the majority of studies support a depressor role for NO in the spinal cord (Chen and Shyr, 2005; del Carmen Garcia et al., 1997; Iida, 1999; Koga et al., 1999). A role for spinal NO as a functional inhibitory regulator of blood pressure has been shown in a previous study demonstrating that endogenous NO acts to limit pressor responses to intrathecal injection of NMDA (Arnolda et al., 2000) and work by Lu et al., (Lu et al., 1999), who determined that intrathecal NOS inhibitors attenuate the decreases in blood pressure induced by haemorrhage. While no studies up to now have directly

examined altered NO signalling in the spinal cord associated with hypertension, there is convincing evidence from the SHR animal model suggesting that the NO signalling pathway is impaired in other central autonomic regions in association with essential hypertension, (Edwards et al., 2004; Kagiyama et al., 1998; Krukoff, 1998; Patel et al., 2001).

The first aim of this study was examine the hypothesis that the number of nNOS containing SPN are lower in the spontaneous hypertensive rat (SHR) compared to its normotensive control, the Wistar Kyoto (WKY), thereby extending the previous conclusion that endogenously produced NO acts to inhibit the activity of SPN (Arnolda et al., 2000). The second aim of this study was to determine the anatomical relationship between nNOS and its classical signalling molecule cGMP in the SPN of both rat strains.

3.2. Methods

3.2.1. Animals

All experiments were carried out with the approval of the Animal Ethics committees of Murdoch University. Data were obtained from 12 male WKY rats (> 6 months old, average systolic blood pressure 120 mm/Hg ± 15) and 12 male SHR rats (> 6 months old, average systolic blood pressure 200 mm/Hg ± 20). Systolic arterial blood pressure was measured 1 week prior to euthanasia using the tail-cuff method (see section 2.2.1).

3.2.2. Tissue preparation

Fourteen days prior to experimentation, (to label SPNs) retrograde tracer Fluorogold® was injected into the intraperitoneal cavity (see section 2.3.3). Animals were perfused transcardially (see section 2.4.1) and the spinal cord was removed and divided into thoracic segments T1-3, T4-5, T6-7, T8-9 and T10-11. Sections were then cut (see section 2.6.1 Spinal Cord), and treated for nicotinamide adenine dinucleotide phosphate (NADPH) histochemistry (see below) and Fluorogold® (FG®) histochemistry (section 2.5.3).

3.2.3. NADPH histochemistry

Detection of NADPH, a co product required in the production of NO, can be used as a marker to identify cells capable of NO production (Nakamura, 1997).

In order to determine which SPN were able to produce NO from SHR and WKY animals (n = 5 each, total n = 10), sections were double labelled for FG® retrograde labelling to identify SPN (section 2.3.1) and beta NADPH (Sigma).

Sections were washed (2 x 30 min; TPBS + 0.3% Triton X (Tx), treated with 2 x 5 min 0.1M Tris Hydrochloride (Tris HCl, pH 7.4) and then incubated in dH_2O containing 0.3% Tx, 1mM NADPH (Sigma) and 0.2mM nitroblue tetrazolium (Sigma) for 30 minutes at 37°C. Sections were then washed for 10 minutes in 0.1M Tris HCl, before undergoing immunohistochemical processing for detection of Fluorogold using DAB (Section 2.5.3) (see Table 3.1 for antibody concentrations).

3.2.4. nNOS, cGMP and ChAT fluorescence immunohistochemistry

To determine the relationship between nNOS, cGMP and choline acetyl transferase (ChAT) in SPN, sections from T1-T9 from 7 SHR and 7 WKY animals were treated for fluorescence immunohistochemistry as described in section 2.5.2. Sections were incubated free floating in primary antibodies directed against nNOS and cGMP (*n*= 4 WKY and 4 SHR) or ChAT and cGMP (*n*= 3 WKY, 3 SHR, Table 3.1). Labelling was detected using species specific secondary antibodies as described in Chapter 2 with dilutions as provided in Table 3.1.

Table 3.1: Antibody combinations used for fluorescence immunohistochemistry in Chapter 3

Animal cohorts	Antibody combination	Dilution	Conjugated to	Dilution
WKY (*n* = 5) & SHR (*n* = 5) 6 months	NADPH rabbit α FG	1:2000	goat α rabbit	1:500
WKY (*n* = 4) & SHR (*n* =4) 6 months	mouse α nNOS rabbit α cGMP	1:400 1:500	FITC: donkey α mouse CY3: donkey α rabbit	1:500 1:500
WKY (*n* = 3) & SHR (*n* = 3) 6 months	goat α ChAT rabbit α cGMP	1:500 1:500	FITC: donkey α goat CY3: donkey α rabbit	1:500 1:500

Table 3.1. Table provides the details of the various combinations used in each of the immunohistochemical experiments. Fluorescence histochemistry experiments were used to investigate the basal levels of nNOS of ChAT with cGMP expression in the IML. Light histochemistry for Fluorogold was coupled with NADPH histochemistry to determine the number of NO expressing SPN in WKY and SHRs. Source, batch and abbreciations detail can be found in Table 2.1.

3.2.5. Analysis

Sections were examined using a light microscope (section 2.6.2) or a confocal dual laser-scanning microscope (section 2.6.1), with appropriate excitation and fluorescence filter sets to discriminate between the fluorophores (fluorescein isothiocyanate [FITC] and indocarbocyanine [CY3]).

3.2.6. Control experiments

For negative controls, tissue sections were treated as described above but sections were incubated with normal rabbit serum (NRS; 1:100, Sigma, St Louis, Missouri, USA) in place of primary antibody, or in blocking solution alone (no-antibody controls). In addition, sections were also treated with anti-cGMP antibody (1: 500) that had undergone pre-adsorption (12 hrs at 4ºC) with cGMP (1mM; Sigma, St Louis, MO) or acetylated cGMP (0.5mM). Acetylation of cGMP was achieved by 1:1 incubation of cGMP with acetylation reagent (33% v/v Triethylamine [Sigma] and 66% v/v Acetic Anhydride [Sigma]). The use of acetylated cGMP was performed based on the manufacturers recommendation that the antibody recognises both free and acetylated cGMP. This polyclonal antibody is specific for cGMP with no significant cross-reaction to other nucleotides at concentrations to 1mM as tested by radioimmunoassay, and was raised against 2'0-succinyl cGMP conjugated to BSA (manufacturer's technical information).

The mouse monoclonal nNOS antibody (Sigma) was raised against a recombinant nNOS fragment (amino acids 1-181) and on western blots reacts specifically with brain NOS and does not react with NOS derived from macrophages (iNOS) or endothelial cells (eNOS) (manufacturer's technical information). The antiserum stains a single band at 150kDa on Western blot staining and controls have

been performed using preabsorption studies with excess nNOS fusion protein (Dinerman et al., 1994). The goat polyclonal ChAT antibody (Chemicon) was raised against human placental ChAT (manufacturer's technical information). Control studies by (Kha et al., 2000) showed that all ChAT staining was abolished by preabsorption with the human placental ChAT antigen. The rabbit anti-FG® antibody (Chemicon) was prepared against the whole molecule FG® (hydroxystilbamidine; manufacturers technical information). Staining of sections of spinal cord produced a pattern of FG-immunoreactivity identical to that seen when sections were viewed under ultraviolet light (direct visualisation of FG® molecule), and was the same pattern of staining as described previously with IP FG® as a retrograde label to identify SPN (Anderson and Edwards, 1994). Histochemical controls omitting the substrate NADPH were performed to test for non-specific deposition of formazan (Rothe et al., 1998).

3.2.7. Quantification of labelled neurons within the IML region and statistical analysis

Cells with a nucleus were counted if they were FG® immunoreactive and were located in the IML bordering the white and grey matter, or associated with that cell group but lying in the lateral funiculus. Thus cells from both the intermediolateralis pars funicularis and intermediolateralis pars principalis were included. The presence or absence of NADPH-diaphorase staining was then noted. On average, 5 sagittal sections from each of the spinal segmental regions contained SPN. The total number of labelled cells from each spinal cord region for each animal were then tallied to give a total cell count breakdown per animal, testing the hypothesis that there were reduced numbers of NADPH reactive SPN in the thoracic spinal cord of the SHR, compared to the WKY. Individual regions of the thoracic spinal cord were not

assessed separately in order to limit inflated risk of type 1 error, when testing multiple null hypotheses from a single experiment (Ludbrook, 1998). No correction factor was applied to cell counts. The number of FG®/NADPH labelled cells were calculated as a percentage of the total number of FG® positive cells in each rat strain. Statistical comparison of the total number of FG® labelled SPN and percentage of FG®/NADPH between the two strains was calculated using a single factor ANOVA using Microsoft Excel (2004). Significance was set at $p < 0.05$. All figures were assembled and labelled using Photo Shop software (version 7, Adobe Systems, Mountain View, CA). Overall image levels and contrast were adjusted equally for all images, but no other modifications were made.

3.3. Results

3.3.1. General observations

Within each spinal cord segment, the general anatomical arrangement of SPN in the IML of the WKY and SHR animals were distinctly different. Classically, the distribution of SPN is known for its' clustered appearance, which resembles a ladder like pattern (Henry and Calaresu, 1972). The WKY showed this characteristic distribution, with clusters of SPN easily recognised when stained for FG® (Fig. 3.1A), ChAT, nNOS or cGMP. On the other hand, the SHR demonstrated a more continuous distribution (Fig. 3.1B) with the distribution of SPN neurons evenly spread along the rostro-caudal axis of the IML. The dendritic pattern of SPN in the SHR also appeared to be altered in comparison to the WKY, with marked reduction in the number of mediolateral projections relative to those in the rostro-caudal dimension.

Figure 3.1: Differences in neuroanatomical arrangement of SPN between SHRs and WKY

Fluorescent images illustrating neuroanatomical arrangement of SPN labelled for Fluorogold® (FG®) in WKY (A) and SHR (B). (A) WKY animal demonstrating clusters of SPN with prominent mediolateral dendritic projections. (B) SHR animal demonstrating a more continuous distribution of SPN with less obvious mediolateral dendritic projections. Small numbers of neurons immunoreactive for FG® can also be seen around the central canal in panel B. Scale bar in B depicts 500 μm in both panels

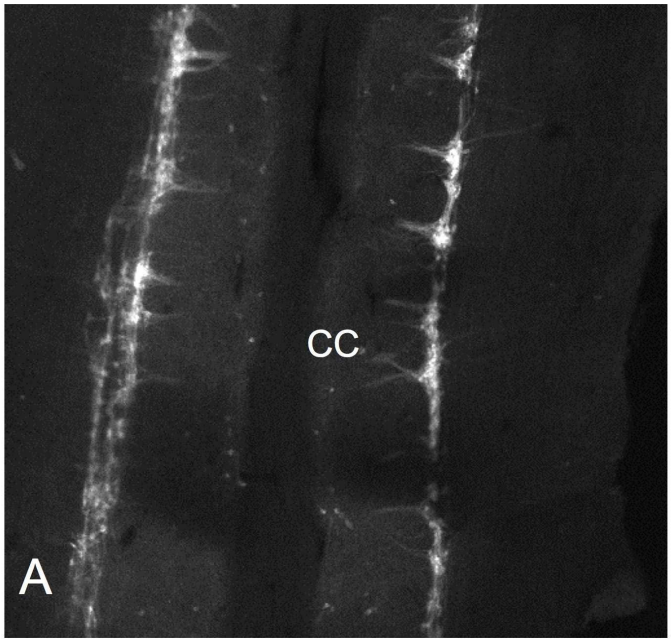
CC
A

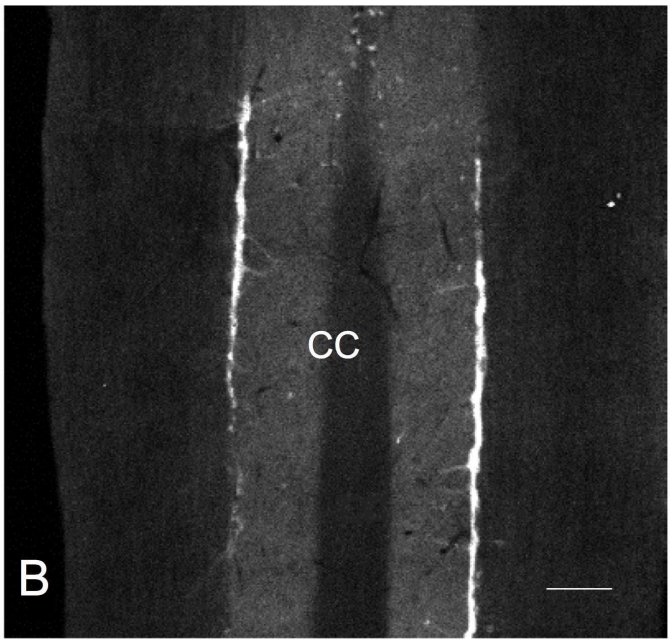
CC
B

3.3.2. Number of SPN and the relationship with NADPH-diaphorase

Combined NADPH-diaphorase histochemistry and immunohistochemistry for the retrograde tracer FG® was used to determine (1) whether there was any difference in the total number of SPN between the WKY (n = 5) and SHR (n = 5) in the IML region of the thoracic spinal cord (T1-T11), and (2) if there was any variation in the proportion of SPN containing NOS, as determined by NADPH-diaphorase histochemistry. The total number of FG® labelled SPN in the thoracic IML region of WKY (T1-T11) was 6542 ± 828 cells, and in the SHR was 6091 ± 820 and these were not significantly different (Table 3.2). All NADPH-diaphorase positive cells in the IML region were labelled with FG®, but not all FG® immunoreactive cells were positive for NADPH-diaphorase (Fig 3.2A-B, Table 3.2). The double-labelled NADPH/FG® were usually located more laterally in the IML than the FG®-only labelled cells. There were significantly less NADPH-diaphorase positive SPN in the SHR animals when compared to WKY (Table 3.2) and as a proportion of the total number of FG® labelled cells, this was equivalent to 64.4 ± 5.1% NADPH reactive FG® cells in the WKY vs. 55.6 ± 2.1% in the SHR (n = 10, $p \leq 0.05$). Cells reactive for NADPH-diaphorase only were noted in the region of the central canal (Fig 3.2C).

Figure 3.2: Retrograde labelling of SPN, with NADPH histochemistry of SHRs and WKY

Light microscopy images depicting Fluorogold® (FG®) retrograde labelling of SPN detected with immunohistochemistry combined with NADPH-diaphorase histochemistry for NOS in T1-3 in WKY (A) and SHR (B, C). In A and B, the central canal is to the right of the image, white matter to the left. In C, the region of the central canal is in the middle of the image. Double-labelled cells appear black while single labelled cells (FG®-only) are brown (arrows) and are located predominantly in the medial region of the IML. Cells labelled for NADPH-diaphorase only appear blue and are illustrated in panel C. Note the dense rostro-caudal dendritic tree reactive for NADPH only (arrow heads B) in the SHR. Scale bar in C depicts 100μM for all panels.

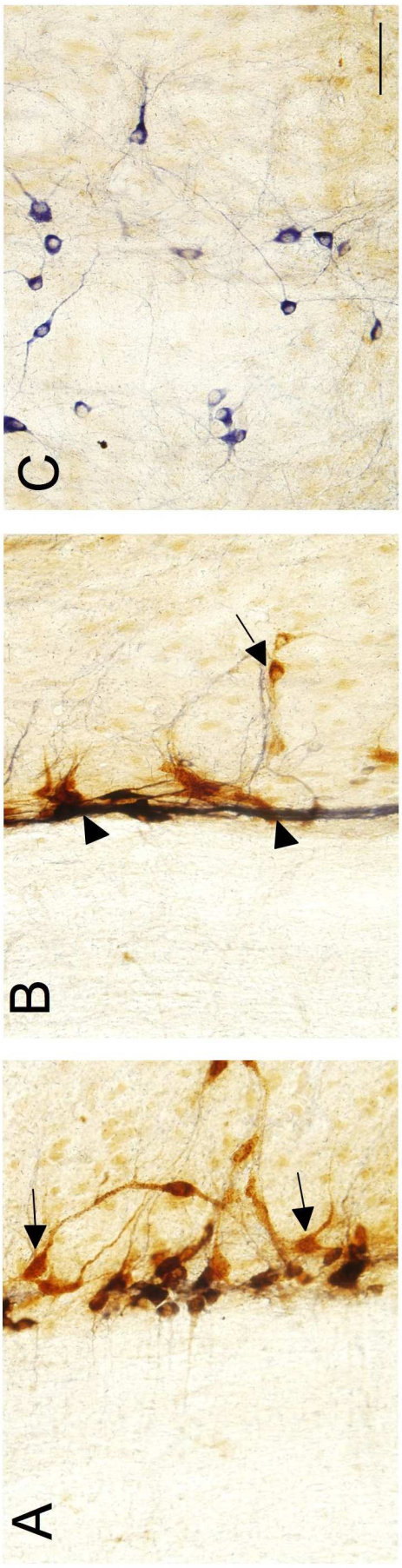
C
B
A

Table 3.2: SPN cell counts in thoracic IML region of WKY and SHR

Animal	FG only	FG and NADPH	Total FG	% NADPH re total FG
WKY1	2047	3667	5726	64.04%
WKY2	2041	4558	6599	69.07%
WKY3	1782	3970	5754	69.00%
WKY4	3029	3935	6956	56.57%
WKY5	2786	4883	7675	63.62%
Mean ± SD WKY	2337 ± 538.6	4202.6 ± 500.5	6542 ± 828.4	64.4 ± 5.1%
SHR1	2333	2764	5099	54.21%
SHR2	2527	3098	5661	54.73%
SHR3	3039	3563	6588	54.08%
SHR4	2424	3501	5905	59.29%
SHR5	3179	4019	7203	55.80%
Mean ± SD SHR	2700.4 ± 382.5	3389 ± 478.3	6091.2 ± 819.6	55.6 ± 2.1%

Table 3.2. Uncorrected bilateral counts for FG-labelled neurons and FG/NADPH diaphorase double-labelled neurons in the thoracic IML spinal cord region (T1 – T11) for each WKY and SHR animal examined.

Cells immunoreactive for nNOS showed strong cytoplasmic staining that extended into the proximal dendrites in both WKY and SHR (Figs 3.3A, C). A consistent and unexpected finding was the co-localisation of cGMP in all nNOS immunoreactive neurons in the IML (Figs 3.3B, D) in both the SHR (n = 4) and WKY (n = 4) animals. In contrast, nNOS immunoreactive cells positioned near the central canal were never co-localised with cGMP (data not shown). Further, we identified a subpopulation of IML neurons that were immunoreactive only for cGMP and these were found predominantly in the medial part of the IML. In contrast the double-labelled cGMP/nNOS neurons were located mainly in the lateral regions of the IML (Fig 3.3). This distribution was similar to that described above for NAPDH/FG® double labelled vs. FG® only labelled SPN. These cGMP only neurons were found in both the WKY and SHR in all thoracic segments of the spinal cord examined. Immunoreactivity for cGMP was cytoplasmic and had distinct punctate or granular appearance that extended into associated process. Blood vessels in the region also showed cGMP immunoreactivity (Fig 3.3B).

Figure 3.3: Relationship of nNOS and cGMP in SPN in WKY and SHRs

Confocal images illustrating co-localisation of nNOS (A, C) with cGMP (B, D) in cells from the IML of the thoracic spinal cord (T4-T6) in WKY (A, B) and SHR (C, D). Central canal is to the left of the image, white matter to the right. All nNOS positive neurons contain cGMP, but there is a subpopulation of cells, located predominantly in the medial region of the IML that are immunoreactive for cGMP-only (asterix). Arrows indicate blood vessels labelled with cGMP. Scale bar in D depicts 20μm in all panels.

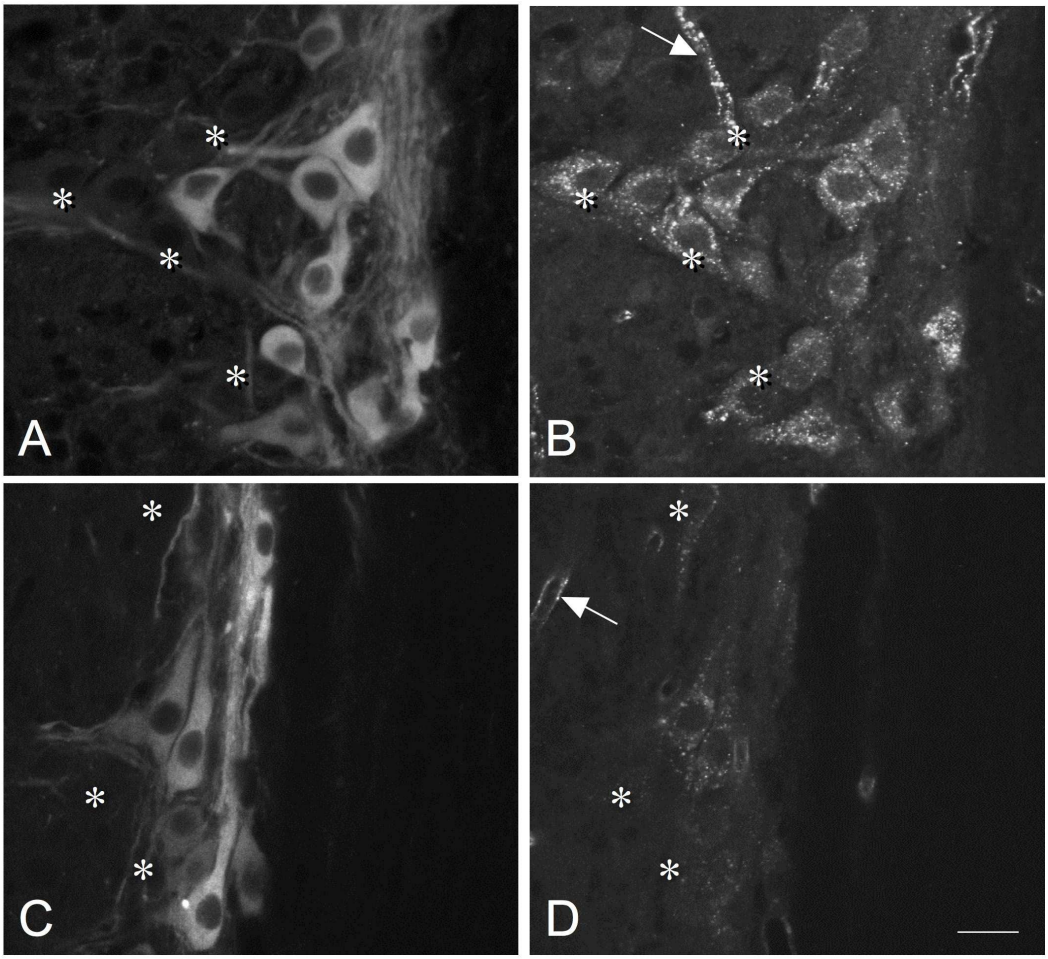
A
B
C
D

3.3.3. Cyclic GMP and ChAT immunoreactivity

To determine if the cGMP-immunoreactive neurons in the IML region were SPN, double labelling of sections for ChAT and cGMP was performed (*n* = 3 WKY, *n* = 3 SHR). Incompatibility of primary antibodies prevented the use of FG® in these experiments. No difference was found between SHR and WKY and so results have been combined. Overall, 98% of ChAT immunoreactive neurons in the IML region were double labelled for cGMP-immunoreactivity (97.94 % ± 2.06%; *n* = 3 WKY animals, 3 SHR animals; 650 cells counted in total across T1-T9, Fig 3.4A, B). In conjunction with the total cell count and nNOS/cGMP double labelling experiments, these results confirm that all the cGMP (i.e. both the nNOS-positive and nNOS-negative populations) labelled cells within the IML are SPN. Further, they indicate that there is no difference in the total number of cGMP immunoreactive SPN between the two rat strains.

3.3.4. Control experiments.

Sections processed in the absence of primary antibody did not show any staining. Pre-absorption of the anti-cGMP antibody with free cGMP caused a significant reduction of cGMP immunoreactivity in spinal cord segments from both SHR and WKY, and pre-absorption of the anti-cGMP antibody with acetylated cGMP abolished cGMP immunoreactivity (Fig 3.4C). These results are similar to a study by de Vente (De Vente et al., 1998) using a different anti cGMP antibody. Negative controls using NRS did not show any preferential staining of neuronal cells, instead demonstrating weak, non-specific staining of all cells. Histochemical controls omitting the substrate NADPH showed no staining.

Figure 3.4: Relationship of ChAT and cGMP in SPN

Confocal images illustrating double labelling of horizontal cord section (T4-T6) with ChAT (A) and cGMP (B) in the IML of a WKY animal. Central canal is to the left of the image, white matter to the right. Images demonstrate double labelling of ChAT with cGMP in all SPN shown. Panel C is a control image depicting lack of staining after the cGMP antibody had been pre-incubated in acetylated cGMP prior to use for fluorescence immunohistochemistry. Scale bar in C depicts 20μm in both panels

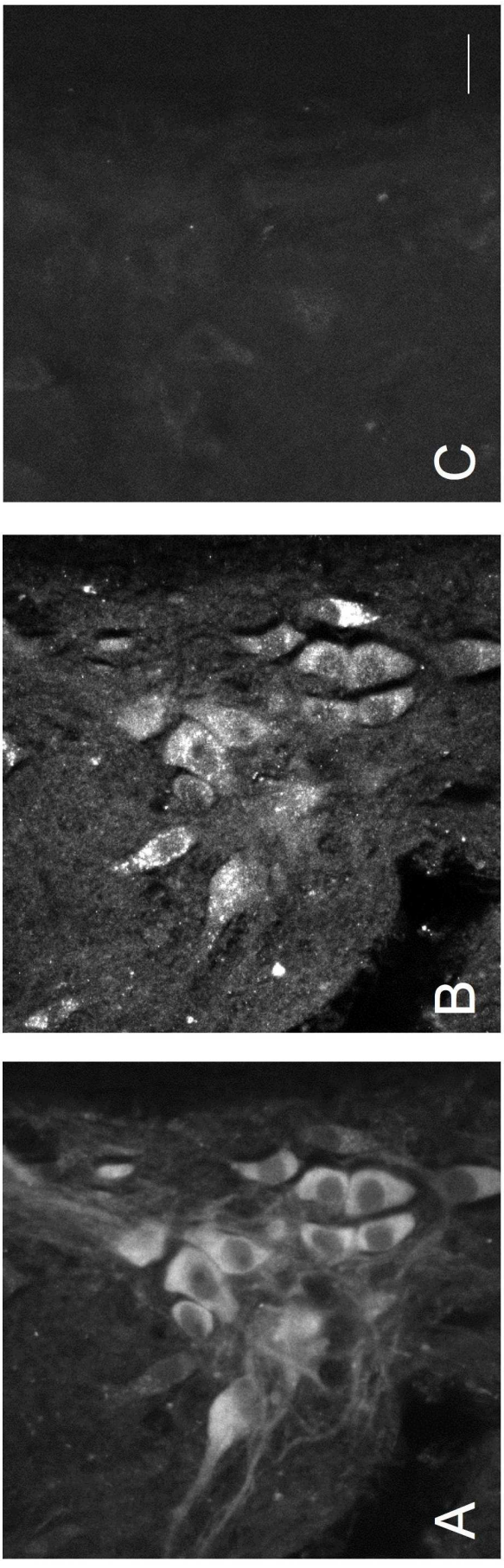
A
B
C

3.4. Discussion

This is the first detailed neuroanatomical analysis of cGMP and nNOS expression in the SPN population within the IML of the thoracic spinal cord. These novel results have determined that two subpopulations of cGMP immunoreactive SPN exist (1) those SPN that contain both cGMP and nNOS, and (2) a population of cGMP only SPN. These subpopulations were identified in both SHR and WKY. Further, we have comprehensively demonstrated that in the SHR, there is a significant reduction in the number of SPN expressing NOS when compared to the WKY, despite a comparable number of SPN in each strain.

3.4.1. Co-localisation of nNOS and cGMP in SPN

In the present study, there was a consistent and strong co-localisation of cGMP and nNOS within SPN in the IML region of thoracic spinal cord. This is in contrast to a number of studies, most notably work of (Wu et al., 1997) and (Vles et al., 2000), who assessed nNOS and cGMP immunoreactivity in the spinal cord of Sprague-Dawley and Lewis rats, but did not report cGMP in cell bodies in the IML region, only in nerve fibres. Other detailed analyses of cGMP and nNOS neuroanatomy in the brain and cervical spinal cord (De Vente et al., 1998; Vles et al., 2000), describe co-localisation of nNOS and cGMP as the exception rather than the rule. The only other neuronal populations in which a consistent co-expression of nNOS and cGMP has previously been described are cerebellar granule cells (De Vente et al., 1998) and within the supraoptic nucleus (Stern and Zhang, 2005). Our control experiments suggest the cGMP immunoreactivity is specific and additionally, the punctate cytoplasmic staining pattern for cGMP in this study is similar to that shown in cervical spinal cord laminae (Vles et al., 2000) and the supraoptic nucleus

(Stern and Zhang, 2005). A number of studies utilising immunocytochemistry to determine cGMP expression pre-treat with the phosphodiesterase inhibitor isobutylmethylxanthine (IBMX) to enhance detection (Allaerts et al., 1998; De Vente et al., 1998; Vles et al., 2000). However, in our preliminary studies, we compared results using pre-perfusate saline solution with and without IBMX (1mM) prior to fixation, and found that cGMP expressing cells in the IML could be readily detected in the absence of IBMX. By omitting IBMX, we believe our results are representative of basal cGMP levels in the regions examined.

Levels of cGMP are directly regulated by guanylyl cyclases, and NO is a potent activator of sGC. It has been argued that the concentrations of Ca^{2+} required for the activation of nNOS inhibits sGC, such that NO should not be able to induce the up-regulation of cGMP in the same cell (Knowles et al., 1989; Parkinson et al., 1999). However, through its linkage to the NMDA receptor via postsynaptic density protein PSD95 (Christopherson et al., 1999), nNOS is effectively compartmentalised to subcellular regions that are exposed to relatively high Ca^{2+} levels (Kiedrowski et al., 1992). This would provide a mechanism by which nNOS and sGC are exposed to different Ca^{2+} concentrations. Given that we find co-localisation of NO and cGMP in SPN, we hypothesise that such partitioning of nNOS and cGMP within the confines of the soma would permit autocrine signalling in these neurons.

Cyclic GMP levels can also be regulated by membrane bound, or particulate guanylyl cyclases, including the receptors for the atrial natriuretic peptide (ANP), brain (BNP) and C-type NP. While the natriuretic peptides are expressed in the spinal cord (Cameron et al., 1996), and increased CNP expression has been documented in the SHR (Kuchel et al., 1988), their ability to elicit cGMP synthesis in SPN has not been elucidated and would warrant further investigation.

3.4.2. Chemical phenotype and strain dependent organisation of thoracic SPN

A subpopulation of cGMP-only immunoreactive neurons were also identified in the IML region. Their identity as SPN was confirmed by the presence of ChAT. The description of this new sub-population supports the theory of chemical coding within the SPN, where neurons can be linked to functional roles by the presence of discrete combinations of neurochemical markers as has been described previously (Afework and Burnstock, 1995; Cao and Morrison, 2001; Holgert et al., 1995; Morrison and Cao, 2000; Murphy et al., 2003). Interestingly, in both the WKY and SHR, double labelled cGMP/nNOS and FG®/NADPH SPN were predominantly located laterally within the IML. We have recently described a similar pattern of location for tonically activated subpopulations of SPN, including those within the functionally defined adrenal SPN subpopulation (via immunoreactivity to phosphorylated extracellular signal regulated kinase 1/2 (p-ERK1/2) (Springell et al., 2005). A mediolateral topographic organisation of functionally distinct populations of SPN is present within the IML, with lateral SPN having a vasomotor function and the more medial SPN having a motility regulating function (Janig and McLachlan, 1986; Pyner and Coote, 1994).

Our study also indicated an unusual dendritic tree for the SPN in the SHR when compared to the WKY and previous reported studies in Sprague-Dawley rats, the cat and hamster (Pyner and Coote, 1995; Reuss and Reuss, 2001; Tang et al., 1995b). Tang et al (Tang et al., 1995b) propose that the different receptive field may restrict inputs to SPN in the SHR.

3.4.3. Reduced expression of NOS in SPN of the upper thoracic spinal cord of the SHR

The other primary finding in this study was the reduced number of SPN that express NOS in the SHR when compared to the WKY, despite comparable numbers of SPN in the two rat strains. Given that all NOS isoforms exhibit NADPH-diaphorase activity the application of NADPH-diaphorase histochemistry to identify nNOS neurons deserves comment. While in some regions, including the lateral collateral pathway of the sacral spinal cord (Doone et al., 1999), NADPH-diaphorase does not match nNOS-immunoreactivity, it has been shown previously in the IML that there is consistent double labelling of the two markers (Doone et al., 1999; Okamura et al., 1995).

Our finding of a decreased number of NOS containing SPN in the thoracic spinal cord significantly advances the work of Tang et al (Tang et al., 1995a) who demonstrated a decreased proportion of NOS containing SPN, but only in those SPN that project to the superior cervical ganglion and only in the intermediolateralis pars funicularis. Our finding are based on total thoracic IML SPN cell numbers and indicate this phenomena is not limited to one subpopulation of SPN but is consistent across the thoracic spinal cord region, and will therefore potentially affect multiple sympathetic outflow pathways (Strack et al., 1988). Decreased numbers of nNOS neurons has also been described in other sites in SHR including the PVN (DiCarlo et al., 2002). In addition to studies supporting a depressor role for endogenous NO in the spinal cord (Chen and Shyr, 2005; del Carmen Garcia et al., 1997), work from our laboratory has previously demonstrated that endogenous NO attenuates pressor responses induced by NMDA (Arnolda et al., 2000), suggesting that NO acts as an inhibitory modulator of descending excitatory cardiovascular signals. While it is not

possible to argue causation on the basis of our neuroanatomical data, a reduction in NO in the IML of SHR could be associated with a corresponding decrease in cGMP expression, and may contribute to the increase in sympathetic activity associated with hypertension. The next chapter in this thesis explores these possibilities, examining the downstream expression of cGMP and its functional activity in SPN of WKY and SHR.

3.4.4. Conclusion

We have demonstrated for the first time that cGMP and nNOS are co-localised in a subpopulation of SPN, and that cGMP can now be used to discriminate SPN according to a unique profile of neurochemicals. Further, we have convincingly demonstrated that the number of SPN in the thoracic IML expressing NOS is significantly less in the SHR than in the WKY, despite each species having comparable numbers of total SPN in this region.

It has recently been demonstrated that physiologically relevant inputs to SPN arise from intraspinal sources (Llewellyn-Smith et al., 2005). This, combined with our findings, raises the possibility of functional autocrine and paracrine NO signalling in the IML, and provides an anatomical substrate for altered SPN activity arising from differential supraspinal, intraspinal and local inputs in the SHR.

4. Cyclic GMP demonstrates differential expression levels and functional pressor activity in the spinal cord of Spontaneously Hypertensive and Wistar Kyoto rats

4.1. Introduction

One of the most widely studied and best-understood signalling pathways for nitric oxide (NO) is the activation of the primary neuronal receptor for NO, soluble guanylate cyclase (sGC), and the subsequent generation of intracellular 3', 5'-cyclic guanosine monophosphate (cGMP; (Ahern et al., 2002; Knowles et al., 1989). In Chapter 3, we determined that all sympathetic preganglionic neurons (SPN) within the thoracic intermediolateral (IML) cell column of the spinal cord express cGMP and that the SPN can be further coded by the presence or absence of neuronal NO synthase (nNOS). Further, we demonstrated that there are significantly fewer NOS-containing SPN in the spontaneously hypertensive rat (SHR), compared to its normotensive control, the Wistar Kyoto (WKY). In this chapter we look to see whether this has had a translational effect upon cGMP expression and functional activity within SPN.

Given the direct relationship between NO activity and the formation of cGMP, it would be reasonable to hypothesise that a reduced capacity by SPN to produce NO in the SHR animals would translate into lower cGMP levels. This is supported by previous work in other systems. For example, reduced production and/or bioavailability of NO has been associated with reduced activity of the sGC/cGMP

system in the vasculature of hypertensive rats (Kojda et al., 1998; Ruetten et al., 1999) and experiments utilising NO donors and inhibitors show parallel increases and decreases in cGMP levels, respectively. The NO donor sodium nitroprusside (SNP) increases the level of cGMP content in the subfornical organ (Rauch et al., 1997) and in the cerebellum, blockade of NMDA receptors reduces not only NO production but also reduces basal cerebellar cGMP levels (Yamada et al., 1996). Finally, in olfactory neurons, a progressive reduction in nNOS expression induced by targeted gene deletion is followed by decreased cGMP production (Chen et al., 2004a).

Cyclic GMP production may also be stimulated when the natriuretic peptides - atrial natriuretic peptide (ANP), brain (BNP) and C-type NP (CNP) bind their cognate receptors, membrane bound guanylyl cyclases (Lucas et al., 2000). In the rat, the major subtype of natriuretic peptide receptor in the central nervous system (CNS) is the ANP-B receptor and the ligand for the ANP-B receptor is CNP. Thus the ligand CNP/ANP-B receptor system may be the most important in the rat (Imura et al., 1992). To date, while it has been shown that natriuretic peptides are expressed in the spinal cord (Cameron et al., 1996), their ability to elicit cGMP synthesis in SPN has not been elucidated.

In the thoracic region of the spinal cord, SPN play a key role in the control of arterial pressure and heart rate. The effects of intrathecal injections of NO donors and NOS inhibitors are conflicting, with inconsistent pressor (Hakim et al., 1995; Lee et al., 1996) and depressor responses described (Chen and Shyr, 2005; del Carmen Garcia et al., 1997; Iida, 1999; Koga et al., 1999). To date, only one study has directly examined the role of spinal cGMP in modulating cardiovascular parameters. Work by members of our group (Malik et al., 2007) has recently demonstrated that intrathecally delivered cGMP not only raises mean arterial pressure (MAP) in a dose

dependent fashion, but also supports MAP during haemorrhage. This effect is mimicked by the intrathecal administration of L-arginine, and blocked by intrathecal delivery of the selective sGC inhibitor 1H-[1,2,4] oxadiazole [4,3-a] quinoxaline-1-one (ODQ), suggesting that within the spinal cord, sympathoexcitatory effects of spinal NO are mediated by a cGMP-dependent mechanism.

The aim of this study therefore was to determine if (i) reduced nNOS levels correlate with reduced detectable cGMP in the SPN of SHR vs. WKY animals and (ii) if intrathecal administration of cGMP analogue 8-bromo-cGMP would elicit different functional pressor effects in the two strains.

4.2. Materials and methods

4.2.1. General methods

The experiment was divided into two parts. The first part was designed to compare the amount of cGMP detected in thoracic SPN of SHR and WKY rats using immunohistochemical methods. The second part compared the effects of intrathecal administration of the membrane permeable analogue of cGMP, 8-Bromo-cGMP (8-Br-cGMP), in the spinal cord of WKY and SHR rats on MAP.

All surgical and recording procedures were performed in the Medical Research Facility, Royal Perth Hospital, Western Australia, and the immunohistochemistry was performed at Murdoch University, Western Australia, in accordance with the National Health and Medical Research Council of Australia guidelines on the use of animals for scientific purposes. Experiments were approved by the Animal Ethics Committee of Royal Perth Hospital and Murdoch University.

Animals used for immunohistochemical experiments were deeply anaesthetised with an intraperitoneal (IP) injection of sodium pentobarbitone (100mg/kg). The depth of the anaesthesia was monitored using the corneal or the paw and tail pinch reflex. Animals used for surgical experiments were anaesthetised with urethane (ethyl carbamate, Sigma, St Louis, MO, USA) injected intraperitoneally (1.2g/kg body weight).

*4.2.2. **Immunohistochemistry***

Processing

Details for the immunohistochemical techniques used in this project have been provided in Chapter 2, General Materials and Methods. Briefly, 50 μm horizontal thoracic spinal cord sections (T2 – 9) from WKY (n = 4, 6 month old, males) and SHR (n = 4, 6 month old, males) rats were cut on a vibrating microtome (see section 2.5.1) and immunoperoxidase immunohistochemistry (section 2.5.3) was performed using a rabbit anti-cGMP antibody (1:2000; Chemicon, Temecula, CA, USA). Control sections were processed in parallel without the addition of primary antibody.

Immunohistochemistry analysis:

Preparations were examined using an Olympus BX51 light microscope (Olympus, Waverly, Australia) under bright field microscopy. Images of SPN within the IML region were acquired and densitometry used to undertake relative assessment of the level of immunoreactivity using Image J (Rasband, W.S., ImageJ, U. S. National Institutes of Health, Bethesda, Maryland, USA, http://rsb.info.nih.gov/ij/, 1997-2007). Only neurons that had their full profile visible were selected for analysis. Arbitrary units (limited to the grey scale range of 0 – 255) were then expressed as a reciprocal of luminance, giving a direct measure of immunoreactive staining intensity. Raw density measurements were then adjusted for background staining, which allowed comparison of data between different animals (Fuller et al., 2006). For each animal, 20 SPN cellular intensity values were determined and the averages calculated. Average values from each animal were then used for statistical analysis, by using a paired two-tailed Student's t-test (Microsoft Excel, 2004), with the assumption of equal variance and significance set at $p \leq 0.05$.

4.2.3. ***Surgical preparation***

The surgical procedures were performed by Dr D.J McKitrick and Dr V.V Holobotovskyy at the Medical Research Facility, Royal Perth Hospital, Perth, Western Australia.

WKY (*n* = 12; 8 – 10 weeks, male) and SHR (*n* = 12; 8 – 10 weeks, male) rats were used for the study. Six rats of each strain were assigned to each of 2 groups, 8-Bromo-cGMP-treated and phosphate buffered saline (PBS)-treated (8-Bromo-cGMP vehicle) groups.

Placement of femoral artery catheter for blood pressure recordings

Animals were anaesthetised with urethane diluted in 0.9% saline administered ip. Once anaesthetised, animals were positioned supine and the left leg was shaved and cleaned with 70% ethanol. The femoral vein and artery were exposed and the artery dissected from the vein. The artery was tied distally with a silk ligature (4-0 silk Ethicon; Johnson and Johnson, Australia) and occluded proximally in a similar fashion, but not tied off. The artery was elevated and a small incision made on the surface to allow insertion of a bevelled polyethylene catheter (Dural Plastic Engineering, NSW, Australia; internal diameter 0.8mm, outer diameter 1.0mm), filled with sterile heparinised saline (0.9 % NaCl with 2 I.U/ml heparin (Jurox, Rutherford, Australia), into the artery (~5 cm). This was secured with the proximal silk tie. The catheter was then anchored with the distal ligature. The catheter was connected to a pressure transducer (Bell and Howell, California, USA),

Upon completion of the study, animals were killed with pentobarbital sodium (100mg/kg; Lethabarb, Virbac, Australia) administered via the arterial catheter.

Intrathecal injection

Animals were secured in a stereotaxic frame (David Kopf, Tujunga, CA, USA) and the cervical spinal region was exposed to the atlanto-occipital membrane. The atlanto-occipital membrane and dura mater were pierced with a 25-gauge needle. A cannula (polyethylene, internal diameter 0.28mm, outer diameter; 0.61mm, Dural Plastic Engineering) was inserted into the subarachnoid space and the tip progressed caudally (7.0 cm) to lie above the dorsal surface of the spinal cord, at the level of the T12 vertebra. Placement of the catheter was confirmed with an injection of methylene blue (10µl) upon completion of the experiment**.** Catheters were filled with cGMP analogue, 8-Bromo-cGMP (Sigma Aldrich) or control solution PBS (0.1M pH 7.4).

Experimental procedures

Doses of 1, 30 and 100 µM 8-bromo-cGMP dissolved in PBS were used. Prior to the intrathecal injection, MAP values were monitored for two minutes. At two minutes 10µl of 8-Br cGMP [1, 30 and 100 µM (assigned in random order)] was injected into the subarachnoid space and the haemodynamic effects monitored for a further 10 minutes. Control animals received only PBS (10µL). At 10 minutes (or longer until MAP had returned to preinjection values) a subsequent doses of 8-Br-cGMP (or repeated 10 µL PBS in the control groups) was given until each experimental rat had received 3 intrathecal injections.

Recording procedures and analysis

The pressure transducer was connected to an IBM compatible computer equipped with Power Lab (AD Instruments, Version 5.5.4, 2007, NSW, Australia) hardware and Chart software (AD Instruments). The digitised output was presented

as pulsatile pressure sampled at 0.01s intervals. Pulsatile AP information was mathematically converted to MAP and the results recorded and displayed in mmHg. Baseline values are presented as the average MAP ± standard error of the mean (SEM). Mean arterial pressure values before and after drug administration were compared for strain/dose interactions using two-way ANOVA. Changes in MAP values were compared by one-way ANOVA, followed by Tukey's Multiple Comparison post-hoc test (Graphpad Prism version 3.02, Graphpad Software, San Diego USA). Results are presented as the average change in MAP ± SEM for each strain and dose, and a *p* value of ≤ 0.05 was taken to indicate significant differences for all tests.

4.3. Results

4.3.1. Immunohistochemistry

As described in the previous chapter, the general anatomical arrangement of the SPN of the IML was different between the two strains. Figure 4.1 provides representative images of cGMP staining in WKY and SHR. Analysis of cGMP immunoreactivity of SPN within the IML of SHR and WKY rats is summarised in Fig 4.2A. WKY rats had an average intensity score that was 3-fold greater than that of the SHR (Fig 4.2B).

4.3.2. Effects of intrathecal 8-Br-cGMP on MAP

Prior to intrathecal injections, the baseline MAP was recorded in all experimental and control groups. The baseline recordings for the WKY groups, experimental and control were 97.0 $\pm$ 3.0 mmHg (n = 6), and 91.17 $\pm$ 3.6 mmHg (n = 6) respectively and were not significantly different (overall average MAP 94.085 $\pm$ 2.3 n = 12). The baseline MAP recordings for the SHR groups, experimental and control were 134.7 $\pm$ 0.5 mmHg (n = 6), and 130.8 $\pm$ 3.3 mmHg respectively and were not significantly different (overall average 136.75 $\pm$ 1.4 n = 12).

Changes in MAP in response to intrathecal administration of 8-Br-cGMP are illustrated in Figure 4.3. One-way ANOVA indicated a significant difference between all groups ($p \leq 0.0001$). Post hoc analysis indicated that in the SHR, each dose significantly increased MAP ($p \leq 0.01$) compared to PBS, and that the response seen with 100 μM 8-Br-cGMP was significantly greater than that seen with 1 μM and 30 μM 8-Br-cGMP ($p \leq 0.05$, respectively). In contrast, intrathecal 8-Br-cGMP did not cause a significant change in MAP in WKY animals. A 2-way ANOVA (strain

vs. dose of 8-Br-cGMP) indicated significant strain affect ($p \leq 0.0001$). The WKY data therefore reanalysed independently of the SHR. One-way ANOVA indicated a significant difference between groups ($p = 0.0036$) and post-hoc analysis showed that the 100 µM intrathecal dose of 8-Br-cGMP in the WKY caused a change in MAP that was significantly different to both the PBS and 1 and 30 µM injections ($p \leq 0.01$).

Figure 4.1: Relative expression levels of cGMP in SPN in SHRs and WKY

Light microscopy images depicting Cyclic GMP labeling of SPN detected with diaminobenzidase (DAB) immunohistochemistry in WKY (male, 6 months) (**A, C**) and SHR (male, 6 months) (**B, D**). In all images the central canal is to the right of the image, white matter to the left. Images A and B demonstrate distinct differences in SPN arrangement between the WKY (A) and SHR. Images C and D demonstrate individual SPN (*) which were further assessed for cGMP immunoreactivity intensity, corrected for background staining. It is apparent from these images by visual assessment that there is a difference in the level of intensity of staining. Scale bar equals 50μm (A, B), and 100 μm in (C, D).

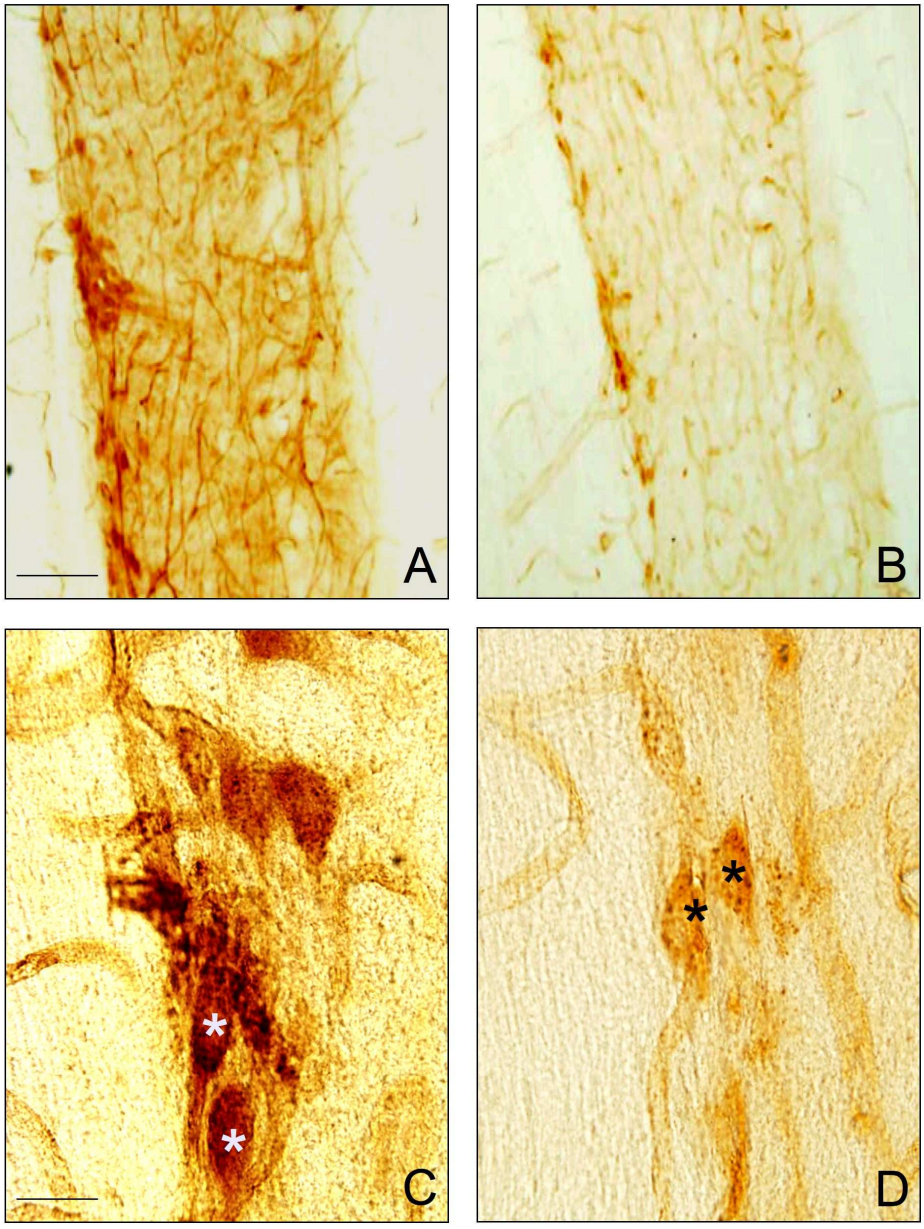
A
B
C
D

Figure 4.2: Arbitrary readings for cGMP expression in SHRs and WKY

Panel A provides the uncorrected arbitrary intensity readings for cGMP immunoreactivity (cGMP-IR) straining for individual WKY and SHR adult animals *(n* = 4, each). Figure 4.2B graphically represents the differences in cGMP expression between the SHR and WKY. The Y-axis indicates the difference of cGMP-IR intensity between cell and background (arbitrary units, scale 0 – 255). Results show that WKY have relative intensity reading that is 3 fold greater that that seen in the SHR when corrected for background staining ($p \leq 0.05$).

A Intensity of cGMP-IR for each WKY and SHR

	Intensity of cGMP-IR	
Animal No	WKY	SHR
1	108.62	72.76
2	168.67	42.5
3	169.26	67.52
4	170.31	49.53

B Average intensity of cGMP-IR in WKY and SHR

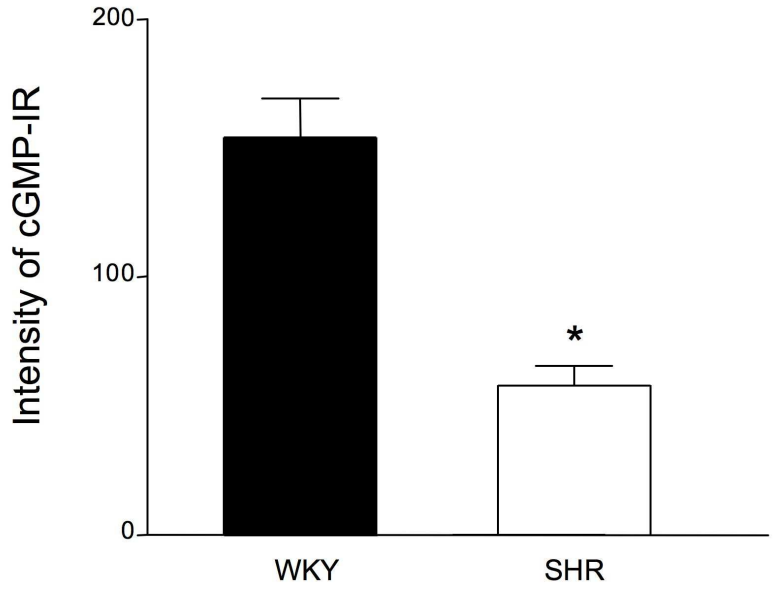

Figure 4.3: Change in MAP for SHRs and WKYs in response to intrathecal 8-br-cGMP

Changes in mean arterial pressure (MAP) in WKY and SHR in response to intrathecal administration of the cGMP [8-bromo-cGMP: 8-Br-cGMP, 1, 30 and 100 µM dissolved in phosphate buffered saline (PBS; 0.1M, pH 7.4)]. Results are presented as the average change in MAP ± sem. for each animal strain and dose used. *Response to 100 µM 8-Br-cGMP in the WKY were significantly different to PBS, 1 and 30 µM ($p \leq 0.01$). ** Response to 100 µM 8-Br-cGMP in the SHR is significantly different to that PBS, 1 and 30 µM of 8-Br-cGMP ($p \leq 0.05$). All dosages of 8-Br-cGMP significantly increased MAP compared to PBS.

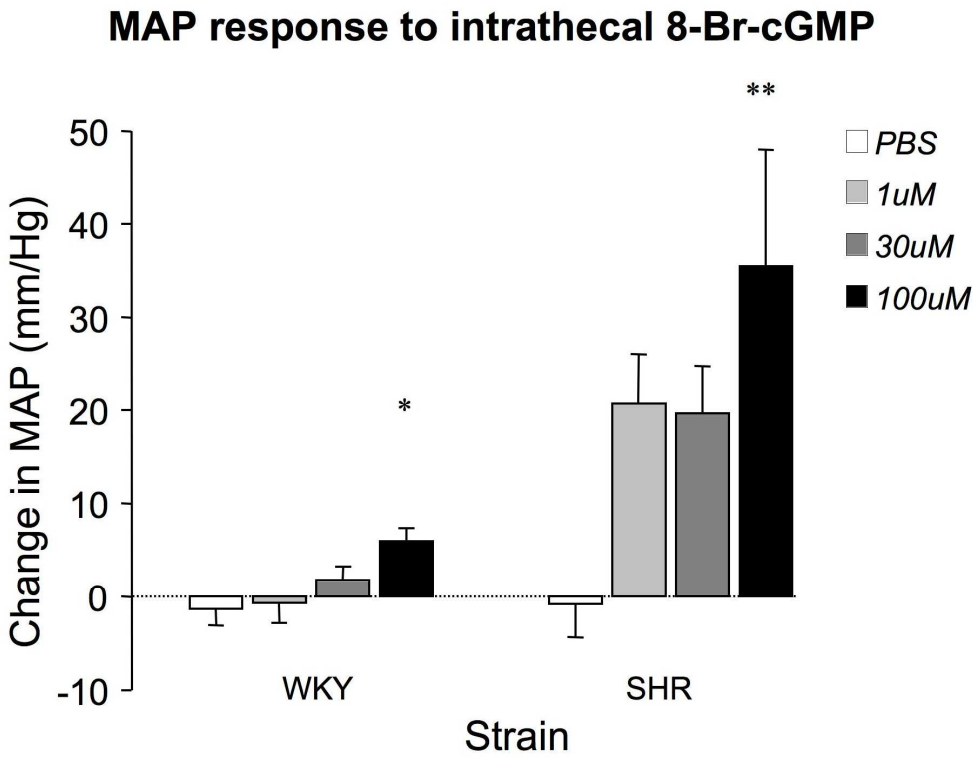
MAP response to intrathecal 8-Br-cGMP
Change in MAP (mm/Hg)
50
40
30
20
10
0
-10
*
**
WKY
SHR
Strain
PBS
1uM
30uM
100uM

4.4. Discussion

The major findings of this study are (i) that the basal detection of cGMP levels within the SPN, as shown using immunohistochemistry, is significantly less in SHR compared to WKY rats, correlating with our finding of a reduced number of nNOS producing SPN (Chapter 3) and (ii), that intrathecal administration of exogenous 8-Br-cGMP induces a marked increased in MAP in the SHR, while in the WKY, only a small increase in MAP could be elicited at the highest dose used. These results agree with recent work by our group looking at intrathecal pressor response to cGMP in Sprague Dawley rats (Malik et al 2007), but highlight significant strain variation that may be linked to the degree of autonomic tone. Overall, these results suggest that while there is less endogenous cGMP in SPN of the SHR under basal conditions, the functional response to exogenous cGMP is not diminished and indeed is enhanced.

4.4.1. Methodological issues

Catheter placement is a key issue with regard to the outcome of the intrathecal injection experiments. In 1976, Yaksh and Rudy (Yaksh and Rudy, 1976) examined intrathecal spread of drug in the spinal cord and demonstrated that drugs injected at the level of T12 (tip of the cannula) flow further rostral than they do caudal. Furthermore, the spread of a 10μL injection from T12 is restricted to the upper thoracic region of the spinal cord, where the majority of the SPN that provide cardiac and vascular sympathetic innervation are located (Malik et al., 2007). Our placement of the catheter tip at T12 was therefore appropriate and would have further served to prevent distribution of the drug to brainstem cardiovascular centres.

Given that intrathecal injection will affect all parts of the spinal cord to which the drugs spreads, it could be argued that the changes in MAP recorded were not

solely due to changes in the activity of SPN. However, based on our work (Chapter 3) and that of others (Anderson, 1992 (Chapter 3); Tang et al., 1995b), the localisation of cGMP, and NOS within the upper thoracic spinal cord is limited to SPN and the dorsal horn, where presumably, NO serves to modulate pain pathways (Dun et al., 1992; Reuss and Reuss, 2001). We can therefore speculate that the responses to intrathecal 8-Br-cGMP injection were modulated by the SPN in the IML regions targeted.

4.4.2. Reduced cGMP expression within SPN

The reduced expression of cGMP in the SPN of SHRs relative to WKY was predicted in accord with the results of Chapter 3. Our demonstration of cGMP in all SPN indicate it is a key signalling molecule in this cell population, and our finding of both a reduced number of NOS neurons (Chapter 3) and reduced basal level of cGMP suggests that NO-cGMP signalling is altered in SHR, and may therefore be associated with the hypertension seen in these animals. Such a phenomena is described in the RVLM of SHR, where decreased activity of the L-arginine-NO pathway is also thought to contribute to hypertension in this model (Kagiyama et al., 1998).

As described in Chapter 1, cGMP is formed within neurons when NO binds to sGC. For activity, both α and β isoforms of the sGC are required in 1:1 stoichiometry (Cabilla et al., 2006) and the balance of these subunits is critical to cGMP production. It is possible that in the SHR, decreased expression or malfunctioning of sGC receptors in the SPN could inhibit or reduce their capacity to produce cGMP. For example, it has been shown in pituitary tissue that the application of estradiol causes both the mRNA and protein levels of the $\alpha 1$ subunit to increase, and $\beta 1$ to decrease (Cabilla et al., 2006). This imbalance results in unstable sGC subunits and

consequently a reduction in cGMP (Cabilla et al., 2006). Further support for this hypothesis arises from studies using ANP. Stimulation of primary brainstem cultures with ANP show that there is significantly less cGMP produced in SHRs comparative to WKYs (Tang et al., 1993) and this down regulation has been attributed to a reduction of guanylate cyclase-coupled ANP receptors. Future studies aimed at elucidating the level of expression of the α and β isoforms of sGC in SPN, and the capacity for natriuretic peptide to regulate cGMP synthesis in SPN would be warranted.

4.4.3. Intrathecal administration of exogenous cGMP

While our initial work (Chapter 3) led us to consider that reduced NO, and therefore cGMP levels in the SPN of SHR was a "causal" mechanism that drove increased sympathetic drive at the level of the spinal cord, this hypothesis required revisiting based on recent studies from our group examining the effect of intrathecal delivery of (the membrane permeable analogue of cGMP) 8-Br-cGMP (Malik et al., 2007). In that study it was shown MAP in Sprague-Dawley rats increased in response to exogenous cGMP in a dose dependent manner. We therefore predicted that the intrathecal injection of 8-Br-cGMP would result in an increase in blood pressure in both strains. This is indeed what we were able to demonstrate, however, the results also show a significant strain-dependent effect, with the SHR demonstrating much greater pressor responses at all doses tested. Like the Sprague-Dawley (Malik et al., 2007), both strains showed the greatest response to 8-Br-cGMP at the highest 100μM dosage, but again this was significantly more pronounced in the SHR. It is possible therefore that in the SHR, the SPN have a heightened responsiveness to the NO-sGC-cGMP cascade, and that it has functional consequences. Such a differential

responsiveness has been documented in WKY and SHR previously. In the aorta of the SHR, despite a reduced basal level of cGMP, stimulation with the excitatory drug YC-1 produces a significantly greater increase in cGMP compared to the WKY (Ruetten et al., 1999), and the use of the adenoviral vector, Ad.PRS-nNOS, which drives nNOS, reverses the attenuated production of cGMP (Li et al., 2007). These results suggest a compensatory increased sensitivity or effectiveness of the NO-sGC-cGMP pathway in the SHR (Ruetten et al., 1999).

Alternatively, the increase in blood pressure seen in response to 8-bromo-cGMP administration may be due to a decreased capacity to breakdown cGMP in the SHR. An approach to address this would be to radio isotope tag 8-Br-cGMP, and then measure the break down rate using radioimmunoassay on slices of spinal cord taken at various time points. This approach has been used by (Rengasamy et al., 1997), to demonstrate the effect of inhaled anaesthetics on NO and cGMP production.

Another possibility is that the increased responsiveness to intrathecal 8-Br-cGMP in the SHR is due to heightened downstream effects. A number of secondary pathways, including the protein kinase G (PKG) and cGMP modulated ion channels may be modified in these animals. It has already been shown that the stimulation of protein kinase C in aortic tissue of SHRs results in heightened sensitivity compared to the WKY, as the aorta of these rats display increased contractility and decreased ability to relax (Bruschi et al., 1988).

An interesting study by Schmid and Pehl (Schmid and Pehl, 1996) examined the electrophysiological effect of NO donors and cGMP donor on neurons in the spinal cord. Lumbar spinal cord slices were superfused with NO donor sodium nitroprusside (SNP) and then 8-Br-cGMP. In the lamina I and II neurons, 32% of neurons were excited by both SNP or 8-Br-cGMP, 46% were inhibited by both SNP

or 8-Br-cGMP and 22% had no response to either compound. If there are similar excitatory and inhibitory NO-cGMP dependent responses in SPN, is it possible that the proportions change in the SHR relative to the WKY. In Chapter 3, we illustrated neurochemical and anatomical differences in the SPN of the SHR, which may perhaps also reflect altered inhibitory/excitatory neuron distribution.

4.4.4. Conclusion

The work by Malik et al. (Malik et al., 2007) determined that not only does intrathecal 8-Br-cGMP and L-arginine increase blood pressure, but in the case of haemorrhage, preadministration of 8-Br-cGMP attenuates the fall in MAP while ODQ augments it. Interestingly, intrathecal ODQ did not alter basal MAP, suggesting that the endogenous formation of cGMP is not a key factor driving resting MAP, but that it assumes greater importance under relevant physiological stimuli. As the NO-cGMP pathway in the SHR appears to be sensitised, it would therefore fit that only small changes in cGMP levels, as through exogenous administration, would elicit a pronounced response.

Given our combined neuroanatomical and functional findings, it is now possible to speculate that reduced levels of cGMP expression in the SHR are not necessarily contributing to the hypertension, but that they are instead a consequence. Down regulation of the levels of cGMP, mediated by reduced endogenous NO production, are a reflex response mediating the pressor effects of cGMP.

5. Differential expression of neuronal nitric oxide synthase and inducible nitric oxide synthase in the rostral ventrolateral medulla of the Spontaneously Hypertensive rat

5.1. Introduction

Brain pathways controlling arterial pressure are distributed throughout the neuraxis in discrete topographically arranged networks. Within the rostral ventrolateral medulla (RVLM) sympathoexcitatory neurons directly innervate sympathetic preganglionic neurons (SPN) in the spinal cord and are critical to the tonic and reflex regulation of sympathetic tone and therefore of arterial blood pressure (Lipski et al., 1997). The activity of these RVLM neurons is regulated not only by baroreceptor input via the nucleus tractus solitarii (NTS) and caudal ventrolateral medulla (CVLM) (Loewy, 1991), but also by synaptic inputs from many other areas of the central nervous system. An increase in sympathoexcitatory output from the RVLM has been reported in different forms of hypertension, despite different initiating mechanisms (Campese, 2000; Colombari et al., 2001; Rahn et al., 1999).

Recently, evidence for interactions between nitric oxide (NO) and sympathetic output via the RVLM has been presented (Chan et al., 2003a; Chan et al., 2001b). However, the role of this molecule is controversial, for although inhibitory effects evoked by NO within the RVLM have been described (Maeda et al., 1999), excitatory effects have also been reported (Hirooka et al., 1996; Martins-Pinge et al., 1999). It

has been proposed that NO produced from different sources [i.e. neuronal NO synthase (nNOS) vs. inducible NO synthase (iNOS)] mediate differing effects on sympathetic output and blood pressure. In a study by Chan (2003), application of nNOS or iNOS blockers in anaesthetised rats resulted in a respective reduction or increase in mean arterial pressure (MAP) (Chan et al., 2001c). Furthermore, investigations in conscious rats have indicated that microinjection of nNOS inhibitors appears to decrease MAP, while iNOS inhibitors increases MAP (Martins-Pinge et al., 2007). These studies indicate nNOS having an excitatory action, while iNOS is inhibitory. Furthermore, co-injecting iNOS inhibitors with glutamate, which has an excitatory action on bulbospinal RVLM neurons, appears to accentuate the action of glutamate, while the opposite happens when nNOS is applied, further adding support to iNOS and nNOS having differential effects (Martins-Pinge et al., 2007).

Given the discrepancies in the literature and the indication that different isoforms of NOS within the RVLM affect blood pressure differentially, the present study was designed to investigate if differences in the expression of NOS isoforms exist between the normotensive Wistar Kyoto (WKY) rat and the Spontaneously Hypertensive Rat (SHR). As nNOS appears to enhance MAP, we predicted that the relative expression of nNOS would be greater in the SHR, compared to the WKY. Reverse transcription polymerase chain reaction (RT-PCR) experiments were designed to assess differential expression of iNOS and nNOS mRNA followed by assessment of protein levels using immunohistochemistry.

5.2. Materials and methods

5.2.1. Animals

All experiments were carried out with the approval of the Animal Ethics Committee of Murdoch University, Western Australia. Gene expression data was obtained from mature male WKY and SHR rats (n = 9 each strain, 16-23 weeks old). Systolic arterial blood pressure was measured 1-2 weeks prior to tissue collection for mRNA analysis using the tail-cuff method. Blood pressure values for WKY and SHR were, respectively, 127.6 ± 16.7 mm Hg (n = 9) and 198.4 ± 18.8 mm Hg (n = 9). Prior to decapitation for tissue removal, animals were anaesthetised with carbon dioxide (CO_2). A further 3 SHR and 4 WKY male animals (12-14 weeks old) were used for immunohistochemical testing of nNOS protein expression in the RVLM. These animals were lightly anaesthetised with CO_2, and then deeply anaesthetised with sodium pentobarbitone by intraperitoneal (IP) injection (Nembutal; Nembutal Sodium Solution; Abbott Laboratories, Co. Ltd., Chicago, IL, USA; 100mg/kg) prior to perfusion with fixative through the ascending aorta.

5.2.2. Reverse transcription-polymerase chain reaction (RT-PCR)

Polymerase chain reaction experiments were performed by Mrs Rhonda Loxley and Mr Mark Edwards at Murdoch University, South St, Murdoch.

Tissue preparation and RNA extraction

The brainstem was removed and frozen with dry ice in sterile 0.1M phosphate buffer (PB). Sections (200 μm) were cut on a freezing cryostat, and the RVLM region of the ventrolateral medulla identified under a light microscope (Wild M7 S, Wild Heerbrugg, Switzerland). Bilateral tissue punches were taken from sections

containing the RVLM (6-8 punches in total from 3-4 slices from each animal) with a sharpened needle (external and internal diameters, 1.2 and 1.0 mm respectively). The RVLM was identified as that region extending caudally 600-800 μm from the caudal pole of the facial nucleus. This corresponds to -12.5 mm to -11.7 mm caudal to Bregma (Paxinos and Watson, 1998). The region was bounded laterally by the spinal trigeminal tract, medially by the inferior olive and pyramids, and dorsally by the compact formation of the nucleus ambiguus, as described by us previously (Fig. 5.1) (Phillips et al., 2001). The punches were transferred into isolation reagent (Promega Total RNA Isolation System; Promega, WI, USA) and total RNA extracted according to the manufacturer's instructions. Contaminating genomic DNA was destroyed using RQ1 DNAse 1 (1U, Promega) in 1X buffer at 37^{o} C for 20 min, containing 40U of RNAsin (Promega). RNA was re-extracted with phenol/chloroform/isoamyl alcohol and Phase Lock Gel Tubes (Eppendorf; Brinkman Instruments, NY, USA) and precipitated in 100% ethanol with 20 U glycogen (Roche) and 0.3 M sodium acetate (pH 4.0).

Figure 5.1: Location of the RVLM

Photograph illustrating the location of the tissue punch site, RVLM, NTS, inferior olive, pyramidal tracts and the compact formation of the nucleus ambiguus.

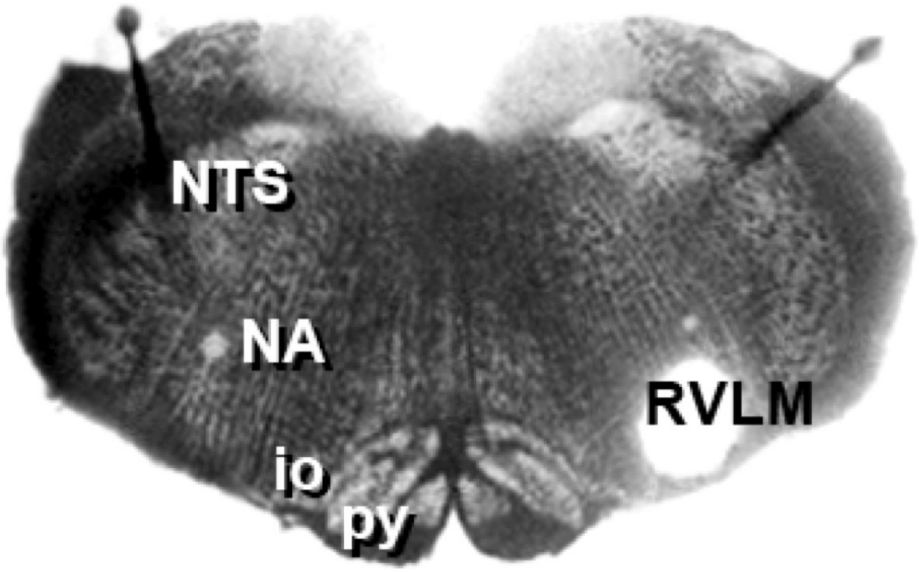
NTS
NA
RVLM
io
py

Reverse transcription – polymerase chain reaction

The RNA was reverse transcribed in a 20 µl final volume using Superscript II (100U, Invitrogen, CA, USA) in 1X RT buffer, with 2.5 ng/µl random primers, 1 mM each deoxynucleoside-triphosphate (dNTPs), 5 mM dithiotreitol and 20 U RNAsin at 42^{o}C for 45 min and then 50^{o}C for 30 min. The RT enzyme was heat inactivated (90^{o}C for 5 min).

Only samples that tested positive for the catecholaminergic marker phenylethanolamine N-methyltransferase (PNMT) were used for subsequent analysis. This gene was used as a control for regional location, given the position of the catecholaminergic C1 cell group in the RVLM (Paxinos and Watson, 1999). Primers for PNMT were as described by Andreassi *et al.* (Andreassi et al., 1998). Not all genes could be tested in all samples due to the small amounts of RNA extracted from each region and therefore results were pooled. Each result represents data obtained from a minimum of three separate animals.

Quantitative Real-Time PCR

Real time PCR was performed using an ABI Prism 7700 Sequence Detection System (Applied Biosystems). The reactions were performed in the presence of conventional forward and reverse primers and an MGB Taqman probe labelled with a fluorescent reporter dye (FAM or VIC©). Primers and probes for nNOS and iNOS were designed using Primer Express (Applied Biosystems) software (see Table 5.1 for primer and probe details). Expression of nNOS and iNOS were normalised to an endogenous control gene (neuronal specific enolase; NSE) to give a ΔCt value (see *Real-time data analysis*). This allowed us to account for variability in the initial

starting amount of cDNA. Multiplexed reactions (where target and control gene primers and probes were amplified in the same tube) were compared with non-multiplexed reactions to check that one primer pair was not limiting the performance of the other. For the iNOS primers, the Ct values from the reactions could not be matched, and subsequent reactions were therefore performed in separate tubes. Linear range analysis (diluting template cDNA 10 - 1000 fold; n = 3) was used to assess amplification efficiency. For both sets of primers, the ΔCt value between target and NSE remained constant.

Table 5.1: Primer and Probe Sequences and Conditions used for Real-Time PCR

Primer/ Probe	Sequence	Product Size (bp)	Sequence GenBank ID	Conc. (nM) [(a)]
PNMT		288		
Forward primer	5′-CAACAACTACGCGCCTCCTC-3′			200
Reverse primer	5′-TGAGGCCAGACATGCTGGCTAT-3′			200
Taqman probe				
NSE		89	M11931	120
Forward primer	5′-GGGCACTCTACCAGGACTTTGTC-3′			120
Reverse primer	5′-TGGACCAAGCTGCCCAGT-3′			250
Taqman probe	5′-FAM-CATGGAAAAACACAATTAC-3′			
nNOS		84	X59949	
Forward primer	5′-ATCGGCGTCCGTGACTACTG-3′			300
Reverse primer	5′-TCCTCATGTCCAAATCCATCTTCT-3′			300
Taqman probe	5′-FAM-CCTGGAGGAAGTAGCCA-3′			250
iNOS		95	U03699	
Forward primer	5′-TGGCCTCCCTCTGGAAAGA-3′			900
Reverse primer	5′-GGTGGTCCATGATGGTCACAT-3′ 5′-			900
Taqman probe	FAM-CTGCTTCTGAAAACTAT-3′			250

Table 5.1. Table depicts the primer and probe sequences used to identify the mRNA for nNOS and iNOS; (a) concentration of primer or probe used in the real time PCR reaction.

Real-time data analysis

Results obtained using primers for NSE were used to normalise the data. To determine relative concentrations of DNA during the exponential phase of the reactions, level of fluorescence is plotted against cycle number on a logarithmic scale, so an exponentially increasing quantity will give a straight line. A threshold for detection of fluorescence above background is determined. The cycle at which the fluorescence from a sample crosses the detection threshold is called the cycle threshold (Ct). The NSE Ct values were subtracted from the Ct value for each gene (to give ΔCt values). These values were used to carry out statistical comparisons between genes and within strains. For graphical representation, the fold variation was then determined using the $2^{-(\Delta\Delta Ct)}$ method according to published protocols (Livak and Schmittgen, 2001) and the manufacturer's recommendations. Fold-variation was calculated by determining the difference in ΔCt values between a chosen reference and test sample (ΔΔCt value), and applying the $2^{-(\Delta\Delta Ct)}$ formula. The range values were then determined using the formula $2^{-(\Delta\Delta Ct \pm SD\ \Delta Ct)}$ (Livak and Schmittgen, 2001). When comparing individual genes between rat strains, the reference was expression levels of each gene in the WKY animal. For determination of relative expression of the NOS isoform expression, nNOS was used as the reference gene.

Statistical analysis

Values are reported as mean ± standard deviation (sd) of the ΔCt values. Reported *n* values indicate actual PCR reaction numbers. Duplicate or triplicates reactions from a minimum of three animals were pooled. Statistical analysis was performed using the SPSS Statistical Package (SPSS Inc., IL, USA). A two-tailed

Students t-test was used for analysis with the assumption of equal variance to compare individual genes in SHR vs. WKY and iNOS vs. nNOS.

5.2.3. Immunohistochemistry

Processing

Animals were perfused with ice-cold solutions of 0.9% saline with heparin (1000 IU/ml), followed by a 4% solution of formaldehyde in 0.1M phosphate buffer (PB; pH 7.4). The brainstem was then removed and post fixed for 2 – 4 hours at 4°C. Horizontal sections of brain stem (50 μm thick) were cut on a vibrating microtome (section 2.5.1) and alternate sections were collected in series for subsequent examination. Sections were treated for immunofluorescence immunohistochemistry as per section 2.5.2. Table 5.2 lists the nNOS antibody and dilution used for this experiment. Control experiments were processed in parallel without the addition of primary antibody.

Table 5.2: Antibody combination used for fluorescence immunohistochemistry in Chapter 5

Animal	Combination	Dilution	Conjugated to	Dilution
WKY (*n* = 3) & SHR (*n* = 3) 10 - 12 weeks	mouse α nNOS	1:400	FITC: donkey α mouse	1:500
WKY (*n* = 3) & SHR (*n* = 3) 10 - 12 weeks	sheep α PNMT	1:500	CY2: donkey α sheep	1:500

Table 5.2. Table details the various antibody combinations used in each of the immunohistochemical experiments investigating the basal levels of nNOS or PNMT expression in the RVLM in WKYs and SHRs. Alternating sections were taken from each animal, one series being processed for nNOS, the other series being processed for PNMT. Source, batch and abbreviations detail can be found in Table 2.1.

Imaging and quantitation

Sections were imaged as detailed in section 2.6.1. To count cell numbers, composite figures of the RVLM region were assembled using PhotoShop software (Version 7, Adobe Systems, Mountain View, CA). Overall colour balance and contrast were adjusted; however no other changes were made. Only nNOS immunoreactive cell profiles that included a nucleus or PNMT neurons with a complete profile were counted. A total of 8 sections were examined from each animal, extending 800 μm from the facial nucleus as described for the tissue punch RNA extraction (Section 5.2.2). Rostrocaudal distribution patterns represent bilateral cell counts made every 100 μm. The mean ± sd was calculated from a minimum of three animals. Statistical difference was calculated using a two tailed Students t-test assuming equal variance.

5.3. Results

5.3.1. Quantitative analysis of NOS isoform expression in the RVLM

Table 5.3 presents the NOS isoform mean ΔCt scores ± sd. and results of analysis for significant difference between variables. Data was then transformed to show fold variation and range.

Comparative analysis of expression levels of each gene *between* rat strains, utilising the WKY as the reference, indicated that nNOS expression in the SHR was 1.76 times higher than the WKY (Fig. 5.2, $p \leq 0.05$ determined using the ΔCt values; Table 5.3). Although there was a trend towards higher levels of iNOS mRNA expression in the SHR, there was no significant difference in the levels between the two strains. Comparison of the isoform data indicated that iNOS mRNA was expressed at significantly lower levels than nNOS within the RVLM of both rat strains ($p \leq 0.05$) being 0.03 (± 0.01) that of nNOS in both the SHR and WKY.

Figure 5.2: Relative mRNA expression within the RVLM of NOS isoforms in WKY and SHRs

Relative expression of NOS isoforms in RVLM punches taken from SHR and WKY. Data presented as fold difference ± range values, determined using the $2^{-(\Delta\Delta Ct)}$ and $2^{-(\Delta\Delta Ct \pm S.D.\ \Delta Ct)}$ formulas, respectively, relative to the expression level in WKY animals (= 1). Significant differences were seen in the levels of nNOS (higher level in the SHR) (**$p \leq 0.05$). Data represent sample results pooled from a minimum of three animals each.

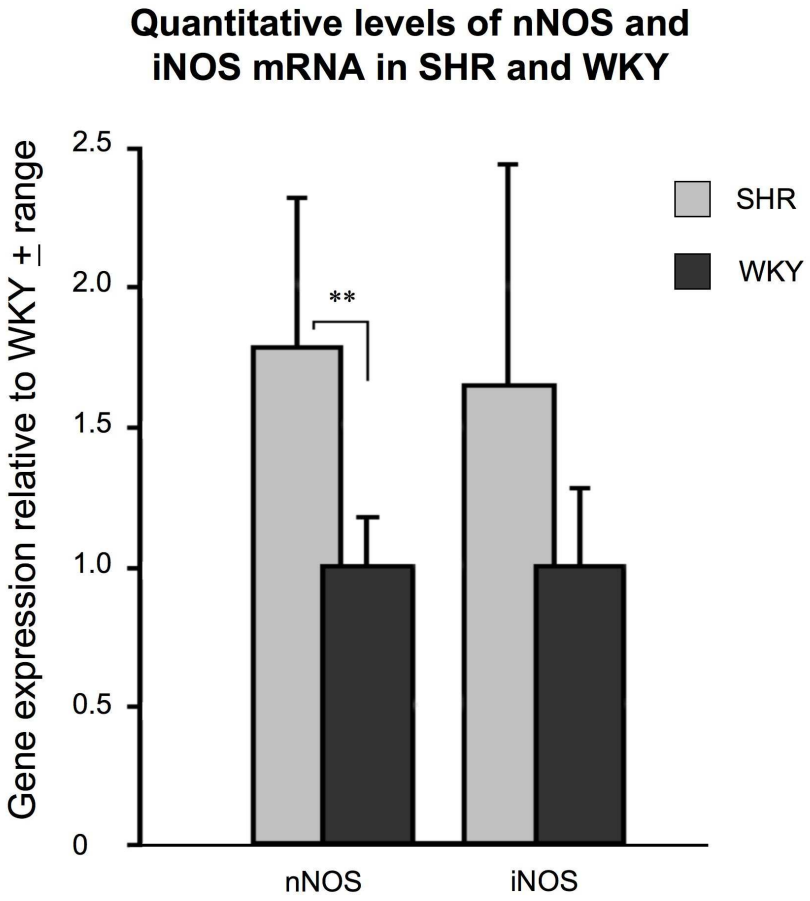
Quantitative levels of nNOS and iNOS mRNA in SHR and WKY
Gene expression relative to WKY ± range
2.5
2.0
1.5
1.0
0.5
0
**
SHR
WKY
nNOS
iNOS

Table 5.3: Means and standard deviation of ΔCt values for NOS isoform genes from each rat strain

	nNOS	iNOS
SHR	$^{9}4.58+0.38_{a,b}$	$^{7}9.84+0.94_{a}$
WKY	$^{8}5.41+0.27_{b,c}$	$^{7}10.56+0.47_{c}$

Table 5.3. Italic superscript indicates value of n for each sample. Means labelled with the same alphabetical subscript are statistically different (p <0.05), as determined by Student's t-test for paired comparisons (nNOS vs. iNOS and SHR vs. WKY). Note lower ΔCt values indicate higher relative levels of mRNA expression.

5.3.2. nNOS immunoreactivity in the RVLM

In order to confirm the finding of increased nNOS expression in the RVLM of SHR animals, fluorescence immunohistochemistry was performed using an antibody directed against nNOS. Confocal imaging demonstrated a cluster of nNOS immunoreactive neurons located predominantly in the region of the lateral paragigantocellular nucleus (Fig. 5.3.). The rostrocaudal distribution of nNOS immunoreactive cells was assessed along the axis of the RVLM. There was some variability between individual animals, but the majority of nNOS cells were located caudal to the facial nucleus. When comparing the SHR and WKY animals, the total number of cells counted in the RVLM region was not significantly different (SHR = 573 ± 164.9 n=3 vs. WKY = 357.5 ± 122 n=4) but when individual rostrocaudal levels were compared using a students' t-test, significantly greater numbers were seen at the rostral end of the RVLM in the SHR ($p \leq 0.05$). Control experiments that did not contain any primary antibody did not show any labelled cells.

Figure 5.3: Neuronal NOS immunoreactivity in RVLM

(A) Confocal image illustrating nNOS immunoreactivity in the RVLM of an SHR. Midline is located to the left and ventrolateral edge by the dotted line. The nNOS-immunoreactive cells were predominantly located adjacent to the inferior olive (io). Scale bar equals 100 μm. (B) Rostrocaudal distribution pattern of nNOS immunoreactivity in neurons of the RVLM of SHR and WKY animals. Figure shows mean ± sd of cells counted bilaterally in RVLM region in sections taken every 100 μm. Results illustrate that the majority of the nNOS immunoreactive neurons are located in the region caudal to the facial nucleus (7th) and that there are significantly more cells staining for nNOS in this area in the SHR as compared to the WKY (**$p \leq 0.05$, n=7).

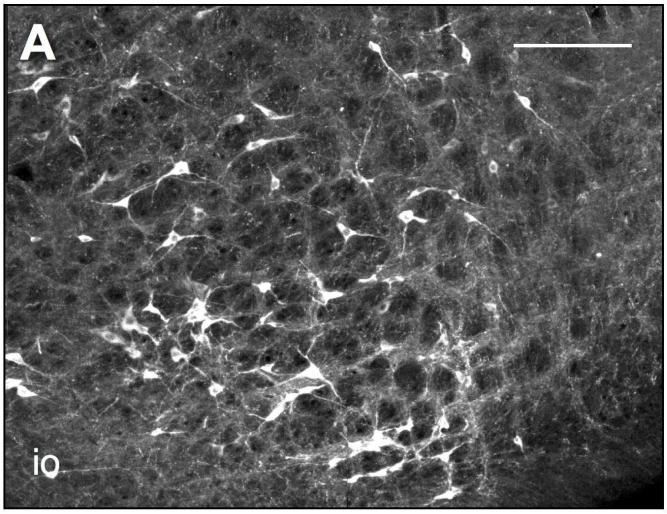
A
io

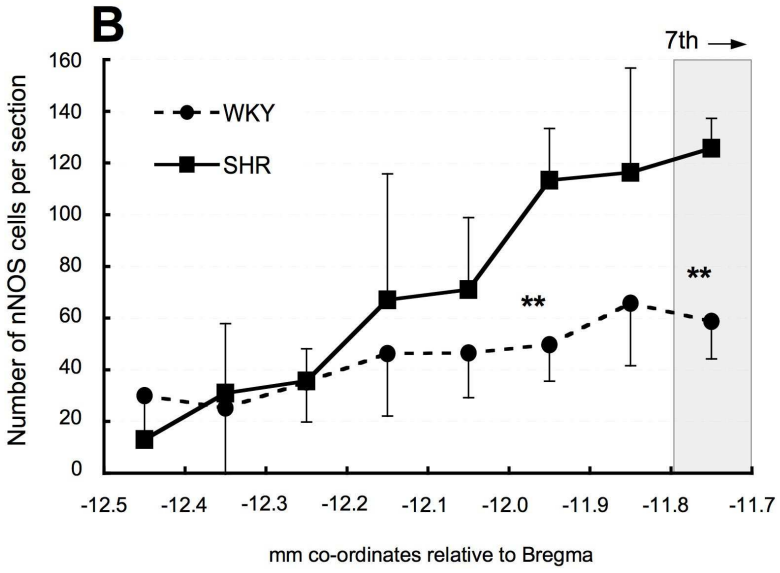
B
7th
160
140
120
100
80
60
40
20
0
WKY
SHR
**
**
Number of nNOS cells per section
-12.5
-12.4
-12.3
-12.2
-12.1
-12.0
-11.9
-11.8
-11.7
mm co-ordinates relative to Bregma

5.4. Discussion

This study has demonstrated differential expression of nNOS in the RVLM of SHR as compared to the WKY rat strain. Quantitative analysis showed nNOS mRNA levels were greater in SHR animals than WKY and that iNOS levels were at significantly lower levels than nNOS for both strains. The nNOS finding was confirmed using immunohistochemistry to assess nNOS protein expression throughout the RVLM region.

5.4.1. Methodological considerations

Quantitative real-time PCR was used for this study as it is an accepted highly sensitive methodology that allowed us to compare a large number of genes from a very small amount of starting material. Neuron specific enolase, which was used to normalise gene expression levels, is a glycolytic enzyme responsible for converting 2-phospho-D-glycerate to phosphoenolpyruvate (Marangos et al., 1978). To confirm the suitability of NSE as an endogenous housekeeping gene, work from our colleagues has shown previously that the levels of this gene do not vary in central sites between rat strains (Reja et al., 2002c). Further evidence for NSE as a sound endogenous control are studies that show constant mRNA levels of this gene despite various neuronal states, including status epilepticus and traumatic brain injury (Iino et al., 2003; Schreiber et al., 1999).

Our results show some differences from the quantitative mRNA data reported previously regarding the level of expression of NOS isoforms within the RVLM (Chan et al., 2001a; Chan et al., 2003b; Plochocka-Zulinska and Krukoff, 1997). A number of factors may have contributed to these differences. First, our study

analysed gene expression levels in older animals (≥ 16 weeks), while the study by Chan *et al*., 2001 (Chan et al., 2001a) used 8-10 week old animals. Second, both the type and time of anaesthesia prior to euthanasia may be a contributing factor, resulting in a change in transcription. For example, in the work by Chan *et al*., 2001, 2003 (Chan et al., 2001a; Chan et al., 2003b) both sodium pentobarbitone and propofol were used, and then the animals were paralysed with pancuronium which would have resulted in a much longer time frame between anaesthetic induction and death/tissue removal compared to our study that involved the use of CO_2 and decapitation. This may have caused different gene expression levels and such a possibility is supported by work conducted in other brain areas. For example, NR2C message in the hippocampus and cortex is up-regulated in the long-term, but not immediately following a hypoxic episode (Perez-Velazquez and Zhang, 1994). We suggest that our study, which used a very short time frame between induction of anaesthesia and death, more closely represents basal expression levels of the NOS isoforms. However, the possibility of post transcriptional and translational regulation applies limitations to any inferences drawn from mRNA analysis.

5.4.2. Neuronal nitric oxide synthase expression

Our study demonstrated a significant increase in the mRNA and protein expression of nNOS in the RVLM of the SHR. Both the mRNA and immunohistochemical data from tissue punches and the rostral portion of the RVLM, respectively, showed close to twice as much nNOS in the SHR as compared to WKY. While the population of nNOS neurons in the RVLM has been described previously (Chang et al., 2003; Iadecola et al., 1993; Paxinos and Watson, 1999), this is the first study to show increased expression of nNOS at both the protein and mRNA levels in

a hypertensive rat strain. These nNOS containing cells do not project to the spinal cord (Iadecola et al., 1993), but they have been implicated in central autonomic control by their proximity to the RVLM and it is possible they form part of a network of modulatory interneurons in the region (Zanzinger, 1999).

Microinjection studies indicate that the neurons within the RVLM are susceptible to modulation by NO, with both inhibitory and excitatory effects over sympathetic output from the region being described (Maeda et al., 1999). An alteration in the balance between nNOS and iNOS activity may underlie the genesis of augmented sympathetic vasomotor tone during hypertension. This was elegantly demonstrated by Chan *et al*., 2001 (Chan et al., 2001c), who using selective blockade of nNOS and iNOS in the RVLM, elicited a reduction or enhancement of sympathetic vasomotor outflow, respectively. More recent work by this group (Chan et al., 2003b) showed that NO derived from nNOS in the RVLM induces sympathoexcitation via activation of both NMDA and non-NMDA receptors, and sympathoinhibition elicited by NO generated by iNOS is mediated by $GABA_A$ receptors. Our finding that nNOS has a comparatively greater expression than iNOS in both strains suggests that the proposed sympathoexcitatory effects of NO production may generally predominate in the RVLM. While not examined in our study, higher levels of nNOS expression could therefore be considered as a potential factor contributing to increased sympathetic tone from the region. Alternatively, it is possible that increased expression of nNOS in the RVLM of SHR is a compensatory response to elevated blood pressure. A study by Plochocka-Zulinska and Krukoff (Plochocka-Zulinska and Krukoff, 1997), demonstrated increased nNOS expression in the hypothalamus, dorsal medulla and CVLM of adult SHR, but not in young pre-hypertensive rats or WKY and Sprague Dawley rats. The

inference drawn from these studies was that NO production is up-regulated in specific brain regions in response to increased sympathetic activity in order to re-establish homeostatic balance. Obviously further studies will be required to address these issues.

5.4.3. No difference in iNOS expression between the two strains

This study also demonstrated that there appeared to be no difference in the level of iNOS mRNA expression between the two strains. As no differences were found at the mRNA level, subsequent analysis of protein expression was not performed.

This is an interesting result as previous work has indicated that not only are there dose dependent changes in MAP in response to microinjection or blockade of iNOS (Chan et al., 2003b; Chan et al., 2001c), there have been previous studies detailing lower expression of iNOS in SHR rats compared to WKY (Chan et al., 2003a; Chan et al., 2001a). However, these studies were done in rats younger than the ones we tested, suggesting that the relative levels of iNOS in the SHR increases with age. Apart from the activation of sGC, NO can readily react with superoxide to form peroxynitrite (Ohkuma and Katsura, 2001), which can stimulate the release of GABA, providing NO with an alternative way of influencing neurotransmission (Mayorov, 2005). Increasing levels of iNOS through the use of an adenovirus in the RVLM causes a pressor response in awake normotensive rats, a result that is said to be in response to an increase in oxidative stress (Kimura et al., 2005). This is consistent with recent work has shown an increase in superoxide in the brain playing a key role in sympathoexcitation after myocardial infarction (Gao et al., 2004; Lindley et al., 2004). Finally, studies show that superoxide is involved in the tonic regulation of sympathetic outflow in the RVLM of WKY and SHRs, as

microinjection of superoxide dismutase, the enzyme that converts superoxide into oxygen and hydrogen peroxidase, reduces HR and MAP (Tai et al., 2005). The Chan study (Chan et al., 2001a) indicated that though both WKYs and SHRs respond to microinjections of iNOS with increases in MAP, the onset latency in SHRs was much faster, indicating increased relative sensitivity to NO production in the SHR.

5.4.4. Conclusions

This study has demonstrated that nNOS expression is significantly greater in SHR rats, while iNOS mRNA levels do not appear to be different. While this study has not addressed issues of cause versus effect, it has highlighted key differences that may underlie some of the functional diversity that has been described in the literature. Determining physiological relevance will be a key focus for future studies.

6. Immunohistochemical detection of soluble guanylate cyclase (sGC) and cyclic guanosine monophosphate (cGMP) within the rostral ventrolateral medulla

6.1. Introduction

The rostral ventrolateral medulla (RVLM) contributes significant excitatory drive to sympathetic preganglionic neurons (Lipski et al., 1995) via two well characterised phenotypic populations of neurons, the C1 (adrenergic) and non-C1 cell groups, which project monosynaptically to the spinal cord (Phillips et al., 2001; Stornetta et al., 2002). While glutamate is the major neurotransmitter driving sympathetic activity within the RVLM nitric oxide (Gordon and Sved, 2002) (NO) is thought to play a key role in regulating glutamate induced pressor responses, and therefore modulating the activity of RVLM neurons and in turn homeostatic blood pressure mechanisms (Chen et al., 2001; Huang et al., 2003; Wu et al., 2001). In the previous chapter (Chapter 5) we demonstrated an increase in NO expression in spontaneously hypertensive rats (SHR), and altered NO signalling in the RVLM is associated with increased sympathetic outflow in a number of animal models of hypertension (Krukoff, 1998), however the mechanism of action is unclear, with a range of effects attributed to NO being reported including NO-mediated pressor, depressor or neutral responses (Hirooka et al., 1996; Martins-Pinge et al., 1997; Tseng et al., 1996).

As described in Chapter 1, one of the most widely studied and best-understood NO second messenger systems is the activation of NO-receptor, soluble guanylate cyclase (sGC) and the subsequent generation of intracellular 3',5'-cyclic guanosine monophosphate (cGMP) (Ahern et al., 2002; Lucas et al., 2000). Soluble GC is a heme-containing heterodimer of α and β subunits, with the β1 subunit being the major subunit, as there is no catalytic activity in its' absence (Friebe et al., 2007; Mergia et al., 2003). Activation of NMDA receptors can drive this pathway, with increased intracellular Ca stimulating the Ca^{2+}/calmodulin NO system, promoting conversion of L-Arginine to NO. Intracellular cGMP levels can also be regulated by membrane bound, or particulate guanylyl cyclases, incorporating the receptors for atrial (ANP), brain (BNP) and C-type (CNP) natriuretic peptides (Lucas et al., 2000). As a second messenger, cGMP can target various protein kinases and ion channels, and its activity is limited through degradation by phosphodiesterases (PDE) (Lucas et al., 2000).

Nitric oxide has alternative neuromodulatory mechanisms. This includes the s-nitrosylation of proteins and in particular that of NMDA receptors (Ahern et al., 2002), and interactions with superoxide, with the resultant peroxynitrite having potent oxidising properties that convey a variety of physiological and pathophysiological effects (Ohkuma and Katsura, 2001).

While all three NO synthase (NOS) isoforms are present in the RVLM, as described in chapter 5, work by Chan *et al*. (Chan et al., 2003b) suggests that the relative balance of functional nNOS vs. inducible (i)NOS activity determines RVLM output, and further, that the different NOS isoforms activate different downstream signals, with nNOS driving sGC/cGMP-dependent sympathoexcitatory responses, and NO produced by iNOS driving peroxynitrite formation and sympathoinhibitory

responses (Chan et al., 2005). Glutamate-induced pressor responses in the RVLM are in general proposed to be modulated by NO-sGC/cGMP (Chen et al., 2001; Morimoto et al., 2000; Wu et al., 2001) and this is supported by electrophysiological studies showing cGMP-dependent potentiation of glutamate currents in RVLM slice preparations (Huang et al., 2003).

To date, no studies have described the immunohistochemical localisation of neurons capable of expressing cGMP within the C1 region (De Vente et al., 1998). Given the strong evidence that NO signalling plays a functional role in the RVLM we sought to identify the cellular targets for NO in the RVLM, visualising cGMP and its neuroanatomical relationship with the C1 cell group, as identified by the presence of phenylethanolamine N-methyltransferase (PNMT) and the more medially located nNOS expressing cell population (previous chapter; (Iadecola et al., 1993). Given the results presented in Chapter 5 showing significantly higher expression of nNOS in SHR compared to the Wistar Kyoto (WKY), and studies that show augmented responses to microinjection of glutamate in the RVLM in the SHR (Tsuchihashi et al., 2000; Tsuchihashi et al., 1998), we considered the hypothesis that downstream signalling pathways (i.e. the NO/sCG/cGMP pathway) may be altered. Our initial aim therefore was to determine if altered cGMP expression, as determined using immunohistochemistry, could be demonstrated in the RVLM of the SHR. Additional studies sought to increase synthesis of cGMP in fresh RVLM brain slices and examine sGC immunoreactivity (IR) throughout the region also.

6.2. Materials and methods

6.2.1. Animals

Male rats were used in all experiments. WKY (n = 22 in total) and SHR (n = 3 total) were used in the different age groups as detailed in each experimental protocol (Table 6.1 and 6.2).

6.2.2. Animal tissue preparation for immunohistochemistry

Rats were anaesthetised with sodium pentobarbitone (Thiobarb, Jurox, Rutherford, Australia; 100mg/kg) administered intraperitoneally. A pre-fixation solution of ice-cold heparinised saline was perfused via the ascending aorta as detailed in section 2.4. In one set of experiments, the phosphodiesterase inhibitor isobutylmethylxanthine (IBMX; 0.5mM Sigma, St Louis, MO, USA) was added to the pre-fixation saline solution. Brains were removed and sectioned on a vibrating microtome, as per section 2.5.1. Sections were split into two alternate series, with each section therefore 100 um apart. Sections were then treated for the immunohistochemistry in the combinations detailed as in Table 6.1, using the protocol described in section 2.5.2. Previous studies and manufacturers product information have documented the specificity of antibody reactions for cGMP (Chapter 3), nNOS (Dinerman et al., 1994), sGC (Gutierrez-Mecinas et al., 2005) and PNMT (Rinaman, 2001). Negative controls sections were processed in parallel with primary antibody experiments.

Table 6.1: Antibody combinations used for fluorescence immunohistochemistry in Chapter 6

Animal	Exp. Condition	Combination	Dilution	Conjugated to	Dilution
WKY (*n* = 3) & SHR (*n* = 3)	Aged animals (6 months)	mouse α nNOS rabbit α cGMP	1:400 1:500	FITC: donkey α mouse CY3: donkey α rabbit	1:500 1:500
WKY (*n* = 3) & SHR (*n* = 3)	Aged animals (6 months)	sheep α PNMT rabbit α cGMP	1:500 1:500	CY2: donkey α sheep CY3: donkey α rabbit	1:500 1:500
WKY + IBMX (*n* = 3) - IBMX (*n* = 3)	Young animals (10 weeks)	mouse α nNOS rabbit α cGMP	1:400 1:500	FITC: donkey α mouse CY3: donkey α rabbit	1:500 1:500
WKY + IBMX (*n* = 3) - IBMX (*n* = 3)	Young animals (10 weeks)	sheep α PNMT rabbit α cGMP	1:500 1:500	CY2: donkey α sheep CY3: donkey α rabbit	1:500 1:500
WKY (*n* = 3)	Young animals (10 weeks)	mouse α nNOS rabbit α sGC	1:400 1:500	FITC: donkey α mouse CY3: donkey α rabbit	1:500 1:500
WKY (*n* = 3)	Young animals (10 weeks)	sheep α PNMT rabbit α sGC	1:500 1:500	CY2: donkey α sheep CY3: donkey α rabbit	1:500 1:500

Table 6.1. Table details the various combinations used in each of the immunohistochemical experiments investigating the basal levels of cGMP of presence of sGC expression in the RVLM in WKYs (*n* = 12, total) and SHR (*n* = 3, total). Alternating sections were taken from each animal, and therefore more than one antibody combination could be used for each animal. Source, batch and abbreviations detail can be found in Table 2.1.

Table 6.2: Antibody combinations used for fluorescence immunohistochemistry after slice incubation in Chapter 6

Animal	Exp. Condition	Combination	Dilution	Conjugated to	Dilution
WKY (n=3)	DETA-NO (100μM)	mouse α nNOS rabbit α cGMP	1:400 1:500	FITC: donkey α mouse CY3: donkey α rabbit	1:500 1:500
WKY (n=3)	DETA-NO (100μM)	sheep α PNMT rabbit α cGMP	1:500 1:500	CY2: donkey α sheep CY3: donkey α rabbit	1:500 1:500
WKY (n=3)	NMDA (100μM)	mouse α nNOS rabbit α cGMP	1:400 1:500	FITC: donkey α mouse CY3: donkey α rabbit	1:500 1:500
WKY (n=3)	NMDA (100μM)	sheep α PNMT rabbit α cGMP	1:500 1:500	CY2: donkey α sheep CY3: donkey α rabbit	1:500 1:500
WKY (n=3)	Control	mouse α nNOS rabbit α cGMP	1:400 1:500	FITC: donkey α mouse CY3: donkey α rabbit	1:500 1:500
WKY (n=3)	Control	sheep α PNMT rabbit α cGMP	1:500 1:500	CY2: donkey α sheep CY3: donkey α rabbit	1:500 1:500

Table 6.2. Table details the various combinations used for each of the immunohistochemical experiments investigating levels of cGMP in the RVLM of WKYs (n = 9), after slice incubation. Alternating sections were taken from each animal, and therefore more than one antibody combination could be used for animal. Source, back and abbreviation detail can be found in Table 2.1.

6.2.3. Animal tissue preparation for brainstem slice in-vitro incubation

The following experiments were done with the assistance of Anna Barron, at the School of Veterinary and Biomedical Sciences, Murdoch University, Australia.

Animals were anaesthetised and perfused as for the immunohistochemical experiments using a perfusate that consisted of ice-cold sucrose based cutting solution (2 mM KCl, 2 mM MgSO4, 1.25 mM NaH2PO4, 1 mM $MgCl_2$, 26 mM $NaHCO_3$, 0.1 mM $CaCl_2$, 10 mM D-glucose, 248 mM sucrose, 95% O_2/ 5% CO_2, pH 7.4 (Moyer and Brown, 1998) containing IBMX (0.5 mM) and heparin 1000 IU/mL (Jurox). The brains were removed immediately and coronal RVLM sections (400 μm) were cut on a vibrating microtome while immersed in the same ice-cold sucrose cutting solution.

After cutting, brain slices were warmed to 37 °C over 20 min in an artificial cerebrospinal fluid (aCSF) solution (124 mM NaCl, 2 mM KCl, 2 mM $MgSO_4.7H_2O$, 1.25 mM NaH_2PO_4, 26 mM $NaHCO_3$, 2 mM $CaCl_2$, 10 mM D-glucose, 0.5 mM IBMX, 95%O_2 5% CO_2, pH 7.4) (Moyer and Brown, 1998). Once at 37 °C, slices were incubated for a further 30 min, prior to incubation in either 100 μM NMDA (Sigma, Castle Hill, Newcastle, Australia) plus 10uM glycine for 1 x 5 min (Lerma et al., 1989) or 100 μM DETA-NO (Sigma) for 1 x 15 min (Sandirasegarane and Diamond, 1999) in aCSF solution. Twenty minutes prior to use, DETA-NO was prepared in aCSF buffer and warmed to 37 °C to stabilise NO release. The reaction was terminated by submerging the slices in ice-cold 3.7% formalin. Control slices were incubated in aCSF solution only. Slices were post-fixed for 2 h in 3.7 % formalin at 4 °C, followed by washing for in 0.1M PBS (1 x 30 min). Slices were then cryoprotected in 30% sucrose in 0.1M PBS and sodium azide (0.1%; overnight) prior to cutting 50 μm sections on a cryostat (Leica CM1510; Leica Microsystems GmbH, Wetzlar, Germany) at -17°C for subsequent immunohistochemistry using

alternate sections as described above. Antibody combinations for each experimental condition are as detailed in Table 6.2.

6.2.4. Imaging and analysis

Imaging of sections were performed on a BioRad MRC-1024 confocal laser scanning microscope as detailed in section 2.6.1. No statistical analysis was performed.

6.3. Results

6.3.1. Detection of cGMP-IR in the RVLM

Initial experiments were undertaken in mature WKY and SHR animals (> 18 weeks, *n* = 3 of each strain). The distribution of cells expressing PNMT and nNOS were used as markers to delineate the neuronal populations of interest within the RVLM. PNMT neurons defined the rostro-caudal axis of the C1 cell group while nNOS cell bodies bounded the medial RVLM region (Paxinos and Watson, 1998). Very few cGMP immunoreactive neurons could be detected in the RVLM in association with either the PNMT C1 or the nNOS cells groups in either strain of the aged animals (Fig 6.1). No double labelling was noted for any cells for cGMP and PNMT or cGMP and nNOS (Fig 6.1 A-F). In contrast, there was strong cGMP-IR in the NA (Fig 6.1B, 6.1F). In these cells, staining was punctate in appearance and localised to the cytoplasm and extending neurites. Cyclic GMP-IR was visible in the vasculature throughout the sections (Fig 6.1 B, D and F).

As there was no apparent difference in cGMP expression in the neurons of the RVLM between the SHR and WKY, all subsequent experiments were performed in WKY animals.

To control for rapid degradation of cGMP under the experimental conditions, additional adult WKY animals were assessed after perfusion with IBMX (0.5mM, *n* = 3) in the pre-perfusate solution. To assess the influence of animal age, immunohistochemistry was also repeated in young male WKY animals (10 weeks; *n* = 3). Neither the presence of IBMX in the pre-perfusate solution or the use of younger animals uncovered cGMP-IR neurons in the RVLM. The use of IBMX did not alter PNMT or nNOS-IR but visibly increased the intensity of staining for cGMP

in cells of the NA, and within blood vessels in the region (Figure 6.2).

To confirm that the cGMP antibody was detecting both neuronal and vascular elements, a cGMP/ mouse anti α smooth muscle actin double label combination was used (anti α-SMA, mouse monoclonal, 1:500, A5228 clone 1A4: Sigma). The α-SMA labels smooth muscle cells of precapillary arterioles in the brain (Boado and Pardridge, 1994), and showed co-localisation with cGMP (Fig. 6.5A). Furthermore, the overall pattern of vascular/microvascular cGMP staining in the brain is as described by (Tassorelli et al., 2004). Parallel control experiments lacking primary antibody showed no staining.

Figure 6.1: Relationship of cGMP with either nNOS or PNMT

Confocal images depicting double labelling for PNMT/ cGMP (A, B) and nNOS/ cGMP (C, D) in the RVLM of adult WKY in the absence of IBMX, and PNMT/ cGMP (E, F) in the RVLM of an adult SHR in the absence of IBMX. PNMT-immunoreactivity (A, E) indicates the location of the C1 adrenergic cell group. Panel C illustrates nNOS immunoreactive cells, located adjacent to the inferior olive (IO) in the ventromedial region of the RVLM. cGMP-IR in the neurons of the nucleus ambiguus (NA) and in blood vessels (arrows) is evident (panels B, D, F) however there is no double labelling of neurons with cGMP in association with either the PNMT or nNOS cell groups. A single cGMP-IR neuron is visible (arrow head, panel F) in the C1 region of the SHR animal. Scale bar in Panel B = 200um for panels (A-B). Scales bars in panels D and F equal 100μm for panels (C-D) and (E-F), respectively.

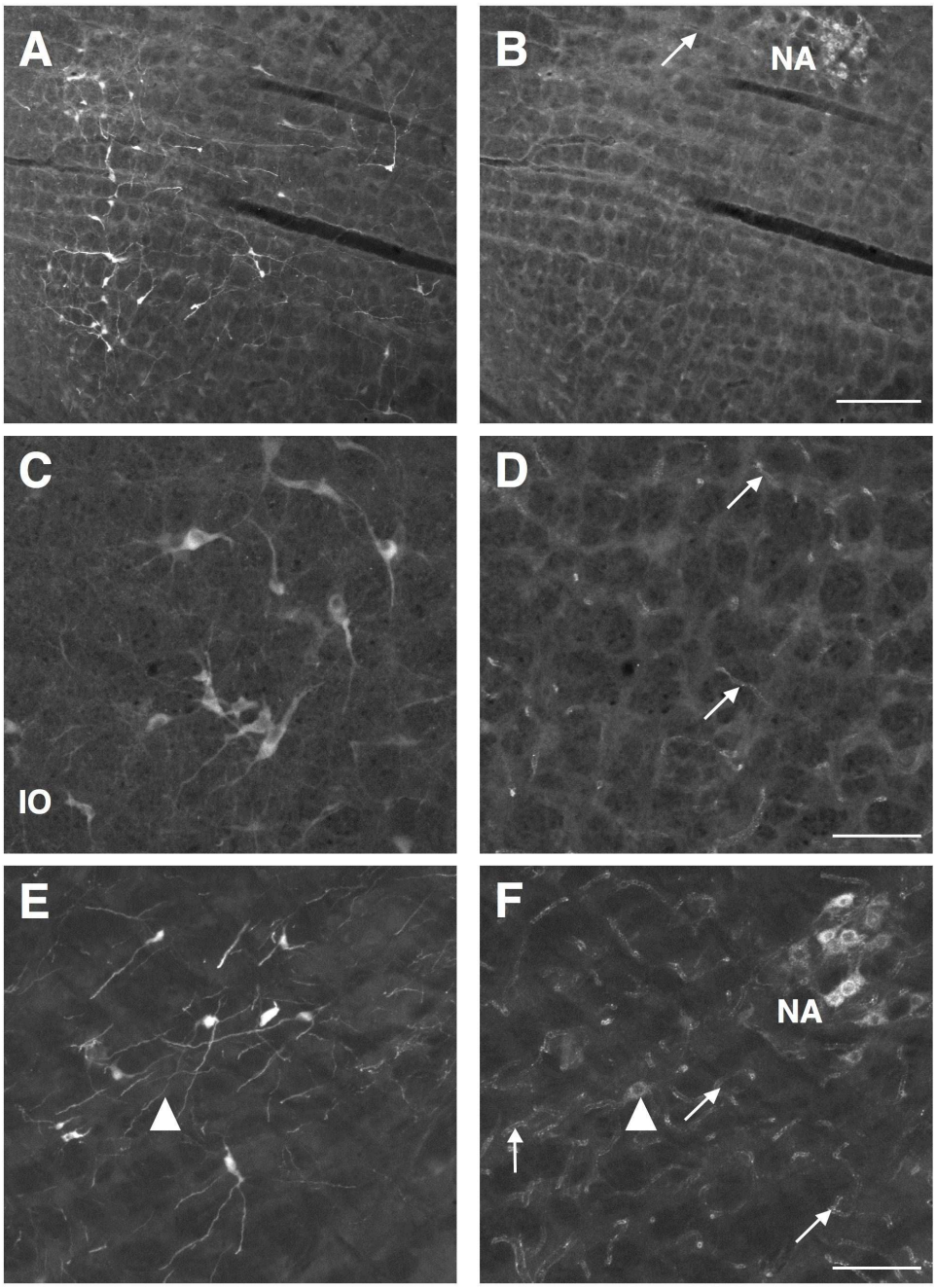
A
B
NA
C
IO
D
E
F
NA

Figure 6.2: Cyclic GMP expression in sections preincubated with IBMX

Confocal images illustrating cGMP in RVLM sections taken from adult WKY (A) and SHR (B) animals treated with IBMX in the pre-perfusate solution. Midline is located to the left and ventral surface of the medulla towards the base. Figures show the marked increase in detection of cGMP in the vasculature (arrows) and cells of the nucleus ambiguus (NA) when compared to Figure 6.1, however very few neurons expressing cGMP were detected in the RVLM region. Individual neurons showing cGMP-IR above the level of background staining are shown (arrow heads). Scale bar in A equals 200μm, scale bar in panel B equals 100 μm.

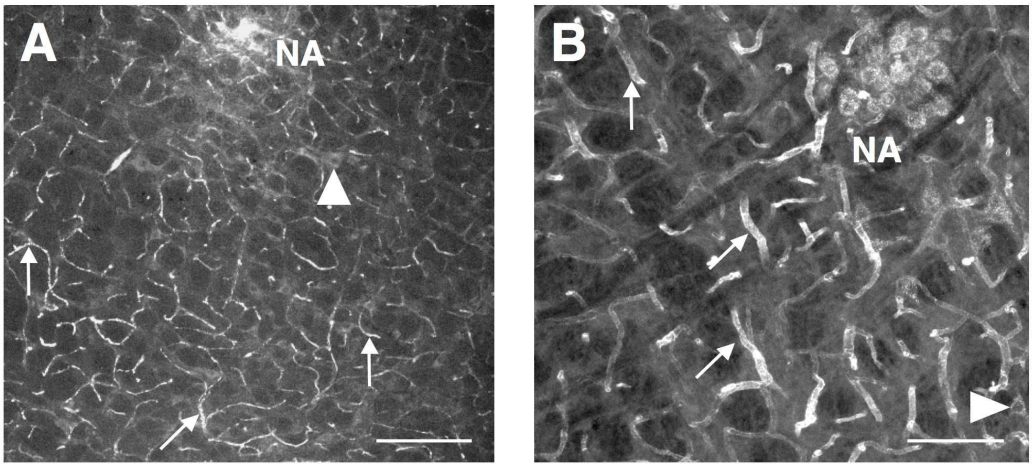
A
NA
B
NA

6.3.2. Detection of cGMP–IR in brainstem slices after incubation in-vitro

Given the lack of detection of cGMP in the RVLM, cGMP-IR in the RVLM was re-examined in brainstem slices that were treated *in-vitro* using experimental paradigms designed to increase cGMP synthesis. Due to the extended time frame of the experimental protocol, all experiments were performed in the presence of IBMX (0.5mM). Sections were examined after incubation of brainstem slices *in-vitro in* aCSF (control), with 100uM NMDA or the NO donor DETA-NO (100uM; n = 3 for each experiment, total n = 9 WKY 10 week old animals). In the aCSF control experiments, the location of neuronal cGMP staining was comparable with that from the fixation perfused experiments (Figure 6.3A/B). However, tissue integrity and overall fluorescence was reduced in this series of experiments due to the incubation protocol and the requirement for cryoprotection prior to sectioning. In those brainstem slice preparations incubated with NMDA or DETA-NO, cGMP staining in the vasculature and NA was notably brighter when compared to control (aCSF) preparations, but no additional neuronal staining in RVLM neurons was uncovered (Figs 6.3C - F).

6.3.3. Detection of sGC-IR in the RVLM

Given that there was no cGMP immunofluorescence, immunohistochemistry was performed for the presence of the NO receptor sGC. Sections from 3 male WKY animals (10 weeks) were examined for sGC/NOS and sGC/PNMT-IR. Within the RVLM region, sGC-IR was widely distributed and unlike the PNMT and nNOS immunoreactive neuronal populations, sGC cells could not be defined as belonging to a distinct group or nuclei. While cells immunoreactive for sGC were often in close

proximity to nNOS or PNMT immunoreactive cells there was no co-localisation (Fig 6.4A and B). Control experiments for sGC in the cerebellum showed the typical sGC-IR staining in cerebellar Purkinje (Fig. 6.5B) as previously described by Ding et al (Ding et al., 2004).

Figure 6.3: Cyclic GMP expression in RVLM sections incubated with NO donors

Confocal images depicting cGMP (B, D, E) and either PNMT (A, C) or nNOS-IR (E) in RVLM sections from WKY rats after treatment *in-vitro* to increase cGMP synthesis. Panels A/B show the PNMT/cGMP IR, respectively under control incubation conditions. Panels C/D illustrate PNMT/cGMP-IR respectively after *in-vitro* incubation in NMDA (100 μm 2 min). Panels E/F show nNOS/cGMP-IR, respectively after incubation in DETA-NO (100 μm 15 min). Insets B', D'& F' illustrate cGMP expression in the nucleus ambiguus (NA) under control, NMDA and DETA-NO experimental conditions, respectively. All experiments were performed in the presence of 0.5mM IBMX. Despite cGMP-IR in blood vessels (arrows) and NA being enhanced by the in-vitro treatments, they failed to reveal the presence of additional cGMP-IR neurons in the RVLM regions in association with either the PNMT or nNOS cell groups. Scale bar in F equals 100μm for panels (A-F). Scale bar in F' equals 100μm for panels (B', D' and F').

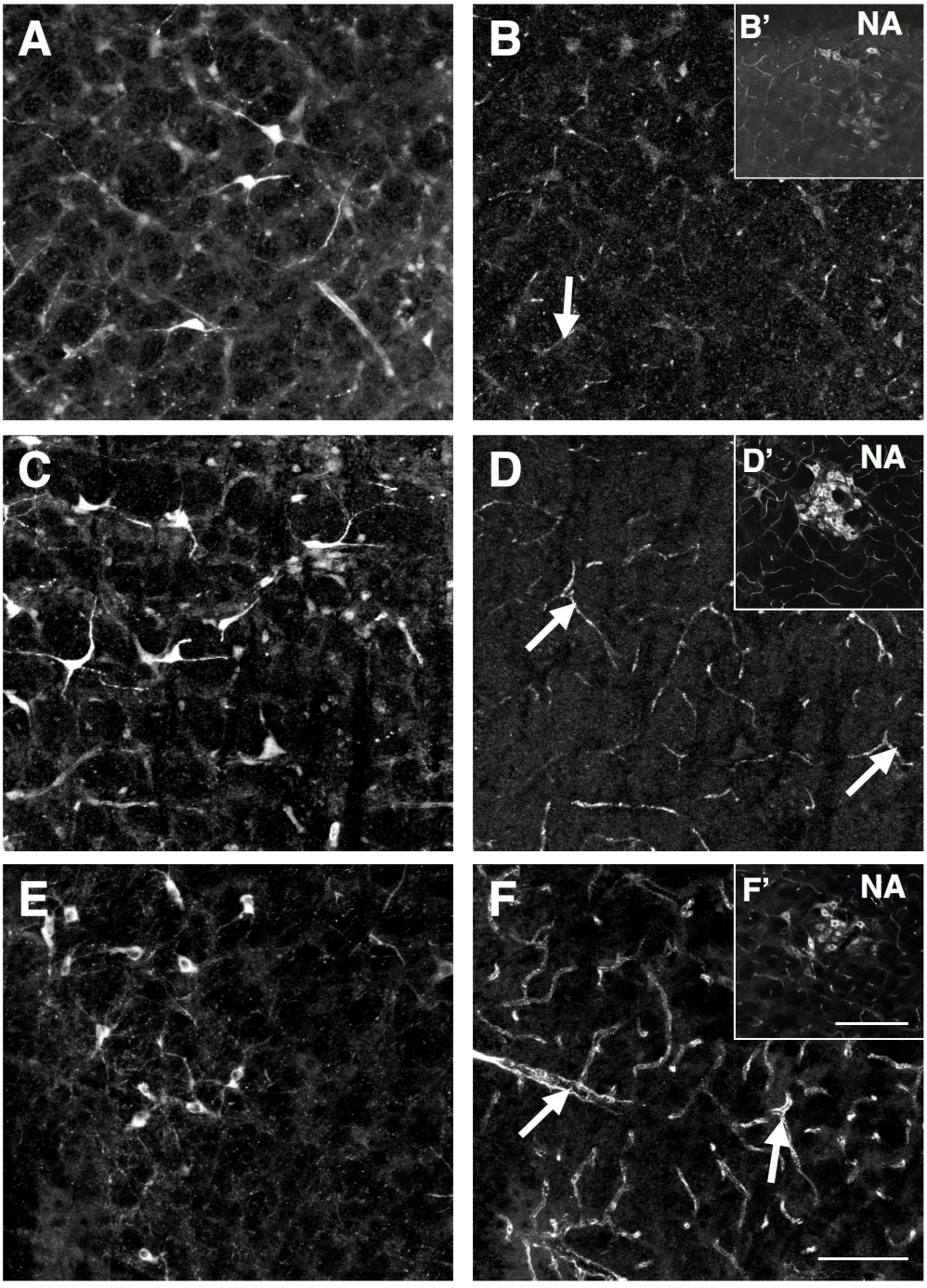
A
B
B'
NA
C
D
D'
NA
E
F
F'
NA

Figure 6.4: Relationship of PNMT or nNOS with sGC

Confocal images illustrating double labelling for PNMT/sGC in RVLM from WKY animals (male, 10 weeks old). Panels A/B/C show PNMT and sGC as individual images and then overlain in colour, respectively, and illustrate cells immunoreactive for PNMT (#; red) and sGC (arrows; green) but lack of co localisation. Scale bar in C equal 100μm for panels (A-C).

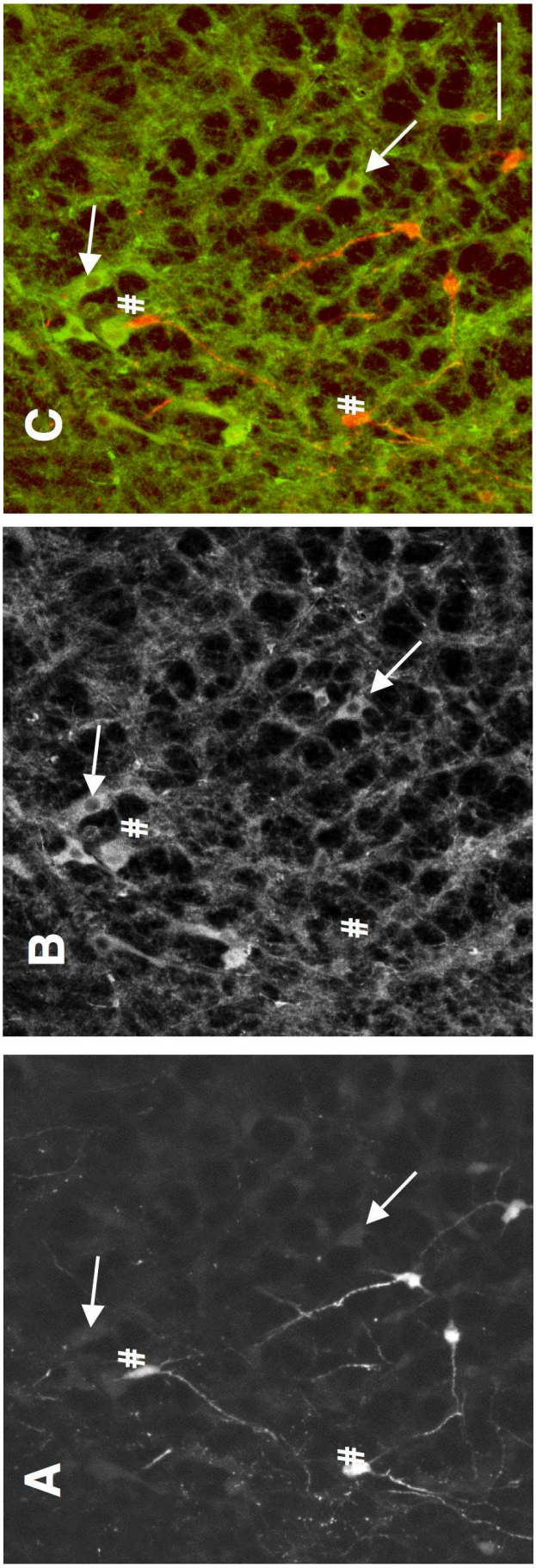
C
B
A

Figure 6.5: Control sections depicting specificity of cGMP and sGC

Control experimental results. Panel A shows control experiments assessing the vascular expression of cGMP. Sections were double labelled for α-smooth muscle actin (α-SMA; green – FITC secondary antibody) and cGMP (red – CY3 antibody). All α-SMA-IR structures showed clear co-localisation with cGMP as illustrated. The cGMP expression can be seen to extend from the larger precapillary arteriole (arrows) to the microvasculature, where it is expressed in pericytes (the contractile elements of the brain microvasculature), that do not label for α-SMA {Poeggel, 1992 #865; Ehler, 1995 #899}. Panel B shows intense labelling for sGC (red – CY3 secondary antibody) in the cerebellum. Scale bar in A equals 20um and scale bar in panel B equals 50μm.

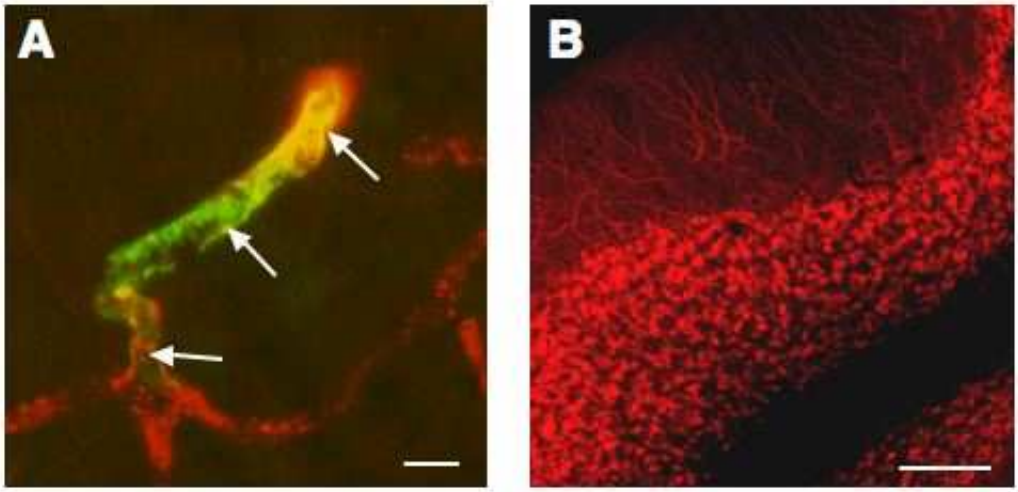
A
B

6.4. Discussion

It is well documented that the premotor sympathetic neurons in the RVLM are critical to the maintenance and control of blood pressure (Dampney, 1994) and that endogenous NO is an important mediator in this regulatory process (Hirooka et al., 1996; Martins-Pinge et al., 1997; Morimoto et al., 2000). Functional studies provide strong evidence that NO acts through the sGC-cGMP signalling pathway in the RVLM to drive sympathoexcitatory responses (Chan et al., 2005; Martins-Pinge et al., 1999; Mayorov, 2005; Wu et al., 2001), however, we were unable to detect cGMP in neurons of the C1 region of either the SHR or WKY rat strains. This was despite the use of PDE inhibitors of the use of specific stimulators of cGMP synthesis in slice preparations. We were able to demonstrate abundant sGC-IR in neurones throughout the RVLM region.

6.4.1. Cyclic GMP in the RVLM

The detection of cGMP expression in the adjacent brainstem regions of the NA, as well as expression in the blood vessels within the RVLM lessens methodological concerns regarding the adequacy of antigen recognition and/or antibody penetration. The lack of detectable cGMP expression is in accord with a detailed study by De Vente *et al.* (De Vente et al., 1998), who similarly observed cGMP expression in the NA and nucleus tractus solitarii in the brain stem region, but do not comment on its expression in the RVLM, despite the use of *in-vitro* stimulation paradigms as applied in this study. In the work by De Vente *et al*., the importance of IBMX to reveal otherwise non-detectable cGMP populations was stressed (De Vente et al., 1990; De Vente et al., 1998) and this has also been noted by other authors (Allaerts et al., 1998). For this reason, IBMX was used in a subset of studies in

perfusion fixed rats and for the brainstem slice *in-vitro* incubation experiments. However, while we found that IBMX did increase the levels of cGMP in already visible cell populations and in blood vessels in the brainstem, it did not uncover new cGMP-IR neurons in the RVLM, suggesting IBMX-sensitive PDE activity did not limit detection. This concurs with data presented in Chapter 3 where we were able to show that cGMP expressing sympathetic preganglionic neurons could be readily detected in the absence of IBMX.

The effects of anaesthetic on cGMP levels also require consideration. For this project, anaesthetic was an ethical requirement. Results from studies investigating the effect of anaesthetic on cGMP in the central nervous system are conflicting, with some reports describing the effects of anaesthetics as inhibitory, while others suggest no effect or indeed an increase in cGMP levels (Galley, 2000). Thiopentone was chosen for this study on the rationale that intravenous agents are less likely to depress cGMP levels than inhalation anaesthetics (Tobin et al., 1994), and that pentobarbital drugs specifically do not depress cGMP levels in the brainstem (Galley et al., 2001). Given that our brainstem slice *in-vitro* incubation experiments failed to uncover cGMP-IR in the RVLM, despite the demonstration of an increase of detectable cGMP in surrounding tissues, and the time available for anaesthetic wash-out, it is likely the effects of anaesthetic were minimal in this study.

The use of NMDA and NO donors to increase detectable cGMP in brain slice *in-vitro* preparations has been demonstrated previously in various tissues including the paraventricular nucleus (Vacher et al., 2003) cerebellum (De Vente et al., 1990; De Vente et al., 1998) and hippocampus and thalamus (van Staveren et al., 2005). The choice of DETA-NO as a donor was based on its ability to spontaneously liberate NO in aqueous solutions in a stable, time-controlled fashion (Keefer, 2005). It has

been proposed that the type of NO donor can make a significant difference to the way in which cGMP is stimulated (Butt et al., 1995), however a recent study comparing the effects of NONOates to the classical NO donor sodium nitroprusside found limited difference in their ability to stimulate sGC or influence cGMP staining patterns in brain slice preparations (van Staveren et al., 2005). Similar to our study, nitroglycerin, another NO donor, has been shown to increase cGMP-IR in both neuronal and vascular elements of the brain but did not uncover any additional or previously undetected cGMP immunoreactive neuronal cell groups (Tassorelli et al., 2004).

6.4.2. Soluble guanylate cyclase expression within the RVLM

The widespread detection of sGC within neurones of the RVLM is in accord with previous studies that have demonstrated both mRNA and protein for sGC within the medulla (Campese et al., 2007; Krukoff et al., 1995). It is likely to be a functional form of sGC, as the antibody we used was specific for the β1 subunit, which is the obligatory subunit for functional sGC (Friebe et al., 2007), and has been shown to co-localise extensively with the α subunit throughout the CNS of the adult rat brain (Ding et al., 2004).

While we did not demonstrate co-localisation of sGC with the nNOS cell population, they were often in close association. This pattern of expression is consistent with other brain regions, where NO responsive and NO producing structures are not necessarily found within the same neuronal profile (De Vente et al., 1998; Ding et al., 2004; Schmidt et al., 1992). An exception is the NTS, where nNOS and sGC have been shown to co-localise (Lin and Talman, 2005). Similarly, we saw sGC in close association but not co-localised with the C1 cell group. Additional

studies aimed at determining the cell population which expresses sGC should include retrograde labelling as a means of identification of the non-C1 bulbospinal group (Phillips et al., 2001), and double labelling for markers such as neuropeptide Y to identify neurons which project to the hypothalamus (Verberne et al., 1999), or markers to enable identification of glutamatergic and GABAergic neurons (Stornetta et al., 2002). This would then allow potential functional relevance to be attributed to sGC expression in the region. Interestingly, in an *in-vivo* study of the cat, nNOS-sGC co-localisation was present in the RVLM only after activation by bradykinin (as identified by the presence of *c-fos*) (Guo and Longhurst, 2006). This raises the hypothesis that functional network inputs, such as the sympathetic baroreflex pathway (Mayorov, 2005) are required to drive a sGC/cGMP cascade in the RVLM.

6.4.3. Conclusion

Despite our lack of detection of cGMP in the neurons of the C1 region, a number of physiological studies indicate that NO can modulate pressor responses in this region via a sGC/cGMP dependent mechanism (Huang et al., 2003; Martins-Pinge et al., 1999; Wu et al., 2001), including facilitation of sympathetic baroreflex transmission (Mayorov, 2005). Given the properties of NO as a freely diffusible molecule, and its tight coupling to both the NMDA receptor and sGC, the dynamics of NO signalling can be very confined, short lived and discrete (Garthwaite, 2005). The kinetics of the cGMP signalling in the RVLM may therefore be finely tuned to respond to very low NO concentrations. A recent study has shown that in similar conditions to ours, the use of a NO donor in the presence of IBMX was not sufficient to maximise cGMP detection in the hippocampus, but instead required the further addition of YC-1 or BAY 41-2272, NO-independent activators of sGC (van Staveren et al., 2005).

The expression of an IBMX-insensitive cGMP-specific phosphodiesterase (PDE9) in the RVLM may be another important factor limiting detection of cGMP accumulation (Soderling et al., 1998; van Staveren et al., 2005). As basal cGMP levels in neurons have been shown to result from a dynamic equilibrium between synthesis by sGC tonically stimulated by endogenous NO, and degradation by PDEs, including PDE9 (Hepp et al., 2007), we can speculate that these mechanisms may participate in maintaining cGMP levels in the RVLM at undetectable low levels. Examination of the role of NO-independent activation of sGC and specific phosphodiesterases is therefore required before the role of cGMP as a contributor to altered sympathetic tone in the SHR can be ascertained.

In conclusion, if present in the RVLM, cGMP does not exist in detectable quantities in the resting state and cannot be elicited by NMDA receptor stimulation, NO donor or by PDE inhibition. This finding raises questions now as to whether endogenous NO in the RVLM is truly working through this pathway.

7. Heterogeneous distribution of basal cyclic guanosine monophosphate within distinct neuronal populations in the hypothalamic paraventricular nucleus

7.1. Introduction

The sympathetic nervous system is critical to the regulation of physiological homeostasis under basal conditions (Kenney et al., 2003; Patel et al., 2001). Substantial data indicates that forebrain, brainstem and spinal networks are involved in this process (Dampney, 1994). Located either side of the third ventricle, the paraventricular hypothalamus (PVN) is a convergence point for many regions involved in the maintenance of homeostasis, including roles in fluid regulation, metabolism, immunological responses and thermoregulation (Benarroch, 2005), as well as being pivotal in the maintenance of cardiovascular function (Coote, 2005; Guyenet, 2006).

The PVN is a complex nucleus made up of three functionally distinct subsets of neurons: magnocellular neurosecretory neurons, parvocellular neuroendocrine neurons (Swanson and Sawchenko, 1983) and parvocellular preautonomic neurons (Swanson and Sawchenko, 1983). The magnocellular neurons produce oxytocin (OT) and arginine vasopressin (AVP) peptides, and innervate the posterior pituitary gland. The parvocellular neuroendocrine neurons project to the median eminence, and regulate the release of hormones from the anterior pituitary gland. Parvocellular preautonomic neurons send descending projections to brainstem regions including the

nucleus tractus solitarii (NTS), rostral ventrolateral medulla (RVLM), and sympathetic preganglionic neurons (SPNs) located the intermediolateral (IML) column of the spinal cord (Armstrong et al., 1980; Dampney, 1994; Portillo et al., 1998; Pyner and Coote, 1999; Ranson et al., 1998; Shafton et al., 1998; Stern, 2001; Swanson and Sawchenko, 1980).

Significant evidence supports a major role for preautonomic PVN neurons in the control of tonic and reflex autonomic function, including modulation of renal sympathetic nerve activity (Chen and Toney, 2001; Kannan et al., 1987; Malpas and Coote, 1994; Zhang et al., 1997) as well as the baroreceptor reflex (Patel and Schmid, 1988; Zhang and Ciriello, 1985a) and volume expansion reflex (Haselton et al., 1994; Pyner and Coote, 2000). Autonomic outflow from the PVN is regulated by the action of numerous neurotransmitters, including glutamate, GABA and angiotensin II (Chen et al., 2003; Li et al., 2001; Tagawa and Dampney, 1999; Zhang and Patel, 1998). Of particular interest is nitric oxide (NO), a ubiquitous modulatory molecule that acts as a non-conventional neurotransmitter in the central nervous system (Schuman and Madison, 1994). In general, NO is believed to act as an inhibitory molecule within central regions involved in autonomic and neuroendocrine control (see (Krukoff, 1999) and (Kadekaro, 2004) for review). For example, incremental increases in NO levels within the PVN result in diminished neurohumoral secretion, decreased sympathetic nerve activity, and concomitant decreases in blood pressure and heart rate (Hashiguchi et al., 1997; Li et al., 2001; Zhang et al., 1997). Importantly, NO is constitutively produced within the PVN and supraoptic nucleus (SON) (Stern, 2004), and basal NO levels restrain neurohumoral output from these regions. This is supported by recent studies indicating that inhibitors of NO synthase (NOS) activity within the PVN result in sympathoexcitation and increased blood pressure (Zhang and

Patel, 1998). Further, diminished basal NO availability within the PVN has been shown to contribute to elevated neurohumoral drive in pathological conditions such as hypertension, heart failure and diabetes (DiCarlo et al., 2002; Zhang et al., 2001; Zheng et al., 2007).

Accumulating evidence indicates that NO effects on neuroendocrine and autonomic outputs from the SON and PVN are mediated by inhibition of the electrical activity of both magnocellular (Bains and Ferguson, 1997; Liu et al., 1997; Stern, 2001; Stern and Zhang, 2005) and preautonomic neurons (Li et al., 2002; Li et al., 2003b), and that these actions are mediated through an enhancement of GABAergic transmission (Li et al., 2003a; Li et al., 2003b; Yang et al., 2007). One of the classical mechanisms underlying NO signalling in neurons involves activation of soluble guanylyl cyclase (sGC) (Knowles et al., 1989). Recent studies indicate that NO facilitation of GABAergic function and inhibitory effects in PVN preautonomic neurons involves activation of a cGMP-dependent pathway (Li et al., 2003a; Yang et al., 2007). Altogether, this supports the NO-cGMP signalling cascade as a key mechanism controlling ongoing neuronal activity and neurohumoral output from the PVN.

In the present chapter, we aim to expand on this knowledge by performing a detailed anatomical characterization of constitutive NO-receptive, cGMP producing neuronal populations within the PVN. Retrograde labelling techniques have been combined with immunohistochemistry to visualise cGMP within functionally, neurochemically and topographically discrete PVN neuronal populations.

7.2. Materials and methods

7.2.1. ***Animals***

All experiments were carried out with the approval of the Animal Ethics committees of Murdoch University and the University of Cincinnati. Data were obtained from 12 male Wistar rats (aged 7 – 8 weeks old, 250g). Animals were housed and treated as per methods section 2.1.

7.2.2. ***Microinjection of retrograde tracer Fluorobeads***

Individual animals had retrograde tracer injected in one site only, being either the RVLM (n = 4), NTS (n = 4) or IML (n = 4).

The candidate conducted IML injections with the assistance of Mr Courtney Reddrop, at the School of Veterinary and Biomedical Sciences, Murdoch University, Australia. RVLM and NTS microinjections were undertaken by Dr Vinicia Biancardi, and Associate Professor Javier Stern, at the University of Cincinnati, OH, USA.

Fluorobeads™ (Lumafluor, Naple, Fl, USA) are latex microspheres labelled with a fluorescent marker, (either fluorescein or rhodamine) and utilise the retrograde axonal system to be transported from motor end plate to soma (Katz et al., 1984). Fluorobeads were used in this study to identify hypothalamic neurons with projections to the IML, RVLM and NTS regions.

Retrograde label from sympathetic preganglionic neurons

Anaesthesia was induced with an intramuscular (IM) injection of ketamine/xylazine combination (40 mg/kg: 5 mg/kg; Ketamil 100mg/ml: Xylazil 20 mg/ml, both Ilium Troy Laboratories, NSW Australia), and subsequently maintained

using isofluorane by mask administration (Isorane, Veterinary Companies of Australia, NSW, Australia; 2 – 5%; 1 L/min).

Animals were placed in the prone position and a midline incision made between T1 and T4. After dissection through the muscle layers, the dorsal surface of T2 and T3 was removed with rongeurs. A bent 25-gauge needle was used to pierce the pia mater, which was then cleared from the dorsal surface of the spinal cord. Once exposure of the spinal cord was completed the animal was placed into a stereotaxic frame. A glass micropipette (Socorex, Ecublens, Switzerland; tip diameter 50 – 70 μm) was filled with Fluorobeads™ (Green) and inserted 0.6mm lateral to the midline, to a depth of 0.7 mm below the dorsal surface (Kantzides and Badoer, 2003). Two bilateral injections (200 nl each) were undertaken in separate sites 200 μm apart, running in a rostral to caudal fashion (total of 4 injections) (Cham et al., 2006). To minimise leakage of tracer from the injection site, administration was undertaken over a 5-minute period (Cham et al., 2006; Kantzides and Badoer, 2003). The location of the IML injections were examined and verified histologically at the end of the experiment, and only animals ($n = 4$) in which the injected tracer covered the IML were utilised. As per the Cham study (Cham et al., 2006) the tracer also spread to parts of the tractus rubrospinalis, tractus corticothalamicus lateralis and the tractus corticothalmucus lateralis.

Upon completion the overlying muscles were sutured with silk (4-0; Ethicon; Johnson and Johnson, Australia) and the skin incision closed with Vicryl (4-0; Ethicon). Preoperatively, animals received penicillin (100mg/kg IM Norcillin L.A. 1000 units/ml, Norbrook Laboratories, Northern Ireland) and the non-steroidal anti-inflammatory drug Carprofen (4 mg/kg; Rimadyl 50mg/ml, Pfizer, NSW, Australia).

Additional analgesia (Carprofen 4 mg/kg) was administered 24 and 48 hours post surgery. Animals were monitored daily for a week post surgery.

Retrograde labelling from NTS and RVLM

Rats were anaesthetised by injection of ketamine/xylazine mixture (90 mg/kg: 5 mg/kg respectively) administered IP. Animals were placed in a stereotaxic frame, and ear and nose bars were fixed so that the head was horizontal. For injections in the NTS, the dorsal medulla was exposed after retraction of the overlying muscles and occipital membranes. A small part of the occipital bone was removed to increase the exposure of the medulla. Rhodamine-labelled microspheres (Lumafluor, Naples, FL, USA) were pressure-injected unilaterally (200 nl) into the NTS at the level of the obex. The injection site was 12mm caudal to Bregma, 1 mm lateral to the midline and 0.8 mm below the dorsal surface. To minimise the leakage of the tracer from the injection administration was undertaken over a 5-minute period. Following injection the muscles were sutured together and the incision closed as described above.

For injections in the RVLM, a 4-mm burr hole was made in the skull and the same tracer was injected at the co-ordinates 12.0 mm caudal to Bregma, 2 mm lateral to the midline and 8 mm below the dorsal surface. Injections and aftercare were made as per the NTS injections. The location of the tracer was verified histologically, as previously reported (Stern, 2001; Stern et al., 2003).

7.2.3. Tissue removal and immunohistochemistry

Seven days post surgery for retrograde labelling, animals were anaesthetised (Section 2.4), and tissue was removed after transcardial perfusion with ice-cold heparinised saline, followed by 4% formalin (as per section 2.4.1). To determine the relationship between cGMP and either OT or AVP in cell populations differentially

identified by retrograde labelling, sections were prepared for fluorescence immunohistochemistry (section 2.5) and treated with the combinations of primary antibody as outlined in Table 7.1. When double labelling for OT and cGMP, primary antibodies were incubated consecutively, each for 24 hours. Negative controls were processed in parallel in the absence of primary antibody. Previous studies and manufacturers product information have documented the specificity of antibody reactions for the cGMP (Chapter 3) OT (Wainwright et al., 2004) and AVP (Nylen et al., 2001b) antibodies.

Table 7.1 Antibody combinations used for fluorescence immunohistochemistry in Chapter 7

Animal number (Wistar)	**Origin of retrograde label**	**Combination**	**Dilution**	**Conjugated to**	**Dilution**
n = 4	IML	mouse α OT	1:20000	CY5: donkey α mouse	1:500
n = 4	RVLM	rabbit α cGMP	1:500	CY3: donkey α rabbit	1:500
n = 4	NTS				
n = 4	IML	guinea pig α AVP	1:50000	CY5: donkey α sheep	1:500
n = 4	RVLM	rabbit α cGMP	1:500	CY3: donkey α rabbit	1:500
n = 4	NTS				

Table 7.1. Table details the various combinations of antibodies used in this chapter, to explore the relationship between cGMP and the subpopulations of neurons found in the PVN, based on peptide expression or the identification of retrograde label. Source, batch and abbreviations detail can be found in Table 2.1.

7.2.4. Quantification and analysis

Sections were examined using a confocal microscope under fluorescence microscopy and images acquired of the PVN regions ranging from Bregma -1.40 mm through Bregma -2.10 mm. Cells were included in the analysis if they contained single, double or triple staining and if the nucleus was clearly visible. Analysis was undertaken using Image Pro Plus software (Media Cybernetics, Silver Spring, MD, USA). Images were opened as a stack and the following regions of the PVN were examined for labelling: lateral magnocellular (LM), dorsal cap (DC), ventromedial parvocellular (VM) and posterior parvocellular (PaPo) subnucleus. OT/AVP immunoreactive and/or retrogradely labelled positive cells were traced using a free hand tool within the Image Pro Plus programme. To detect and quantify cGMP immunoreactivity (IR), the mean intensity of cGMP signal within traced neurons was calculated and expressed as fluorescence arbitrary units, ranging from 0 (absolute black) to 255 (absolute green). Background fluorescence was subtracted from all images. Neurons were arbitrarily considered to be cGMP positive when the fluorescence intensity within the neurons was 30% greater than background (see also (Stern and Zhang, 2005). The percentage of total magnocellular neurosecretory neurons (determined by their location and OT/AVP IR) or preautonomic neurons (determined by presence of retrograde label) containing cGMP was determined and statistically compared.

7.2.5. Statistical analysis

To determine differences in the incidence of cGMP IR among the various neuronal populations sampled, a Chi Square test was used. Values were compared to

a χ^2_{crit} values table, obtained from Pagano (Pagano, 1994), with level of significance set to $p \leq 0.01$.

7.3. Results

7.3.1. General cGMP immunoreactivity within the PVN

The majority of retrograde labelling from the three different regions (IML, RVLM and NTS) was concentrated in mid to caudal regions of the PVN (Bregma -1.3 mm through -2.1 mm). Neurons were clustered within the DC, VM and PaPo parvocellular PVN subnuclei. Conversely, OT and AVP magnocellular neurosecretory neurons were concentrated in the LM and in the medial magnocellular (MM) region (see Fig 7.1). In general, cGMP IR was diffusely observed throughout the PVN. Within neuronal profiles, a characteristic clustered pattern of cGMP was observed, whereas a more diffuse pattern was observed within PVN capillaries and arterioles. Representative examples of cGMP IR at different rostro-caudal PVN levels are shown in Fig. 7.1 A2-C2. As has been recently reported in the supraoptic nucleus (Stern and Zhang, 2005) control experiments that involved preincubation of hypothalamic slices containing the PVN in the presence of the NOS antagonists (1 mM L-NAME) or the NO scavenger c-PTIO (500 µM) almost completely abolished cGMP IR (not shown), indicating that most basal cGMP levels within the PVN is NO-driven.

Figure 7.1: Photomicrographs depicting retrogradely labelled

Confocal photomicrographs at three different rostro-caudal levels of the PVN (A: Bregma -1.40; B: Bregma -1.80; C: Bregma -2.0) depicting retrogradely-labeled PVN-IML projecting (green) and OT immunoreactive neurons (red) (A1-C1), and corresponding cGMP immunoreactivity (IR) (A2-C2). Arrows point to examples of cGMP immunoreactive capillaries (B2) and arterioles (C2). 3V, third ventricle. DC: dorsal cap; LM: lateral magnocellular; MM: medial magnocellular; PaPo: posterior parvocellular; VM: ventromedial parvocellular. Figure serves to demonstrate the cGMP IR of the region from which neurons were counted.

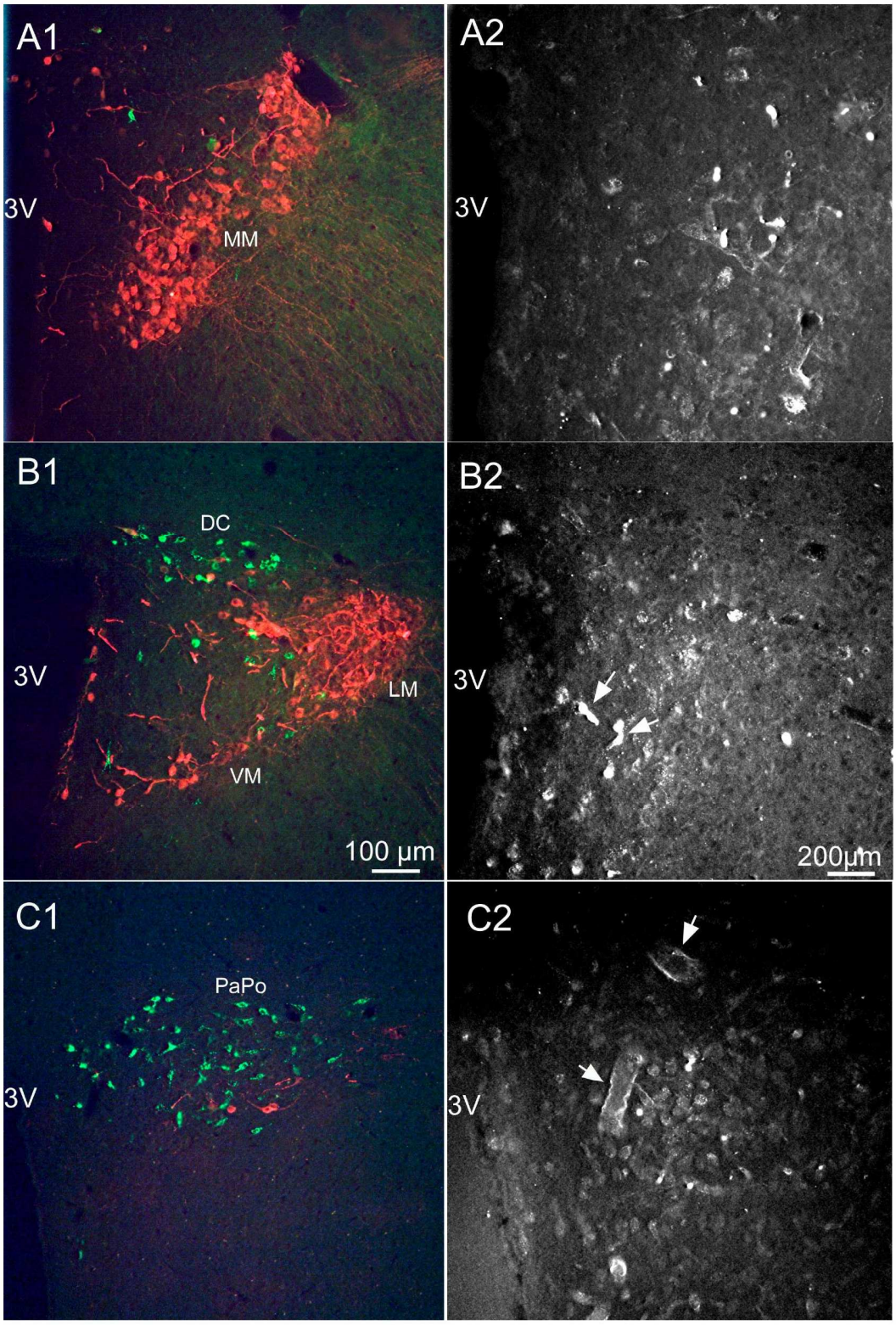
A1
3V
MM
A2
3V
B1
DC
3V
LM
VM
100 µm
B2
3V
200µm
C1
PaPo
3V
C2
3V

7.3.2. Heterogeneous distribution of cGMP expression within neurosecretory and preautonomic PVN neuronal populations

Double labelling fluorescent immunohistochemistry combined with retrograde tracing was performed to determine co-localisation of cGMP within identified magnocellular neurosecretory or preautonomic PVN neurons. Representative examples are shown in Fig. 7.2. A total of 173 and 860 magnocellular and preautonomic neurones, respectively, were sampled for this study. Of the magnocellular neurons, 119 were shown to contain cGMP (68.8%). In contrast, only 80 preautonomic neurons expressed cGMP (9.3%), a proportion significantly less than that observed in magnocellular cells ($p < 0.01$) (Fig 7.3).

7.3.3. Oxytocin and vasopressin magnocellular neurons express similar basal cGMP levels.

Analysis was undertaken to determine if there was any difference in cGMP IR between magnocellular neurons that expressed OT and those that expressed AVP. Of the 173 cells counted, 90 and 83 neurons were OT and AVP immunoreactive, respectively. Both populations showed similar levels of colocalisation. Each subgroup showed ~69% of magnocellular neurones were also immunoreactive for cGMP (62/90 OT and 57/83 AVP, $p > 0.5$ Fig. 7.4), indicating that basal cGMP levels in magnocellular neurosecretory neurons are not dependent on their neurochemical identity.

Figure 7.2: Cyclic GMP reactivity within magnosecretory and presympathetic PVN neurons

Basal cGMP immunoreactivity in representative magnocellular neurosecretory and presympathetic PVN neurons. **A**; Confocal images depicting cGMP immunostaining (**A1**) and OT immunoreactive neurons (**A2**). In **A3**, both images are superimposed to illustrate colocalisation. Arrows point to examples of double-labeled neurons. Asterisks point to examples of cGMP immunoreactive neurons that are OT immunonegative. **B**; Confocal images depicting cGMP immunostaining **(B1**) and retrogradely-labeled PVN-IML projecting neurons (**B2**, green) and OT immunoreactive neurons (**B2**, blue, respectively). In **B3**, both images are superimposed to illustrate colocalisation. An arrow points to an example of PVN-IML, cGMP double-labeled neuron. Arrowheads point to examples of PVN-IML neurons lacking cGMP immunoreactivity. Asterisks point to examples of cGMP immunoreactive neurons that are OT immunonegative and do not contain retrograde label. Scale bar: 20 μm.

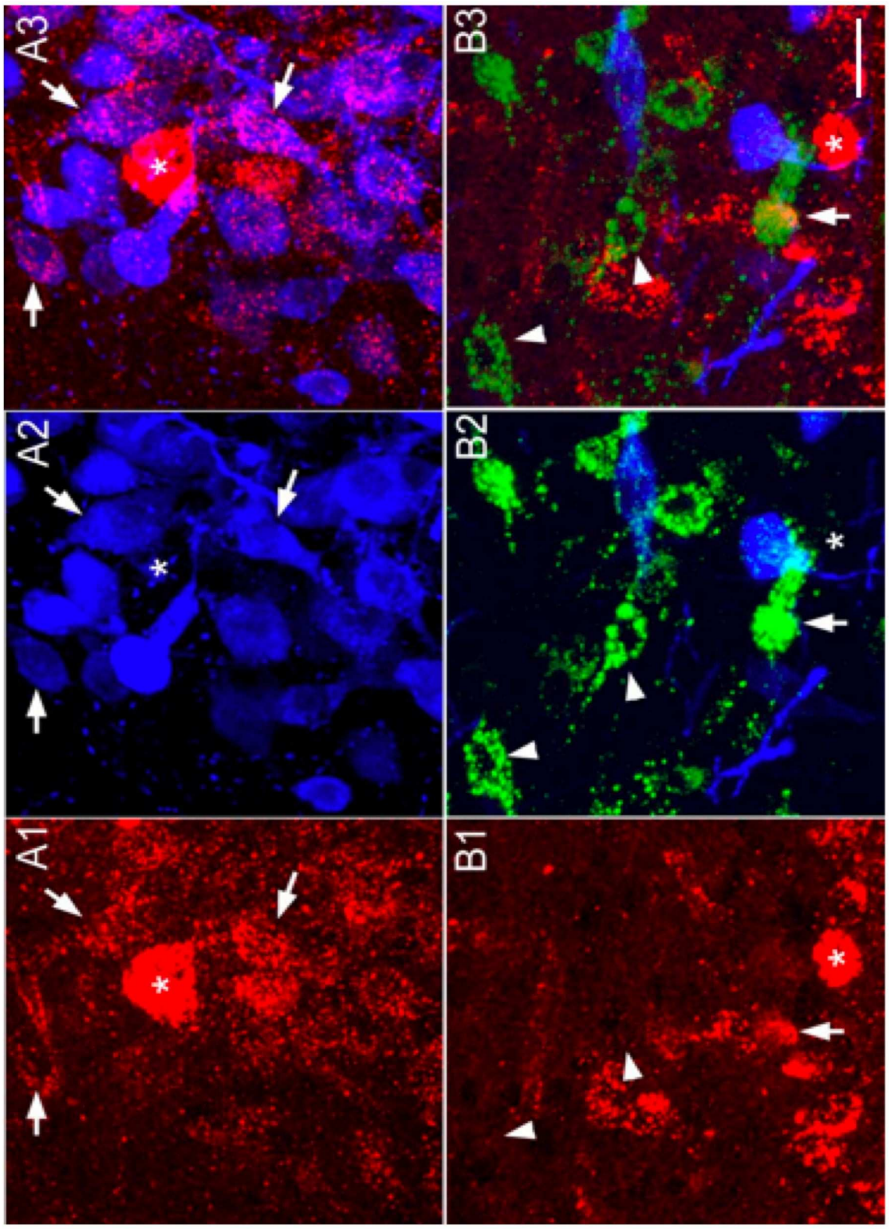
A3
B3
A2
B2
A1
B1

Figure 7.3: Relationship of magnocellular and preautonomic neurons with cGMP

Summary data showing percentage of magnocellular and preautonomic neurons that colocalised with cGMP. Magnocellular neurons were identified through the presence of either OT or AVP immunoreactivity. Preautonomic neurons were identified by retrograde labelling from either the IML, RVLM or NTS. The incidence of double-labeled cells was significantly higher in magnocellular neurosecretory as compared to preautonomic neurons (* $p<0.01$; n = 173 magnocellular total, 119 cGMP positive, and 860 preautonomic neurones total, 80 cGMP positive).

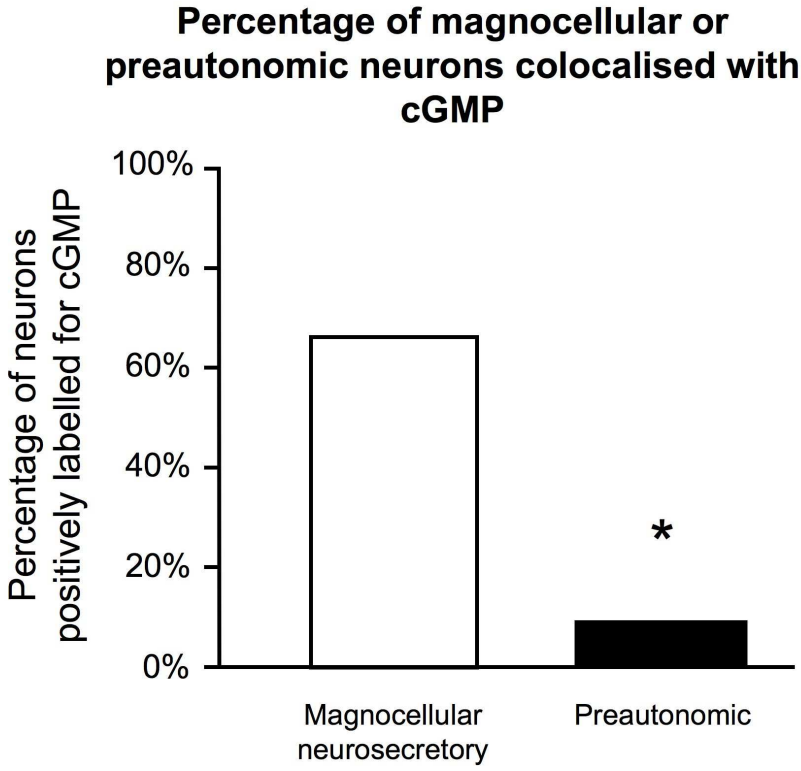
Percentage of magnocellular or preautonomic neurons colocalised with cGMP
Percentage of neurons positively labelled for cGMP
100%
80%
60%
40%
20%
0%
*
Magnocellular neurosecretory
Preautonomic

Figure 7.4: Relationship of OT and AVP magnocellular neurons and cGMP

Summary data showing percentage of oxytocin and vasopressin magnocellular neurosecretory cells that express cGMP. Magnocellular oxytocin and vasopressin cells were identified through immunoreactivity to OT and AVP respectively. Both populations showed similar levels of colocalisation ($p>0.01$; $n = 173$ cells total).

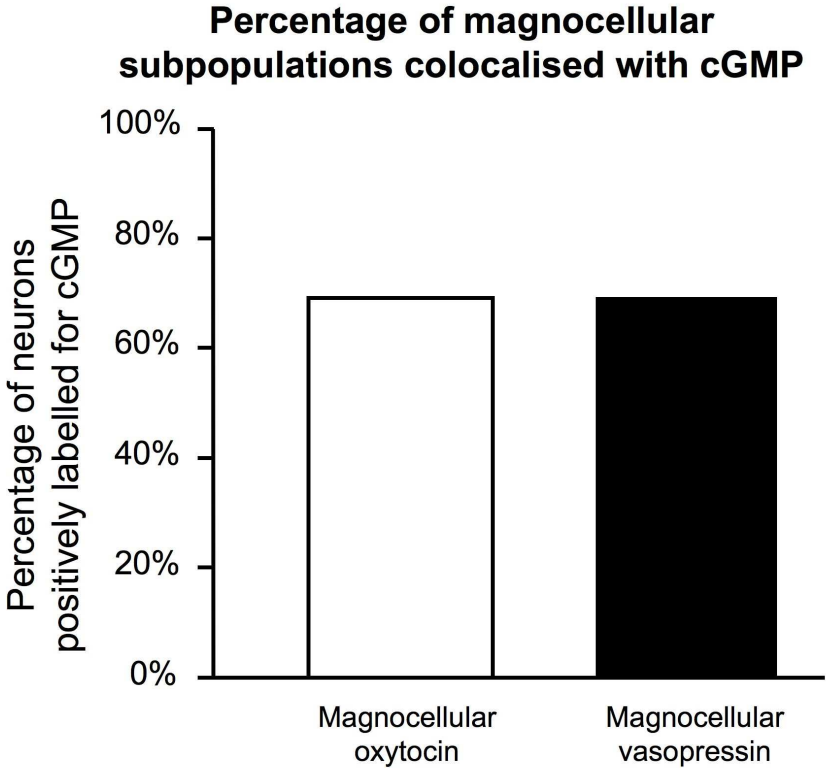
Percentage of magnocellular subpopulations colocalised with cGMP
Percentage of neurons positively labelled for cGMP
100%
80%
60%
40%
20%
0%
Magnocellular oxytocin
Magnocellular vasopressin

7.3.4. Comparison of cGMP immunoreactivity among preautonomic neurons according to their subnuclei distribution.

Previous data from the laboratory of Stern et al (Stern, 2001) supports the presence of subnuclei-dependent differences in functional and structural properties of preautonomic PVN neurons. Thus, we aimed to determine whether basal cGMP IR in preautonomic PVN neurons was dependent on their subnuclei distribution, regardless of their projection target (see below). Therefore, we compared the expression of cGMP among retrogradely labelled neurones located in the VM, DC and PaPo subnuclei (Fig 7.5A). Within the VM, only 6.3% (21/332) of PA neurons expressed cGMP, while in the DC and PaPo, 10% (24/240) and 12.15% (35/288) of neurons, respectively, were found to express cGMP. Our results indicated no significant difference in the distribution of cGMP among these topographically distinct preautonomic neuronal populations ($p > 0.1$).

7.3.5. Comparison of cGMP immunoreactivity among preautonomic neurons according to their innervated target

We next analysed whether cGMP levels in preautonomic PVN neurons varied according to their innervated targets (i.e., NTS, RVLM or IML). Within the NTS-, RVLM- and IML-projecting PVN neuronal populations, 7.9% (24/301), 2.4% (3/121) and 12.1% (53/438), respectively, were found to be cGMP immunoreactive. Basal cGMP IR between these target-specific PVN populations was not significantly different (Fig 7.5B).

7.3.6. Comparison of cGMP immunoreactivity among preautonomic neurons according to their neurochemical phenotype

Preautonomic PVN neurons are known to be neurochemically heterogeneous (Hallbeck et al., 2001). Similar to magnocellular neurosecretory neurons, a proportion of preautonomic neurons express OT and AVP peptides. Thus, we performed triple fluorescence labelling (i.e., OT or AVP, retrograde labelling and cGMP) to determine whether cGMP levels in preautonomic PVN neurons may be dependent, at least in part, on their neurochemical identity. Of the total number of preautonomic cells sampled, we were able to identify 253 and 185 as OT and AVP immunoreactive, respectively. Within the OT population, 15.4% (39/253) were found to contain cGMP. Within the AVP population, 7.5% (14/185) contained cGMP. Although twice as many OT preautonomic neurons were shown to express cGMP, this was not statistically significant (Fig 7.5C). When the incidence of cGMP IR in neurochemically identified OT and AVP neurons was compared between magnocellular and preautonomic PVN neurons, significantly higher levels were observed in magnocellular neurons [OT: 68.8% *versus* 16.4% in magnocellular (total $n = 90$, cGMP positive $n = 62$) and preautonomic (total $n = 256$, cGMP positive $n = 42$), respectively, $p < 0.01$; AVP: 68.6% *versus* 8.5% in magnocellular (total $n = 83$, cGMP positive $n = 57$) and preautonomic (total $n = 187$, cGMP positive $n = 16$) respectively, $p < 0.01$]. These results indicate that basal cGMP levels in major PVN neuronal populations is largely dependent on their overall function (i.e., magnocellular neurosecretory *versus* preautonomic), rather than on their neurochemical phenotype, topographical distribution and/or autonomic-related innervated target.

Figure 7.5: Basal cGMP expression in identified preautonomic PVN subpopulations

Basal cGMP immunoreactivity in identified preautonomic PVN subpopulations. Summary data showing the incidence of cGMP immunoreactivity in PVN preautonomic neurons according to their subnuclei location (**A**), their innervated targed (**B**) and their neurochemical phenotype (**C**). No significant differences were observed in any cases ($p > 0.01$). The Y-axis depicts the percentage of cells that expressed cGMP. VM: ventromedial; DC: dorscal cap; PaPo: posterior parvocellular; NTS: nucleus of the solitarii tract; RVLM: rostral-ventrolateral medulla; IML: intermediolateral cell column; OT: oxytocin; VP: Vasopressin.

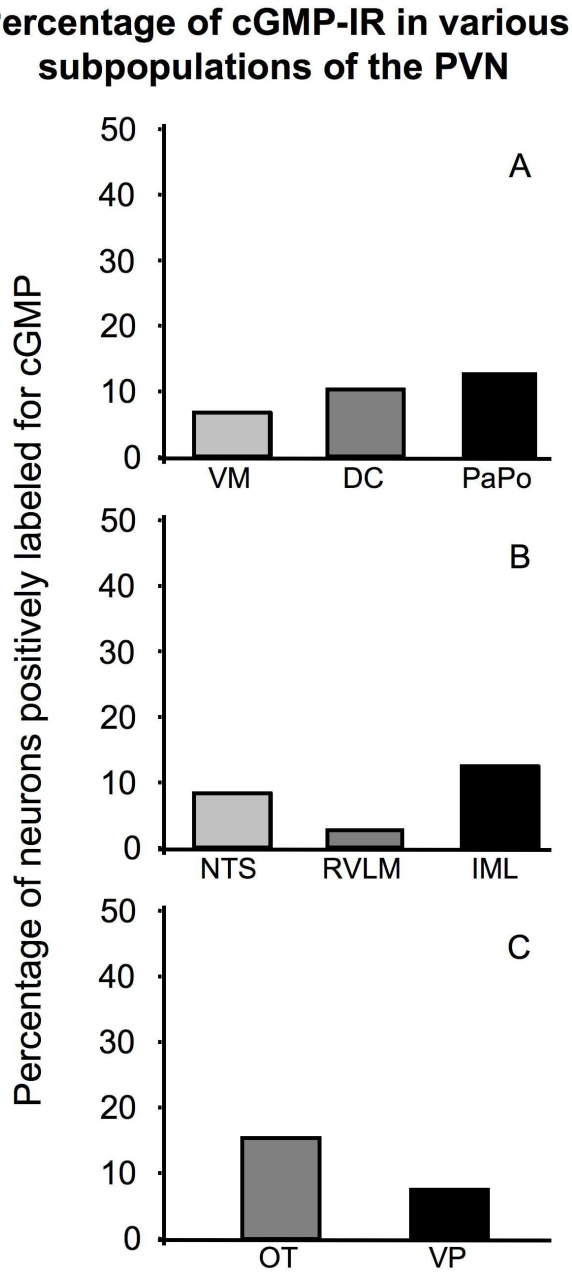
Percentage of cGMP-IR in various subpopulations of the PVN
Percentage of neurons positively labeled for cGMP
A
B
C
50
40
30
20
10
0
VM
DC
PaPo
NTS
RVLM
IML
OT
VP

7.4. Discussion

Since it's discovery, NO has been shown to be a key signalling molecule in a number of central and peripheral processes including the regulation of sympathetic activity (Krukoff, 1999). In the PVN, NO inhibits neuronal activity, of both presympathetic (Li et al., 2003b), and magnocellular neurons (Stern and Ludwig, 2001). As a membrane permeant neuronal messenger, NO produces its biological actions through distinct signal transduction pathways (Ahern et al., 2002; Stamler et al., 1997), such as the modification of proteins (S-Nitrosylation) (Jaffrey et al., 2001) or the formation of peroxynitrite (Trabace and Kendrick, 2000). However, the most common NO signalling cascade is the activation of sGC, which subsequently elevates intracellular cGMP (Southam and Garthwaite, 1993). Indeed, a cGMP-dependent cascade was recently demonstrated to mediate inhibition of presympathetic PVN neuronal activity in response to SNAP, an NO donor (Li et al., 2004). Moreover, it has been shown that NO is constitutively produced within the PVN (Stern and Zhang, 2005), where it restrains ongoing presympathetic neuronal firing activity (Li et al., 2003b). Constitutively produced NO has also been shown to inhibit PVN-driven renal sympathetic nerve discharge (Zhang and Patel, 1998). However, whether or not cGMP is the actual mediator of constitutively produced NO actions within the PVN is unknown, and a detailed characterisation of NO-receptive, cGMP producing PVN neuronal populations, and specifically preautonomic ones, is lacking. In this study, we evaluated cGMP expression within various cell populations within the mid rostro-caudal portion of the PVN, including preautonomic IML, RVLM and NTS- projecting neurons, and magnocellular neurosecretory OT and AVP neurons. Our results support a heterogeneous distribution of basal cGMP levels within PVN neuronal

populations, with relatively high levels found in magnocellular neurosecretory neurons. Conversely, a relatively small proportion of preautonomic PVN neurons, regardless of their innervated target, topographical distribution or neurochemical identity, were found to be cGMP immunoreactive.

7.4.1. Methodological considerations

To identify target-specific populations of preautonomic PVN neuronal populations, a retrograde tracer was injected at three different targets, namely the IML, RVLM and NTS. Based on the nature of the tracer used (highly restricted and well-defined injection sites, and lack of labelling of fibres in passage (Katz et al., 1984), as well as the trajectory and topography of descending axonal projections from the PVN (Luiten et al., 1985; Swanson, 1977), it is very unlikely that PVN neurons projecting to areas other than the targeted ones were labelled. Essentially separate populations of PVN neurons have been shown to project to sympathetic and parasympathetic preganglionic neurons (Portillo et al., 1996; 1998) and the distinct anatomical segregation of descending PVN axonal projections at the level of the medulla (Luiten et al., 1985; Swanson, 1977) precluded the simultaneous labelling of different PVN descending pathways (e.g., NTS- and RVLM-projecting neurons) following a single site injection. It is worth noting however, that a small subpopulation of PVN-RVLM neurons (between 5 and 16%) has been shown to send axon collaterals to the spinal cord (Pyner and Coote, 2000; Shafton et al., 1998). Thus, our experimental approach based on a single tracer injection at a single target site precluded us from differentiating this small population of RLVM- and IML-projecting neurons. Further, it is well established that virtually no neurons project both to autonomic-related medulla centres and the pituitary or median eminence (Swanson et al., 1980), and that magnocellular and preautonomic neuronal

populations are topographically segregated within the PVN (Armstrong et al., 1980; Swanson and Sawchenko, 1983). Thus, we believe that all the above considerations support the specificity of the different PVN neuronal populations sampled in our studies.

7.4.2. Cyclic GMP is highly expressed in PVN magnocellular neurosecretory neurons

Consistent with recent studies on supraoptic neurons (Stern and Zhang, 2005), we found the majority of PVN magnocellular neurosecretory neurons to contain high basal levels of cGMP. However, whereas significantly higher levels of cGMP (as well as endogenous NO levels) were observed in AVP as compared to OT neurons in the SON (Stern and Zhang, 2005), similar cGMP levels between these two populations were observed in the present study in the PVN. Interestingly, results from this study and previous work by Stern et al in the SON, differ from those previously reported in mice by Vacher and colleagues, who showed cGMP-IR was not co-localised with either AVP or OT expressing neurons, and only found cGMP-IR in astrocyte-like cells and blood vessels (Vacher et al., 2003). We currently lack a clear explanation for the differences reported in detectable cGMP levels, given that in work not included as part of this thesis, Stern et al (Stern et al, unpublished observations) have been able to clearly demonstrate cGMP in the cell bodies of neurons in the PVN of a transgenic mouse that expresses enhanced Green Fluorescent Protein (eGFP) driven by the glutamic decarboxylase (GAD67) promoter (Oliva et al., 2000). Moreover, cGMP IR was also readily identified within GFP-labelled PVN axonal terminals of the transgenic mouse. However, since cGMP levels in our work and that of Vacher have been evaluated in the absence of the phosphodiesterase inhibitor IBMX, it is possible that a differential degradation of cGMP by endogenous

phosphodiesterases exists under the different experimental paradigms between the laboratories and has resulted in different detection sensitivities.

Magnocellular SON and PVN neurosecretory neurons are known to express high levels of nNOS (Arevalo et al., 1992; Hatakeyama et al., 1996; Stern and Zhang, 2005), expression of which is enhanced in an activity-dependent manner (Kadowaki et al., 1994; Srisawat et al., 2000; Ueta et al., 1995). Moreover, both the α1 and β1 subunits of sGC are highly expressed in the SON and PVN (Furuyama et al., 1993). In addition, Stern et al have recently demonstrated a high degree of colocalisation of nNOS, constitutive NO levels (measured as NO-induced fluorescence) and cGMP within SON magnocellular neurons (Stern and Zhang, 2005). Altogether, these studies, along with a well established role of the NO-cGMP pathway in the control of the magnocellular neurosecretory system (Briski, 1999; Li et al., 2003b; Stern and Zhang, 2005; Vacher et al., 2003; Yang and Hatton, 1999; Zhang et al., 2007) (see however, (Ozaki et al., 2000; Terrell et al., 2003), support the NO-cGMP cascade as an important autocrine pathway by which magnocellular neurosecretory neurons regulate their own degree of activity.

Interestingly, in addition to magnocellular neurosecretory neurons (Stern and Zhang, 2005), colocalisation of nNOS and cGMP has only been reported previously in cerebellar granule cells (De Vente et al., 1998) and in our study examining sympathetic preganglionic neurons in the spinal cord (Chapter 3). Thus, a NO-sGC-cGMP autoregulatory dependent pathway seems to be highly restricted to specific CNS neuronal populations. In fact, since the concentration of Ca^{2+} required for the activation of nNOS inhibits sGC, it has been argued that nNOS expressing cells should not be able to auto-regulate their own activity through changes in cGMP levels (Knowles et al., 1989; Parkinson et al., 1999). However, compartmentalisation of

nNOS to specific subcellular regions, largely through its linkage to NMDA receptors through the postsynaptic density protein PSD95 (Christopherson et al., 1999), provides a mechanism by which nNOS and sGC could be differentially exposed to different Ca^{2+} concentrations within the same cell. This mechanism may support findings that show activation of NMDA receptors constitutes a major mechanism driving constitutive NO production in magnocellular neurosecretory neurons (Bains and Ferguson, 1997; Stern and Zhang, 2005).

7.4.3. Preautonomic PVN neurons express relatively low levels of basal cGMP

In contrast to magnocellular neurosecretory neurons, our results indicate a very low incidence (< than 10%) of preautonomic subject neurons expressing cGMP under basal conditions. This was the case regardless of their innervated target, their topographical distribution within the PVN, and whether or not they were immunoreactive for OT or AVP. Previous functional studies by the Stern group have shown that NO has an inhibitory effect on presympathetic (Li et al., 2003b), and magnocellular neurons (Stern and Ludwig, 2001). Electrophysiology studies showed that retrodialysis of NO donors or precursors of NO on identified magnocellular neurons (Stern and Ludwig, 2001) inhibits the spontaneous firing rate of neurons, while nNOS inhibitors increase the firing rate. Based on our results showing a significantly higher basal cGMP level in magnocellular neurosecretory compared to preautonomic OT/AVP immunoreactive neurons, it is reasonable to conclude that it is not the neurochemical phenotype, but rather the overall functional setting (i.e., neurosecretory vs. preautonomic) that is associated with the highly heterogeneous distribution of basal cGMP levels in the PVN. This is in line with work by Nylen et al (Nylen et al., 2001a), which looked at the difference in co-localisation of NO

within presympathetic spinally projecting neurons, OT magnocellular or VP magnocellular neurons. They found that over 80% of neurons expressing NO were magnocellular, which lends itself logically to the idea that there would be an increase in the downstream cGMP of these neurons.

Despite the absence and/or low levels of endogenous cGMP found in preautonomic PVN neurons, it is now well established that constitutive NO efficiently restrains PVN neuron firing activity, and consequently autonomic outflow from the region (Li et al., 2002; Li et al., 2003b; Li et al., 2001; Zhang and Patel, 1998). Thus, NO actions on this subpopulation of PVN neurons are likely mediated through a direct, cGMP-dependent mechanism, and/or alternatively, NO effects are indirectly mediated. While cGMP-independent mechanisms cannot be ruled out, such as S-nitrosylation, several lines of evidence support that GABA, the dominant inhibitory neurotransmitter in the PVN (Decavel and Van den Pol, 1990), indirectly mediates NO effects on preautonomic PVN neurons. Firstly, results from the Stern laboratory show that constitutive NO inhibitory actions on PVN-RVLM and PVN-NTS projecting neurons require intact and functional local GABAergic terminals, and that enhanced NO availability increased the frequency of GABAergic inhibitory currents (Li et al., 2003b) see also: (Li et al., 2004). Secondly, work from the Patel laboratory shows that when acting in the PVN, NO inhibition of renal sympathetic nerve activity also required the presence of functional GABAergic inputs (Zhang and Patel, 1998). Finally, recent work indicates that NO-mediated increased GABAergic activity in the PVN is mediated through a cGMP signalling cascade (Li et al., 2004; Yang et al., 2007). Altogether, these data are consistent with the notion that the PVN GABAergic interneuronal population is a key NO receptive, cGMP-producing neuronal group within the PVN.

Unlike magnocellular neurons, our preliminary studies (data not included) show that only a relatively small proportion of preautonomic PVN neurons express detectable levels of nNOS, agreeing with the work of a number of other groups (Kantzides and Badoer, 2005; Li et al., 2003b; Weiss et al., 2001). Thus, it is likely that the NO modulating preautonomic PVN neuronal activity likely originates from an alternative cellular source with projections to the PVN region.

7.4.4. Conclusion

In summary, results from our study indicate that basal cGMP immunoreactive levels are heterogeneously distributed within functionally segregated PVN neuronal populations. The high levels of basal cGMP found in the majority of magnocellular neurosecretory neurons suggest that constitutive NO, likely acting in an autocrine manner, directly modulates magnocellular neurosecretory activity through a cGMP-dependent pathway. Conversely, taking into account the literature and our results showing relatively low basal cGMP levels in levels in preautonomic PVN neurons, it is likely that that NO from inputs to the PVN acts in a paracrine manner to stimulate GABAergic inhibitory activity via a cGMP-dependent pathway, which in turn results in inhibition of preautonomic neuronal function.

8. Final discussion

The neural control of blood pressure involves a vast network of autonomic centres that must work in close collaboration, communicating via both direct and indirect anatomical connections and numerous neurotransmitters, receptors and intracellular signalling pathways. Since its discovery, NO and the role it plays in blood pressure control has generated much interest and controversy. The initial premise of this thesis was that central NO signalling is perturbed in the hypertensive state, and that basal levels of NO and its signalling cascade messenger cGMP would therefore be different when comparing a hypertensive rat model and its genetically related control. We also aimed to determine the relationship between NO and cGMP in the key central autonomic control regions of the spinal cord, brainstem and hypothalamus. Our research supports an underlying difference in the level of expression of NO and cGMP between the spontaneously hypertensive rat (SHR) and the genetically related normotensive Wistar Kyoto rat (WKY) in the central nervous system regions studied, however a number of novel and unanticipated results were also found.

8.1. Is there a difference in the basal expression of NO?

The immunohistochemical results from Chapter 3 examining nNOS expression in SPN, and the studies in Chapter 5 examining both nNOS mRNA and protein levels in the RVLM do support the notion that there is a difference in the basal or resting levels of potential NO production when comparing the hypertensive and normotensive rat strains. Within the RVLM, we saw that there was significantly

higher nNOS mRNA expression in the SHRs, compared to the WKYs, and that there was significantly more nNOS mRNA expression in both strains when compared to iNOS. Interestingly, while there was no overall significant difference in the number of cells expressing nNOS in the region between the two strains, when the data is was analysed along a rostro-caudal gradient, there were significantly more nNOS neurons in the rostral portion of the RVLM in the SHR animals, suggesting that there may be a NO gradient within the RVLM. This has functional relevance given that projection sites differ between rostral and caudal regions of the RVLM, with the rostral RVLM containing mainly bulbospinal neurons that project to the spinal cord (Kanjhan et al., 1995), and the caudal RVLM containing neurons that project to the PVN. (Day et al., 1980; Sakumoto et al., 1978; Sawchenko and Swanson, 1982). Localised microinjection studies that clearly distinguish between the rostral and caudal regions of the RVLM, and studies aiming to compare responses to NO and/or the blockade of endogenous NO production between the two regions of the RVLM, may therefore provide an answer to the discrepancies reported in the literature regarding regulation and its functional role of NO activity in the RVLM region.

In the spinal cord however, rather than seeing increased nNOS expression, we demonstrated reduced number of SPN expressing nNOS in the SHR, which was in turn reflected downstream through reduced cGMP detection. These results suggest that global predictions regarding a change of NO expression levels, and the direction of that change in association with hypertension in the SHR cannot be made. Others have demonstrated similar variable directional changes in the expression of other neurotransmitters between the SHR and WKY. Sweerts and colleagues have shown that galanin levels were significantly lower in the SHR in the supraoptic nerve when compared to the WKY, but significantly higher in the RVLM (Sweerts et al., 1999).

Furthermore, Boone and McMillen (Boone and McMillen, 1994) found that gene expression of proenkephalin in the NTS, CVLM and RVLM was lower in the SHR, while in the locus coeruleus, anterior and lateral hypothalamus, it was significantly increased. In contrast, work by Reja and colleagues (Reja et al., 2002b) showed that within the SHR, there are significantly higher levels of the alpha 1A adrenergic receptor in the hypothalamus, RVLM, spinal cord, myocardium and adrenal medulla, but constantly significantly lower levels of the alpha 2A adrenergic receptor in the same region. In this case, the authors were able to attribute the changes to global changes in the SHR.

8.2. Functionality of the NO-cGMP signalling pathway in central autonomic nuclei

In Chapter 3, we made the novel discovery that all nNOS SPN also contained cGMP. Furthermore, we demonstrated a medially located population of SPN that contained cGMP in the absence of nNOS. In Chapter 4, this finding was extended to demonstrate that in parallel with decreased levels of nNOS, there appeared to be down regulation of cGMP in individual SPN. From a neuroanatomical perspective, these results have two implications. Firstly, they support both a paracrine and autocrine role for NO within SPN. It is predominantly assumed that NO works in a paracrine fashion, as the level of calcium required to activate NOS inhibits the guanylate cyclases (Thippeswamy and Morris, 2001). However, studies have shown that in specific regions of the brain, nNOS is immunohistochemically co-localised with sGC (Burette et al., 2001). Also, within the vasculature, sGC has been co-localised with both L-arginine and eNOS (Buchwalow et al., 2004) indicating the potential for NO to work in an autocrine manner. An autocrine action of NO has been

described in baroreceptor neurons of the nodose ganglion (Li et al., 1998), although in this region NO, has been shown to work through S-nitrosylation, rather than via cGMP-dependent mechanisms. The issue of excessive calcium inhibiting guanylate cyclases and therefore preventing an autocrine action of NO can be countered by cellular compartmentalisation, whereby spatial confinement of the various pathways allows NO signals to have independent, and even opposite effects through the recruitment of different downstream pathways. For example, it has been shown that the endoplasmic reticulum comes into close apposition to the plasma membrane, which is believed to limit the spatial spread of Ca^{2+} and Na^{+} in hair cells (Martin and Fuchs, 1992), arterial smooth muscle cells (Arnon et al., 2000) and cardiac myocytes (Bridge et al., 1990; Leblanc and Hume, 1990; Lederer et al., 1990). A structural barrier overcomes the limiting factor of calcium inhibiting the guanylate cyclases, thereby allowing signalling to occur in different locations within the cell.

Secondly, the anatomical differences between the cGMP expressing SPN cell groups suggest that there may be functional distinctions between the medial and lateral SPN populations (neurochemically defined as cGMP positive/nNOS negative and cGMP positive/nNOS positive, respectively). This is supported by our complementary work that describes a comparable distribution of tonically activated subpopulations of SPNs, [identified via immunoreactivity to phosphorylated extracellular signal regulated kinase 1/2 (p-ERK1/2)] including those within the functionally defined adrenal SPN subpopulation (Springell et al., 2005). Further, a mediolateral topographic organisation of functionally distinct populations of SPN has been proposed within the IML, with lateral SPN having a vasomotor function and the more medial SPN having a motility regulating function (Janig and McLachlan, 1986; Pyner and Coote, 1994). Indeed**,** there is increasing evidence to suggest that SPN are

chemically coded and that each discrete group regulates a single autonomic target tissue (Minson et al., 2002), with SPN containing neurokinin-1 receptor (Grkovic and Anderson, 1996; Llewellyn-Smith et al., 1997b) or calcium binding proteins (Grkovic and Anderson, 1995; 1997) having specific targets.

Our experiments investigating the presence of cGMP in the RVLM (Chapter 6) failed to demonstrate its expression in association with the C1 RVLM cell group or nNOS populations. These experiments were initially designed in the light of evidence indicating that NO was influencing the area in a cGMP dependent manner (Zanzinger, 2002). Similarly, in the PVN, we found that very few preautonomic neurons actually co-express cGMP. The lack of expression of cGMP either in, or nearby our neurons of interest raises questions as to how NO is influencing these regions and more specifically, regulating autonomic outflow.

Our initial foray into the signalling of NO within the RVLM was based on the functional studies mentioned in chapter 5. In many of these studies, NO was exogenously added to the RVLM via a number of different NO donors, or the NO pathway was excited using various drugs, such as NMDA and studying the subsequent change in blood pressure. The experiments went on to clarify the role of cGMP by either blocking the NO-cGMP receptor sGC, with a specific guanylate cyclase inhibitor, or by studying the downstream cascade of cGMP, PKG. While these are valid approaches designed to test the effect NO has on blood pressure regulation, the results do not necessarily confirm that the NO-cGMP pathway mediates physiological responses in the regions. It may be that the neurons involved contain the necessary components to create cGMP, but stimulation via an exogenous NO mechanism is different to that evoked by endogenous NO. In the RVLM, the lack of cGMP in the region suggests that endogenous NO may be working via a non-

cGMP dependent pathway. To elucidate this better, we need to understand the chemical biology of NO.

Rather than traditional protein receptor-ligand interactions, the biological effects of NO are determined by chemical reactions, such as binding to sGC or phosphorylating receptors for other transmitters, thereby allowing NO to influence a number of different cellular regulatory pathways. The effects of NO can be divided into two main categories; direct, which means the reaction occurs fast enough to allow direct interaction with the target molecule; and indirect, which requires an interaction with oxygen or superoxide to generate free radicals which subsequently react with biological targets (Wink et al., 1996). One significant difference between the direct and indirect interactions is the concentration of NO – direct interactions require concentrations of NO that are under 1μM, while indirect interactions require concentrations of NO of 1μM or higher (Thomas et al., 2008). Furthermore, it has been demonstrated in a study on tumour development that different concentrations of NO activate different pathways. Tumour development engages an intricate set of molecular events, with several key events being critical to the process, such as phosphorylation of extracellular signal-related kinase (ERK) and activation of proteins p53 and hypoxic inducible factor 1 alpha (HIF-1α) (Thomas et al., 2004). Nitric oxide is known to activate these events during tumourogenesis (Hofseth et al., 2003a; Hofseth et al., 2003b; Hussain et al., 2003) (although the process through which NO affects these proteins is unclear). In the study by Thomas (Thomas et al., 2004), they correlated the concentrations of NO with when each of these events occurred. They found that phosphorylation of ERK occurred when the tumour cells were exposed to NO concentrations of ≥1μM, but that HIF-1α activation and p53 activation did not occur until there was at least a concentration of 50μM and 100μM,

respectively, as detected by gas probe (Thomas et al., 2004). Though these proteins are not pertinent to our study, what this experiment highlights is that different concentrations of NO may induce different pathways.

Importantly, it has been shown that the NO concentration required to stimulate catecholamines, and more specifically our C1 cells, has been estimated at around 1μM, which is the breakpoint between direct and indirect signalling by NO (Thomas et al., 2008). It is possible therefore that the functional responses attributed to NO in the RVLM is mediated via a non-direct pathway, not through the cGMP cascade. Given this information it would be reasonable to study the concentration of NO in our areas of interest using for example 4,5-diaminofluorescein-2-diacetate (DAF-2), a NO-sensitive indicator which can visually identify NO production in neurons, with confocal microscopy to visualise and quantify the NO expression (Kono et al., 2004), as the fluorescence signal generated is proportional to the amount of NO present (Kojima et al., 1998). When using NO donors, it would be prudent to measure the NO concentrations generated, given that the levels of NO may differentially drive a specific pathway that is not stimulated by endogenous NO.

However, it is important to note here that NO can modulate other neurotransmitters to elicit various effects. For example, microdialysis studies have shown that within the PVN, both GABAergic and glutamatergic mechanisms are modulated by NO, as when NO is introduced to the PVN, there is a significant increase in the level of both GABA and glutamate release (Horn et al., 1994). Further, throughout the brain NO, may be produced both pre and post synaptically (Garthwaite, 2008), and could be modulating transmission as well. Many brain areas express prototypic coupling with post synaptic NMDA receptors, as discussed in chapter 1. Presynaptically, NO could effect transmitter release by regulating changes

in the intracellular Ca^{2+}, either by modulating the external Ca^{2+}, influx, or by regulating the release from intracellular stores (Zanzinger et al., 1995). Indeed within the hippocampus, it has been shown that presynaptic interneurons express the $\alpha1\beta1$ heterodimer of the sGC receptor, while the $\alpha2\beta1$ is predominantly in the postsynaptic pyramidal neurons. Studies have shown that the $\alpha1\beta1$ isoform is cytosolic, while the $\alpha2\beta1$ is associated with the PDZ-domain containing PSD-95 Russwurm, 2001 #917}. Furthermore, it has been shown that PSD-95 can interact with all components of the NO-cGMP cascade (Russwurm and Koesling, 2002). It has therefore been suggested that within hippocampal pyramidal cells, excitatory transmission occurs by PSD-95 binding the $\alpha2\beta1$ sGC receptor to nNOS and NMDA receptors postsynaptically (Szabadits et al., 2007). However, within the presynaptic interneurons, as $\alpha1\beta1$ is cytosolic, NO can bind to PDZ-domain scaffolding proteins. (Szabadits et al., 2007). It has been postulated that the lack of the $\alpha2$ subunit means that within interneurons sGC is now no longer targeted, therefore altering transmission.

8.3. Is NO excitatory or inhibitory and is its increase a causal or compensatory response to hypertension?

While our initial work (Chapter 3) led us to consider that reduced NO, and therefore cGMP levels in the SPN of SHR was a "causal" mechanism that drove increased sympathetic drive at the level of the spinal cord, this hypothesis required revisiting based on work from our group examining the effect of intrathecal delivery of 8-Br-cGMP (Malik et al., 2007). In that study it was shown MAP in Sprague-Dawley rats increased in response to exogenous cGMP in a dose dependent manner. We therefore predicted that the intrathecal injection of the membrane permeable analogue of cGMP, 8-Br-cGMP would result in an increase in blood pressure in both

strains. This is indeed what we were able to demonstrate, however the results also show a significant strain-dependent effect, with the SHR demonstrating much greater pressor responses at all doses tested. Like the Sprague-Dawley, both strains showed the greatest response to 8-Br-cGMP at the highest 100μM dosage, but again this was significantly more pronounced in the SHR. It is possible therefore that in the SHR, the SPN have a heightened responsiveness to the NO-sGC-cGMP cascade with functional consequences. We can speculate that reduced levels of cGMP expression in the SHR are not necessarily contributing to the hypertension, but that they are instead a consequence. Down regulation of the levels of cGMP, mediated by reduced endogenous NO production, are a compensatory response to the hypertensive state. This would support the idea that within the baroreceptor reflex pathway, NO is a sympathoexcitatory molecule at the level of the SPN.

However, within the RVLM, it has been demonstrated by Chan et al (2001c), that when carboxyl-PTIO, a scavenger that obliterates the effects of NO is administered there is a significant increase in the MAP (Chan et al., 2001c), indicating that NO acts as a sympathoinhibitory molecule in this region. Furthermore, when selective iNOS and nNOS blockers were applied together, their combined effects were similar to carboxyl-PTIO, indicating that both iNOS and nNOS are both involved in cardiovascular actions within the RVLM (Chan et al., 2001c). When the selective NOS blockers are administered separately, it was found that blocking nNOS caused a reduction in MAP and HR, while blocking iNOS caused an increase in MAP and HR. This indicated that nNOS is acting in a sympathoexcitatory manner, while iNOS acts in a sympathoinhibitory fashion in controlling cardiovascular function (Chan et al., 2001c).

Our work demonstrated a relatively higher levels of nNOS protein and mRNA within the RVLM of the SHR when compared to the WKY. One way to interpret this is that given nNOS appears to be excitatory, the increase in nNOS seen in the SHR is driving sympathetic output, the outcome being a pressor response. However, another valid interpretation would be to again look at the chemical biology of NO. It has been shown that iNOS produces large amounts of NO, up to 20 times the amount that constitutive NOS produces (Bruckdorfer, 2005). Given that iNOS appears to have a sympathoinhibitory effect on cardiovascular function, it would lead to the suggestion that the high concentration of NO have a sympathoinhibitory function. The increase in nNOS seen in the SHR therefore may be a mechanism by which NO concentration can be increased, and can therefore be alternatively interpreted as a compensatory response designed to counter the increased sympathetic drive. The driver of this increased sympathetic tone is still open to speculation but may arise from higher centres in the CNS.

8.4. Conclusion

The key issue this thesis highlights is that unlike in the periphery, where NO has been identified as having a vasodilatory role, in central autonomic control centres, its effects can be either excitatory or inhibitory, resulting in both pressor or depressor responses. This means that there is limited value in assessing mechanisms that would have a global and therefore non-specific effect on NO production in the CNS, and instead targeted delivery of NO modifying agents to specific regions would be required.

8.5. So where to from here?

In conclusion, this thesis has shown that hypertensive and normotensive rats do show regional and species differences in components of the NO expression and signalling pathways. Importantly, we have demonstrated that while expression of cGMP can be used as a marker of sites of NO activity, it doesn't necessarily explain functional significance.

Genetic factors can cause differences not only in expression of neurotransmitters and receptors, but also changes in the sensitivity of the response. It has been shown that although SHRs and WKY can respond to the same NO-mediated stimuli in the same manner, e.g. both can respond to microinjections in specific regions with a decrease in blood pressure, the latency period can differ as can the degree of change induced (Thomas et al., 2008). This suggests an inherent change in sensitivity to NO signalling. A change in the levels of expression in the NO signalling pathway may therefore not necessarily translate into a corresponding functional change. To fully understand the mechanisms by which NO is acting and its contribution to hypertension, I propose that looking at changes in receptors, sensitivity and downstream pathways will be the most informative in defining the true nature of NO's role in hypertension.

9. References

Afework M, Burnstock G. 1995. Colocalization of neuropeptides and NADPH-diaphorase in the intra-adrenal neuronal cell bodies and fibres of the rat. Cell Tissue Res 280(2):291-295.

Agarwal SK, Calaresu FR. 1991. Monosynaptic connection from caudal to rostral ventrolateral medulla in the baroreceptor reflex pathway. Brain Res 555(1):70-74.

Aghajanian GK, Rogowski MA. 1983. The Physiological role of alpha adrenoceptors in the CNS: new concepts from single-cell studies. Trends Pharmacol Sci 4:315 - 317.

Ahern GP, Klyachko VA, Jackson MB. 2002. cGMP and S-nitrosylation: two routes for modulation of neuronal excitability by NO. Trends Neurosci 25(10):510-517.

Aicher SA, Kurucz OS, Reis DJ, Milner TA. 1995. Nucleus tractus solitarius efferent terminals synapse on neurons in the caudal ventrolateral medulla that project to the rostral ventrolateral medulla. Brain Res 693(1-2):51-63.

Aicher SA, Milner TA, Pickel VM, Reis DJ. 2000. Anatomical substrates for baroreflex sympathoinhibition in the rat. Brain Res Bull 51(2):107-110.

Aicher SA, Sharma S, Pickel VM. 1999. N-methyl-D-aspartate receptors are present in vagal afferents and their dendritic targets in the nucleus tractus solitarius. Neuroscience 91(1):119-132.

Alderton WK, Cooper CE, Knowles RG. 2001. Nitric oxide synthases: structure, function and inhibition. The Biochemical journal 357(Pt 3):593-615.

Allaerts W, De Vente J, Markerink-Van Ittersum M, Tuinhof R, Roubos EW. 1998. Topographical relationship between neuronal nitric oxide synthase immunoreactivity and cyclic 3',5'-guanosine monophosphate accumulation in the brain of the adult Xenopus laevis. J Chem Neuroanat 15(1):41-56.

Allen AM, Chai SY, Clevers J, McKinley MJ, Paxinos G, Mendelsohn FA. 1988a. Localization and characterization of angiotensin II receptor binding and angiotensin converting enzyme in the human medulla oblongata. J Comp Neurol 269(2):249-264.

Allen AM, Chai SY, Sexton PM, Lewis SJ, Verberne AJ, Jarrott B, Louis WJ, Clevers J, McKinley MJ, Paxinos G, et al. 1987. Angiotensin II receptors and angiotensin converting enzyme in the medulla oblongata. Hypertension 9(6 Pt 2):III198-205.

Allen AM, Dampney RA, Mendelsohn FA. 1988b. Angiotensin receptor binding and pressor effects in cat subretrofacial nucleus. Am J Physiol 255(5 Pt 2):H1011-1017.

Allen AM, Guyenet PG. 1993. Alpha 2-adrenoceptor-mediated inhibition of bulbospinal barosensitive cells of rat rostral medulla. Am J Physiol 265(5 Pt 2):R1065-1075.

Anderson CR. 1992. NADPH diaphorase-positive neurons in the rat spinal cord include a subpopulation of autonomic preganglionic neurons. Neurosci Lett 139(2):280-284.

Anderson CR. 1998. Identification of cardiovascular pathways in the sympathetic nervous system. Clin Exp Pharmacol Physiol 25(6):449-452.

Anderson CR, Edwards SL. 1994. Intraperitoneal injections of Fluorogold reliably labels all sympathetic preganglionic neurons in the rat. J Neurosci Methods 53(2):137-141.

Anderson CR, McLachlan EM, Srb-Christie O. 1989a. Distribution of sympathetic preganglionic neurons and monoaminergic nerve terminals in the spinal cord of the rat. J Comp Neurol 283(2):269-284.

Anderson EA, Sinkey CA, Lawton WJ, Mark AL. 1989b. Elevated sympathetic nerve activity in borderline hypertensive humans. Evidence from direct intraneural recordings. Hypertension 14(2):177-183.

Andreassi JL, 2nd, Eggleston WB, Fu G, Stewart JK. 1998. Phenylethanolamine N-methyltransferase mRNA in rat hypothalamus and cerebellum. Brain Res 779(1-2):289-291.

Andresen MC, Doyle MW, Bailey TW, Jin YH. 2004. Differentiation of autonomic reflex control begins with cellular mechanisms at the first synapse within the nucleus tractus solitarius. Braz J Med Biol Res 37(4):549-558.

Andresen MC, Kunze DL. 1994. Nucleus tractus solitarius--gateway to neural circulatory control. Annu Rev Physiol 56:93-116.

Andrew PJ, Mayer B. 1999. Enzymatic function of nitric oxide synthases. Cardiovasc Res 43(3):521-531.

Andrezik JA, Chan-Palay V, Palay SL. 1981. The nucleus paragigantocellularis lateralis in the rat. Conformation and cytology. Anat Embryol (Berl) 161(4):355-371.

Arevalo R, Sanchez F, Alonso JR, Carretero J, Vazquez R, Aijon J. 1992. NADPH-diaphorase activity in the hypothalamic magnocellular neurosecretory nuclei of the rat. Brain Res Bull 28(4):599-603.

Armstrong WE, Warach S, Hatton GI, McNeill TH. 1980. Subnuclei in the rat hypothalamic paraventricular nucleus: a cytoarchitectural, horseradish peroxidase and immunocytochemical analysis. Neuroscience 5(11):1931-1958.

Arnal JF, Dinh-Xuan AT, Pueyo M, Darblade B, Rami J. 1999. Endothelium-derived nitric oxide and vascular physiology and pathology. Cell Mol Life Sci 55(8-9):1078-1087.

Arnolda LF. 2002. Inducible nitric oxide synthase and cardiac dysfunction in salt-sensitive hypertension. J Hypertens 20(12):2355-2356.

Arnolda LF, McKitrick DJ, Llewellyn-Smith IJ, Minson JB. 2000. Nitric oxide limits pressor responses to sympathetic activation in rat spinal cord. Hypertension 36(6):1089-1092.

Arnon A, Hamlyn JM, Blaustein MP. 2000. Ouabain augments Ca(2+) transients in arterial smooth muscle without raising cytosolic Na(+). Am J Physiol Heart Circ Physiol 279(2):H679-691.

Averill DB. 2000. Neurochemical and peptidergic pathways of the baroreflex arc in the medulla oblongata: an introduction. Brain Res Bull 51(2):103-105.

Averill DB, Diz DI. 2000. Angiotensin peptides and baroreflex control of sympathetic outflow: pathways and mechanisms of the medulla oblongata. Brain Res Bull 51(2):119-128.

Babic T, Ciriello J. 2004. Medullary and spinal cord projections from cardiovascular responsive sites in the rostral ventromedial medulla. J Comp Neurol 469(3):391-412.

Backman SB, Henry JL. 1983. Effects of GABA and glycine on sympathetic preganglionic neurons in the upper thoracic intermediolateral nucleus of the cat. Brain Res 277(2):365-369.

Badoer E. 1998. Neurons in the hypothalamic paraventricular nucleus that project to the rostral ventrolateral medulla are not activated by hypotension. Brain Res 801(1-2):224-227.

Badoer E. 2001. Hypothalamic paraventricular nucleus and cardiovascular regulation. Clin Exp Pharmacol Physiol 28(1-2):95-99.

Bains JS, Ferguson AV. 1995. Paraventricular nucleus neurons projecting to the spinal cord receive excitatory input from the subfornical organ. Am J Physiol 268(3 Pt 2):R625-633.

Bains JS, Ferguson AV. 1997. Nitric oxide regulates NMDA-driven GABAergic inputs to type I neurones of the rat paraventricular nucleus. J Physiol 499 (Pt 3):733-746.

Baranano DE, Snyder SH. 2001. Neural roles for heme oxygenase: contrasts to nitric oxide synthase. Proc Natl Acad Sci U S A 98(20):10996-11002.

Barzon L, Fallo F, Sonino N, Boscaro M. 2002. Development of overt Cushing's syndrome in patients with adrenal incidentaloma. Eur J Endocrinol 146(1):61-66.

Bellamy TC, Garthwaite J. 2001. Sub-second kinetics of the nitric oxide receptor, soluble guanylyl cyclase, in intact cerebellar cells. J Biol Chem 276(6):4287-4292.

Benarroch EE. 2005. Paraventricular nucleus, stress response, and cardiovascular disease. Clin Auton Res 15(4):254-263.

Bergamaschi C, Campos RR, Schor N, Lopes OU. 1995. Role of the rostral ventrolateral medulla in maintenance of blood pressure in rats with Goldblatt hypertension. Hypertension 26(6 Pt 2):1117-1120.

Bernard C. 1865. An introduction to the Study of Experimental Medicine. Dover: MacMillan & Co.

Bhat GK, Mahesh VB, Lamar CA, Ping L, Aguan K, Brann DW. 1995. Histochemical localization of nitric oxide neurons in the hypothalamus: association with gonadotropin-releasing hormone neurons and co-localization with N-methyl-D-aspartate receptors. Neuroendocrinology 62(2):187-197.

Blair ML, Piekut D, Want A, Olschowka JA. 1996. Role of the hypothalamic paraventricular nucleus in cardiovascular regulation. Clin Exp Pharmacol Physiol 23(2):161-165.

Blessing WW. 1988. Depressor neurons in rabbit caudal medulla act via GABA receptors in rostral medulla. Am J Physiol 254(4 Pt 2):H686-692.

Blessing WW, Goodchild AK, Dampney RA, Chalmers JP. 1981. Cell groups in the lower brain stem of the rabbit projecting to the spinal cord, with special reference to catecholamine-containing neurons. Brain Res 221(1):35-55.

Blessing WW, Reis DJ. 1982. Inhibitory cardiovascular function of neurons in the caudal ventrolateral medulla of the rabbit: relationship to the area containing A1 noradrenergic cells. Brain Res 253(1-2):161-171.

Blessing WW, Reis DJ. 1983. Evidence that GABA and glycine-like inputs inhibit vasodepressor neurons in the caudal ventrolateral medulla of the rabbit. Neurosci Lett 37(1):57-62.

Blessing WW, Sved AF, Reis DJ. 1982. Destruction of noradrenergic neurons in rabbit brainstem elevates plasma vasopressin, causing hypertension. Science 217(4560):661-663.

Boado RJ, Pardridge WM. 1994. Differential expression of alpha-actin mRNA and immunoreactive protein in brain microvascular pericytes and smooth muscle cells. J Neurosci Res 39(4):430-435.

Bonham AC, Jeske I. 1989. Cardiorespiratory effects of DL-homocysteic acid in caudal ventrolateral medulla. Am J Physiol 256(3 Pt 2):H688-696.

Boone JB, Jr., McMillen D. 1994. Proenkephalin gene expression is altered in the brain of spontaneously hypertensive rats during the development of hypertension. Brain Res Mol Brain Res 24(1-4):320-326.

Boscan P, Allen AM, Paton JF. 2001. Baroreflex inhibition of cardiac sympathetic outflow is attenuated by angiotensin II in the nucleus of the solitary tract. Neuroscience 103(1):153-160.

Boudaba C, Di S, Tasker JG. 2003. Presynaptic noradrenergic regulation of glutamate inputs to hypothalamic magnocellular neurones. J Neuroendocrinol 15(8):803-810.

Bredt DS. 1999. Endogenous nitric oxide synthesis: biological functions and pathophysiology. Free Radic Res 31(6):577-596.

Bredt DS, Glatt CE, Hwang PM, Fotuhi M, Dawson TM, Snyder SH. 1991. Nitric oxide synthase protein and mRNA are discretely localized in neuronal populations of the mammalian CNS together with NADPH diaphorase. Neuron 7(4):615-624.

Bredt DS, Hwang PM, Snyder SH. 1990. Localization of nitric oxide synthase indicating a neural role for nitric oxide. Nature 347(6295):768-770.

Brenman JE, Bredt DS. 1997. Synaptic signaling by nitric oxide. Curr Opin Neurobiol 7(3):374-378.

Brenman JE, Chao DS, Gee SH, McGee AW, Craven SE, Santillano DR, Wu Z, Huang F, Xia H, Peters MF, Froehner SC, Bredt DS. 1996. Interaction of nitric oxide synthase with the postsynaptic density protein PSD-95 and alpha1-syntrophin mediated by PDZ domains. Cell 84(5):757-767.

Bridge JH, Smolley JR, Spitzer KW. 1990. The relationship between charge movements associated with ICa and INa-Ca in cardiac myocytes. Science 248(4953):376-378.

Briski KP. 1999. Pharmacological manipulation of central nitric oxide/guanylate cyclase activity alters Fos expression by rat hypothalamic vasopressinergic neurons during acute glucose deprivation. J Chem Neuroanat 17(1):13-19.

Broillet MC. 1999. S-nitrosylation of proteins. Cell Mol Life Sci 55(8-9):1036-1042.

Brown MR, Fisher LA. 1984. Brain peptide regulation of adrenal epinephrine secretion. Am J Physiol 247(1 Pt 1):E41-46.

Brownstein MJ, Palkovits M. 1984. Catecholamines, serotonin, acetylcholine, and GABA-aminobutyric acid in the rat brain:biochemical studies. In: Bjorklund A, Hokfelt T, editors. Classical Transmitters in the CNS. Amsterdam: Elsevier Science Publishing. p 23 - 54.

Bruckdorfer R. 2005. The basics about nitric oxide. Mol Aspects Med 26(1-2):3-31.

Bruschi G, Bruschi ME, Capelli P, Regolisti G, Borghetti A. 1988. Increased sensitivity to protein kinase C activation in aortas of spontaneously hypertensive rats. J Hypertens Suppl 6(4):S248-251.

Buchwalow IB, Podzuweit T, Samoilova VE, Wellner M, Haller H, Grote S, Aleth S, Boecker W, Schmitz W, Neumann J. 2004. An in situ evidence for autocrine function of NO in the vasculature. Nitric Oxide 10(4):203-212.

Burette A, Petrusz P, Schmidt HH, Weinberg RJ. 2001. Immunohistochemical localization of nitric oxide synthase and soluble guanylyl cyclase in the ventral cochlear nucleus of the rat. J Comp Neurol 431(1):1-10.

Burman KJ, Sartor DM, Verberne AJ, Llewellyn-Smith IJ. 2004. Cocaine- and amphetamine-regulated transcript in catecholamine and noncatecholamine presympathetic vasomotor neurons of rat rostral ventrolateral medulla. J Comp Neurol 476(1):19-31.

Butler AR, Flitney FW, Williams DL. 1995. NO, nitrosonium ions, nitroxide ions, nitrosothiols and iron-nitrosyls in biology: a chemist's perspective. Trends Pharmacol Sci 16(1):18-22.

Butt E, Pohler D, Genieser HG, Huggins JP, Bucher B. 1995. Inhibition of cyclic GMP-dependent protein kinase-mediated effects by (Rp)-8-bromo-PET-cyclic GMPS. Br J Pharmacol 116(8):3110-3116.

Cabilla JP, Diaz Mdel C, Machiavelli LI, Poliandri AH, Quinteros FA, Lasaga M, Duvilanski BH. 2006. 17 beta-estradiol modifies nitric oxide-sensitive guanylyl cyclase expression and down-regulates its activity in rat anterior pituitary gland. Endocrinology 147(9):4311-4318.

Cameron VA, Aitken GD, Ellmers LJ, Kennedy MA, Espiner EA. 1996. The sites of gene expression of atrial, brain, and C-type natriuretic peptides in mouse fetal development: temporal changes in embryos and placenta. Endocrinology 137(3):817-824.

Campagnole-Santos MJ, Diz DI, Ferrario CM. 1988. Baroreceptor reflex modulation by angiotensin II at the nucleus tractus solitarii. Hypertension 11(2 Pt 2):I167-171.

Campese VM. 2000. Neurogenic factors and hypertension in renal disease. Kidney Int Suppl 75:S2-6.

Campese VM, Krol E. 2002. Neurogenic factors in renal hypertension. Curr Hypertens Rep 4(3):256-260.

Campese VM, Sindhu RK, Ye S, Bai Y, Vaziri ND, Jabbari B. 2007. Regional expression of NO synthase, NAD(P)H oxidase and superoxide dismutase in the rat brain. Brain Res 1134(1):27-32.

Campos Junior RR, Guertzenstein PG. 1989. Role of the glycine sensitive area in the regulation of cardiac output. Prog Brain Res 81:243-251.

Cannon RO, 3rd. 1998. Role of nitric oxide in cardiovascular disease: focus on the endothelium. Clin Chem 44(8 Pt 2):1809-1819.

Cao WH, Morrison SF. 2001. Differential chemoreceptor reflex responses of adrenal preganglionic neurons. Am J Physiol Regul Integr Comp Physiol 281(6):R1825-1832.

Card JP, Sved JC, Craig B, Raizada M, Vazquez J, Sved AF. 2006. Efferent projections of rat rostroventrolateral medulla C1 catecholamine neurons: Implications for the central control of cardiovascular regulation. J Comp Neurol 499(5):840-859.

Cary SP, Winger JA, Derbyshire ER, Marletta MA. 2006. Nitric oxide signaling: no longer simply on or off. Trends Biochem Sci 31(4):231-239.

Casadei B. 2006. The emerging role of neuronal nitric oxide synthase in the regulation of myocardial function. Exp Physiol 91(6):943-955.

Chalmers J. 1998. Volhard Lecture. Brain, blood pressure and stroke. J Hypertens 16(12 Pt 2):1849-1858.

Chalmers J, Pilowsky P. 1991. Brainstem and bulbospinal neurotransmitter systems in the control of blood pressure. J Hypertens 9(8):675-694.

Cham JL, Badoer E. 2008. Hypothalamic paraventricular nucleus is critical for renal vasoconstriction elicited by elevations in body temperature. Am J Physiol Renal Physiol 294(2):F309-315.

Cham JL, Klein R, Owens NC, Mathai M, McKinley M, Badoer E. 2006. Activation of spinally projecting and nitrergic neurons in the PVN following heat exposure. Am J Physiol Regul Integr Comp Physiol 291(1):R91-101.

Chan JY, Chan SH, Li FC, Tsai CY, Cheng HL, Chang AY. 2005. Phasic cardiovascular responses to mevinphos are mediated through differential activation of cGMP/PKG cascade and peroxynitrite via nitric oxide generated in the rat rostral ventrolateral medulla by NOS I and II isoforms. Neuropharmacology 48(1):161-172.

Chan JY, Wang LL, Chao YM, Chan SH. 2003a. Downregulation of basal iNOS at the rostral ventrolateral medulla is innate in SHR. Hypertension 41(3):563-570.

Chan JY, Wang LL, Wu KL, Chan SH. 2001a. Reduced functional expression and molecular synthesis of inducible nitric oxide synthase in rostral ventrolateral medulla of spontaneously hypertensive rats. Circulation 104(14):1676-1681.

Chan JY, Wang SH, Chan SH. 2001b. Differential roles of iNOS and nNOS at rostral ventrolateral medulla during experimental endotoxemia in the rat. Shock 15(1):65-72.

Chan RK, Sawchenko PE. 1994. Spatially and temporally differentiated patterns of c-fos expression in brainstem catecholaminergic cell groups induced by cardiovascular challenges in the rat. J Comp Neurol 348(3):433-460.

Chan SH, Wang LL, Chan JY. 2003b. Differential engagements of glutamate and GABA receptors in cardiovascular actions of endogenous nNOS or iNOS at rostral ventrolateral medulla of rats. Br J Pharmacol 138(4):584-593.

Chan SH, Wang LL, Wang SH, Chan JY. 2001c. Differential cardiovascular responses to blockade of nNOS or iNOS in rostral ventrolateral medulla of the rat. Br J Pharmacol 133(4):606-614.

Chang AY, Chan JY, Chan SH. 2003. Differential distribution of nitric oxide synthase isoforms in the rostral ventrolateral medulla of the rat. J Biomed Sci 10(3):285-291.

Chen CH, Shyr MH. 2005. Blockade of spinal nitric oxide synthase on blood pressure variability and hepatic microcirculation. Acta Anaesthesiol Taiwan 43(2):67-72.

Chen J, Tu Y, Moon C, Matarazzo V, Palmer AM, Ronnett GV. 2004a. The localization of neuronal nitric oxide synthase may influence its role in neuronal precursor proliferation and synaptic maintenance. Dev Biol 269(1):165-182.

Chen QH, Toney GM. 2001. AT(1)-receptor blockade in the hypothalamic PVN reduces central hyperosmolality-induced renal sympathoexcitation. Am J Physiol Regul Integr Comp Physiol 281(6):R1844-1853.

Chen R, Iwai M, Wu L, Suzuki J, Min LJ, Shiuchi T, Sugaya T, Liu HW, Cui TX, Horiuchi M. 2003. Important role of nitric oxide in the effect of angiotensin-converting enzyme inhibitor imidapril on vascular injury. Hypertension 42(4):542-547.

Chen SY, Mao SP, Chai CY. 2001. Role of nitric oxide on pressor mechanisms within the dorsomedial and rostral ventrolateral medulla in anaesthetized cats. Clin Exp Pharmacol Physiol 28(3):155-163.

Chen XQ, Du JZ, Wang YS. 2004b. Regulation of hypoxia-induced release of corticotropin-releasing factor in the rat hypothalamus by norepinephrine. Regul Pept 119(3):221-228.

Cho KO, Hunt CA, Kennedy MB. 1992. The rat brain postsynaptic density fraction contains a homolog of the Drosophila discs-large tumor suppressor protein. Neuron 9(5):929-942.

Chowdhary S, Townend JN. 1999. Role of nitric oxide in the regulation of cardiovascular autonomic control. Clin Sci (Lond) 97(1):5-17.

Chowdhary S, Townend JN. 2001. Nitric oxide and hypertension: not just an endothelium derived relaxing factor! J Hum Hypertens 15(4):219-227.

Christopherson KS, Hillier BJ, Lim WA, Bredt DS. 1999. PSD-95 assembles a ternary complex with the N-methyl-D-aspartic acid receptor and a bivalent neuronal NO synthase PDZ domain. J Biol Chem 274(39):27467-27473.

Ciriello J. 1983. Brainstem projections of aortic baroreceptor afferent fibers in the rat. Neurosci Lett 36(1):37-42.

Ciriello J, Kline RL, Zhang TX, Caverson MM. 1984. Lesions of the paraventricular nucleus alter the development of spontaneous hypertension in the rat. Brain Res 310(2):355-359.

Collingridge GL, Lester RA. 1989. Excitatory amino acid receptors in the vertebrate central nervous system. Pharmacol Rev 41(2):143-210.

Colombari E, Sato MA, Cravo SL, Bergamaschi CT, Campos RR, Jr., Lopes OU. 2001. Role of the medulla oblongata in hypertension. Hypertension 38(3 Pt 2):549-554.

Contestabile A. 2000. Roles of NMDA receptor activity and nitric oxide production in brain development. Brain Res Brain Res Rev 32(2-3):476-509.

Coote JH. 1995. Cardiovascular function of the paraventricular nucleus of the hypothalamus. Biol Signals 4(3):142-149.

Coote JH. 2005. A role for the paraventricular nucleus of the hypothalamus in the autonomic control of heart and kidney. Exp Physiol 90(2):169-173.

Coote JH, Macleod VH, Fleetwood-Walker S, Gilbey MP. 1981. The response of individual sympathetic preganglionic neurones to microelectrophoretically applied endogenous monoamines. Brain Res 215(1-2):135-145.

Coote JH, Yang Z, Pyner S, Deering J. 1998. Control of sympathetic outflows by the hypothalamic paraventricular nucleus. Clin Exp Pharmacol Physiol 25(6):461-463.

Crane BR, Arvai AS, Gachhui R, Wu C, Ghosh DK, Getzoff ED, Stuehr DJ, Tainer JA. 1997. The structure of nitric oxide synthase oxygenase domain and inhibitor complexes. Science 278(5337):425-431.

Crane BR, Arvai AS, Ghosh DK, Wu C, Getzoff ED, Stuehr DJ, Tainer JA. 1998. Structure of nitric oxide synthase oxygenase dimer with pterin and substrate. Science 279(5359):2121-2126.

Craven KB, Zagotta WN. 2006. CNG and HCN channels: two peas, one pod. Annu Rev Physiol 68:375-401.

Cravo SL, Morrison SF, Reis DJ. 1991. Differentiation of two cardiovascular regions within caudal ventrolateral medulla. Am J Physiol 261(4 Pt 2):R985-994.

Dahlstroem A, Fuxe K. 1964. Evidence for the Existence of Monoamine-Containing Neurons in the Central Nervous System. I. Demonstration of Monoamines in the Cell Bodies of Brain Stem Neurons. Acta Physiol Scand Suppl:SUPPL 232:231-255.

Dahlstrom A, Fuxe K. 1965. Evidence for the existence of an outflow of noradrenaline nerve fibres in the ventral roots of the rat spinal cord. Experientia 21(7):409-410.

Dampney RA. 1994. Functional organization of central pathways regulating the cardiovascular system. Physiol Rev 74(2):323-364.

Dampney RA, Coleman MJ, Fontes MA, Hirooka Y, Horiuchi J, Li YW, Polson JW, Potts PD, Tagawa T. 2002. Central mechanisms underlying short- and long-term regulation of the cardiovascular system. Clin Exp Pharmacol Physiol 29(4):261-268.

Dampney RA, Goodchild AK, McAllen RM. 1987. Vasomotor control by subretrofacial neurones in the rostral ventrolateral medulla. Can J Physiol Pharmacol 65(8):1572-1579.

Dampney RA, Horiuchi J, Tagawa T, Fontes MA, Potts PD, Polson JW. 2003a. Medullary and supramedullary mechanisms regulating sympathetic vasomotor tone. Acta Physiol Scand 177(3):209-218.

Dampney RA, Polson JW, Potts PD, Hirooka Y, Horiuchi J. 2003b. Functional organization of brain pathways subserving the baroreceptor reflex: studies in conscious animals using immediate early gene expression. Cell Mol Neurobiol 23(4-5):597-616.

Davies PF. 1995. Flow-mediated endothelial mechanotransduction. Physiol Rev 75(3):519-560.

Davis KL, Martin E, Turko IV, Murad F. 2001. Novel effects of nitric oxide. Annu Rev Pharmacol Toxicol 41:203-236.

Dawson TM, Snyder SH. 1994. Gases as biological messengers: nitric oxide and carbon monoxide in the brain. J Neurosci 14(9):5147-5159.

Dawson VL, Dawson TM. 1998. Nitric oxide in neurodegeneration. Prog Brain Res 118:215-229.

Day TA, Blessing W, Willoughby JO. 1980. Noradrenergic and dopaminergic projections to the medial preoptic area of the rat. A combined horseradish peroxidase/catecholamine fluorescence study. Brain Res 193(2):543-548.

De Groat WC, Ryall RW. 1967. An excitatory action 0f 5-hydroxytryptamine on sympathetic preganglionic neurones. Exp Brain Res 3(4):299-305.

de Sousa Buck H, Caous CA, Lindsey CJ. 2001. Projections of the paratrigeminal nucleus to the ambiguus, rostroventrolateral and lateral reticular nuclei, and the solitary tract. Auton Neurosci 87(2-3):187-200.

De Vente J, Bol JG, Berkelmans HS, Schipper J, Steinbusch HM. 1990. Immunocytochemistry of cGMP in the Cerebellum of the Immature, Adult, and Aged Rat: the Involvement of Nitric Oxide. A Micropharmacological Study. Eur J Neurosci 2(10):845-862.

De Vente J, Hopkins DA, Markerink-Van Ittersum M, Emson PC, Schmidt HH, Steinbusch HW. 1998. Distribution of nitric oxide synthase and nitric oxide-receptive, cyclic GMP-producing structures in the rat brain. Neuroscience 87(1):207-241.

de Wardener HE. 2001. The hypothalamus and hypertension. Physiol Rev 81(4):1599-1658.

de Wit C, Schafer C, von Bismarck P, Bolz SS, Pohl U. 1997. Elevation of plasma viscosity induces sustained NO-mediated dilation in the hamster cremaster microcirculation in vivo. Pflugers Arch 434(4):354-361.

Dean C, Seagard JL. 1995. Expression of c-fos protein in the nucleus tractus solitarius in response to physiological activation of carotid baroreceptors. Neuroscience 69(1):249-257.

Decavel C, Van den Pol AN. 1990. GABA: a dominant neurotransmitter in the hypothalamus. J Comp Neurol 302(4):1019-1037.

del Carmen Garcia M, Celuch SM, Adler-Graschinsky E. 1997. Possible participation of spinal nitric oxide in the control of the blood pressure in anesthetized rats. Brain Res 764(1-2):67-74.

Deuchars SA, Morrison SF, Gilbey MP. 1995. Medullary-evoked EPSPs in neonatal rat sympathetic preganglionic neurones in vitro. J Physiol 487 (Pt 2):453-463.

DiCarlo SE, Zheng H, Collins HL, Rodenbaugh DW, Patel KP. 2002. Daily exercise normalizes the number of diaphorase (NOS) positive neurons in the hypothalamus of hypertensive rats. Brain Res 955(1-2):153-160.

Dinerman JL, Dawson TM, Schell MJ, Snowman A, Snyder SH. 1994. Endothelial nitric oxide synthase localized to hippocampal pyramidal cells: implications for synaptic plasticity. Proc Natl Acad Sci U S A 91(10):4214-4218.

Ding JD, Burette A, Nedvetsky PI, Schmidt HH, Weinberg RJ. 2004. Distribution of soluble guanylyl cyclase in the rat brain. J Comp Neurol 472(4):437-448.

Dobbins EG, Feldman JL. 1994. Brainstem network controlling descending drive to phrenic motoneurons in rat. J Comp Neurol 347(1):64-86.

Doone VG, Pelissier N, Manchester T, Vizzard AM. 1999. Distribution of NADPH-d and nNOS-IR in the thoracolumbar and sacrococcygeal spinal cord of the guinea pig. J Auton Nerv Syst 77(2-3):98-113.

Dun NJ, Dun SL, Forstermann U, Tseng LF. 1992. Nitric oxide synthase immunoreactivity in rat spinal cord. Neurosci Lett 147(2):217-220.

Edwards MA, Loxley RA, Powers-Martin K, Lipski J, McKitrick DJ, Arnolda LF, Phillips JK. 2004. Unique levels of expression of N-methyl-D-aspartate receptor subunits and neuronal nitric oxide synthase in the rostral ventrolateral medulla of the spontaneously hypertensive rat. Brain Res Mol Brain Res 129(1-2):33-43.

Egan B, Panis R, Hinderliter A, Schork N, Julius S. 1987. Mechanism of increased alpha adrenergic vasoconstriction in human essential hypertension. J Clin Invest 80(3):812-817.

Ellenberger HH, Feldman JL. 1990. Brainstem connections of the rostral ventral respiratory group of the rat. Brain Res 513(1):35-42.

Ellenberger HH, Vera PL, Feldman JL, Holets VR. 1992. Multiple putative neuromessenger inputs to the phrenic nucleus in rat. J Chem Neuroanat 5(5):375-382.

Engelmann M, Landgraf R, Wotjak CT. 2004. The hypothalamic-neurohypophysial system regulates the hypothalamic-pituitary-adrenal axis under stress: an old concept revisited. Front Neuroendocrinol 25(3-4):132-149.

Esler M, Jennings G, Biviano B, Lambert G, Hasking G. 1986. Mechanism of elevated plasma noradrenaline in the course of essential hypertension. J Cardiovasc Pharmacol 8 Suppl 5:S39-43.

Esler M, Kaye D. 1998. Increased sympathetic nervous system activity and its therapeutic reduction in arterial hypertension, portal hypertension and heart failure. J Auton Nerv Syst 72(2-3):210-219.

Ezerman EB, Forehand CJ. 1996. Development and segmental organization of rostrocaudal dendrites of rat sympathetic preganglionic neurons. J Auton Nerv Syst 57(1-2):29-35.

Fagard RH. 2001. Exercise characteristics and the blood pressure response to dynamic physical training. Med Sci Sports Exerc 33(6 Suppl):S484-492; discussion S493-484.

Feil R, Hofmann F, Kleppisch T. 2005. Function of cGMP-dependent protein kinases in the nervous system. Rev Neurosci 16(1):23-41.

Feldberg W, Guertzenstein PG. 1972. A vasodepressor effect of pentobarbitone sodium. J Physiol 224(1):83-103.

Feldberg W, Guertzenstein PG. 1976. Vasodepressor effects obtained by drugs acting on the ventral surface of the brain stem. J Physiol 258(2):337-355.

Ferguson AV, Samson WK. 2003. The orexin/hypocretin system: a critical regulator of neuroendocrine and autonomic function. Front Neuroendocrinol 24(3):141-150.

Ferrari MF, Fior-Chadi DR. 2005. Differential expression of nNOS mRNA and protein in the nucleus tractus solitarii of young and aged Wistar-Kyoto and spontaneously hypertensive rats. J Hypertens 23(9):1683-1690.

Fesler P, Ribstein J, du Cailar G, Mimran A. 2005. Determinants of cardiorenal damage progression in normotensive and never-treated hypertensive subjects. Kidney Int 67(5):1974-1979.

Folkow B. 1982. Physiological aspects of primary hypertension. Physiol Rev 62(2):347-504.

Foster MW, McMahon TJ, Stamler JS. 2003. S-nitrosylation in health and disease. Trends Mol Med 9(4):160-168.

Friebe A, Mergia E, Dangel O, Lange A, Koesling D. 2007. Fatal gastrointestinal obstruction and hypertension in mice lacking nitric oxide-sensitive guanylyl cyclase. Proc Natl Acad Sci U S A 104(18):7699-7704.

Fuller PI, Reddrop C, Rodger J, Bellingham MC, Phillips JK. 2006. Differential expression of the NMDA NR2B receptor subunit in motoneuron populations susceptible and resistant to amyotrophic lateral sclerosis. Neurosci Lett 399(1-2):157-161.

Furchgott RF. 1983. Role of endothelium in responses of vascular smooth muscle. Circ Res 53(5):557-573.

Furchgott RF, Zawadzki JV. 1980. The obligatory role of endothelial cells in the relaxation of arterial smooth muscle by acetylcholine. Nature 288(5789):373-376.

Furuyama T, Inagaki S, Takagi H. 1993. Localizations of alpha 1 and beta 1 subunits of soluble guanylate cyclase in the rat brain. Brain Res Mol Brain Res 20(4):335-344.

Galley HF. 2000. Anaesthesia and the nitric oxide-cyclic GMP pathway in the central nervous system. Br J Anaesth 84(2):141-143.

Galley HF, Le Cras AE, Logan SD, Webster NR. 2001. Differential nitric oxide synthase activity, cofactor availability and cGMP accumulation in the central nervous system during anaesthesia. Br J Anaesth 86(3):388-394.

Gao L, Wang W, Li YL, Schultz HD, Liu D, Cornish KG, Zucker IH. 2004. Superoxide mediates sympathoexcitation in heart failure: roles of angiotensin II and NAD(P)H oxidase. Circ Res 95(9):937-944.

Garcia-Cardena G, Oh P, Liu J, Schnitzer JE, Sessa WC. 1996. Targeting of nitric oxide synthase to endothelial cell caveolae via palmitoylation: implications for nitric oxide signaling. Proc Natl Acad Sci U S A 93(13):6448-6453.

Garthwaite J. 2005. Dynamics of cellular NO-cGMP signaling. Front Biosci 10:1868-1880.

Garthwaite J. 2008. Concepts of neural nitric oxide-mediated transmission. Eur J Neurosci 27(11):2783-2802.

Garthwaite J, Charles SL, Chess-Williams R. 1988. Endothelium-derived relaxing factor release on activation of NMDA receptors suggests role as intercellular messenger in the brain. Nature 336(6197):385-388.

Garthwaite J, Garthwaite G. 1987. Cellular origins of cyclic GMP responses to excitatory amino acid receptor agonists in rat cerebellum in vitro. J Neurochem 48(1):29-39.

Garthwaite J, Garthwaite G, Palmer RM, Moncada S. 1989. NMDA receptor activation induces nitric oxide synthesis from arginine in rat brain slices. Eur J Pharmacol 172(4-5):413-416.

Gatti PJ, Norman WP, Taveira Dasilva AM, Gillis RA. 1986. Cardiorespiratory effects produced by microinjecting L-glutamic acid into medullary nuclei associated with the ventral surface of the feline medulla. Brain Res 381(2):281-288.

Gavras I, Gavras H. 2001. Role of alpha2-adrenergic receptors in hypertension. Am J Hypertens 14(6 Pt 2):171S-177S.

Gbadegesin M, Vicini S, Hewett SJ, Wink DA, Espey M, Pluta RM, Colton CA. 1999. Hypoxia modulates nitric oxide-induced regulation of NMDA receptor currents and neuronal cell death. Am J Physiol 277(4 Pt 1):C673-683.

Gibbins IL. 1992. Vasoconstrictor, vasodilator and pilomotor pathways in sympathetic ganglia of guinea-pigs. Neuroscience 47(3):657-672.

Giuliano F, Rampin O. 2004. Neural control of erection. Physiol Behav 83(2):189-201.

Goldstein DS. 1983. Plasma catecholamines and essential hypertension. An analytical review. Hypertension 5(1):86-99.

Goodchild AK, Dampney RA. 1985. A vasopressor cell group in the rostral dorsomedial medulla of the rabbit. Brain Res 360(1-2):24-32.

Gordon FJ, McCann LA. 1988. Pressor responses evoked by microinjections of L-glutamate into the caudal ventrolateral medulla of the rat. Brain Res 457(2):251-258.

Gordon FJ, Sved AF. 2002. Neurotransmitters in central cardiovascular regulation: glutamate and GABA. Clin Exp Pharmacol Physiol 29(5-6):522-524.

Goto A, Ikeda T, Tobian L, Iwai J, Johnson MA. 1981. Brain lesions in the paraventricular nuclei and catecholaminergic neurons minimize salt hypertension in Dahl salt-sensitive rats. Clin Sci (Lond) 61 Suppl 7:53s-55s.

Gow AJ, Chen Q, Gole M, Themistocleous M, Lee VM, Ischiropoulos H. 2000. Two distinct mechanisms of nitric oxide-mediated neuronal cell death show thiol dependency. Am J Physiol Cell Physiol 278(6):C1099-1107.

Granata AR, Ruggiero DA, Park DH, Joh TH, Reis DJ. 1985. Brain stem area with C1 epinephrine neurons mediates baroreflex vasodepressor responses. Am J Physiol 248(4 Pt 2):H547-567.

Graudal NA, Galloe AM, Garred P. 1998. Effects of sodium restriction on blood pressure, renin, aldosterone, catecholamines, cholesterols, and triglyceride: a meta-analysis. JAMA 279(17):1383-1391.

Griffith OW, Stuehr DJ. 1995. Nitric oxide synthases: properties and catalytic mechanism. Annu Rev Physiol 57:707-736.

Grkovic I, Anderson CR. 1995. Calretinin-containing preganglionic nerve terminals in the rat superior cervical ganglion surround neurons projecting to the submandibular salivary gland. Brain Res 684(2):127-135.

Grkovic I, Anderson CR. 1996. Distribution of immunoreactivity for the NK1 receptor on different subpopulations of sympathetic preganglionic neurons in the rat. J Comp Neurol 374(3):376-386.

Grkovic I, Anderson CR. 1997. Calbindin D28K-immunoreactivity identifies distinct subpopulations of sympathetic pre- and postganglionic neurons in the rat. J Comp Neurol 386(2):245-259.

Guertzenstein PG. 1973. Blood pressure effects obtained by drugs applied to the ventral surface of the brain stem. J Physiol 229(2):395-408.

Guertzenstein PG, Silver A. 1974. Fall in blood pressure produced from discrete regions of the ventral surface of the medulla by glycine and lesions. J Physiol 242(2):489-503.

Guo ZL, Longhurst JC. 2006. Responses of neurons containing VGLUT3/nNOS-cGMP in the rVLM to cardiac stimulation. Neuroreport 17(3):255-259.

Gutierrez-Mecinas M, Crespo C, Blasco-Ibanez JM, Gracia-Llanes FJ, Marques-Mari AI, Martinez-Guijarro FJ. 2005. Soluble guanylyl cyclase appears in a specific subset of periglomerular cells in the olfactory bulb. Eur J Neurosci 21(5):1443-1448.

Guyenet PG. 1990. Role of the ventral medulla oblongata in blood pressure regulation. Loewy A, Spyer K, editors. New York: Oxford University Press. 145 - 167 p.

Guyenet PG. 2006. The sympathetic control of blood pressure. Nat Rev Neurosci 7(5):335-346.

Guyenet PG, Koshiya N, Huangfu D, Baraban SC, Stornetta RL, Li YW. 1996. Role of medulla oblongata in generation of sympathetic and vagal outflows. Prog Brain Res 107:127-144.

Guyenet PG, Schreihofer AM, Stornetta RL. 2001. Regulation of sympathetic tone and arterial pressure by the rostral ventrolateral medulla after depletion of C1 cells in rats. Ann N Y Acad Sci 940:259-269.

Guyenet PG, Stornetta RL, Schreihofer AM, Pelaez NM, Hayar A, Aicher S, Llewellyn-Smith IJ. 2002. Opioid signalling in the rat rostral ventrolateral medulla. Clin Exp Pharmacol Physiol 29(3):238-242.

Guyton AC. 1990. Long-term arterial pressure control: an analysis from animal experiments and computer and graphic models. Am J Physiol 259(5 Pt 2):R865-877.

Haibara AS, Colombari E, Chianca DA, Jr., Bonagamba LG, Machado BH. 1995. NMDA receptors in NTS are involved in bradycardic but not in pressor response of chemoreflex. Am J Physiol 269(4 Pt 2):H1421-1427.

Hakim MA, Hirooka Y, Coleman MJ, Bennett MR, Dampney RA. 1995. Evidence for a critical role of nitric oxide in the tonic excitation of rabbit renal sympathetic preganglionic neurones. J Physiol 482 (Pt 2):401-407.

Hallbeck M, Larhammar D, Blomqvist A. 2001. Neuropeptide expression in rat paraventricular hypothalamic neurons that project to the spinal cord. J Comp Neurol 433(2):222-238.

Hamilton MO, Papka RE, O'Donoghue DL, Vaidya AM, Williams SJ, Poff CR, McNeill DL. 1995. Spinal projection neurons to the laterodorsal pontine tegmental

nucleus: relationship to preganglionic neurons and nitric oxide synthase. J Comp Neurol 353(1):1-8.

Hardy SG. 2001. Hypothalamic projections to cardiovascular centers of the medulla. Brain Res 894(2):233-240.

Haselton JR, Goering J, Patel KP. 1994. Parvocellular neurons of the paraventricular nucleus are involved in the reduction in renal nerve discharge during isotonic volume expansion. J Auton Nerv Syst 50(1):1-11.

Haselton JR, Guyenet PG. 1989. Electrophysiological characterization of putative C1 adrenergic neurons in the rat. Neuroscience 30(1):199-214.

Hashiguchi H, Ye SH, Ross-Cisneros F, Alexander N. 1997. Central nitric oxide donors attenuate cardiovascular and central norepinephrine responses to stress. Am J Physiol 272(5 Pt 2):R1447-1453.

Hatakeyama S, Kawai Y, Ueyama T, Senba E. 1996. Nitric oxide synthase-containing magnocellular neurons of the rat hypothalamus synthesize oxytocin and vasopressin and express Fos following stress stimuli. J Chem Neuroanat 11(4):243-256.

Hegde LG, Shukla R, Dikshit M, Srimal RC. 1994. Study on the involvement of the L-arginine/nitric oxide pathway in the central cardiovascular regulation in the chloralose-anaesthetized cat. Arch Int Pharmacodyn Ther 328(2):155-164.

Hemmens B, Mayer B. 1998. Enzymology of nitric oxide synthases. Methods Mol Biol 100:1-32.

Henry JL, Calaresu FR. 1972. Topography and numerical distribution of neurons of the thoraco-lumbar intermediolateral nucleus in the cat. J Comp Neurol 144(2):205-214.

Hepp R, Tricoire L, Hu E, Gervasi N, Paupardin-Tritsch D, Lambolez B, Vincent P. 2007. Phosphodiesterase type 2 and the homeostasis of cyclic GMP in living thalamic neurons. J Neurochem 102(6):1875-1886.

Herman JP, Figueiredo H, Mueller NK, Ulrich-Lai Y, Ostrander MM, Choi DC, Cullinan WE. 2003. Central mechanisms of stress integration: hierarchical circuitry controlling hypothalamo-pituitary-adrenocortical responsiveness. Front Neuroendocrinol 24(3):151-180.

Herman JP, Mueller NK, Figueiredo H. 2004. Role of GABA and glutamate circuitry in hypothalamo-pituitary-adrenocortical stress integration. Ann N Y Acad Sci 1018:35-45.

Herzig TC, Buchholz RA, Haywood JR. 1991. Effects of paraventricular nucleus lesions on chronic renal hypertension. Am J Physiol 261(3 Pt 2):H860-867.

Hevel JM, Marletta MA. 1992. Macrophage nitric oxide synthase: relationship between enzyme-bound tetrahydrobiopterin and synthase activity. Biochemistry 31(31):7160-7165.

Hirooka Y. 2006. Localized gene transfer and its application for the study of central cardiovascular control. Auton Neurosci 126-127:120-129.

Hirooka Y, Polson JW, Dampney RA. 1996. Pressor and sympathoexcitatory effects of nitric oxide in the rostral ventrolateral medulla. J Hypertens 14(11):1317-1324.

Hofmann F, Feil R, Kleppisch T, Schlossmann J. 2006. Function of cGMP-dependent protein kinases as revealed by gene deletion. Physiol Rev 86(1):1-23.

Hofseth LJ, Hussain SP, Wogan GN, Harris CC. 2003a. Nitric oxide in cancer and chemoprevention. Free Radic Biol Med 34(8):955-968.

Hofseth LJ, Saito S, Hussain SP, Espey MG, Miranda KM, Araki Y, Jhappan C, Higashimoto Y, He P, Linke SP, Quezado MM, Zurer I, Rotter V, Wink DA, Appella E, Harris CC. 2003b. Nitric oxide-induced cellular stress and p53 activation in chronic inflammation. Proc Natl Acad Sci U S A 100(1):143-148.

Hokfelt T, Johansson O, Goldstein M. 1984a. Central catecholamine neurons as revealed by immunohistochemistry with special reference to adrenaline neurons. In: Bjorklund A, Hokfelt T, editors. Classical Transmitters in the CNS. Amsterdam: Elsevier Science Publishing. p 157 - 276.

Hokfelt T, Johansson O, Goldstein M. 1984b. Central catecholamine neurons as revealed by immunohistochemistry with special reference to adrenaline neurons. Bjorklund A, Hokfelt T, editors. Amsterdam: Elsevier. 157 - 276 p.

Hokfelt T, Martensson R, Bjorklund A, Kleinau S, Goldstein M. 1984c. Distrubutional maps of tyrosine-hydroxylase-immuno-reactive neurons in the rat brain. In: Bjorklund A, Hokfelt T, editors. Classical transmitters in the CNS. Amsterdam: Elsevier Science Publishing. p 277 - - 379.

Holgert H, Aman K, Cozzari C, Hartman BK, Brimijoin S, Emson P, Goldstein M, Hokfelt T. 1995. The cholinergic innervation of the adrenal gland and its relation to enkephalin and nitric oxide synthase. Neuroreport 6(18):2576-2580.

Hollmann M, Heinemann S. 1994. Cloned glutamate receptors. Annu Rev Neurosci 17:31-108.

Horn T, Smith PM, McLaughlin BE, Bauce L, Marks GS, Pittman QJ, Ferguson AV. 1994. Nitric oxide actions in paraventricular nucleus: cardiovascular and neurochemical implications. Am J Physiol 266(1 Pt 2):R306-313.

Huang CC, Chan SH, Hsu KS. 2003. cGMP/protein kinase G-dependent potentiation of glutamatergic transmission induced by nitric oxide in immature rat rostral ventrolateral medulla neurons in vitro. Mol Pharmacol 64(2):521-532.

Huang PL, Huang Z, Mashimo H, Bloch KD, Moskowitz MA, Bevan JA, Fishman MC. 1995. Hypertension in mice lacking the gene for endothelial nitric oxide synthase. Nature 377(6546):239-242.

Hussain SP, Hofseth LJ, Harris CC. 2003. Radical causes of cancer. Nat Rev Cancer 3(4):276-285.

Iadecola C, Faris PL, Hartman BK, Xu X. 1993. Localization of NADPH diaphorase in neurons of the rostral ventral medulla: possible role of nitric oxide in central autonomic regulation and oxygen chemoreception. Brain Res 603(1):173-179.

Iida N. 1999. Nitric oxide mediates sympathetic vasoconstriction at supraspinal, spinal, and synaptic levels. Am J Physiol 276(3 Pt 2):H918-925.

Iino M, Nakatome M, Ogura Y, Fujimura H, Kuroki H, Inoue H, Ino Y, Fujii T, Terao T, Matoba R. 2003. Real-time PCR quantitation of FE65 a beta-amyloid precursor protein-binding protein after traumatic brain injury in rats. Int J Legal Med 117(3):153-159.

Imaizumi T, Granata AR, Benarroch EE, Sved AF, Reis DJ. 1985. Contributions of arginine vasopressin and the sympathetic nervous system to fulminating hypertension after destruction of neurons of caudal ventrolateral medulla in the rat. J Hypertens 3(5):491-501.

Imura H, Nakao K, Itoh H. 1992. The natriuretic peptide system in the brain: implications in the central control of cardiovascular and neuroendocrine functions. Front Neuroendocrinol 13(3):217-249.

Inokuchi H, Yoshimura M, Trzebski A, Polosa C, Nishi S. 1992a. Fast inhibitory postsynaptic potentials and responses to inhibitory amino acids of sympathetic preganglionic neurons in the adult cat. J Auton Nerv Syst 41(1-2):53-59.

Inokuchi H, Yoshimura M, Yamada S, Polosa C, Nishi S. 1992b. Fast excitatory postsynaptic potentials and the responses to excitant amino acids of sympathetic preganglionic neurons in the slice of the cat spinal cord. Neuroscience 46(3):657-667.

Jaffrey SR, Erdjument-Bromage H, Ferris CD, Tempst P, Snyder SH. 2001. Protein S-nitrosylation: a physiological signal for neuronal nitric oxide. Nat Cell Biol 3(2):193-197.

Jaffrey SR, Snyder SH. 1995. Nitric oxide: a neural messenger. Annu Rev Cell Dev Biol 11:417-440.

Janig W, McLachlan EM. 1986. Identification of distinct topographical distributions of lumbar sympathetic and sensory neurons projecting to end organs with different functions in the cat. J Comp Neurol 246(1):104-112.

Janig W, McLachlan EM. 1987. Organization of lumbar spinal outflow to distal colon and pelvic organs. Physiol Rev 67(4):1332-1404.

Jansen AS, Wessendorf MW, Loewy AD. 1995. Transneuronal labeling of CNS neuropeptide and monoamine neurons after pseudorabies virus injections into the stellate ganglion. Brain Res 683(1):1-24.

Jeske I, McKenna KE. 1992. Quantitative analysis of bulbospinal projections from the rostral ventrolateral medulla: contribution of C1-adrenergic and nonadrenergic neurons. J Comp Neurol 324(1):1-13.

Jeske I, Morrison SF, Cravo SL, Reis DJ. 1993. Identification of baroreceptor reflex interneurons in the caudal ventrolateral medulla. Am J Physiol 264(1 Pt 2):R169-178.

Jeske I, Reis DJ, Milner TA. 1995. Neurons in the barosensory area of the caudal ventrolateral medulla project monosynaptically on to sympathoexcitatory bulbospinal neurons in the rostral ventrolateral medulla. Neuroscience 65(2):343-353.

Johnson ML, Ely DL, Turner ME. 1992. Genetic divergence between the Wistar-Kyoto rat and the spontaneously hypertensive rat. Hypertension 19(5):425-427.

Ju G, Han ZS, Fan LZ. 1989. Fluorogold as a retrograde tracer used in combination with immunohistochemistry. J Neurosci Methods 29(1):69-72.

Julius S. 1986. The emerging field of borderline hypertension. J Cardiovasc Pharmacol 8 Suppl 5:S4-7.

Kaczmarek L, Kossut M, Skangiel-Kramska J. 1997. Glutamate receptors in cortical plasticity: molecular and cellular biology. Physiol Rev 77(1):217-255.

Kadekaro M. 2004. Nitric oxide modulation of the hypothalamo-neurohypophyseal system. Braz J Med Biol Res 37(4):441-450.

Kadowaki K, Kishimoto J, Leng G, Emson PC. 1994. Up-regulation of nitric oxide synthase (NOS) gene expression together with NOS activity in the rat hypothalamo-hypophysial system after chronic salt loading: evidence of a neuromodulatory role of nitric oxide in arginine vasopressin and oxytocin secretion. Endocrinology 134(3):1011-1017.

Kagiyama S, Tsuchihashi T, Abe I, Fujishima M. 1997. Cardiovascular effects of nitric oxide in the rostral ventrolateral medulla of rats. Brain Res 757(1):155-158.

Kagiyama S, Tsuchihashi T, Abe I, Fujishima M. 1998. Enhanced depressor response to nitric oxide in the rostral ventrolateral medulla of spontaneously hypertensive rats. Hypertension 31(4):1030-1034.

Kanjhan R, Lipski J, Kruszewska B, Rong W. 1995. A comparative study of pre-sympathetic and Botzinger neurons in the rostral ventrolateral medulla (RVLM) of the rat. Brain Res 699(1):19-32.

Kannan H, Niijima A, Yamashita H. 1987. Inhibition of renal sympathetic nerve activity by electrical stimulation of the hypothalamic paraventricular nucleus in anesthetized rats. J Auton Nerv Syst 21(1):83-86.

Kantzides A, Badoer E. 2003. Fos, RVLM-projecting neurons, and spinally projecting neurons in the PVN following hypertonic saline infusion. Am J Physiol Regul Integr Comp Physiol 284(4):R945-953.

Kantzides A, Badoer E. 2005. nNOS-containing neurons in the hypothalamus and medulla project to the RVLM. Brain Res 1037(1-2):25-34.

Katz LC, Burkhalter A, Dreyer WJ. 1984. Fluorescent latex microspheres as a retrograde neuronal marker for in vivo and in vitro studies of visual cortex. Nature 310(5977):498-500.

Kaupp UB, Seifert R. 2002. Cyclic nucleotide-gated ion channels. Physiol Rev 82(3):769-824.

Keefer LK. 2005. Nitric oxide (NO)- and nitroxyl (HNO)-generating diazeniumdiolates (NONOates): emerging commercial opportunities. Curr Top Med Chem 5(7):625-636.

Kenney MJ, Weiss ML, Haywood JR. 2003. The paraventricular nucleus: an important component of the central neurocircuitry regulating sympathetic nerve outflow. Acta Physiol Scand 177(1):7-15.

Kha HT, Finkelstein DI, Pow DV, Lawrence AJ, Horne MK. 2000. Study of projections from the entopeduncular nucleus to the thalamus of the rat. J Comp Neurol 426(3):366-377.

Kiedrowski L, Costa E, Wroblewski JT. 1992. Glutamate receptor agonists stimulate nitric oxide synthase in primary cultures of cerebellar granule cells. J Neurochem 58(1):335-341.

Kiely JM, Gordon FJ. 1993. Non-NMDA receptors in the rostral ventrolateral medulla mediate somatosympathetic pressor responses. J Auton Nerv Syst 43(3):231-239.

Kimura KA, Reynolds JN, Brien JF. 2000. Ethanol neurobehavioral teratogenesis and the role of the hippocampal glutamate-N-methyl-D-aspartate receptor-nitric oxide synthase system. Neurotoxicol Teratol 22(5):607-616.

Kimura Y, Hirooka Y, Sagara Y, Ito K, Kishi T, Shimokawa H, Takeshita A, Sunagawa K. 2005. Overexpression of inducible nitric oxide synthase in rostral ventrolateral medulla causes hypertension and sympathoexcitation via an increase in oxidative stress. Circ Res 96(2):252-260.

Kistner U, Wenzel BM, Veh RW, Cases-Langhoff C, Garner AM, Appeltauer U, Voss B, Gundelfinger ED, Garner CC. 1993. SAP90, a rat presynaptic protein related to the product of the Drosophila tumor suppressor gene dlg-A. J Biol Chem 268(7):4580-4583.

Knowles RG, Palacios M, Palmer RM, Moncada S. 1989. Formation of nitric oxide from L-arginine in the central nervous system: a transduction mechanism for stimulation of the soluble guanylate cyclase. Proc Natl Acad Sci U S A 86(13):5159-5162.

Koga N, Takano Y, Honda K, Saito R, Kamiya H. 1999. Roles of nitric oxide in the spinal cord in cardiovascular regulation in rats. Neurosci Lett 267(3):173-176.

Kojda G, Kottenberg K, Hacker A, Noack E. 1998. Alterations of the vascular and the myocardial guanylate cyclase/cGMP-system induced by long-term hypertension in rats. Pharm Acta Helv 73(1):27-35.

Kojima H, Nakatsubo N, Kikuchi K, Kawahara S, Kirino Y, Nagoshi H, Hirata Y, Nagano T. 1998. Detection and imaging of nitric oxide with novel fluorescent indicators: diaminofluoresceins. Anal Chem 70(13):2446-2453.

Koller A, Kaley G. 1990. Prostaglandins mediate arteriolar dilation to increased blood flow velocity in skeletal muscle microcirculation. Circ Res 67(2):529-534.

Koller A, Sun D, Kaley G. 1993. Role of shear stress and endothelial prostaglandins in flow- and viscosity-induced dilation of arterioles in vitro. Circ Res 72(6):1276-1284.

Kono T, Chisato N, Ebisawa Y, Asama T, Sugawara M, Ayabe T, Kohgo Y, Kasai S, Yoneda M, Takahashi T. 2004. Impaired nitric oxide production of the myenteric plexus in colitis detected by a new bioimaging system. J Surg Res 117(2):329-338.

Koshiya N, Huangfu D, Guyenet PG. 1993. Ventrolateral medulla and sympathetic chemoreflex in the rat. Brain Res 609(1-2):174-184.

Krukoff TL. 1998. Central regulation of autonomic function: no brakes? Clin Exp Pharmacol Physiol 25(6):474-478.

Krukoff TL. 1999. Central actions of nitric oxide in regulation of autonomic functions. Brain Res Brain Res Rev 30(1):52-65.

Krukoff TL, Gehlen F, Ganten D, Wagner J. 1995. Gene expression of brain nitric oxide synthase and soluble guanylyl cyclase in hypothalamus and medulla of two-kidney, one clip hypertensive rats. Hypertension 26(1):171-176.

Krukoff TL, Harris KH, Linetsky E, Jhamandas JH. 1994. Expression of c-fos protein in rat brain elicited by electrical and chemical stimulation of the hypothalamic paraventricular nucleus. Neuroendocrinology 59(6):590-602.

Krumenacker JS, Hanafy KA, Murad F. 2004. Regulation of nitric oxide and soluble guanylyl cyclase. Brain Res Bull 62(6):505-515.

Kubo T, Hagiwara Y, Sekiya D, Chiba S, Fukumori R. 2000. Cholinergic inputs to rostral ventrolateral medulla pressor neurons from hypothalamus. Brain Res Bull 53(3):275-282.

Kubo T, Kihara M. 1987. Evidence for the presence of GABAergic and glycine-like systems responsible for cardiovascular control in the nucleus tractus solitarii of the rat. Neurosci Lett 74(3):331-336.

Kubo T, Kihara M. 1990. Modulation of the aortic baroreceptor reflex by neuropeptide Y, neurotensin and vasopressin microinjected into the nucleus tractus solitarii of the rat. Naunyn-Schmiedeberg's archives of pharmacology 342(2):182-188.

Kuchel O, Debinski W, Thibault G, Cantin M, Genest J. 1988. Ganglionic, spinal cord and hypothalamic atrial natriuretic factor: its distribution, origin and possible role in spontaneously hypertensive rats. J Hypertens Suppl 6(4):S279-281.

Kuypers HGJM, Maisky V. 1975. Retrograde axonal transport of horseradish peroxidase from spinal cord to the brainstem groups in the cat. Neurosci Lett 1:9-14.

Lage RC, Campagnole-Santos MJ, Fontes MA, Santos RA. 1999. Cardiovascular effects produced by nitric oxide-related drugs in the caudal ventrolateral medulla. Neuroreport 10(4):731-735.

Lawes CM, Vander Hoorn S, Law MR, Elliott P, MacMahon S, Rodgers A. 2006. Blood pressure and the global burden of disease 2000. Part II: estimates of attributable burden. J Hypertens 24(3):423-430.

Lawrence AJ, Jarrott B. 1993. Nitric oxide increases interstitial excitatory amino acid release in the rat dorsomedial medulla oblongata. Neurosci Lett 151(2):126-129.

Lawrence AJ, Jarrott B. 1996. Neurochemical modulation of cardiovascular control in the nucleus tractus solitarius. Prog Neurobiol 48(1):21-53.

Leblanc N, Hume JR. 1990. Sodium current-induced release of calcium from cardiac sarcoplasmic reticulum. Science 248(4953):372-376.

Lederer WJ, Niggli E, Hadley RW. 1990. Sodium-calcium exchange in excitable cells: fuzzy space. Science 248(4953):283.

Lee SB, Koh HC, Kim ON, Sung KW, Kim SY. 1996. Intrathecal administration of sodium nitroprusside, a nitric oxide donor, increases blood pressure in anesthetized rats. Neurosci Lett 203(1):53-56.

Lerma J, Kushner L, Zukin RS, Bennett MV. 1989. N-methyl-D-aspartate activates different channels than do kainate and quisqualate. Proc Natl Acad Sci U S A 86(6):2083-2087.

Li D, Wang L, Lee CW, Dawson TA, Paterson DJ. 2007. Noradrenergic cell specific gene transfer with neuronal nitric oxide synthase reduces cardiac sympathetic neurotransmission in hypertensive rats. Hypertension 50(1):69-74.

Li DP, Atnip LM, Chen SR, Pan HL. 2005. Regulation of synaptic inputs to paraventricular-spinal output neurons by alpha2 adrenergic receptors. J Neurophysiol 93(1):393-402.

Li DP, Chen SR, Finnegan TF, Pan HL. 2003a. Signalling pathway of nitric oxide in synaptic GABA release in the rat paraventricular nucleus. J Physiol 554(3):100-110.

Li DP, Chen SR, Finnegan TF, Pan HL. 2004. Signalling pathway of nitric oxide in synaptic GABA release in the rat paraventricular nucleus. J Physiol 554(Pt 1):100-110.

Li DP, Chen SR, Pan HL. 2002. Nitric oxide inhibits spinally projecting paraventricular neurons through potentiation of presynaptic GABA release. J Neurophysiol 88(5):2664-2674.

Li DP, Yang Q, Pan HM, Pan HL. 2008. Pre- and postsynaptic plasticity underlying augmented glutamatergic inputs to hypothalamic presympathetic neurons in spontaneously hypertensive rats. J Physiol 586(6):1637-1647.

Li H, Forstermann U. 2000. Nitric oxide in the pathogenesis of vascular disease. J Pathol 190(3):244-254.

Li H, Poulos TL. 2005. Structure-function studies on nitric oxide synthases. J Inorg Biochem 99(1):293-305.

Li WM, Sato A, Sato Y, Schmidt RF. 1996. Morphine microinjected into the nucleus tractus solitarius and rostral ventrolateral medullary nucleus enhances somatosympathetic A- and C- reflexes in anesthetized rats. Neurosci Lett 221(1):53-56.

Li Y, Zhang W, Stern JE. 2003b. Nitric oxide inhibits the firing activity of hypothalamic paraventricular neurons that innervate the medulla oblongata: role of GABA. Neuroscience 118(3):585-601.

Li YF, Mayhan WG, Patel KP. 2001. NMDA-mediated increase in renal sympathetic nerve discharge within the PVN: role of nitric oxide. Am J Physiol Heart Circ Physiol 281(6):H2328-2336.

Li Z, Chapleau MW, Bates JN, Bielefeldt K, Lee HC, Abboud FM. 1998. Nitric oxide as an autocrine regulator of sodium currents in baroreceptor neurons. Neuron 20(5):1039-1049.

Lifton RP, Gharavi AG, Geller DS. 2001. Molecular mechanisms of human hypertension. Cell 104(4):545-556.

Lin JC, Tsao WL, Wang Y. 1995. Cardiovascular effects of NMDA in the RVLM of spontaneously hypertensive rats. Brain Res Bull 37(3):289-294.

Lin LH, Talman WT. 2005. Soluble guanylate cyclase and neuronal nitric oxide synthase colocalize in rat nucleus tractus solitarii. J Chem Neuroanat 29(2):127-136.

Lind RW. 1988. Angiotensin and the lamina terminalis: illustrations of a complex unity. Clin Exp Hypertens A 10 Suppl 1:79-105.

Lind RW, Swanson LW, Ganten D. 1985. Organization of angiotensin II immunoreactive cells and fibers in the rat central nervous system. An immunohistochemical study. Neuroendocrinology 40(1):2-24.

Lindley TE, Doobay MF, Sharma RV, Davisson RL. 2004. Superoxide is involved in the central nervous system activation and sympathoexcitation of myocardial infarction-induced heart failure. Circ Res 94(3):402-409.

Lipski J, Kanjhan R, Kruszewska B, Rong WF, Smith M. 1997. Presympathetic neurones in the rostral ventrolateral medulla of the rat: electrophysiology, morphology and relationship to adjacent neuronal groups. Acta Neurobiol Exp 56:373 – 384.

Lipski J, Kanjhan R, Kruszewska B, Smith M. 1995. Barosensitive neurons in the rostral ventrolateral medulla of the rat in vivo: morphological properties and relationship to C1 adrenergic neurons. Neuroscience 69(2):601-618.

Liu QS, Jia YS, Ju G. 1997. Nitric oxide inhibits neuronal activity in the supraoptic nucleus of the rat hypothalamic slices. Brain Res Bull 43(2):121-125.

Livak KJ, Schmittgen TD. 2001. Analysis of relative gene expression data using real-time quantitative PCR and the 2(-Delta Delta C(T)) Method. Methods 25(4):402-408.

Llewellyn-Smith IJ. 2002. GABA in the control of sympathetic preganglionic neurons. Clin Exp Pharmacol Physiol 29(5-6):507-513.

Llewellyn-Smith IJ, Arnolda LF, Pilowsky PM, Chalmers JP, Minson JB. 1998. GABA- and glutamate-immunoreactive synapses on sympathetic preganglionic neurons projecting to the superior cervical ganglion. J Auton Nerv Syst 71(2-3):96-110.

Llewellyn-Smith IJ, Cassam AK, Krenz NR, Krassioukov AV, Weaver LC. 1997a. Glutamate- and GABA-immunoreactive synapses on sympathetic preganglionic neurons caudal to a spinal cord transection in rats. Neuroscience 80(4):1225-1235.

Llewellyn-Smith IJ, Dicarlo SE, Collins HL, Keast JR. 2005. Enkephalin-immunoreactive interneurons extensively innervate sympathetic preganglionic neurons regulating the pelvic viscera. J Comp Neurol 488(3):278-289.

Llewellyn-Smith IJ, Martin CL, Fenwick NM, Dicarlo SE, Lujan HL, Schreihofer AM. 2007. VGLUT1 and VGLUT2 innervation in autonomic regions of intact and transected rat spinal cord. J Comp Neurol 503(6):741-767.

Llewellyn-Smith IJ, Martin CL, Minson JB, Pilowsky PM, Arnolda LF, Basbaum AI, Chalmers JP. 1997b. Neurokinin-1 receptor-immunoreactive sympathetic preganglionic neurons: target specificity and ultrastructure. Neuroscience 77(4):1137-1149.

Llewellyn-Smith IJ, Phend KD, Minson JB, Pilowsky PM, Chalmers JP. 1992. Glutamate-immunoreactive synapses on retrogradely-labelled sympathetic preganglionic neurons in rat thoracic spinal cord. Brain Res 581(1):67-80.

Lodish H, Berk A, Zipursky SL, Matsudiara P, Baltimore D, Darnell J. 1997. Molecular Biology of the Cell. New York: W.H Freeman and Company.

Loewy A. 1990. Central Autonomic Pathways. Central Regulation of autonomic functions. AD L, KM S, editors. New York: Oxford. 88 - 103 p.

Loewy AD. 1991. Forebrain nuclei involved in autonomic control. Prog Brain Res 87:253-268.

Louis WJ, Howes LG. 1990. Genealogy of the spontaneously hypertensive rat and Wistar-Kyoto rat strains: implications for studies of inherited hypertension. J Cardiovasc Pharmacol 16 Suppl 7:S1-5.

Lu PP, Shee JJ, Chen HM, Lin CC, Shyr MH. 1999. Spinal nitric oxide participates in the control of the blood pressure during graded hemorrhage in the conscious rat. Shock 12(3):222-226.

Lucas KA, Pitari GM, Kazerounian S, Ruiz-Stewart I, Park J, Schulz S, Chepenik KP, Waldman SA. 2000. Guanylyl cyclases and signaling by cyclic GMP. Pharmacol Rev 52(3):375-414.

Ludbrook J. 1998. Multiple comparison procedures updated. Clin Exp Pharmacol Physiol 25(12):1032-1037.

Luepker RV, Arnett DK, Jacobs DR, Jr., Duval SJ, Folsom AR, Armstrong C, Blackburn H. 2006. Trends in blood pressure, hypertension control, and stroke mortality: the Minnesota Heart Survey. Am J Med 119(1):42-49.

Luiten PG, ter Horst GJ, Karst H, Steffens AB. 1985. The course of paraventricular hypothalamic efferents to autonomic structures in medulla and spinal cord. Brain Res 329(1-2):374-378.

Machado BH, Mauad H, Chianca Junior DA, Haibara AS, Colombari E. 1997. Autonomic processing of the cardiovascular reflexes in the nucleus tractus solitarii. Braz J Med Biol Res 30(4):533-543.

Mackay J, Mensah G. 2004. The Atlas of Heart Disease and Stroke. World Health Organization.

Madden CJ, Ito S, Rinaman L, Wiley RG, Sved AF. 1999. Lesions of the C1 catecholaminergic neurons of the ventrolateral medulla in rats using anti-DbetaH-saporin. Am J Physiol 277(4 Pt 2):R1063-1075.

Madden CJ, Sved AE. 2003. Rostral ventrolateral medulla C1 neurons and cardiovascular regulation. Cell Mol Neurobiol 23(4-5):739-749.

Maddens M, Sowers J. 1987. Catecholamines in critical care. Crit Care Clin 3(4):871-882.

Maeda M, Inoue M, Takao S, Nakai M. 1999. Central control mechanisms of circulation in the medulla oblongata by nitric oxide. Jpn J Physiol 49(6):467-478.

Magoun HW. 1940. Descending connections from the hypothalamus. Res Publ Ass Nerv Ment Dis 20:270 - 285.

Malik V, Holobotovskyy VV, Phillips JK, McKitrick DJ, Arnolda LF. 2007. Intrathecal cGMP elicits pressor responses and maintains mean blood pressure during haemorrhage in anaesthetized rats. J Physiol 581(Pt 2):543-552.

Malpas SC, Coote JH. 1994. Role of vasopressin in sympathetic response to paraventricular nucleus stimulation in anesthetized rats. Am J Physiol 266(1 Pt 2):R228-236.

Mani SK, Allen JM, Rettori V, McCann SM, O'Malley BW, Clark JH. 1994. Nitric oxide mediates sexual behavior in female rats. Proc Natl Acad Sci U S A 91(14):6468-6472.

Marangos PJ, Zis AP, Clark RL, Goodwin FK. 1978. Neuronal, non-neuronal and hybrid forms of enolase in brain: structural, immunological and functional comparisons. Brain Res 150(1):117-133.

Marshall JM. 1994. Peripheral chemoreceptors and cardiovascular regulation. Physiol Rev 74(3):543-594.

Martin AR, Fuchs PA. 1992. The dependence of calcium-activated potassium currents on membrane potential. Proc Biol Sci 250(1327):71-76.

Martin DS, Haywood JR. 1992. Sympathetic nervous system activation by glutamate injections into the paraventricular nucleus. Brain Res 577(2):261-267.

Martins-Pinge MC, Araujo GC, Lopes OU. 1999. Nitric oxide-dependent guanylyl cyclase participates in the glutamatergic neurotransmission within the rostral ventrolateral medulla of awake rats. Hypertension 34(4 Pt 2):748-751.

Martins-Pinge MC, Baraldi-Passy I, Lopes OU. 1997. Excitatory effects of nitric oxide within the rostral ventrolateral medulla of freely moving rats. Hypertension 30(3 Pt 2):704-707.

Martins-Pinge MC, Garcia MR, Zoccal DB, Crestani CC, Pinge-Filho P. 2007. Differential influence of iNOS and nNOS inhibitors on rostral ventrolateral medullary mediated cardiovascular control in conscious rats. Auton Neurosci 131(1-2):65-69.

Masters BS, McMillan K, Sheta EA, Nishimura JS, Roman LJ, Martasek P. 1996. Neuronal nitric oxide synthase, a modular enzyme formed by convergent evolution: structure studies of a cysteine thiolate-liganded heme protein that hydroxylates L-arginine to produce NO. as a cellular signal. FASEB J 10(5):552-558.

Matsuo I, Hirooka Y, Hironaga K, Eshima K, Shigematsu H, Shihara M, Sakai K, Takeshita A. 2001. Glutamate release via NO production evoked by NMDA in the NTS enhances hypotension and bradycardia in vivo. Am J Physiol Regul Integr Comp Physiol 280(5):R1285-1291.

Mayer B, John M, Heinzel B, Werner ER, Wachter H, Schultz G, Bohme E. 1991. Brain nitric oxide synthase is a biopterin- and flavin-containing multi-functional oxido-reductase. FEBS Lett 288(1-2):187-191.

Mayorov DN. 2005. Selective sensitization by nitric oxide of sympathetic baroreflex in rostral ventrolateral medulla of conscious rabbits. Hypertension 45(5):901-906.

McCall RB. 1988. Effects of putative neurotransmitters on sympathetic preganglionic neurons. Annu Rev Physiol 50:553-564.

McDonald LJ, Murad F. 1995. Nitric oxide and cGMP signaling. Adv Pharmacol 34:263-275.

McKitrick DJ, Calaresu FR. 1997. Reciprocal connection between nucleus ambiguus and caudal ventrolateral medulla. Brain Res 770(1-2):213-220.

McKitrick DJ, Krukoff TL, Calaresu FR. 1992. Expression of c-fos protein in rat brain after electrical stimulation of the aortic depressor nerve. Brain Res 599(2):215-222.

McLachlan EM, Anderson CR, Sinclair AD. 1989. Are there bulbospinal catecholaminergic neurones in the guinea pig equivalent to the C1 cell group in the rat and rabbit? Brain Res 481(2):274-285.

Mendelsohn FA, Allen AM, Clevers J, Denton DA, Tarjan E, McKinley MJ. 1988. Localization of angiotensin II receptor binding in rabbit brain by in vitro autoradiography. J Comp Neurol 270(3):372-384.

Mergia E, Russwurm M, Zoidl G, Koesling D. 2003. Major occurrence of the new alpha2beta1 isoform of NO-sensitive guanylyl cyclase in brain. Cell Signal 15(2):189-195.

Messerli FH, Williams B, Ritz E. 2007. Essential hypertension. Lancet 370(9587):591-603.

Milner TA, Morrison SF, Abate C, Reis DJ. 1988. Phenylethanolamine N-methyltransferase-containing terminals synapse directly on sympathetic preganglionic neurons in the rat. Brain Res 448(2):205-222.

Minami N, Imai Y, Hashimoto J, Abe K. 1995. The role of nitric oxide in the baroreceptor-cardiac reflex in conscious Wistar rats. Am J Physiol 269(3 Pt 2):H851-855.

Minson J, Arnolda L, Llewellyn-Smith I, Pilowsky P, Chalmers J. 1996. Altered c-fos in rostral medulla and spinal cord of spontaneously hypertensive rats. Hypertension 27(3 Pt 1):433-441.

Minson JB, Arnolda LF, Llewellyn-Smith IJ. 2002. Neurochemistry of nerve fibers apposing sympathetic preganglionic neurons activated by sustained hypotension. J Comp Neurol 449(4):307-318.

Minson JB, Llewellyn-Smith IJ, Arnolda LF, Pilowsky PM, Chalmers JP. 1997. C-fos expression in central neurons mediating the arterial baroreceptor reflex. Clin Exp Hypertens 19(5-6):631-643.

Miyagawa A, Okamura H, Ibata Y. 1994. Coexistence of oxytocin and NADPH-diaphorase in magnocellular neurons of the paraventricular and the supraoptic nuclei of the rat hypothalamus. Neurosci Lett 171(1-2):13-16.

Mollace V, De Francesco EA, Nistico G. 1992. Evidence that pharmacological manipulations of central L-arginine-NO pathway influence blood pressure and heart rate in rats. Neurosci Lett 137(1):87-90.

Monahan KD. 2007. Effect of Aging on Baroreflex Function in Humans. Am J Physiol Regul Integr Comp Physiol.

Monyer H, Burnashev N, Laurie DJ, Sakmann B, Seeburg PH. 1994. Developmental and regional expression in the rat brain and functional properties of four NMDA receptors. Neuron 12(3):529-540.

Morimoto S, Sasaki S, Miki S, Kawa T, Nakamura K, Itoh H, Nakata T, Takeda K, Nakagawa M, Fushiki S. 2000. Nitric oxide is an excitatory modulator in the rostral ventrolateral medulla in rats. Am J Hypertens 13(10):1125-1134.

Moriyoshi K, Masu M, Ishii T, Shigemoto R, Mizuno N, Nakanishi S. 1991. Molecular cloning and characterization of the rat NMDA receptor. Nature 354(6348):31-37.

Morrison SF. 2003. Glutamate transmission in the rostral ventrolateral medullary sympathetic premotor pathway. Cell Mol Neurobiol 23(4-5):761-772.

Morrison SF, Cao WH. 2000. Different adrenal sympathetic preganglionic neurons regulate epinephrine and norepinephrine secretion. Am J Physiol Regul Integr Comp Physiol 279(5):R1763-1775.

Morrison SF, Milner TA, Reis DJ. 1988. Reticulospinal vasomotor neurons of the rat rostral ventrolateral medulla: relationship to sympathetic nerve activity and the C1 adrenergic cell group. J Neurosci 8(4):1286-1301.

Moyer JR, Jr., Brown TH. 1998. Methods for whole-cell recording from visually preselected neurons of perirhinal cortex in brain slices from young and aging rats. J Neurosci Methods 86(1):35-54.

Murad F. 1994. Regulation of cytosolic guanylyl cyclase by nitric oxide: the NO-cyclic GMP signal transduction system. Adv Pharmacol 26:19-33.

Muratani H, Averill DB, Ferrario CM. 1991. Effect of angiotensin II in ventrolateral medulla of spontaneously hypertensive rats. Am J Physiol 260(5 Pt 2):R977-984.

Murphy SM, McAllen R, Campbell GD, Howe PR, Anderson CR. 2003. Re-establishment of neurochemical coding of preganglionic neurons innervating transplanted targets. Neuroscience 117(2):347-360.

N'Diaye A, Sevoz-Couche C, Nosjean A, Hamon M, Laguzzi R. 2001. Stimulation of 5-HT2 receptors in the nucleus tractus solitarius enhances NMDA receptor-mediated reflex-evoked bradycardiac responses in the rat. Auton Neurosci 92(1-2):45-55.

Nakahara T, Ishii K, Iwamoto K, Nakayama K. 1995. Differential significance of nitric oxide in hypotensive mechanisms of acetylcholine and histamine in dogs. Res Commun Mol Pathol Pharmacol 89(1):77-84.

Nakahara T, Moriuchi H, Yunoki M, Kubota Y, Tanaka Y, Sakamato K, Shigenobu K, Ishii K. 2000. Involvement of K(+) channel in procainamide-induced relaxation of bovine tracheal smooth muscle. Eur J Pharmacol 402(1-2):143-149.

Nakamura H. 1997. NADPH-diaphorase and cytosolic urea cycle enzymes in the rat spinal cord. J Comp Neurol 385(4):616-626.

Nakanishi S. 1992. Molecular diversity of glutamate receptors and implications for brain function. Science 258(5082):597-603.

Nathan C, Xie QW. 1994. Nitric oxide synthases: roles, tolls, and controls. Cell 78(6):915-918.

Nazu M, Thippeswamy T. 2002. Nitric oxide signalling system in rat brain stem: immunocytochemical studies. Anat Histol Embryol 31(4):252-256.

Nelson EJ, Connolly J, McArthur P. 2003. Nitric oxide and S-nitrosylation: excitotoxic and cell signaling mechanism. Biol Cell 95(1):3-8.

Nestel PJ. 1969. Blood-pressure and catecholamine excretion after mental stress in labile hypertension. Lancet 1(7597):692-694.

Newman DB. 1985. Distinguishing rat brainstem reticulospinal nuclei by their neuronal morphology. I. Medullary nuclei. J Hirnforsch 26(2):187-226.

Nylen A, Skagerberg G, Alm P, Larsson B, Holmqvist B, Andersson KE. 2001a. Nitric oxide synthase in the hypothalamic paraventricular nucleus of the female rat; organization of spinal projections and coexistence with oxytocin or vasopressin. Brain Res 908(1):10-24.

Nylen A, Skagerberg G, Alm P, Larsson B, Holmqvist BI, Andersson KE. 2001b. Detailed organization of nitric oxide synthase, vasopressin and oxytocin

immunoreactive cell bodies in the supraoptic nucleus of the female rat. Anat Embryol (Berl) 203(4):309-321.

Ohkuma S, Katsura M. 2001. Nitric oxide and peroxynitrite as factors to stimulate neurotransmitter release in the CNS. Prog Neurobiol 64(1):97-108.

Ohta A, Takagi H, Matsui T, Hamai Y, Iida S, Esumi H. 1993. Localization of nitric oxide synthase-immunoreactive neurons in the solitary nucleus and ventrolateral medulla oblongata of the rat: their relation to catecholaminergic neurons. Neurosci Lett 158(1):33-35.

Okamoto K, Aoki K. 1963. Development of a strain of spontaneously hypertensive rats. Jpn Circ J 27:282-293.

Okamura H, Umehara K, Tadaki N, Hisa Y, Esumi H, Ibata Y. 1995. Sympathetic preganglionic neurons contain nitric oxide synthase and project to the superior cervical ganglion: combined application of retrograde neuronal tracer and NADPH-diaphorase histochemistry. Brain Res Bull 36(5):491-494.

Oliva AA, Jr., Jiang M, Lam T, Smith KL, Swann JW. 2000. Novel hippocampal interneuronal subtypes identified using transgenic mice that express green fluorescent protein in GABAergic interneurons. J Neurosci 20(9):3354-3368.

Ozaki M, Shibuya I, Kabashima N, Isse T, Noguchi J, Ueta Y, Inoue Y, Shigematsu A, Yamashita H. 2000. Preferential potentiation by nitric oxide of spontaneous inhibitory postsynaptic currents in rat supraoptic neurones. J Neuroendocrinol 12(3):273-281.

Pagano R. 1994. Understanding statistics in behavioural sciences. Rose S, editor. Minneapolis: West Publishing Company.

Parkinson SJ, Jovanovic A, Jovanovic S, Wagner F, Terzic A, Waldman SA. 1999. Regulation of nitric oxide-responsive recombinant soluble guanylyl cyclase by calcium. Biochemistry 38(20):6441-6448.

Patel KP, Li YF, Hirooka Y. 2001. Role of nitric oxide in central sympathetic outflow. Exp Biol Med (Maywood) 226(9):814-824.

Patel KP, Schmid PG. 1988. Role of paraventricular nucleus (PVH) in baroreflex-mediated changes in lumbar sympathetic nerve activity and heart rate. J Auton Nerv Syst 22(3):211-219.

Paton JF, Kasparov S. 1999. Differential effects of angiotensin II on cardiorespiratory reflexes mediated by nucleus tractus solitarii - a microinjection study in the rat. J Physiol 521 Pt 1:213-225.

Paxinos G, Watson C. 1998. The Rat Brain in Stereotaxic Coordinates. Press A, editor. San Diego.

Paxinos G, Watson C. 1999. Chemoarchitectonic Atlas of the Rat Brainstem. San Diego: Academic Press.

Pelto-Huikko M, Salminen T, Hervonen A. 1985. Localization of enkephalins in adrenaline cells and the nerves innervating adrenaline cells in rat adrenal medulla. Histochemistry 82(4):377-383.

Perez-Velazquez JL, Zhang L. 1994. In vitro hypoxia induces expression of the NR2C subunit of the NMDA receptor in rat cortex and hippocampus. J Neurochem 63(3):1171-1173.

Phillips JK. 2005. Pathogenesis of hypertension in renal failure: role of the sympathetic nervous system and renal afferents. Clin Exp Pharmacol Physiol 32(5-6):415-418.

Phillips JK, Goodchild AK, Dubey R, Sesiashvili E, Takeda M, Chalmers J, Pilowsky PM, Lipski J. 2001. Differential expression of catecholamine biosynthetic enzymes in the rat ventrolateral medulla. J Comp Neurol 432(1):20-34.

Pilowsky PM, Goodchild AK. 2002. Baroreceptor reflex pathways and neurotransmitters: 10 years on. J Hypertens 20(9):1675-1688.

Pineda J, Kogan JH, Aghajanian GK. 1996. Nitric oxide and carbon monoxide activate locus coeruleus neurons through a cGMP-dependent protein kinase: involvement of a nonselective cationic channel. J Neurosci 16(4):1389-1399.

Plochocka-Zulinska D, Krukoff TL. 1997. Increased gene expression of neuronal nitric oxide synthase in brain of adult spontaneously hypertensive rats. Brain Res Mol Brain Res 48(2):291-297.

Pohl U, Herlan K, Huang A, Bassenge E. 1991. EDRF-mediated shear-induced dilation opposes myogenic vasoconstriction in small rabbit arteries. Am J Physiol 261(6 Pt 2):H2016-2023.

Pollock JS, Forstermann U, Mitchell JA, Warner TD, Schmidt HH, Nakane M, Murad F. 1991. Purification and characterization of particulate endothelium-derived relaxing factor synthase from cultured and native bovine aortic endothelial cells. Proc Natl Acad Sci U S A 88(23):10480-10484.

Porter JP, Brody MJ. 1985. Neural projections from paraventricular nucleus that subserve vasomotor functions. Am J Physiol 248(3 Pt 2):R271-281.

Portillo F, Carrasco M, Vallo JJ. 1996. Hypothalamic neuron projection to autonomic preganglionic levels related with glucose metabolism: a fluorescent labelling study in the rat. Neurosci Lett 210(3):197-200.

Portillo F, Carrasco M, Vallo JJ. 1998. Separate populations of neurons within the paraventricular hypothalamic nucleus of the rat project to vagal and thoracic autonomic preganglionic levels and express c-Fos protein induced by lithium chloride. J Chem Neuroanat 14(2):95-102.

Pyner S, Coote JH. 1994. Evidence that sympathetic preganglionic neurones are arranged in target-specific columns in the thoracic spinal cord of the rat. J Comp Neurol 342(1):15-22.

Pyner S, Coote JH. 1995. Arrangement of dendrites and morphological characteristics of sympathetic preganglionic neurones projecting to the superior cervical ganglion and adrenal medulla in adult cat. J Auton Nerv Syst 52(1):35-41.

Pyner S, Coote JH. 1999. Identification of an efferent projection from the paraventricular nucleus of the hypothalamus terminating close to spinally projecting rostral ventrolateral medullary neurons. Neuroscience 88(3):949-957.

Pyner S, Coote JH. 2000. Identification of branching paraventricular neurons of the hypothalamus that project to the rostroventrolateral medulla and spinal cord. Neuroscience 100(3):549-556.

Qadri F, Arens T, Schwarz EC, Hauser W, Dendorfer A, Dominiak P. 2003. Brain nitric oxide synthase activity in spontaneously hypertensive rats during the development of hypertension. J Hypertens 21(9):1687-1694.

Rahn KH, Barenbrock M, Hausberg M. 1999. The sympathetic nervous system in the pathogenesis of hypertension. J Hypertens Suppl 17(3):S11-14.

Rand MJ, Li CG. 1995. Nitric oxide as a neurotransmitter in peripheral nerves: nature of transmitter and mechanism of transmission. Annu Rev Physiol 57:659-682.

Ranson RN, Motawei K, Pyner S, Coote JH. 1998. The paraventricular nucleus of the hypothalamus sends efferents to the spinal cord of the rat that closely appose sympathetic preganglionic neurones projecting to the stellate ganglion. Exp Brain Res 120(2):164-172.

Rauch M, Schmid HA, deVente J, Simon E. 1997. Electrophysiological and immunocytochemical evidence for a cGMP-mediated inhibition of subfornical organ neurons by nitric oxide. J Neurosci 17(1):363-371.

Reja V, Goodchild AK, Phillips JK, Pilowsky PM. 2002a. Tyrosine hydroxylase gene expression in ventrolateral medulla oblongata of WKY and SHR: a quantitative real-time polymerase chain reaction study. Auton Neurosci 98(1-2):79-84.

Reja V, Goodchild AK, Pilowsky PM. 2002b. Catecholamine-related gene expression correlates with blood pressures in SHR. Hypertension 40(3):342-347.

Reja V, Goodchild AK, Pilowsky PM. 2002c. Differences in gene expression of the AT1 receptor and intracellular kinases between WKY and SHR,. Proceedings Australian Health and Medical Research Congress Australian Society for Medical Research,:2837.

Renaud LP, Bourque CW. 1991. Neurophysiology and neuropharmacology of hypothalamic magnocellular neurons secreting vasopressin and oxytocin. Prog Neurobiol 36(2):131-169.

Rengasamy A, Pajewski TN, Johns RA. 1997. Inhalational anesthetic effects on rat cerebellar nitric oxide and cyclic guanosine monophosphate production. Anesthesiology 86(3):689-698.

Reuss MH, Reuss S. 2001. Nitric oxide synthase neurons in the rodent spinal cord: distribution, relation to Substance P fibers, and effects of dorsal rhizotomy. J Chem Neuroanat 21(2):181-196.

Rinaman L. 2001. Postnatal development of catecholamine inputs to the paraventricular nucleus of the hypothalamus in rats. J Comp Neurol 438(4):411-422.

Ross CA, Armstrong DM, Ruggiero DA, Pickel VM, Joh TH, Reis DJ. 1981. Adrenaline neurons in the rostral ventrolateral medulla innervate thoracic spinal cord: a combined immunocytochemical and retrograde transport demonstration. Neurosci Lett 25(3):257-262.

Ross CA, Ruggiero DA, Joh TH, Park DH, Reis DJ. 1983. Adrenaline synthesizing neurons in the rostral ventrolateral medulla: a possible role in tonic vasomotor control. Brain Res 273(2):356-361.

Ross CA, Ruggiero DA, Joh TH, Park DH, Reis DJ. 1984a. Rostral ventrolateral medulla: selective projections to the thoracic autonomic cell column from the region containing C1 adrenaline neurons. J Comp Neurol 228(2):168-185.

Ross CA, Ruggiero DA, Park DH, Joh TH, Sved AF, Fernandez-Pardal J, Saavedra JM, Reis DJ. 1984b. Tonic vasomotor control by the rostral ventrolateral medulla: effect of electrical or chemical stimulation of the area containing C1 adrenaline neurons on arterial pressure, heart rate, and plasma catecholamines and vasopressin. J Neurosci 4(2):474-494.

Ross CA, Ruggiero DA, Reis DJ. 1985. Projections from the nucleus tractus solitarii to the rostral ventrolateral medulla. J Comp Neurol 242(4):511-534.

Rothe F, Canzler U, Wolf G. 1998. Subcellular localization of the neuronal isoform of nitric oxide synthase in the rat brain: a critical evaluation. Neuroscience 83(1):259-269.

Ruetten H, Zabel U, Linz W, Schmidt HH. 1999. Downregulation of soluble guanylyl cyclase in young and aging spontaneously hypertensive rats. Circ Res 85(6):534-541.

Ruggiero DA, Cravo SL, Arango V, Reis DJ. 1989. Central control of the circulation by the rostral ventrolateral reticular nucleus: anatomical substrates. Prog Brain Res 81:49-79.

Ruggiero DA, Ross CA, Anwar M, Park DH, Joh TH, Reis DJ. 1985. Distribution of neurons containing phenylethanolamine N-methyltransferase in medulla and hypothalamus of rat. J Comp Neurol 239(2):127-154.

Russwurm M, Koesling D. 2002. Isoforms of NO-sensitive guanylyl cyclase. Molecular and cellular biochemistry 230(1-2):159-164.

Sacks FM, Svetkey LP, Vollmer WM, Appel LJ, Bray GA, Harsha D, Obarzanek E, Conlin PR, Miller ER, 3rd, Simons-Morton DG, Karanja N, Lin PH. 2001. Effects on blood pressure of reduced dietary sodium and the Dietary Approaches to Stop Hypertension (DASH) diet. DASH-Sodium Collaborative Research Group. N Engl J Med 344(1):3-10.

Sah P, McLachlan EM. 1995. Membrane properties and synaptic potentials in rat sympathetic preganglionic neurons studied in horizontal spinal cord slices in vitro. J Auton Nerv Syst 53(1):1-15.

Saha S. 2005. Role of the central nucleus of the amygdala in the control of blood pressure: descending pathways to medullary cardiovascular nuclei. Clin Exp Pharmacol Physiol 32(5-6):450-456.

Sakuma I, Togashi H, Yoshioka M, Saito H, Yanagida M, Tamura M, Kobayashi T, Yasuda H, Gross SS, Levi R. 1992. NG-methyl-L-arginine, an inhibitor of L-arginine-derived nitric oxide synthesis, stimulates renal sympathetic nerve activity in vivo. A role for nitric oxide in the central regulation of sympathetic tone? Circ Res 70(3):607-611.

Sakumoto T, Tohyama M, Satoh K, Kimoto Y, Kinugasa T, Tanizawa O, Kurachi K, Shimizu N. 1978. Afferent fiber connections from lower brain stem to hypothalamus studied by the horseradish peroxidase method with special reference to noradrenaline innervation. Exp Brain Res 31(1):81-94.

Sandirasegarane L, Diamond J. 1999. The nitric oxide donors, SNAP and DEA/NO, exert a negative inotropic effect in rat cardiomyocytes which is independent of cyclic GMP elevation. J Mol Cell Cardiol 31(4):799-808.

Saper CB, Loewy AD, Swanson LW, Cowan WM. 1976. Direct hypothalamo-autonomic connections. Brain Res 117(2):305-312.

Saphier D. 1993. Electrophysiology and neuropharmacology of noradrenergic projections to rat PVN magnocellular neurons. Am J Physiol 264(5 Pt 2):R891-902.

Sapru HN. 1994. Transmitter/receptor mechanisms in cardiovascular control by the NTS:excitatory amino acids, acetylcholine and substance P. Barroco IRA, editor. Boca Raton: CRC Press. 267 - 281 p.

Sartori C, Lepori M, Scherrer U. 2005. Interaction between nitric oxide and the cholinergic and sympathetic nervous system in cardiovascular control in humans. Pharmacol Ther 106(2):209-220.

Sawchenko PE, Brown ER, Chan RK, Ericsson A, Li HY, Roland BL, Kovacs KJ. 1996. The paraventricular nucleus of the hypothalamus and the functional neuroanatomy of visceromotor responses to stress. Prog Brain Res 107:201-222.

Sawchenko PE, Li HY, Ericsson A. 2000. Circuits and mechanisms governing hypothalamic responses to stress: a tale of two paradigms. Prog Brain Res 122:61-78.

Sawchenko PE, Swanson LW. 1982. Immunohistochemical identification of neurons in the paraventricular nucleus of the hypothalamus that project to the medulla or to the spinal cord in the rat. J Comp Neurol 205(3):260-272.

Sawka AM, Jaeschke R, Singh RJ, Young WF, Jr. 2003. A comparison of biochemical tests for pheochromocytoma: measurement of fractionated plasma metanephrines compared with the combination of 24-hour urinary metanephrines and catecholamines. J Clin Endocrinol Metab 88(2):553-558.

Schlossmann J, Hofmann F. 2005. cGMP-dependent protein kinases in drug discovery. Drug discovery today 10(9):627-634.

Schmid HA, Pehl U. 1996. Regional specific effects of nitric oxide donors and cGMP on the electrical activity of neurons in the rat spinal cord. J Chem Neuroanat 10(3-4):197-201.

Schmidt HH. 1992. NO., CO and .OH. Endogenous soluble guanylyl cyclase-activating factors. FEBS Lett 307(1):102-107.

Schmidt HH, Gagne GD, Nakane M, Pollock JS, Miller MF, Murad F. 1992. Mapping of neural nitric oxide synthase in the rat suggests frequent co-localization with NADPH diaphorase but not with soluble guanylyl cyclase, and novel paraneural functions for nitrinergic signal transduction. J Histochem Cytochem 40(10):1439-1456.

Schreiber SS, Sun N, Tocco G, Baudry M, DeGiorgio CM. 1999. Expression of neuron-specific enolase in adult rat brain following status epilepticus. Exp Neurol 159(1):329-331.

Schreihofer AM, Guyenet PG. 1997. Identification of C1 presympathetic neurons in rat rostral ventrolateral medulla by juxtacellular labeling in vivo. J Comp Neurol 387(4):524-536.

Schreihofer AM, Guyenet PG. 2002. The baroreflex and beyond: control of sympathetic vasomotor tone by GABAergic neurons in the ventrolateral medulla. Clin Exp Pharmacol Physiol 29(5-6):514-521.

Schuman EM, Madison DV. 1994. Nitric oxide and synaptic function. Annu Rev Neurosci 17:153-183.

Seagard JL, Dean C, Hopp FA. 2000. Neurochemical transmission of baroreceptor input in the nucleus tractus solitarius. Brain Res Bull 51(2):111-118.

Serino R, Ueta Y, Hanamiya M, Nomura M, Yamamoto Y, Yamaguchi KI, Nakashima Y, Yamashita H. 2001. Increased levels of hypothalamic neuronal nitric oxide synthase and vasopressin in salt-loaded Dahl rat. Auton Neurosci 87(2-3):225-235.

Seyedabadi M, Li Q, Padley JR, Pilowsky PM, Goodchild AK. 2006. A novel pressor area at the medullo-cervical junction that is not dependent on the RVLM: efferent pathways and chemical mediators. J Neurosci 26(20):5420-5427.

Shafton AD, Ryan A, Badoer E. 1998. Neurons in the hypothalamic paraventricular nucleus send collaterals to the spinal cord and to the rostral ventrolateral medulla in the rat. Brain Res 801(1-2):239-243.

Shapoval LN, Sagach VF, Pobegailo LS. 1991. Nitric oxide influences ventrolateral medullary mechanisms of vasomotor control in the cat. Neurosci Lett 132(1):47-50.

Shaul PW, Smart EJ, Robinson LJ, German Z, Yuhanna IS, Ying Y, Anderson RG, Michel T. 1996. Acylation targets endothelial nitric-oxide synthase to plasmalemmal caveolae. J Biol Chem 271(11):6518-6522.

Simonian SX, Herbison AE. 1996. Localization of neuronal nitric oxide synthase-immunoreactivity within sub-populations of noradrenergic A1 and A2 neurons in the rat. Brain Res 732(1-2):247-252.

Soderling SH, Bayuga SJ, Beavo JA. 1998. Identification and characterization of a novel family of cyclic nucleotide phosphodiesterases. J Biol Chem 273(25):15553-15558.

Southam E, Garthwaite J. 1993. The nitric oxide-cyclic GMP signalling pathway in rat brain. Neuropharmacology 32(11):1267-1277.

Souza HC, Ballejo G, Salgado MC, Da Silva VJ, Salgado HC. 2001. Cardiac sympathetic overactivity and decreased baroreflex sensitivity in L-NAME hypertensive rats. Am J Physiol Heart Circ Physiol 280(2):H844-850.

Springell DA, Powers-Martin K, Phillips JK, Pilowsky PM, Goodchild AK. 2005. Phosphorylated extracellular signal-regulated kinase 1/2 immunoreactivity identifies a novel subpopulation of sympathetic preganglionic neurons. Neuroscience 133(2):583-590.

Spyer KM. 1994. Annual review prize lecture. Central nervous mechanisms contributing to cardiovascular control. J Physiol 474(1):1-19.

Srisawat R, Ludwig M, Bull PM, Douglas AJ, Russell JA, Leng G. 2000. Nitric oxide and the oxytocin system in pregnancy. J Neurosci 20(17):6721-6727.

Staessen JA, Wang J, Bianchi G, Birkenhager WH. 2003. Essential hypertension. Lancet 361(9369):1629-1641.

Stamler JS. 1994. Redox signaling: nitrosylation and related target interactions of nitric oxide. Cell 78(6):931-936.

Stamler JS, Toone EJ, Lipton SA, Sucher NJ. 1997. (S)NO signals: translocation, regulation, and a consensus motif. Neuron 18(5):691-696.

Stern JE. 2001. Electrophysiological and morphological properties of pre-autonomic neurones in the rat hypothalamic paraventricular nucleus. J Physiol 537(Pt 1):161-177.

Stern JE. 2004. Nitric oxide and homeostatic control: an intercellular signalling molecule contributing to autonomic and neuroendocrine integration? Prog Biophys Mol Biol 84(2-3):197-215.

Stern JE, Li Y, Zhang W. 2003. Nitric oxide: a local signalling molecule controlling the activity of pre-autonomic neurones in the paraventricular nucleus of the hypothalamus. Acta Physiol Scand 177(1):37-42.

Stern JE, Ludwig M. 2001. NO inhibits supraoptic oxytocin and vasopressin neurons via activation of GABAergic synaptic inputs. Am J Physiol Regul Integr Comp Physiol 280(6):R1815-1822.

Stern JE, Zhang W. 2005. Cellular sources, targets and actions of constitutive nitric oxide in the magnocellular neurosecretory system of the rat. J Physiol 562(Pt 3):725-744.

Stornetta RL, Akey PJ, Guyenet PG. 1999. Location and electrophysiological characterization of rostral medullary adrenergic neurons that contain neuropeptide Y mRNA in rat medulla. J Comp Neurol 415(4):482-500.

Stornetta RL, Morrison SF, Ruggiero DA, Reis DJ. 1989. Neurons of rostral ventrolateral medulla mediate somatic pressor reflex. Am J Physiol 256(2 Pt 2):R448-462.

Stornetta RL, Schreihofer AM, Pelaez NM, Sevigny CP, Guyenet PG. 2001. Preproenkephalin mRNA is expressed by C1 and non-C1 barosensitive bulbospinal neurons in the rostral ventrolateral medulla of the rat. J Comp Neurol 435(1):111-126.

Stornetta RL, Sevigny CP, Schreihofer AM, Rosin DL, Guyenet PG. 2002. Vesicular glutamate transporter DNPI/VGLUT2 is expressed by both C1 adrenergic and nonaminergic presympathetic vasomotor neurons of the rat medulla. J Comp Neurol 444(3):207-220.

Strack AM, Sawyer WB, Marubio LM, Loewy AD. 1988. Spinal origin of sympathetic preganglionic neurons in the rat. Brain Res 455(1):187-191.

Stuehr DJ, Cho HJ, Kwon NS, Weise MF, Nathan CF. 1991. Purification and characterization of the cytokine-induced macrophage nitric oxide synthase: an FAD- and FMN-containing flavoprotein. Proc Natl Acad Sci U S A 88(17):7773-7777.

Sun MK, Guyenet PG. 1985. GABA-mediated baroreceptor inhibition of reticulospinal neurons. Am J Physiol 249(6 Pt 2):R672-680.

Sun MK, Hackett JT, Guyenet PG. 1988. Sympathoexcitatory neurons of rostral ventrolateral medulla exhibit pacemaker properties in the presence of a glutamate-receptor antagonist. Brain Res 438(1-2):23-40.

Sved AF. 1989. PNMT-containing catecholaminergic neurons are not necessarily adrenergic. Brain Res 481(1):113-118.

Sved AF, Cano G, Card JP. 2001. Neuroanatomical specificity of the circuits controlling sympathetic outflow to different targets. Clin Exp Pharmacol Physiol 28(1-2):115-119.

Sved AF, Ito S, Madden CJ. 2000. Baroreflex dependent and independent roles of the caudal ventrolateral medulla in cardiovascular regulation. Brain Res Bull 51(2):129-133.

Sved AF, Mancini DL, Graham JC, Schreihofer AM, Hoffman GE. 1994. PNMT-containing neurons of the C1 cell group express c-fos in response to changes in baroreceptor input. Am J Physiol 266(2 Pt 2):R361-367.

Sved AF, Tsukamoto K, Schreihofer AM. 1992. Stimulation of alpha 2-adrenergic receptors in nucleus tractus solitarius is required for the baroreceptor reflex. Brain Res 576(2):297-303.

Swanson LW. 1977. Immunohistochemical evidence for a neurophysin-containing autonomic pathway arising in the paraventricular nucleus of the hypothalamus. Brain Res 128(2):346-353.

Swanson LW, Kuypers HG. 1980. The paraventricular nucleus of the hypothalamus: cytoarchitectonic subdivisions and organization of projections to the pituitary, dorsal vagal complex, and spinal cord as demonstrated by retrograde fluorescence double-labeling methods. J Comp Neurol 194(3):555-570.

Swanson LW, Sawchenko PE. 1980. Paraventricular nucleus: a site for the integration of neuroendocrine and autonomic mechanisms. Neuroendocrinology 31(6):410-417.

Swanson LW, Sawchenko PE. 1983. Hypothalamic integration: organization of the paraventricular and supraoptic nuclei. Annu Rev Neurosci 6:269-324.

Swanson LW, Sawchenko PE, Wiegand SJ, Price JL. 1980. Separate neurons in the paraventricular nucleus project to the median eminence and to the medulla or spinal cord. Brain Res 198(1):190-195.

Sweerts BW, Jarrott B, Lawrence AJ. 1999. Expression of preprogalanin mRNA following acute and chronic restraint stress in brains of normotensive and hypertensive rats. Brain Res Mol Brain Res 69(1):113-123.

Szabadits E, Cserep C, Ludanyi A, Katona I, Gracia-Llanes J, Freund TF, Nyiri G. 2007. Hippocampal GABAergic synapses possess the molecular machinery for retrograde nitric oxide signaling. J Neurosci 27(30):8101-8111.

Tagawa T, Dampney RA. 1999. AT(1) receptors mediate excitatory inputs to rostral ventrolateral medulla pressor neurons from hypothalamus. Hypertension 34(6):1301-1307.

Tai MH, Wang LL, Wu KL, Chan JY. 2005. Increased superoxide anion in rostral ventrolateral medulla contributes to hypertension in spontaneously hypertensive rats via interactions with nitric oxide. Free Radic Biol Med 38(4):450-462.

Takahashi M, Ishida T, Traub O, Corson MA, Berk BC. 1997. Mechanotransduction in endothelial cells: temporal signaling events in response to shear stress. J Vasc Res 34(3):212-219.

Takahashi T. 2003. Pathophysiological significance of neuronal nitric oxide synthase in the gastrointestinal tract. J Gastroenterol 38(5):421-430.

Takeda K, Nakata T, Takesako T, Itoh H, Hirata M, Kawasaki S, Hayashi J, Oguro M, Sasaki S, Nakagawa M. 1991. Sympathetic inhibition and attenuation of spontaneous hypertension by PVN lesions in rats. Brain Res 543(2):296-300.

Tang FR, Tan CK, Ling EA. 1995a. A comparative study by retrograde neuronal tracing and substance P immunohistochemistry of sympathetic preganglionic neurons in spontaneously hypertensive rats and Wistar-Kyoto rats. J Anat 186 (Pt 1):197-207.

Tang FR, Tan CK, Ling EA. 1995b. A comparative study of NADPH-diaphorase in the sympathetic preganglionic neurons of the upper thoracic cord between spontaneously hypertensive rats and Wistar-Kyoto rats. Brain Res 691(1-2):153-159.

Tang W, Paulding WR, Sumners C. 1993. ANP receptors in neurons and astrocytes from spontaneously hypertensive rat brain. Am J Physiol 265(1 Pt 1):C106-112.

Tassorelli C, Blandini F, Greco R, Nappi G. 2004. Nitroglycerin enhances cGMP expression in specific neuronal and cerebrovascular structures of the rat brain. J Chem Neuroanat 27(1):23-32.

Terrell ML, Salas N, Bui V, Summy-Long JY, Kadekaro M. 2003. NO inhibition of the magnocellular neuroendocrine system in rats is independent of cGMP signaling pathway. Exp Neurol 184(2):846-856.

Textor SC. 2004. Ischemic nephropathy: where are we now? J Am Soc Nephrol 15(8):1974-1982.

Thippeswamy T, Morris R. 2001. Evidence that nitric oxide-induced synthesis of cGMP occurs in a paracrine but not an autocrine fashion and that the site of its release can be regulated: studies in dorsal root ganglia in vivo and in vitro. Nitric Oxide 5(2):105-115.

Thomas DD, Espey MG, Ridnour LA, Hofseth LJ, Mancardi D, Harris CC, Wink DA. 2004. Hypoxic inducible factor 1alpha, extracellular signal-regulated kinase, and p53 are regulated by distinct threshold concentrations of nitric oxide. Proc Natl Acad Sci U S A 101(24):8894-8899.

Thomas DD, Liu X, Kantrow SP, Lancaster JR, Jr. 2001. The biological lifetime of nitric oxide: implications for the perivascular dynamics of NO and O2. Proc Natl Acad Sci U S A 98(1):355-360.

Thomas DD, Ridnour LA, Isenberg JS, Flores-Santana W, Switzer CH, Donzellie S, Hussain P, Vecoli C, Paolocci N, Ambs S, Colton C, Harris C, Roberts DD, Wink DA. 2008. The chemical biology of nitric oxide: Implications in cellular signaling. Free Radic Biol Med.

Tillet Y. 1988. Adrenergic neurons in sheep brain demonstrated by immunohistochemistry with antibodies to phenylethanolamine N-methyltransferase (PNMT) and dopamine-beta-hydroxylase (DBH): absence of the C1 cell group in the sheep brain. Neurosci Lett 95(1-3):107-112.

Tobin JR, Martin LD, Breslow MJ, Traystman RJ. 1994. Selective anesthetic inhibition of brain nitric oxide synthase. Anesthesiology 81(5):1264-1269.

Toda N, Ayajiki K, Okamura T. 2005. Nitric oxide and penile erectile function. Pharmacol Ther 106(2):233-266.

Toda N, Okamura T. 2003. The pharmacology of nitric oxide in the peripheral nervous system of blood vessels. Pharmacol Rev 55(2):271-324.

Togashi H, Sakuma I, Yoshioka M, Kobayashi T, Yasuda H, Kitabatake A, Saito H, Gross SS, Levi R. 1992. A central nervous system action of nitric oxide in blood pressure regulation. J Pharmacol Exp Ther 262(1):343-347.

Toth ZE, Gallatz K, Fodor M, Palkovits M. 1999. Decussations of the descending paraventricular pathways to the brainstem and spinal cord autonomic centers. J Comp Neurol 414(2):255-266.

Trabace L, Kendrick KM. 2000. Nitric oxide can differentially modulate striatal neurotransmitter concentrations via soluble guanylate cyclase and peroxynitrite formation. J Neurochem 75(4):1664-1674.

Tseng CJ, Liu HY, Lin HC, Ger LP, Tung CS, Yen MH. 1996. Cardiovascular effects of nitric oxide in the brain stem nuclei of rats. Hypertension 27(1):36-42.

Tsuchihashi T, Kagiyama S, Matsumura K, Lin Y, Abe I, Fujishima M. 2000. Cardiovascular responses to glutamate and angiotensin II in ventrolateral medulla of hypertension induced by chronic inhibition of nitric oxide. Hypertens Res 23(4):359-364.

Tsuchihashi T, Kagiyama S, Ohya Y, Abe I, Fujishima M. 1998. Antihypertensive treatment and the responsiveness to glutamate in ventrolateral medulla. Hypertension 31(1):73-76.

Tucker DC, Saper CB, Ruggiero DA, Reis DJ. 1987. Organization of central adrenergic pathways: I. Relationships of ventrolateral medullary projections to the hypothalamus and spinal cord. J Comp Neurol 259(4):591-603.

Ueta Y, Levy A, Chowdrey HS, Lightman SL. 1995. Water deprivation in the rat induces nitric oxide synthase (NOS) gene expression in the hypothalamic paraventricular and supraoptic nuclei. Neurosci Res 23(3):317-319.

Vaandrager AB, Hogema BM, de Jonge HR. 2005. Molecular properties and biological functions of cGMP-dependent protein kinase II. Front Biosci 10:2150-2164.

Vacher CM, Hardin-Pouzet H, Steinbusch HW, Calas A, De Vente J. 2003. The effects of nitric oxide on magnocellular neurons could involve multiple indirect cyclic GMP-dependent pathways. Eur J Neurosci 17(3):455-466.

van Staveren WC, Markerink-van Ittersum M, Steinbusch HW, Behrends S, de Vente J. 2005. Localization and characterization of cGMP-immunoreactive structures in rat brain slices after NO-dependent and NO-independent stimulation of soluble guanylyl cyclase. Brain Res 1036(1-2):77-89.

van Tol HH, van den Buuse M, de Jong W, Burbach JP. 1988. Vasopressin and oxytocin gene expression in the supraoptic and paraventricular nucleus of the spontaneously hypertensive rat (SHR) during development of hypertension. Brain Res 464(4):303-311.

Velley L, Milner TA, Chan J, Morrison SF, Pickel VM. 1991. Relationship of Met-enkephalin-like immunoreactivity to vagal afferents and motor dendrites in the nucleus of the solitary tract: a light and electron microscopic dual labeling study. Brain Res 550(2):298-312.

Verberne AJ, Guyenet PG. 1992. Medullary pathway of the Bezold-Jarisch reflex in the rat. Am J Physiol 263(6 Pt 2):R1195-1202.

Verberne AJ, Stornetta RL, Guyenet PG. 1999. Properties of C1 and other ventrolateral medullary neurones with hypothalamic projections in the rat. J Physiol 517 (Pt 2):477-494.

Verberne AJ, Widdop RE, Maccarrone C, Jarrott B, Beart PM, Louis WJ. 1990. Intrathecal kynurenate reduces arterial pressure, heart rate and baroreceptor-heart rate reflex in conscious rats. Neurosci Lett 114(3):309-315.

Vincent SR, Kimura H. 1992. Histochemical mapping of nitric oxide synthase in the rat brain. Neuroscience 46(4):755-784.

Vles JS, de Louw AJ, Steinbusch H, Markerink-van Ittersum M, Steinbusch HW, Blanco CE, Axer H, Troost J, de Vente J. 2000. Localization and age-related changes of nitric oxide- and ANP-mediated cyclic-GMP synthesis in rat cervical spinal cord: an immunocytochemical study. Brain Res 857(1-2):219-234.

Vollmer RR. 1996. Selective neural regulation of epinephrine and norepinephrine cells in the adrenal medulla -- cardiovascular implications. Clin Exp Hypertens 18(6):731-751.

Vollmer RR, Balcita JJ, Sved AF, Edwards DJ. 1997. Adrenal epinephrine and norepinephrine release to hypoglycemia measured by microdialysis in conscious rats. Am J Physiol 273(5 Pt 2):R1758-1763.

Wainwright A, Rutter AR, Seabrook GR, Reilly K, Oliver KR. 2004. Discrete expression of TRPV2 within the hypothalamo-neurohypophysial system: Implications for regulatory activity within the hypothalamic-pituitary-adrenal axis. J Comp Neurol 474(1):24-42.

Webb GD, Lim LH, Oh VM, El Oakley R, Lee CN, Wong PS, Aye WM, Chan ES, Moore PK. 2006. Expression of neuronal nitric oxide synthase in the internal thoracic artery and saphenous vein. J Thorac Cardiovasc Surg 132(5):1131-1136.

Wedel BJ, Garbers DL. 1997. New insights on the functions of the guanylyl cyclase receptors. FEBS Lett 410(1):29-33.

Weiss ML, Chowdhury SI, Patel KP, Kenney MJ, Huang J. 2001. Neural circuitry of the kidney: NO-containing neurons. Brain Res 919(2):269-282.

Willette RN, Barcas PP, Krieger AJ, Sapru HN. 1983. Vasopressor and depressor areas in the rat medulla. Identification by microinjection of L-glutamate. Neuropharmacology 22(9):1071-1079.

Willette RN, Barcas PP, Krieger AJ, Sapru HN. 1984a. Endogenous GABAergic mechanisms in the medulla and the regulation of blood pressure. J Pharmacol Exp Ther 230(1):34-39.

Willette RN, Gatti PA, Sapru HN. 1984b. GABAergic mechanisms in the ventrolateral medulla alter vasopressor responses from the anterior hypothalamus. J Cardiovasc Pharmacol 6(3):476-482.

Willette RN, Punnen S, Krieger AJ, Sapru HN. 1984c. Interdependence of rostral and caudal ventrolateral medullary areas in the control of blood pressure. Brain Res 321(1):169-174.

Willette RN, Punnen-Grandy S, Krieger AJ, Sapru HN. 1987. Differential regulation of regional vascular resistance by the rostral and caudal ventrolateral medulla in the rat. J Auton Nerv Syst 18(2):143-151.

Wink DA, Hanbauer I, Grisham MB, Laval F, Nims RW, Laval J, Cook J, Pacelli R, Liebmann J, Krishna M, Ford PC, Mitchell JB. 1996. Chemical biology of nitric oxide: regulation and protective and toxic mechanisms. Curr Top Cell Regul 34:159-187.

Wolf-Maier K, Cooper RS, Banegas JR, Giampaoli S, Hense HW, Joffres M, Kastarinen M, Poulter N, Primatesta P, Rodriguez-Artalejo F, Stegmayr B, Thamm M, Tuomilehto J, Vanuzzo D, Vescio F. 2003. Hypertension prevalence and blood pressure levels in 6 European countries, Canada, and the United States. JAMA 289(18):2363-2369.

Wu SY, Dun SL, Forstermann U, Dun NJ. 1997. Nitric oxide and excitatory postsynaptic currents in immature rat sympathetic preganglionic neurons in vitro. Neuroscience 79(1):237-245.

Wu WC, Wang Y, Su CK, Chai CY. 2001. The nNOS/cGMP signal transducing system is involved in the cardiovascular responses induced by activation of NMDA receptors in the rostral ventrolateral medulla of cats. Neurosci Lett 310(2-3):121-124.

Yaksh TL, Rudy TA. 1976. Chronic catheterization of the spinal subarachnoid space. Physiol Behav 17(6):1031-1036.

Yamada K, Hiramatsu M, Noda Y, Mamiya T, Murai M, Kameyama T, Komori Y, Nikai T, Sugihara H, Nabeshima T. 1996. Role of nitric oxide and cyclic GMP in the dizocilpine-induced impairment of spontaneous alternation behavior in mice. Neuroscience 74(2):365-374.

Yamaguchi N. 1992. Sympathoadrenal system in neuroendocrine control of glucose: mechanisms involved in the liver, pancreas, and adrenal gland under hemorrhagic and hypoglycemic stress. Can J Physiol Pharmacol 70(2):167-206.

Yang Q, Chen SR, Li DP, Pan HL. 2007. Kv1.1/1.2 channels are downstream effectors of nitric oxide on synaptic GABA release to preautonomic neurons in the paraventricular nucleus. Neuroscience 149(2):315-327.

Yang QZ, Hatton GI. 1999. Nitric oxide via cGMP-dependent mechanisms increases dye coupling and excitability of rat supraoptic nucleus neurons. J Neurosci 19(11):4270-4279.

Yang Z, Coote JH. 2003. Role of GABA and NO in the paraventricular nucleus-mediated reflex inhibition of renal sympathetic nerve activity following stimulation of right atrial receptors in the rat. Exp Physiol 88(3):335-342.

Yoshimura M, Nishi S. 1982. Intracellular recordings from lateral horn cells fo the spinal cord in vitro. J Auton Nerv Syst 6(1):5-11.

Young JB, Rosa RM, Landsberg L. 1984. Dissociation of sympathetic nervous system and adrenal medullary responses. Am J Physiol 247(1 Pt 1):E35-40.

Zagotta WN, Siegelbaum SA. 1996. Structure and function of cyclic nucleotide-gated channels. Annu Rev Neurosci 19:235-263.

Zanzinger J. 1999. Role of nitric oxide in the neural control of cardiovascular function. Cardiovasc Res 43(3):639-649.

Zanzinger J. 2002. Mechanisms of action of nitric oxide in the brain stem: role of oxidative stress. Auton Neurosci 98(1-2):24-27.

Zanzinger J, Czachurski J, Seller H. 1995. Effects of nitric oxide on sympathetic baroreflex transmission in the nucleus tractus solitarii and caudal ventrolateral medulla in cats. Neurosci Lett 197(3):199-202.

Zhang H, Thijs L, Staessen JA. 2006. Blood pressure lowering for primary and secondary prevention of stroke. Hypertension 48(2):187-195.

Zhang K, Li YF, Patel KP. 2001. Blunted nitric oxide-mediated inhibition of renal nerve discharge within PVN of rats with heart failure. Am J Physiol Heart Circ Physiol 281(3):H995-1004.

Zhang K, Mayhan WG, Patel KP. 1997. Nitric oxide within the paraventricular nucleus mediates changes in renal sympathetic nerve activity. Am J Physiol 273(3 Pt 2):R864-872.

Zhang K, Patel KP. 1998. Effect of nitric oxide within the paraventricular nucleus on renal sympathetic nerve discharge: role of GABA. Am J Physiol 275(3 Pt 2):R728-734.

Zhang TX, Ciriello J. 1985a. Effect of paraventricular nucleus lesions on arterial pressure and heart rate after aortic baroreceptor denervation in the rat. Brain Res 341(1):101-109.

Zhang TX, Ciriello J. 1985b. Kainic acid lesions of paraventricular nucleus neurons reverse the elevated arterial pressure after aortic baroreceptor denervation in the rat. Brain Res 358(1-2):334-338.

Zhang Z, Klyachko V, Jackson MB. 2007. Blockade of phosphodiesterase Type 5 enhances rat neurohypophysial excitability and electrically evoked oxytocin release. J Physiol 584(Pt 1):137-147.

Zheng H, Bidasee KR, Mayhan WG, Patel KP. 2007. Lack of central nitric oxide triggers erectile dysfunction in diabetes. Am J Physiol Regul Integr Comp Physiol 292(3):R1158-1164.